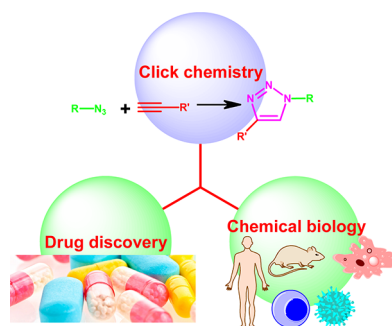


Click Chemistry for Drug Development and Diverse Chemical–Biology Applications

Prakasam Thirumurugan,[†] Dariusz Matusiuk,[‡] and Krzysztof Jozwiak^{*,†}

[†]Laboratory of Medical Chemistry and Neuroengineering, Department of Chemistry, and [‡]Department of Synthesis and Chemical Technology of Pharmaceutical Substances, Medical University of Lublin, Lublin 20093, Poland



CONTENTS

1. Introduction	4905	6. Click Chemistry in Drug Development Using Fragment-Based Drug Discovery	4941
2. Click Chemistry: Overview	4906	7. Click Chemistry and Bioorthogonal Chemistry	4944
3. Application of Click Chemistry in Pharmaceutical Science	4907	7.1. Site-Specific Labeling of Cells, Live Organisms, and Proteins	4947
3.1. Click Chemistry and Drug Discovery	4907	7.2. Site-Specific in Vitro and in Vivo Incorporation of Molecular Probes To Study G-Protein-Coupled Receptors	4950
3.1.1. High-Throughput Screening	4907	7.3. Activity-Based Protein Profiling versus Affinity-Based Protein Profiling	4951
3.1.2. Fragment-Based Drug Discovery	4907	ABPs and AFBPs Used for Targeting Various Protein Classes in Conjunction with Click Chemistry Bioorthogonal Labeling	4952
3.1.3. Dynamic Template-Assisted Strategies in Fragment-Based Drug Discovery	4908	7.4. Labeling and Sequencing of DNA	4952
3.2. Synthetic Utility of Click Chemistry in the Development of Enzyme Inhibitors	4910	7.5. Analysis of G-Quadruplex Structure Using Click Chemistry and G-Quadruplex Stabilizing Ligands	4955
3.2.1. Protein Tyrosine Phosphatase Inhibitors	4910	8. Copper-Free Click Chemistry Reactions for Biological Systems	4959
3.2.2. Protein Kinase Inhibitors	4914	8.1. Design and Synthesis of Bioorthogonal Reagents	4964
3.2.3. Transferase Inhibitors	4914	8.2. Cyclooctyne Derivatives Used in Copper-Free Click Bioorthogonal Chemistry	4967
3.2.4. Glycogen Phosphorylase Inhibitors	4917	8.3. Chemical Tagging Strategies Used Copper-Free Click Chemistry	4970
3.2.5. Serine Hydrolase Inhibitors	4917	9. Conclusion	4973
3.2.6. Cysteine and Serine Protease Inhibitors	4917	Author Information	4973
3.2.7. Metalloproteinase Inhibitors	4920	Corresponding Author	4973
3.2.8. Aspartic Protease Inhibitors	4922	Notes	4973
3.2.9. Oxidoreductase Inhibitors	4923	Biographies	4973
3.2.10. Glycosidase Inhibitors	4925	References	4974
4. In Situ Click Chemistry	4926		
4.1. Mycobacterial Transcriptional Regulator	4926		
4.2. Histone Deacetylase Inhibitors	4927		
4.3. Protein–Protein Interaction Modulators	4928		
4.4. Antibody-like Protein-Capture Agents	4928		
4.5. Acetylcholinesterase Inhibitors	4930		
4.6. HIV Protease Inhibitors	4931		
4.7. Chitinase Inhibitors	4931		
4.8. Carbonic Anhydrase Inhibitors	4931		
4.9. Cell Imaging	4932		
5. Synthetic Utility of Click Chemistry in Receptor–Ligand Binding Studies	4933		
5.1. Selective Agonists	4934		
5.2. Selective Antagonists	4935		
5.3. Selective Binding Ligands	4938		

1. INTRODUCTION

Chemistry, traditionally being the science of synthesis and structural manipulations of molecules, has gradually undertaken the more challenging task of biology-oriented synthesis.¹ The generation of molecules/molecular assemblies possessing well-defined biological functions remains an extremely challenging task; immediate refinements in conventional synthetic tactics are necessary. New and more efficient chemical reactions and methodologies, which may override the laborious protection/deprotection and purification steps in conventional total synthesis, could revolutionize the next-generation chemical and biological research.² A set of chemical reactions, known as bioorthogonal reactions, that are orthogonal to most functional

Received: October 25, 2011

Published: March 27, 2013

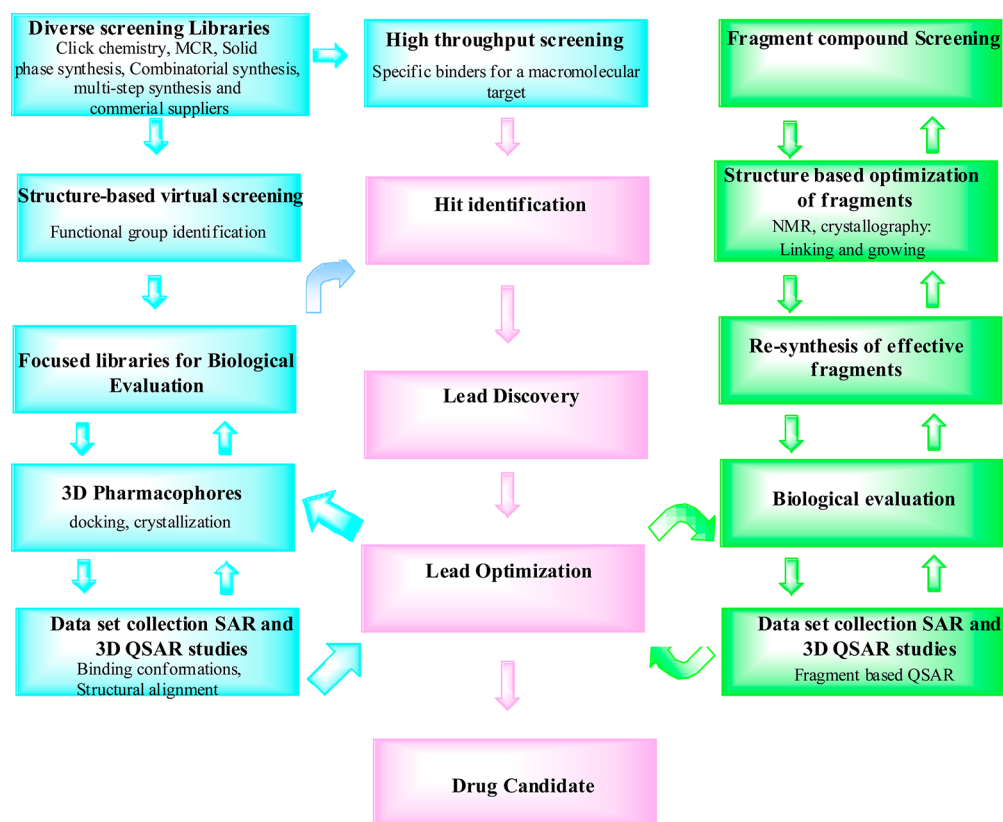


Figure 1. Workflow of the process of hit-to-lead optimization from click chemistry and drug candidate selection. FBDD, SAR, and QSAR studies are essential elements of this complex paradigm. FBDD, fragment-based drug design; QSAR, quantitative SAR; SAR, structure–activity relationship.

groups in biological systems has so far shown promising applications in biological research.³ Of these reactions, the Cu(I)-catalyzed version of the Huisen 1,3-dipolar cycloaddition reaction between azides and terminal alkynes for the construction of triazoles, referred to as a “click chemistry reaction”, was defined by nobel laureate KB Sharpless and associates in 2001.⁴ Click chemistry has recently emerged to become one of the most powerful tools in drug discovery, chemical biology, and proteomic applications. In recent years, the design and synthesis of pharmacologically relevant heterocyclic molecules by combinatorial techniques have proven to be a promising strategy in the search for new pharmaceutical lead structures. Click chemistry is one of the powerful reactions for making carbon–heteroatom–carbon bonds in aqueous environment with a wide variety of chemical and biological applications in various fields.⁵

2. CLICK CHEMISTRY: OVERVIEW

Despite many successes, drug discovery approaches that are based on nature’s secondary metabolites are often hampered by slow and complex syntheses. Through the use of only the most facile and selective chemical transformations, click chemistry simplifies compound synthesis, providing the faster lead discovery and optimization. The click reaction must be modular, wide in scope, give very high yields, generate only inoffensive byproducts that can be removed by nonchromatographic methods, and be stereospecific (but not necessarily enantioselective). The required process characteristics include simple reaction conditions (ideally, the process should be insensitive to oxygen and water), readily available starting materials and reagents, the use of no solvent or a solvent that is

benign (such as water) or easily removed, and simple product isolation.⁶ Purification, if required, must be by nonchromatographic methods, such as crystallization or distillation, and the product must be stable under physiological conditions. The traditional process of drug discovery based on natural secondary metabolites has often been slow, costly, and labor-intensive. Even with the advent of combinatorial chemistry and high-throughput screening in the past two decades, the generation of leads is dependent on the reliability of the individual reactions to construct the new molecular framework.⁷

Click chemistry is a newer approach to the synthesis of drug-like molecules that can accelerate the drug discovery process by utilizing a few practical and reliable reactions. Sharpless and co-workers defined the click reaction as wide in scope and easy to perform, uses only readily available reagents, and is insensitive to oxygen and water.^{4,6} In fact, in several instances, water is the ideal reaction solvent, providing the best yields of the product with the highest rates. For reaction workup and purification, eco-friendly solvents are used that avoid purification techniques like chromatography.⁸

Click reactions share the following attributes:

- (1) Many click components are derived from alkenes and alkynes, and thus ultimately from the cracking of petroleum. Carbon–carbon multiple bonds provide both energy and mechanistic pathways to be elaborated into reactive structures for click connections.
- (2) Most click reactions involve the formation of carbon–heteroatom (mostly N, O, and S) bonds. This stands in contrast to the march of modern synthetic organic

chemistry, which has emphasized the formation of carbon–carbon bonds.

- (3) Click reactions are strongly exothermic, by virtue of either highly energetic reactants or strongly stabilized products.
- (4) Click reactions are usually fusion processes (leaving no byproducts) or condensation processes (producing water as a byproduct).
- (5) Many click reactions are highly tolerant of, and often accelerated by, the presence of water.

The copper(I)-catalyzed 1,2,3-triazole formation from azides and terminal acetylenes is a powerful tool for the generation of privileged medicinal scaffolds, due to its high degree of dependability, complete specificity, and the biocompatibility of the reactants.^{4,9} The triazole scaffolds are found in a number of biologically active compounds exhibiting anti-HIV, antibiotics, antiviral, and antibacterial activities.¹⁰ Click chemistry is one of the powerful tools for the generation of drug candidates. Many researchers used click chemistry as a synthetic tool for the generation of pharmacologically valuable drugs.^{5,9}

3. APPLICATION OF CLICK CHEMISTRY IN PHARMACEUTICAL SCIENCE

Current drug discovery relies on massive screening of chemical libraries against various extracellular and intracellular molecular targets to find novel chemotypes with the desired mode of action. In recent years, high-throughput technologies for combinatorial and multiparallel chemical synthesis, automation technologies for the isolation of natural products, and also availability of large compound collections from commercial sources have substantially increased the size and diversity of compound collections among most Pharma and Biotech companies, in some cases exceeding one million distinct chemical entities.¹¹ At the same time, sequencing of the human genome as well as sequencing the genomes of various pathogens, such as microbes, bacteria, and viruses, have delivered hundreds to thousands of potentially novel biological targets that have poor or no clearly precedented chemical starting point for lead optimization.^{11,12} Click chemistry-based drug discovery mainly falls into three types: (1) high-throughput screening, (2) fragment-based drug discovery, and (3) dynamic template-assisted strategies in fragment-based drug discovery.

3.1. Click Chemistry and Drug Discovery

3.1.1. High-Throughput Screening. High-throughput screening (HTS) is a well-established process for lead drug discovery in pharmaceutical and biotechnology companies and is now also being used for basic and applied research in academia. It comprises the screening of large chemical libraries for activity against biological targets via the use of automation, miniaturized assays, and large-scale data analysis. Today, the tools at hand for lead discovery are expanding and complementing each other: focused screening for well-connected target classes, virtual screening and access to large external chemistry sources (including isolated natural products), structure-based design, and cellular assays of increasing value in understanding compound effects (Figure 1).¹³ All of these tools are important complementary approaches to HTS for providing entry points for lead optimization. A wise use of lead discovery tactics will distinguish successful drug discovery engines. Different engines might be able to afford different options in the menu. As long as we keep learning how to best

select and validate targets linked with human disease and wisely exploit these recently refined technologies (in addition to and not instead of those previously established), we should expect an increase in drugs in the market that help people to live healthier and longer lives.^{14,15}

HTS-based lead discovery falls into a modest set of target families of enzymes such as kinases, proteases, phosphatases, oxidoreductases, phosphodiesterases, and transferases that comprises the majority of biochemical targets in today's lead discovery efforts. Among cell-based targets, many GPCRs (G-protein coupled receptors, 7-transmembrane receptors), nuclear hormone receptors, and some types of voltage-gated and ligand-gated ion channels (e.g., Ca²⁺-channels) are very well suited for screening of large compound collections with today's screening technologies. Despite the large number of human genes (>25 000) and even larger number of gene transcripts and proteins (>100 000), the number of molecular targets with drugs approved is still fairly limited (324 targets). Some targets may be intractable for modulation via low molecular weight compounds. Others, however, might simply be inaccessible by current technologies and therefore constitute not only a great challenge but also a tremendous potential for future lead discovery. Among those, a large number of ion channels, transporters, and transmembrane receptors, but also novel protein–protein, protein–DNA, and protein–RNA interactions, perhaps even RNA/DNA itself, might form innovative targets for modulation via low molecular weight (lmw) compounds as exemplified by some remarkable success stories in recent times.^{16–20}

Click chemistry in combination with high-throughput enzyme assay technologies such as microarrays revolutionized lead-finding and lead-optimization steps in drug discovery. Small molecule libraries assembled using click chemistry have been successfully employed in generating unique inhibitor and activity-based fingerprints of important enzymes. Such fingerprinting strategies may in the future lead to the identification and characterization of new enzyme subclasses and even address the issue of functional convergence of enzymes at a broader scale. Rapid developments in high-throughput screening will continue to be fueled by click chemistry and its novel variants in combination with powerful technologies like microarrays and other ingenious characterization techniques.⁵

3.1.2. Fragment-Based Drug Discovery. Fragment-based drug discovery (FBDD) has become a main-stream alternative to high-throughput screening in the past few years. There are an increasing number of compounds in clinical development, which can trace their origins back to fragment screening, and a number of reviews have been published recently highlighting the progress that has been made.^{21–25} A recent review highlights in FBDD the following concepts: (1) Inappropriate physical properties are a major source of attrition for small molecule drugs. (2) Although weak in potency, fragments actually form high-quality interactions. (3) Ligand efficiency is a way to judge the relative optimizability of differently sized molecules. (4) Relatively small libraries of fragments are required to sample chemical space (Figure 1). It also highlights the following challenges: (1) Specialized methods are needed to detect fragment binding. (2) Efficient optimization of fragment hits is required.

Fragment-based drug discovery is based on the consideration that the free binding energy of a protein ligand results from the contributions of its molecular components. Therefore, small contributions from molecular fragments can add up to yield a

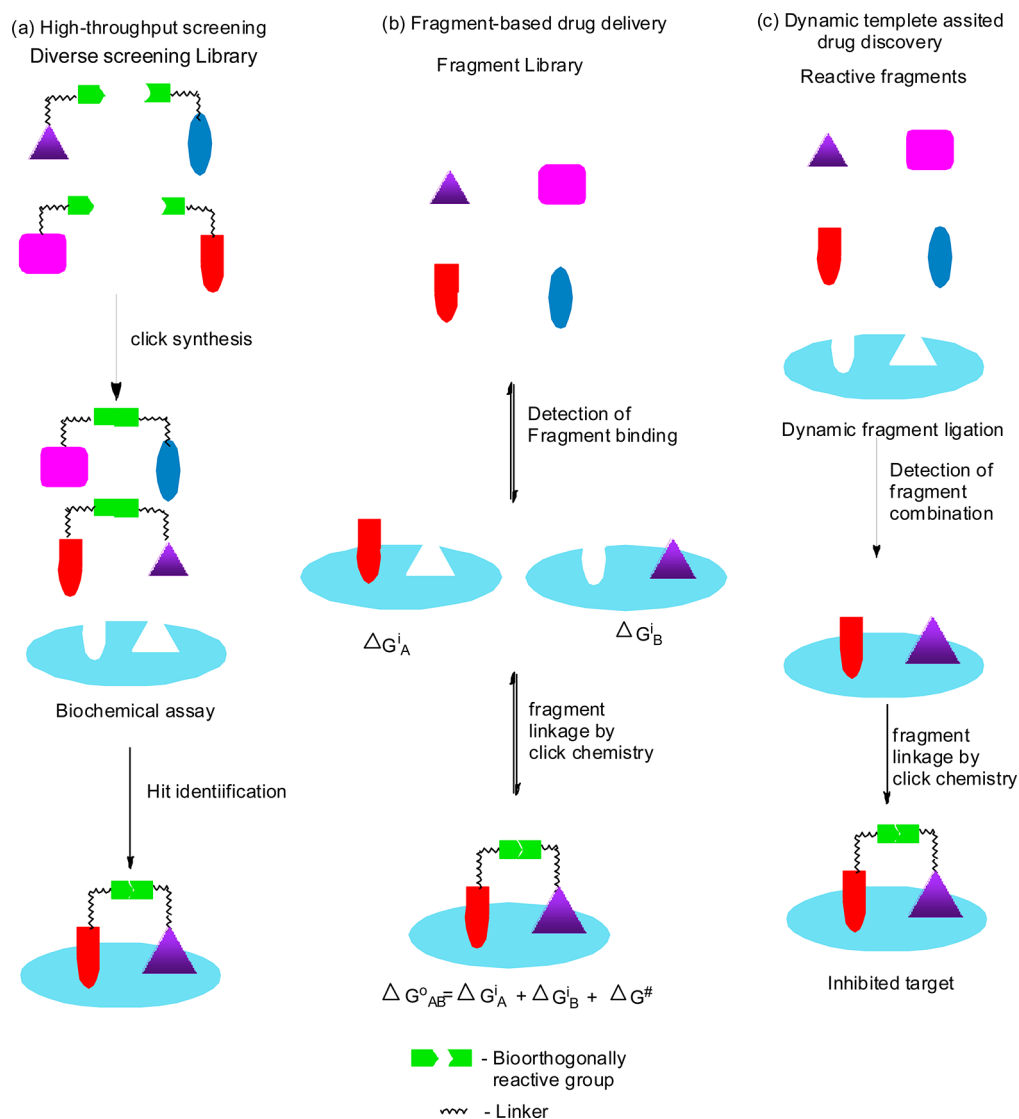


Figure 2. Concepts in lead discovery. (a) High-throughput screening (HTS). A diverse library of chemical compounds is collected and tested against the drug target. (b) Fragment-based lead discovery. The binding of small molecular fragments to the protein is detected. Low-affinity fragments can be linked to provide high-affinity ligands. The binding constant K_{AB} is an exponential function of the binding energy. (c) Dynamic strategies in fragment-based drug discovery. Reactive fragments are incubated with the protein and form specific combinations of fragments on the protein template, which facilitates fragment detection and linkage to a new ligand.

high-affinity protein ligand. First, a small molecule fragment that binds to the protein pocket of interest is identified. The starting fragment is then chemically modified to generate a binder of higher affinity, which is subsequently further optimized to a lead structure. The concept has become very popular for two main reasons. First, initial screening of fragment libraries is expected to sample the chemical space much more efficiently than traditional approaches ever could.²⁴ The second reason is that fragment-derived lead structures have significantly higher ligand efficiency (free binding energy per non-hydrogen atom of the ligand) than molecules discovered by screening of large compound libraries. An investigation of 150 known natural and synthetic ligands revealed that the free binding energy increased in proportion to ligand size up to a maximum of 15 atoms. The maximum average free-energy contribution per heavy atom was -1.5 kcal/mol. For molecules larger than this, no further increase in ligand efficiency was observed. These observations confirm how crucial limiting the molecular size is for the efficiency of protein ligands, thereby

supporting the preference of fragment hits (<12 heavy atoms per molecule) over typical HTS hits. These results also indicate easier optimization and hit-to-lead development of fragment hits relative to that of HTS hits.^{26,27a}

Many enzymes are known to possess multiple binding pockets; yet conventional inhibitor developments generally focus more on only the active site. However, in many cases, the secondary/allosteric binding sites confer selectivity as well as potency. Within this context, click chemistry, due to its highly modular and efficient reaction nature, has been identified as one of the most practical methods toward fragment-based inhibitor assembly where $N + M$ combinations of inhibitor fragments lead to the generation of $N \times M$ potential bidentate inhibitors (Figure 2). Because of the efficiency and water compatible nature of the click reaction, in most cases, the assembled products could be directly screened for inhibition without the need for any purification.^{27b}

3.1.3. Dynamic Template-Assisted Strategies in Fragment-Based Drug Discovery. The major challenges of

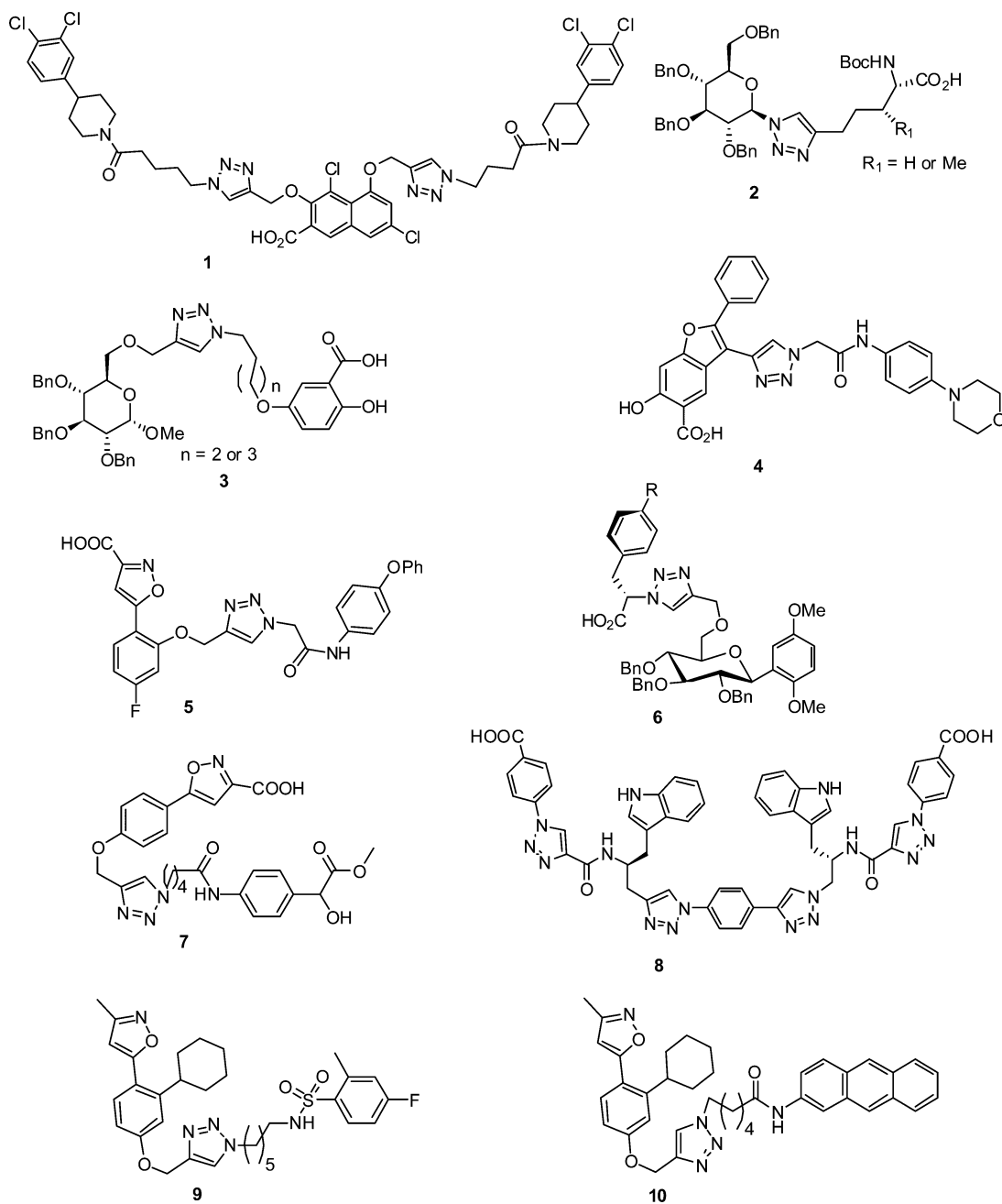


Figure 3. Chemical structures of protein tyrosine phosphatase inhibitors synthesized via click chemistry.

fragment-based drug discovery are the identification of low-affinity fragments and efficient biologically active linkage of the fragments identified. Weakly binding ligands are difficult to detect. To address this problem, alternative so-called dynamic and template-assisted strategies have been proposed for fragment-based drug discovery by researchers. All of these methods use a target protein as a template for selection and/or assembly of optimal fragment combinations. All dynamic template-assisted approaches covered here have in common a chemical reaction (reversible or irreversible, enzymatic or nonenzymatic), which is exploited for detection of the best fragment combination (Figure 2).²⁸

For example, the azide and alkyne reagents are structurally selected to partially interact with the enzymatic binding site. Thus, fragments that interact favorably with the enzyme are selected, and the 1,3-dipolar cycloaddition “click” reaction

connects the fragments to form the final inhibitor. FBDD and TGS both have in common the fact that they capitalize on molecular recognition patterns imprinted on molecular targets to select suitable molecular fragments “ex vivo”, which are then tethered through synthetic optimization (FBDD) or in situ self-assembling to form the final ligands. These ligands can then be resynthesized and scaled up for subsequent biological evaluations through the drug development stages (i.e., in vivo animal models and clinical development). However, when considering Rideout’s ideas and recent developments in TGS together, one could shift this paradigm of fragment-based approaches a step forward toward the use of molecular fragments for direct clinical use (Figure 2). The approach would allow for the in vivo–in situ synthesis of the final ligand already in close proximity to its biological target (protein or DNA) in the host. This innovative research envisages a gene/

protein-specific pharmaceutical composition, which contains the encoded combination of bioorthogonally fragmented prodrugs (two or more than two) to be simultaneously or sequentially administered for in vivo self-assembling of the drug through a synergetic target-driven mechanism.²⁹ As a consequence, highly desirable pharmacological properties associated with low molecular weight drugs could be maintained, while biodistribution problems related to large molecules could be minimized at the plasma level for an optimal clinical application. Another potential benefit could be evasion of drug resistance mechanisms associated with host recognition/metabolization of nonfragmented drugs. In the context of cancer, formation of the final drug only at close proximity of its biological targeted can lead to amplification of selectivity between neoplastic and normal cells. Thus, it is foreseeable that in the future, purposely prepared pharmaceutical compositions of closely related but different fragmented prodrugs could be designed with the help of the click chemistry precursor to synergistically interact with specific molecular targets that have different isoforms (i.e., proteins) or polymorphism (i.e., genes) within patients, paving the way for personalized prodrugs. The template-assisted syn-triazole formation was a more effective inhibitor than that antitriazole for many enzymes using in situ click chemistry.⁵ This is a valuable aspect associated with the uniqueness of molecular scaffolds constructed from fragment-based approaches that could not only be maintained but also applied to current drugs that could be retrosynthetically fragmented, thus creating an attractive setting from the intellectual property standpoint.³⁰

3.2. Synthetic Utility of Click Chemistry in the Development of Enzyme Inhibitors

Enzymes are an integral part of biological systems. They constitute a significant majority of all proteins expressed at an estimated 18–29% within eukaryotic genomes. It thus comes as no major surprise that enzymes have been implicated in many diseases and form the second largest group of drug targets, after receptors. Despite their involvement in a multitude of physiological processes, only a limited number of enzymes have thus far been well-characterized. Consequently, little is understood about the physiological roles, substrate specificity, and downstream targets of the vast majority of these important proteins. Enzyme inhibitors play a significant role in curing diseases, and they are drug targets for many diseases like cancer, tuberculosis, and many incurable diseases.³¹ Within this context, click chemistry, due to its highly modular and efficient reaction nature, has been identified as one of the most practical methods toward fragment-based enzyme inhibitor development. Using fragment pro-inhibitor library screening and click chemistry reaction, researchers developed a large class library of efficient enzyme inhibitors of the following enzymes. Because of the efficiency and water compatible nature of the click reaction, in most cases, the assembled products could be directly screened for inhibition without the need of any purification.³²

3.2.1. Protein Tyrosine Phosphatase Inhibitors. Protein tyrosine phosphatases (PTPs, protein tyrosine phosphatase class enzyme) constitute an important class of signaling enzymes that catalyzes the dephosphorylation of phosphotyrosine residues in a protein substrate. Among them, PTP1B (protein tyrosine phosphatase 1B, nonreceptor phosphotyrosine PTP) has been identified as the major regulator of both insulin and leptin signaling pathways. Malfunctioning of

PTP1B leads to various human diseases like cancer, diabetes, obesity, and inflammation.³³

Zhang and co-workers prepared a highly potent and selective mPTPB inhibitor using a novel, double click chemistry strategy. The most potent mPTPB inhibitor (compound 1, Figure 3) from this approach possesses a K_i value of 160 nM and a >25-fold selectivity for mPTPB over 19 other protein tyrosine phosphatase inhibitors, and molecular docking study of the enzyme–inhibitor complex provides a rationale for the high potency and selectivity of the lead compound and reveals an unusual binding mode ($IC_{50} = 4.9 \mu\text{M}$ against PTP1B and $0.27 \mu\text{M}$ against mPTPB).³⁴

Xie et al. reported new PTP inhibitor entities by simply “clicking” alkynyl amino acids onto diverse azido sugar templates. Triazolyl glucosyl, galactosyl, and mannosyl serine and threonine derivatives were efficiently synthesized via click reaction, one of which (compound 2, Figure 3) was identified as a potent and selective PTP1B inhibitor against a panel of homologous PTPs with $IC_{50} = 5.9 \pm 0.4 \mu\text{M}$ for $R_1 = \text{H}$ against PTP1B and $IC_{50} = 7.1 \pm 1.0 \mu\text{M}$ for $R_1 = \text{Me}$ against PTP1B.³⁵

Tang and co-workers recently reported a library of benzyl 6-triazolo(hydroxy)benzoic glucosides via the Cu(I)-catalyzed azide–alkyne 1,3-dipolar cycloaddition. These glycoconjugates bearing alkyl chain, sugar, and (hydroxy)-benzoic derivatives (compound 3, Figure 3) ($IC_{50} = 8.7 \pm 1.4 \mu\text{M}$ for $n = 2$ and $IC_{50} = 6.7 \pm 0.5 \mu\text{M}$ for $n = 3$) were identified as new PTP1B inhibitors with selectivity over T-Cell PTP (TCPTP), SH2-containing PTP-1 (SHP-1), SHP-2, and leukocyte antigen-related tyrosine phosphatase (LAR).³⁶

Zhou and co-workers recently reported a potent and selective mPTPB inhibitor (compound 4, Figure 3) with highly efficacious cellular activity, from a combinatorial library of bidentate benzofuran salicylic acid derivatives assembled by click chemistry. The inhibition of mPTPB with compound (4) in macrophages reversed the altered host immune responses induced by the bacterial phosphatase and prevents TB growth in host cells with $IC_{50} = 19 \pm 1.5 \mu\text{M}$ against PTP1B, $1.6 \pm 0.22 \mu\text{M}$ against mPTPB, and $77.3 \pm 1.5 \mu\text{M}$ against mPTPA.³⁷

Yao et al. reported a solid-phase reaction strategy for high-throughput synthesis of a 96-member azide library. A 384-member PTP inhibitor library was synthesized by clicking the azide library with an alkyne-modified isoxazole warhead. The entire operation was performed in 96/384-well plates without any purification. From a homologous series of bidentate inhibitors (compound 5, Figure 3) was identified a most potent inhibitor of PTP1B with an IC_{50} of $11.1 \mu\text{M}$.³⁸

Triazole-linked phenylalanine and tyrosine-aryl C-glycoside hybrids were synthesized via microwave-assisted click reaction in high yields. The successive PTP1B biological assay found from the glycoconjugates that contain carboxylic acid and benzyl moieties as more active PTP1B inhibitors (compound 6, Figure 3) is the most potentially successive specific PTP1B inhibitor, which possess at least several-fold selectivity over other homologous PTPs tested with $IC_{50} = 5.6 \mu\text{M}$ for $R = \text{H}$ against PTP1B and $IC_{50} = 5.5 \mu\text{M}$ for $R = \text{OH}$ against PTP1B.³⁹

Yao and co-workers reported the design and synthesis of a small library of protein tyrosine phosphatase (PTP) inhibitors, via click chemistry from alkyne–azide coupling of 66 different bidentate compounds. Subsequent in situ enzymatic screening revealed a potential PTP1B inhibitor (compound 7, Figure 3), which was 10–100-fold more potent ($IC_{50} = 4.7 \mu\text{M}$) than other PTPs.⁴⁰

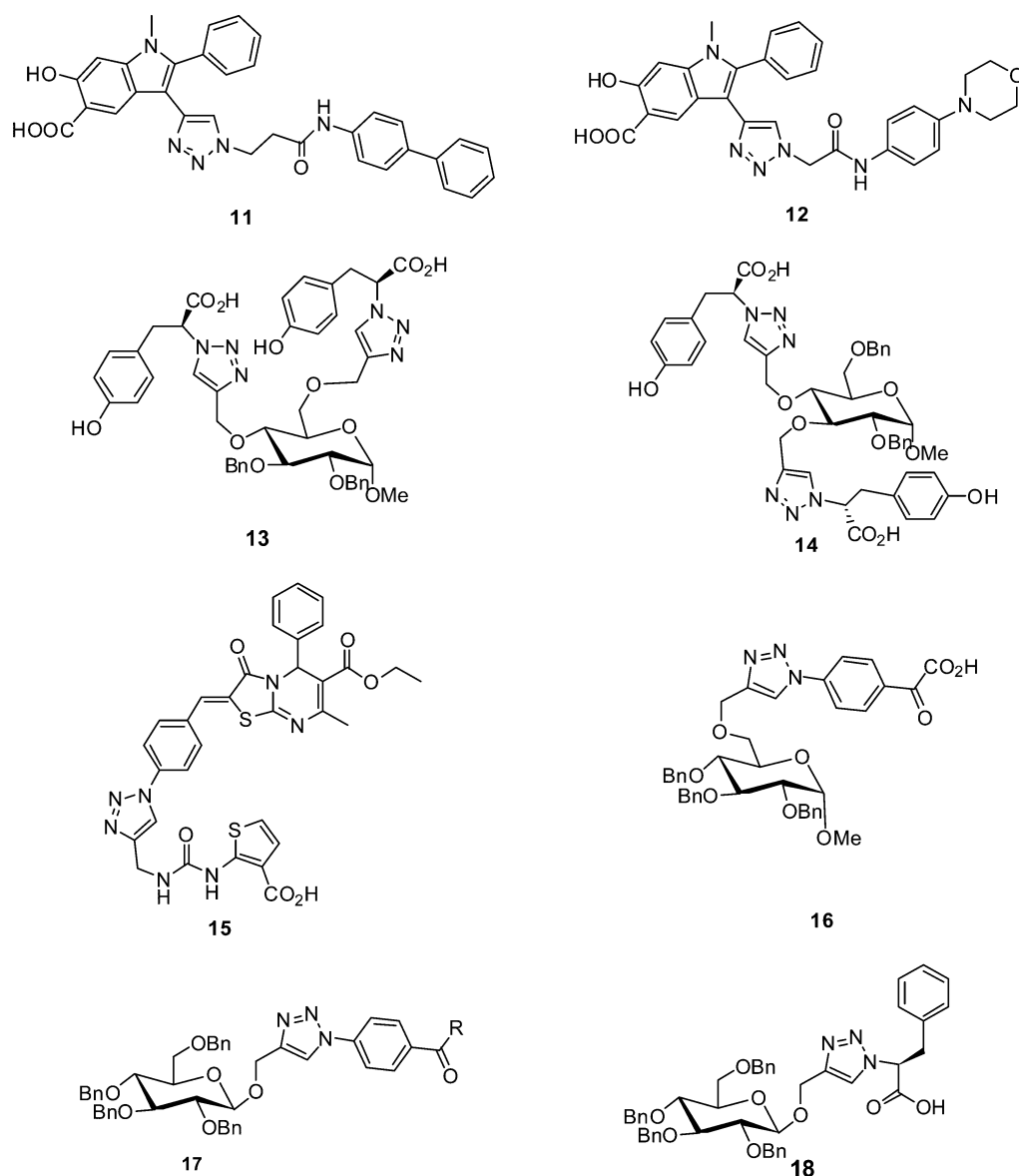


Figure 4. Chemical structures of protein tyrosine phosphatase inhibitors synthesized via click chemistry.

Cu(I)-catalyzed “click” cycloaddition reactions were employed to generate two sequential libraries of PTP inhibitors by Seto et al. In the first stage of the library synthesis, the researchers clicked an azide-functionalized ketocarboxylic acid with 56 different alkynes. The hit identified from this first library was further modified to incorporate an azide functionality and used for the second step click conjugation with the library of 56 alkynes. Subsequent inhibitor screening revealed a potent inhibitor (compound 8, Figure 3), with IC_{50} values of 550 nM against *Yersinia* PTP and 710 nM against TC-PTP.⁴¹

Solid-phase reaction for high-throughput synthesis of a 67-member azide library was done for the development for PTP inhibitor by Yao and co-workers. A 325-member PTP inhibitor library was synthesized by clicking the azide library with an alkyne-modified isoxazole. A triazole library of potential bidentate inhibitors was developed against PTPs using the azide library and several different alkyne warheads. Subsequent high-throughput inhibition assays led to the discovery of highly potent and selective inhibitors of *Mycobacterium tuberculosis*

tyrosine phosphatase (MtpB), and compounds 9 and 10 (Figure 3) were identified as the most potent MtpB inhibitors with $K_i = 150$ and 170 nM.⁴²

Zhang and co-workers reported a salicylic acid derivative-based combinatorial library approach designed to target both the PTP active site and a unique nearby subpocket for enhanced affinity and selectivity. Screening of the library led to the identification of SHP2 inhibitors (compounds 11 and 12, Figure 4) with highly efficacious cellular activity with $IC_{50} = 5.5 \pm 0.4$ and $7.8 \pm 0.8 \mu\text{M}$. Compound 11 blocked growth factor stimulated ERK1/2 activation and hematopoietic progenitor proliferation, providing supporting evidence that chemical inhibition of SHP2 might be therapeutically useful for anticancer and antileukemia treatment.⁴³

Protein tyrosine phosphatase 1B (PTP1B) inhibitors under development are used in the treatment of type 2 diabetes, obesity, and breast cancer. Chen et al. explored click chemistry for the identification of a series of mono- and bis-phenylalaninyl and tyrosinyl glucoside derivatives as novel PTP1B inhibitors. The designed compounds bearing one or two phenylalanine or

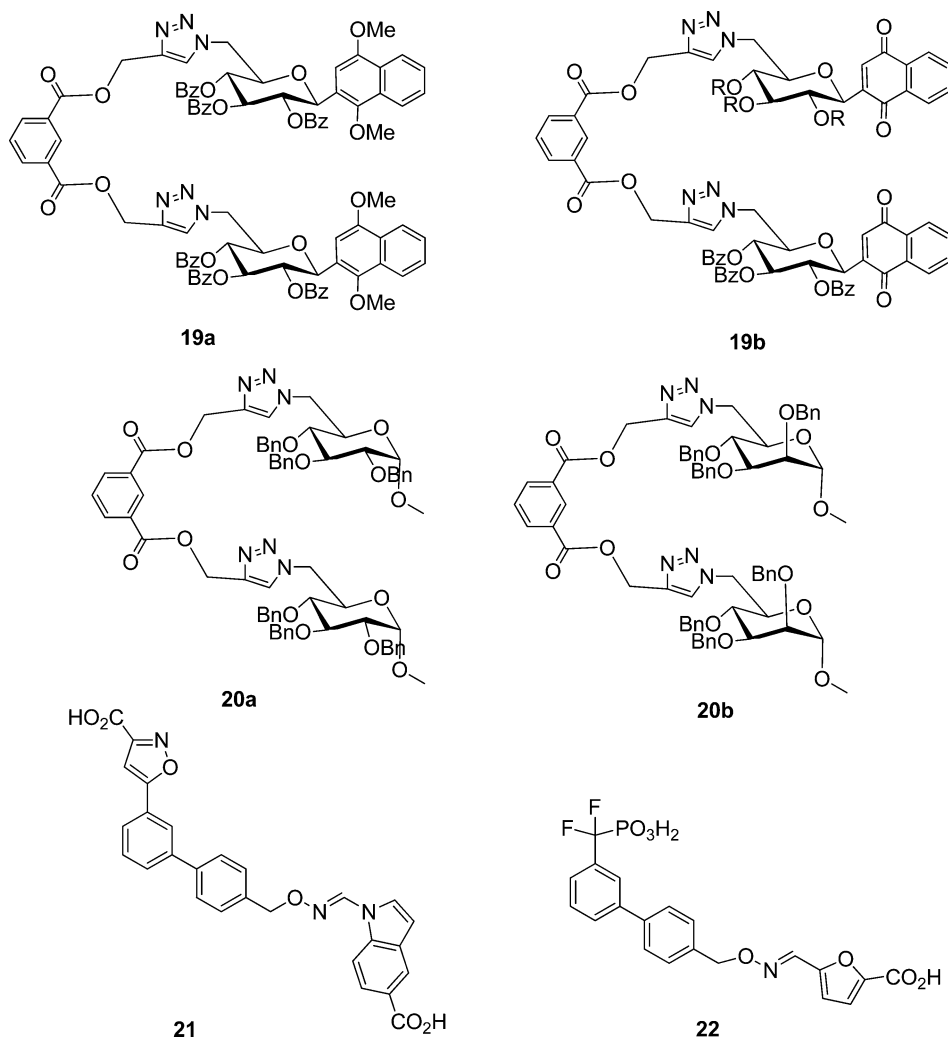


Figure 5. Chemical structures of protein tyrosine phosphatase inhibitors synthesized via click chemistry.

tyrosine derivatives on the 6-, 2,3-, 2,6-, 3,4-, and 4,6-positions of the glucosyl scaffolds were efficiently constructed via the microwave-assisted Cu(I)-catalyzed azide–alkyne cycloaddition in moderate-to-excellent yields. Successive biological assays identified these compounds as novel PTP1B inhibitors, with the 4,6-disubstituted tyrosinyl glucoside being the most potent. A kinetic study established that both mono- and bis-triazole-linked glycosyl acids act as typical competitive inhibitors, whereas the bis-triazolyl ester that also exhibited inhibitory activity on PTP1B displayed a mixed-type inhibition pattern. Compounds **13** and **14** (Figure 4) showed most potent activity against PTP1B in the series with $K_i = 14.4 \mu\text{M}$ against PTP1B and $8.7 \mu\text{M}$ against PTP1B. Also, compound **14** (Figure 4) was effective against TCPTP (T cell protein tyrosine phosphatase) inhibition with $\text{IC}_{50} = 31.0 \pm 9.6 \mu\text{M}$.⁴⁴

Cell division cycle 25 (CDC25) phosphatases regulate key transitions between cell cycle phases during normal cell division, and in the event of DNA damage they are key targets of the checkpoint machinery that ensures genetic stability. Duval et al. reported click chemistry for the rapid synthesis of novel CDC25 phosphatase inhibitors. Triazolobenzylidene-thiazolopyrimidine (TBTP) azide derivative and various substituted alkynes were used for the generation of an 87-member triazole library with good to quantitative yields and high purities. The biological screening results showed that

compound **15** (Figure 4) was the most potent inhibitor of CDC25B when compared to other synthesized TBTP triazole derivatives with $\text{IC}_{50} = 3.0 \pm 0.1 \mu\text{M}$.⁴⁵

The synthesis of glycoconjugates of the triazolyl α -ketocarboxylic acids derivatives was achieved via Cu(I)-catalyzed azide–alkyne cycloaddition from O-propargyl glycoconjugate sugars and various diversely substituted azides. The glycosyl α -ketocarboxylic acid derivatives (compounds **16** and **17**, Figure 4) were identified as promising sugar-based PTP1B inhibitors for several fold selectivities over a panel of homologous PTPs with $\text{IC}_{50} = 3.2 \mu\text{M}$ for compound **16**, $\text{IC}_{50} = 11.1 \mu\text{M}$ when R = OH, and $\text{IC}_{50} = 5.6 \mu\text{M}$ when R = CO₂H for compound **17**.⁴⁶

Yang et al. employed a microwave-accelerated Cu(I)-catalyzed azide–alkyne 1,3-dipolar cycloaddition for the preparation of a series of triazole-linked serinyl, threoninyl, phenylalaninyl, and tyrosinyl 1-O-gluco- or galactosides with high yield of products within only 30 min. Successive biological assay identified these glycopeptidotriazoles as favorable PTP1B and CDC25B inhibitors with selectivity over TCPTP (T-cell protein tyrosine phosphatase), LAR (leukocyte antigen-related PTP receptor), SHP-1 (Src homology region 2 domain containing phosphatase-1), and SHP-2 (Src homology region 2 containing a ubiquitously expressed tyrosine-specific protein phosphatase), which upon subsequent screening revealed

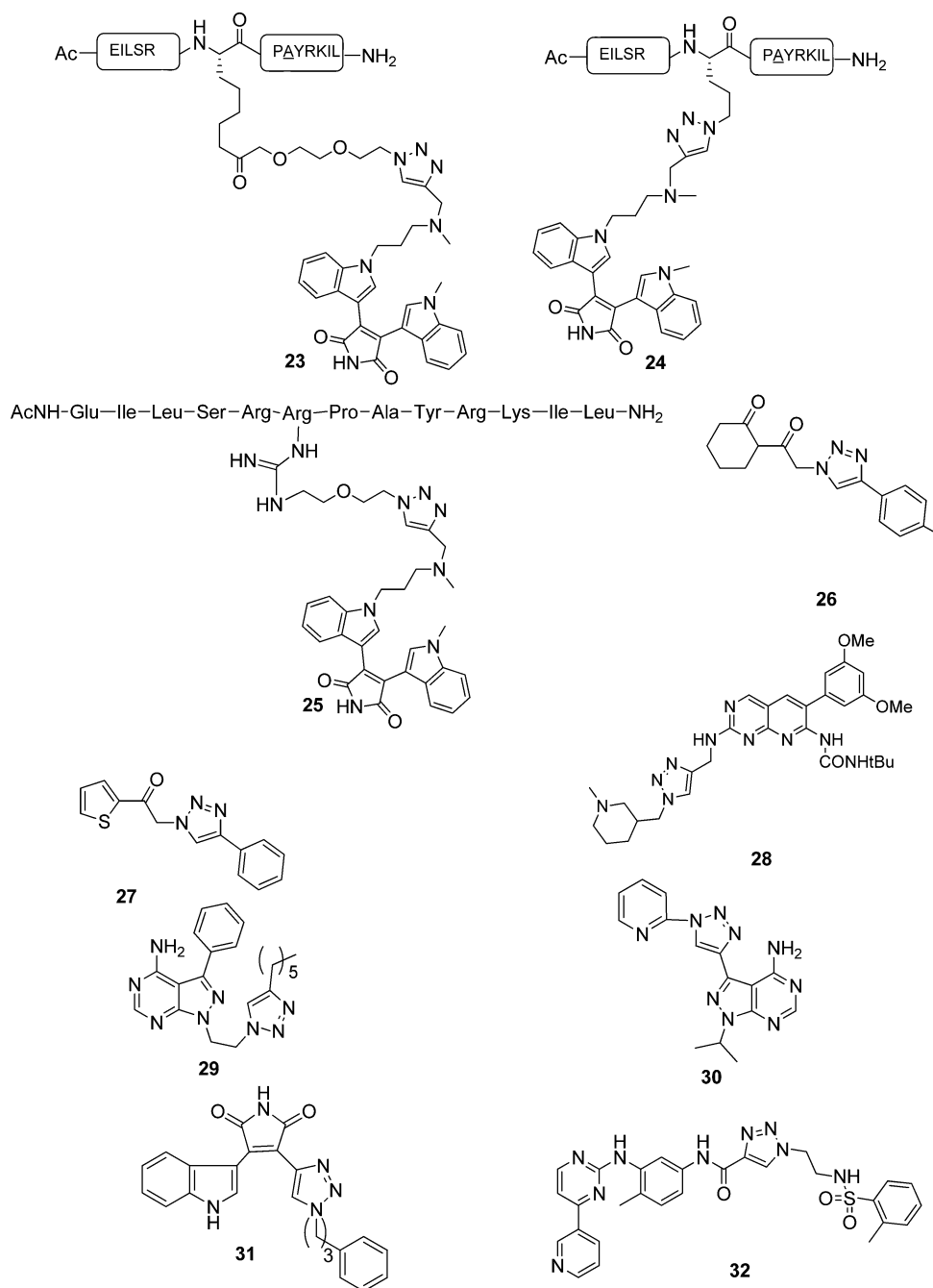


Figure 6. Chemical structures of protein kinases inhibitors synthesized via click chemistry.

compound **18** (Figure 4) as a selective and potent inhibitor of PTP1B over other PTPs tested with $IC_{50} = 5.1 \mu M$.⁴⁷

Xie et al. successfully synthesized dimeric acetylated and benzoylated β -C-D-glucosyl and β -C-D-galactosyl 1,4-dimethoxy benzenes or naphthalenes by click chemistry. These compounds were further transformed into the corresponding β -C-D-glycosyl-1,4-quinone derivatives by CAN oxidation. The in vitro inhibition test of these compounds showed that dimeric benzoylated β -C-D-glycosyl 1,4-dimethoxybenzenes (compound **19a**, Figure 4) or 1,4-benzoquinones (compound **19b**, Figure 4) were good inhibitors of PTP1B ($IC_{50} = 0.62$ – $0.88 \mu M$), with no significant difference between gluco and galacto derivatives.⁴⁸

Monomeric and dimeric benzylated glycosyl benzenes were synthesized via copper-catalyzed [3 + 2] azidealkyne cyclo-

addition. These compounds were then identified as protein tyrosine phosphatase (PTP) 1B inhibitors, which displayed at several fold selectivity over other homologous PTP inhibitors. The triazolyl glycosyl dimers of compounds **20a** and **20b** (Figure 4) showed significant inhibition activity against PTP1B and a panel of homologous PTPs including TCPTP (T-cell protein tyrosine phosphatase) with IC_{50} values of 1.5 ± 0.1 and $5.2 \pm 0.3 \mu M$, respectively.⁴⁹

Burke and his co-workers employed oxime-based click chemistry for the development of 3-isoxazolecarboxylic acid derivative-based inhibitors of *Yersinia pestis* protein tyrosine phosphatase (YopH). The 3-isoxazolecarboxylic acid derivative of compound **21** (Figure 5) showed good inhibition against YopH among homologue series using oxime-based library diversification with $IC_{50} = 3.1 \pm 0.2 \mu M$.⁵⁰

The Gram-negative enterobacterium *Yersinia pestis* (*Y. pestis*) has played an important role in human history as the causative agent of plague, and more recently, it has gained attention because of its possible use as a biological warfare agent. For pathogenicity, *Y. pestis* requires the virulence factor *Yersinia pestis* outer proteinH “YopH”, a highly active PTP. Accordingly, potent and selective YopH inhibitors could provide a basis for new antiplague therapeutics. Burke and co-workers again explored oxime-based click chemistry for the synthesis of a library of nitrophenylphosphate derivatives for generating an inhibitor lead against the *Yersinia pestis* outer protein phosphatase (YopH).⁵⁰ A high activity substrate (*p*-nitrophenylphosphate) identified by this method was converted from a substrate into an inhibitor by replacement of its phosphate group with difluoromethyl phosphonic acid and by attachment of an aminoxy handle for further structural optimization by oxime ligation. A cocrystal structure of this aminoxy-containing platform in complex with YopH allowed the identification of a conserved water molecule proximal to the aminoxy group that was subsequently employed for the design of furanyl-based oxime derivatives. By this process, a potent ($IC_{50} = 190$ nM) and nonpromiscuous inhibitor (compound 22, Figure 5) was developed with good YopH selectivity relative to a panel of phosphatases.^{51c}

3.2.2. Protein Kinase Inhibitors. Protein kinases are key regulators of cell function that constitute one of the largest and most functionally diverse gene families. Kinases are widely recognized as important drug targets involved in many serious diseases, such as cancer and diabetes. Protein kinase phosphorylating enzymes play a pivotal role in cellular signal transduction, and many diseases are characterized by abnormalities in a kinase or its expression level. Protein kinases (PK) are a family of enzymes that are involved in controlling the function of other proteins through the phosphorylation of hydroxyl groups of serine and threonine amino acid residues on these proteins. PK enzymes in turn are activated by signals such as increases in the concentration of diacylglycerol or Ca^{2+} . Hence, PK enzymes play important roles in several signal transduction cascades. Hence, a significant portion of drug discovery efforts has made protein kinases as primary targets.⁵²

Liskamp and co-workers employed bisubstrate-based kinase inhibitors that target the more selective peptide-binding site in addition to the ATP-binding site. Dynamic peptide microarrays were used to find peptide binding site PKa inhibitors. These active binding peptides were linked with chemo-selective click chemistry to an ATP-binding site kinase inhibitor, and this led to novel bisubstrate structures. The most promising potent inhibitors (compounds 23 and 24, Figure 6) had nanomolar affinity and selectivity toward PKC_{α} and PKC_{teta} among three isozymes. Compound 23 showed $IC_{50} = 1.0 \pm 0.2$ μM against PKC_{α} and $IC_{50} = 0.6 \pm 0.1$ μM against PKC_{teta} . On the other hand, compound 24 showed $IC_{50} = 0.43 \pm 0.03$ μM against PKC_{teta} .⁵³

Liskamp et al. employed click chemistry for the synthesis of bisubstrate-based kinase inhibitors using arginine residues featuring acetylene or azide moieties in their side chain. Developed bisubstrate-based kinase inhibitor was tested for affinity and selectivity toward three highly homologous PKC isozymes. The resulting inhibitor (compound 25, Figure 6) showed improved affinity and a highly interesting shift in selectivity toward PKC_{teta} with $IC_{50} = 0.17 \pm 0.029$ μM .⁵⁴

Kumar et al. recently synthesized two classes of 1,4-disubstituted 1,2,3-triazoles using one-pot reaction of α -

tosyloxy ketones/ α -halo ketones, sodium azide, and terminal alkynes in the presence of aqueous PEG (1:1, v/v) using click chemistry. 1,4-Disubstituted 1,2,3-triazoles (compounds 26 and 27, Figure 6) exhibited modest Src kinase inhibitory activity among the synthesized 1,2,3-triazoles with IC_{50} values in the range of 32.5 and 33.9 μM .⁵⁵

Merrer and co-workers reported a library of pyrido[2,3-*d*]pyrimidines as inhibitors of FGFR3 (fibroblast growth factor receptor 3) tyrosine kinase allowing possible interactions with an unexploited region of the ATP binding-site. This library was built-up with an efficient step of click chemistry giving easy access to triazole-based compounds bearing a large panel of substituents. Among the 27 analogues synthesized, more than one-half exhibited 55–89% inhibition of in vitro FGFR3 kinase activity at 2 μM , and one of the pyrido[2,3-*d*]pyrimidine derivatives (compound 28, Figure 6) was able to inhibit autophosphorylation of mutant FGFR3-K650 M in transfected HEK (human embryonic kidney) cells.⁵⁶

Kumar and co-workers recently reported that a series of two classes of 3-phenylpyrazolopyrimidine-1,2,3-triazole conjugates were synthesized using the click chemistry approach. All of these compounds were evaluated for inhibition of Src kinase and human ovarian adenocarcinoma (SK-Ov-3), breast carcinoma (MDA-MB-361), and colon adenocarcinoma (HT-29). Hexyl triazolyl-substituted 3-phenylpyrazolopyrimidine (compound 29, Figure 6) exhibited potent inhibition of Src kinase with an IC_{50} value of 5.6 μM .⁵⁷

Grötl and co-workers employed alkyne/azide-derivatized purine analogues to click to different aromatic azides/alkynes. These synthesized compounds tested against *Plasmodium falciparum* protein kinase 7 (*Pf*PK7) inhibitors and subsequent inhibition assays of the click-products revealed moderately potent inhibitor 30 (Figure 6) of *Pf*PK7 with $IC_{50} = 10$ μM .⁵⁸

Wang and his co-workers successfully synthesized bisaryl maleimide derivatives for natural kinase inhibitors using click chemistry as a synthetic tool. A novel kinase inhibitor (compound 31, Figure 6) with $IC_{50} = 0.10$ μM against GSK-3 β kinase, which targeted only three out of 124 human kinases, was identified, and docking studies revealed a π - π stacking interaction with the Phe67 at the P-loop of GSK-3 β kinase.^{59a}

Yao and co-workers reported the click chemistry technique to generate inhibitors of Abelson (Abl) tyrosine kinase. The researchers first generated a 344-member library of azides, and subsequent inhibition assays revealed a clear preference for short-chain azide scaffolds by the Abl kinase. From the inhibitor screening, the researchers identified compound 32, the most potent hit identified in the screening, shown in Figure 6 with moderate potency and 10–20-fold in selectivity for Abl as compared to other synthesized homologous series with $IC_{50} = 704$ nM.^{59b}

3.2.3. Transferase Inhibitors. Transferase is a large class of enzymes, which play a significant role in many biological processes. Transferase inhibitors are potential drug targets for many diseases like cancer, and many viral and bacterial infection diseases.^{60–62}

3.2.3.1. Glycosyltransferase Inhibitors. The glycosylation and deglycosylation process conducted by glycosyltransferases (GTs; EC 2.4.-) and glycoside hydrolase (GHs, carbohydrases, glycosidases; EC 3.2.1.-) is one series of the important biological processes in the post-translational modifications of protein(s) and lipid(s) functions that greatly influence various molecular recognitions including bacterial and viral infections, cell adhesion, inflammation, immune response, cellular differ-

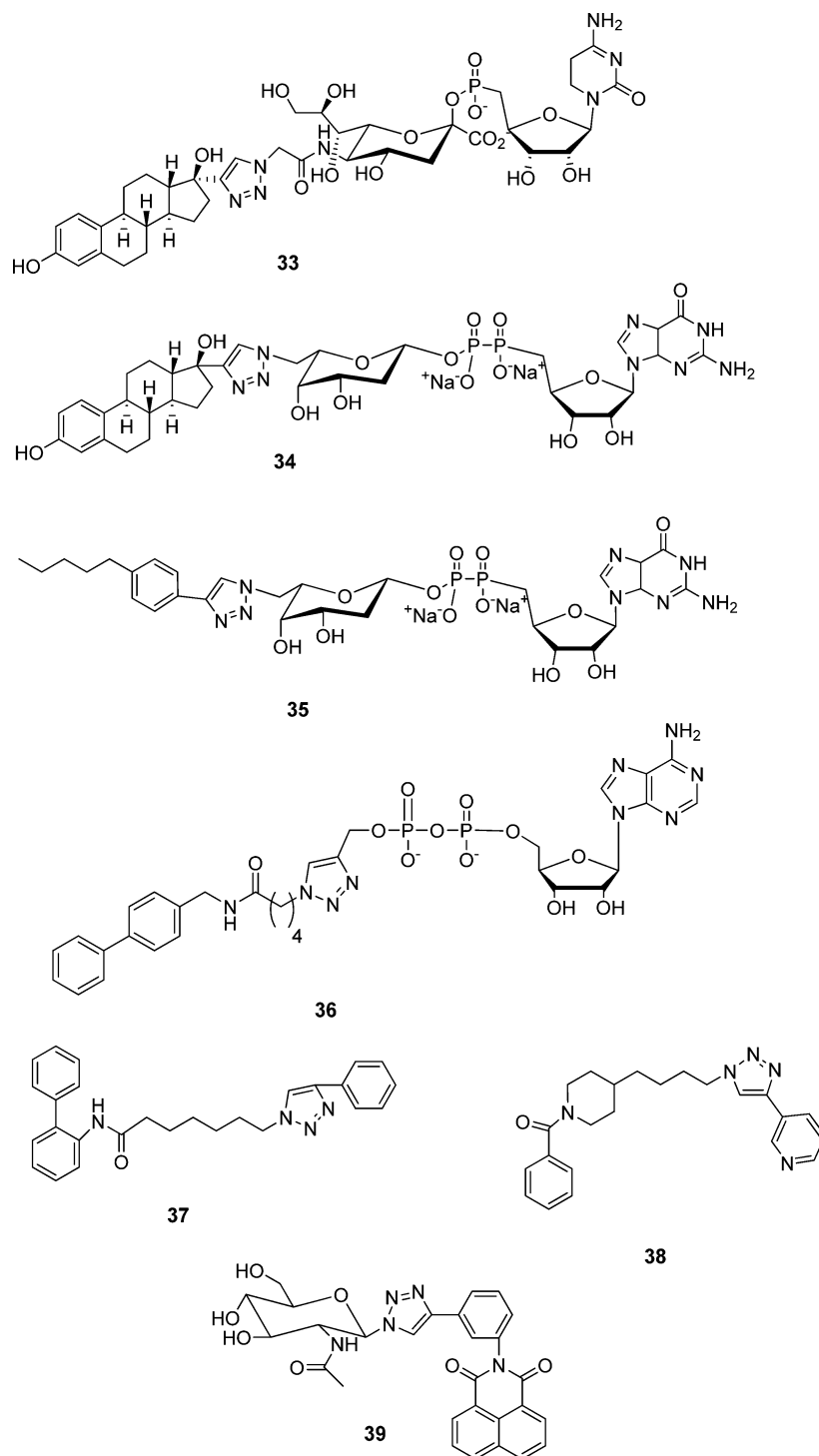


Figure 7. Chemical structures of transferase inhibitors synthesized via click chemistry.

entiation, development, regulation, and many other intercellular communication and signal transductions. Conversely, the biosynthesis of carbohydrates catalyzed by fucosyltransferases involves the transfer of an *L*-fucose moiety from guanosine diphosphate β -*L*-fucose (GDP-fucose) to a specific hydroxyl group of sialyl *N*-acetyl-lactosamine. Selective inhibitors of these enzymes might provide drugs by blocking the synthesis of glycosyl and fucosyl end-products, and the pathology they trigger.⁶⁰

Nishimura and co-workers identified potent and selective inhibitors of glycosyltransferases by high-throughput quantita-

tive MALDI-TOFMS-based screening of focused compound libraries constructed by 1,3-dipolar cycloaddition from the desired azidosugar nucleotides with various alkynes.⁶¹

A non-natural synthetic sugar nucleotide was identified to be the first highly specific inhibitor (compound 33, Figure 7) for rat recombinant α 2,3-(*N*)-sialyltransferase (α 2,3ST, $IC_{50} = 8.2 \mu M$), while this compound was proved to become a favorable substrate for rat recombinant α 2,6-(*N*)-sialyltransferase (α 2,6ST, $K_m = 125 \mu M$, where K_m is the kinetic parameter (Michaelis–Menten constant)). Versatility of this strategy was further demonstrated by identification of two selective

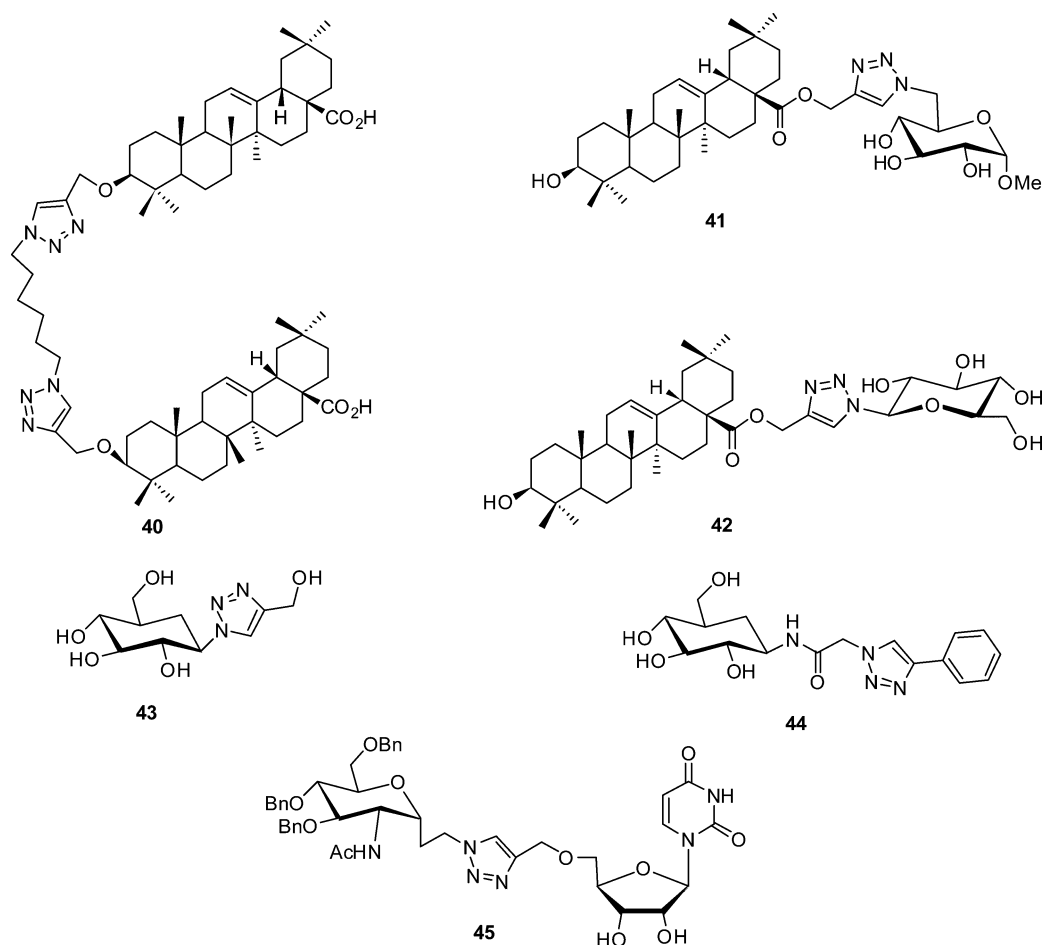


Figure 8. Chemical structures of glycogen phosphorylase inhibitors synthesized via click chemistry.

inhibitors (compounds 34 and 35, Figure 7) for human recombinant α 1,3-fucosyltransferase V (α 1,3-FucT, $K_i = 293$ nM) and α 1,6-fucosyltransferase VIII (R1,6-FucT, $K_i = 13.8$ μ M).⁶¹

Wong et al. reported a nanomolar α -1,3-fucosyltransferase inhibitor was prepared by linking a GDP-derived acetylene to a library of azides, using the copper(I)-catalyzed triazole formation. The excellent yields of the inhibitors and the absence of protecting groups allowed one to test 85 compounds that were rapidly prepared in water and screened straight from the reaction mixture. Hit follow-up, conducted on purified compounds against a panel of fucosyl and galactosyl transferases and kinases, revealed biphenyl derivative (compound 36, Figure 7) as the most potent inhibitor of human α -1,3-fucosyltransferase VI, and it was also revealed to be selective for this enzyme with $K_i = 62$ nM.⁶²

3.2.3.2. Nicotinamide Phosphoribosyltransferase Inhibitors. Interfering with NAD levels might lead to cell death of those cells that have a high usage rate of this pyridine nucleotide, that is, tumoral cells with a high division rate. Indeed, lowering NAD levels will not only hamper those enzymatic reactions that require this pyridine nucleotide as a cofactor but will also alter other cell signaling processes that have been shown to be involved in cancer. Eukaryotic cells possess several mechanisms to replenish NAD, including a de novo synthesis pathway from the amino acid tryptophan and at least two salvage/recycling pathways. One of these pathways relies on the enzyme nicotinamide phosphoribosyltransferase

(NMPRTase) that converts nicotinamide into nicotinamide mononucleotide (NMN) that is subsequently converted to NAD by NMN adenylyltransferase (NMNAT). NMPRTase is the target for the small molecule inhibitor FK866 (APO866) that has been shown to induce apoptosis in tumoral cells and in the same context to lower significantly NAD levels. Indeed, inhibition of this enzyme alone appears to have an important impact on NAD levels in a number of cell types. The inhibition of NAD synthesis or salvage pathways has been proposed as a novel target for antitumoral drugs.⁶³

Colombano et al. recently reported copper-catalyzed [3 + 2] cycloaddition between azides and alkynes to synthesize 185 novel analogues. The most promising compound 37 displayed an IC_{50} for cytotoxicity in vitro of 3.8 ± 0.3 nM and an IC_{50} for NAD depletion of 3.0 ± 0.4 nM. Compound 37 (Figure 7), which presents a 2-aminobiphenyl aromatic group, was the potential inhibitor of nicotinamide phosphoribosyl transferase.⁶³

Canonico et al. successfully constructed a small library of triazole analogues of antitumoral drug FK866 using click chemistry techniques. Among the synthesized triazole analogues, compound 38 (Figure 7) displayed nanomolar potency against depletion of NAD levels. The effect of compound 38 on NAD levels was also consistent with a cytotoxic effect, with an IC_{50} value of approximately 5.7 ± 1.3 nM and a reduction down to the detection limit at concentrations over 100 nm.⁶⁴

3.2.3.3. O-GlcNAcase Inhibitors. Glycosyl transferases are ubiquitous enzymes that catalyze the assembly of glycoconju-

gates throughout all kingdoms of nature. A long-standing problem is the rational design of probes that can be used to manipulate glycosyl transferase activity in cells and tissues. The human glycosyltransferase is responsible for the reversible post-translational modification of nucleocytoplasmic proteins with O-linked *N*-acetyl glucosamine residues (O-GlcNAc). Protein O-GlcNAcylation has been shown to play an important role in a number of biological processes, including regulation of the cell cycle, DNA transcription and translation, signal transduction, and protein degradation. O-GlcNAcase (OGA) is responsible for the removal of O-linked β -*N*-acetylglucosamine (OGlcNAc) from serine or threonine residues, and thus plays a key role in O-GlcNAc metabolism. Potent OGA inhibitors are useful tools for studying the cellular processes of O-GlcNAc and may be developed as drugs for the treatment neurodegenerative diseases.⁶⁵

Wang and his co-workers recently reported that Cu(I)-catalyzed “click” cycloaddition reactions between glycosyl azides and alkynes were exploited to generate inhibitory candidates of O-GlcNAcase. Enzymatic kinetic screening revealed that compound **39** (Figure 7) was a most potent competitive inhibitor of human OGA ($K_i = 185.6 \mu\text{M}$) among the screened compound series.⁶⁵

3.2.4. Glycogen Phosphorylase Inhibitors. Glycogen phosphorylase (GP), a key regulatory enzyme present in most mammals, catalyzes the phosphorolysis of glycogen main-chain, linked through an α -1,4-glucosidic bond, to glucose-1-phosphate (Glc-1-P) that is subsequently converted to α -D-glucose. In view of the pharmaceutical applications in improving glycaemic control in type 2 diabetes, the design of inhibitors of glycogen phosphorylase (GP) is a promising therapeutic strategy.⁶⁶

Recently, oleanolic acid was found to be an inhibitor of glycogen phosphorylase. Cheng et al. synthesized several dimers of oleanolic acid by using amide, ester, or triazole linkage with click chemistry. The synthesized oleanolic acid derivatives were screened against rabbit muscle glycogen phosphorylase. Among the synthesized homologous series of compounds, analogue **40** (Figure 8) was found to be the most potent inhibitor against rabbit muscle glycogen phosphorylase (RMGP), and displayed an IC_{50} value of $2.59 \mu\text{M}$.⁶⁶

Xie et al. reported the synthesis and biological evaluation of glucoconjugates of oleanolic acid, linked by either a triazole moiety or an ester function, as novel inhibitors of glycogen phosphorylase. Several synthesized triterpene–glycoside conjugates exhibited modest inhibitory activity against RMGP. Compound **41** (Figure 8) showed the good inhibition with an IC_{50} value of $1.14 \mu\text{M}$. Structure–activity relationship (SAR) analysis of these inhibitors was also discussed, and possible binding modes of compound **41** were explored by molecular docking simulations.⁶⁷

Propargyl esters of the C-28 carboxylic acids of pentacyclic triterpenes (oleanolic, ursolic, and maslinic acids) were coupled with 2,3,4,6-tetra-*O*-acetyl- β -D-glucopyranosyl azide as well as *N*-(ω -azido-[C-2, C-6, and C-11]alkanoyl)- β -D-glucopyranosylamines under conditions of copper(I)-catalyzed azide–alkyne cycloaddition (CuAAC) to give D-glucose–triterpene heteroconjugates. The newly synthesized compounds were assayed against RMGP a or b enzymes. The heteroconjugate derivative **42** (Figure 8) showed moderate inhibition against RMGP with $\text{IC}_{50} = 26 \mu\text{M}$.⁶⁸

Loganathan and his co-workers reported the crystallographic and computational studies on 4-phenyl-*N*-(β -D-glucopyrano-

syl)-1*H*-1,2,3-triazole-1-acetamide (**43**), an inhibitor of glycogen phosphorylase with $K_i = 17.9 \mu\text{M}$. Xie and his co-workers also employed click chemistry for the synthesis of novel nucleoside conjugates between uridine and *N*-acetylglucosamine or oleanolic acid derivatives.⁶⁹ Compound **44** (Figure 8) showed good inhibitory activity against glycogen phosphorylase with $\text{IC}_{50} = 13.6 \mu\text{M}$.⁷⁰

Chrysin and his co-workers reported that the reaction of per-*O*-acetylated β -D-glucopyranosyl azide and substituted acetylenes gave 1-(β -D-glucopyranosyl)-4-substituted-1,2,3-triazoles in Cu(I)-catalyzed azide–alkyne cycloadditions. Deprotection of these products by the Zemplén method furnished β -D-Glc_p-NHCO-R derivatives as well as 1-(β -D-Glc_p)-4-R-1,2,3-triazoles, which were evaluated as inhibitors of rabbit muscle glycogen phosphorylase b. Pairs of amides versus triazoles with the same R group displayed similar inhibition constants. Compound **45** (Figure 8) showed most potent against inhibition of rabbit muscle glycogen phosphorylase b when compared to newly synthesized compounds with $K_i = 13.7 \mu\text{M}$.⁷¹

3.2.5. Serine Hydrolase Inhibitors. Serine hydrolase is one of the largest and most diverse enzyme classes in eukaryotic and prokaryotic proteomes, with a membership that includes lipases, esterases, thioesterases, peptidases, proteases, and amidases. Mammalian serine hydrolases are nearly equally divided into two major subgroups of ~ 125 serine proteases, mostly from the chymotrypsin and trypsin class, and another ~ 110 “metabolic” enzymes, mostly from the α , β -hydrolase class (Pfam class assignment AB_hydrolase (CL0028)), that hydrolyze metabolites, peptides, or post-translational ester and thioester modifications on proteins. Because of the biological importance of serine hydrolases, clinically approved drugs target members of this enzyme class to treat diseases such as obesity, diabetes, microbial infections, and Alzheimer’s disease.⁷²

Cravatt et al. recently developed a click chemistry that generated triazole urea derivatives with ultra potent inhibition for serine hydrolase with in vivo activity. Rapid lead optimization by click chemistry-enabled synthesis and competitive activity-based profiling identified 1,2,3-triazole ureas that selectively inhibit enzymes from diverse branches of the serine hydrolase class, including peptidases (acyl-peptide hydrolase, or APEH), lipases (platelet-activating factor acetylhydrolase-2, or PAFAH2), and uncharacterized hydrolases (α , β -hydrolase-11, or ABHD11), with exceptional potency in cells (subnanomolar) and mice ($<1 \text{ mg kg}^{-1}$). APEH inhibition leads to accumulation of *N*-acetylated proteins and promotes proliferation in T cells. The triazole urea inhibitors **46**, **47**, and **48** (Figure 9) were highly potent inhibitors against their respective serine hydrolase targets in mouse T-cell proteomes, showing IC_{50} values of 5, 3, and 1 nM for APEH, PAFAH2, and ABHD11, respectively, in competitive gel-based ABPP assay. These data indicate 1,2,3-triazole ureas are a pharmacologically privileged chemotype for serine hydrolase inhibition, combining broad activity across the serine hydrolase class with tunable selectivity for individual enzymes.⁷²

3.2.6. Cysteine and Serine Protease Inhibitors. Many cysteine proteases are essential in regulation of physiological processes and disease propagation, and the proteases play important roles in treatment of cardiovascular diseases, oncology, osteoporosis, and arthritis. In plants also, cysteine proteases play an important role in the growth and development, in senescence and programmed cell death, and in

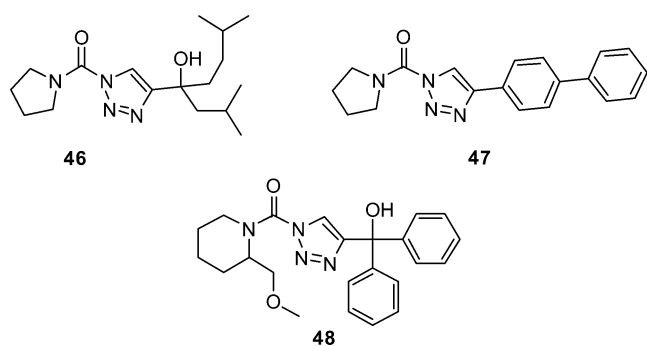


Figure 9. Chemical structures of serine hydrolase inhibitors synthesized via click chemistry.

accumulation and mobilization of storage proteins such as in seeds. In addition, they are involved in signaling pathways and in the response to biotic and abiotic stresses. In humans they are responsible for apoptosis, MHC class II immune responses, prohormone processing, and extracellular matrix remodeling important to bone development. The ability of macrophages and other cells to mobilize elastolytic cysteine proteases to their surfaces under specialized conditions may also lead to accelerated collagen and elastin degradation at sites of inflammation in diseases such as atherosclerosis and emphysema. Many researchers developed the inhibitors of cysteine protease for new drug discovery for the above diseases.^{73–75}

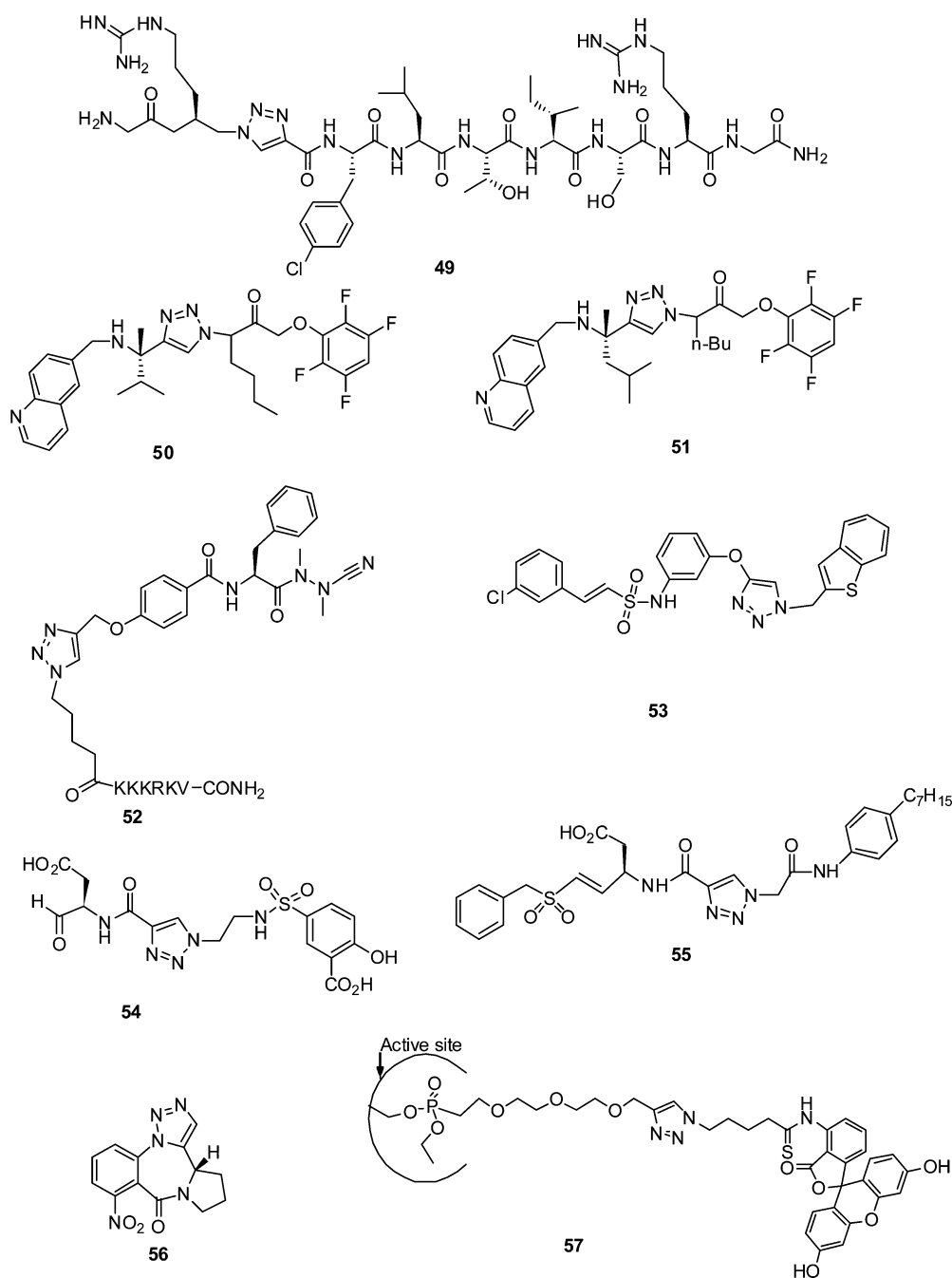


Figure 10. Chemical structures of serine and cysteine protease inhibitors synthesized via click chemistry.

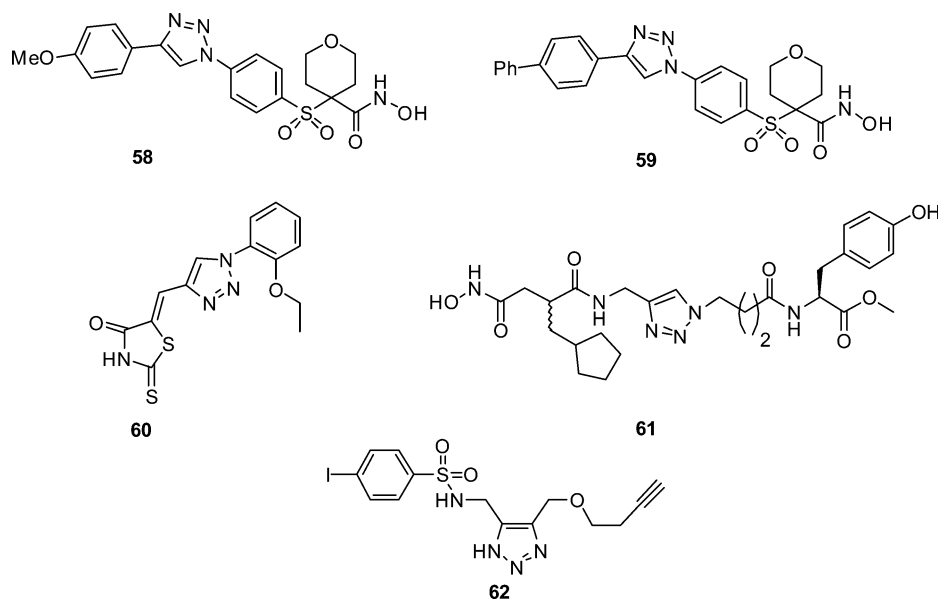


Figure 11. Chemical structures of metalloproteinase inhibitors generated via click chemistry.

A library consisting of about one-half of the 800 000 possible peptidotriazoles on 450 000 beads was prepared by solid-phase peptide synthesis combined with a regioselective copper(I)-catalyzed 1,3-dipolar cycloaddition between a resin-bound alkyne and a protected amino azide. The library was screened on solid phase for inhibitory effect against a recombinant cysteine protease, *Leishmania mexicana* CPB2.8cCTE, and sorted by a high-throughput instrument, COPAS beadsorter (up to 200 000 beads/h). Forty-eight hits were analyzed by MALDI-TOF MS providing structural information about the protease specificity, and **49** (Figure 10) peptidotriazoles were resynthesized and evaluated in solution, with the best inhibitor displaying a K_i value of 76 nM.⁷³

Trypanosoma cruzi parasite is the etiological agent of Chagas disease; treatment is still plagued by limited efficacy, toxicity, and the emergence of drug resistance. The development of inhibitors of the major *T. cruzi* cysteine protease, cruzain, demonstrated to be a promising drug discovery avenue for this neglected disease.^{74a,b} The 1,2,3-triazole-based tetrafluorophenoxymethyl ketone irreversible inhibitor **50** (Figure 10) was found to completely eradicate the *T. cruzi* parasite in cell culture with $IC_{50} = 5.1 \mu\text{M}$ and $K_i = 0.46 \pm 0.4 \mu\text{M}$. In addition to the nonpeptidic nature of inhibitor **50**, the tetrafluorophenoxymethyl ketone functionality represents a very promising mechanism-based pharmacophore due to its high selectivity for cysteine protease inhibition, as well as the lack of toxicity in animal studies, which was established for a tetrafluorophenoxymethyl ketone-based caspase inhibitor that has entered phase II clinical trials.^{74c}

Ellman and his co-workers recently employed click chemistry for the synthesis of 1,4-disubstituted-1,2,3-triazole cruzain inhibitor analogues from aryloxymethyl ketone azide and enantiomerically pure propargyl amine. 1,4-Disubstituted-1,2,3-triazole analogues were screened against *T. cruzi*-infected C3H mice, and tetrafluorophenoxymethyl ketone inhibitor **51** (Figure 10) was found to be the most potent inhibition against *T. cruzi* cysteine protease with $IC_{50} = 3.1 \mu\text{M}$ and $K_i = 0.10 \pm 0.03 \mu\text{M}$.⁷⁵

Yao et al. successfully developed a click chemistry strategy for the synthesis of small molecule inhibitor-peptide conjugates,

which were subsequently used for organelle-specific delivery of inhibitors into cancer cells. Biological testing showed that compound **52** (Figure 10) was successfully delivered to the lysosomes of HepG2 cells, where a greater inhibitory profile against cysteine cathepsins was observed with $IC_{50} = 9.1 \pm 1.1 \mu\text{M}$.⁷⁶

Freire and his co-workers recently reported a small library of 25 triazole/tetrazole-based sulfonamides had been synthesized and further evaluated for their inhibitory activity against thrombin, trypsin, trypsin, and chymase. The triazole-based sulfonamides inhibited thrombin more efficiently than the tetrazole counterparts. Particularly, compound **53** (Figure 10) showed strong thrombin inhibition ($K_i = 880 \text{ nM}$) and significant selectivity against other human-related serine proteases class enzymes such as trypsin ($K_i = 729 \mu\text{M}$).⁷⁷

Caspases are a class of cysteine proteases, which specifically cleave after the aspartic acid residue of protein substrates. As they are the enzymes responsible for apoptotic mode of cell death, inhibitors of caspases may have the potential to be developed into therapeutic agents for both acute cellular degenerative diseases as well as chronic neurodegenerative diseases.⁷⁸

Yao and co-workers employed click chemistry for high-throughput synthesis of caspase inhibitors containing aldehyde and vinyl sulfone warheads. A total of 198 caspase inhibitors were assembled by using click chemistry, and subsequent enzymatic screening with caspases 3 and 7 led to the identification of a moderately potent reversible inhibitor, **54** (Figure 10) ($IC_{50} = 4.67$ and $7.70 \mu\text{M}$ against caspases 3 and 7), and an irreversible vinyl sulfone-based inhibitor, **55** (Figure 10) ($IC_{50} = 5.0 \mu\text{M}$ against caspase 7), for caspases 3 and 7, respectively.⁷⁸

Mohapatra and co-workers reported one-pot synthesis of novel tetracyclic scaffolds that incorporate a fusion of a proline, 1,2,3-triazole ring with [1,4]-benzodiazepin-8(4H)-one ring systems following click chemistry. The new triazole fused benzodiazepine derivatives were screened for their efficacy as enzymatic protease inhibitors such as serine protease, cysteine protease, and aspartase protease. Compound **56** (Figure 10)

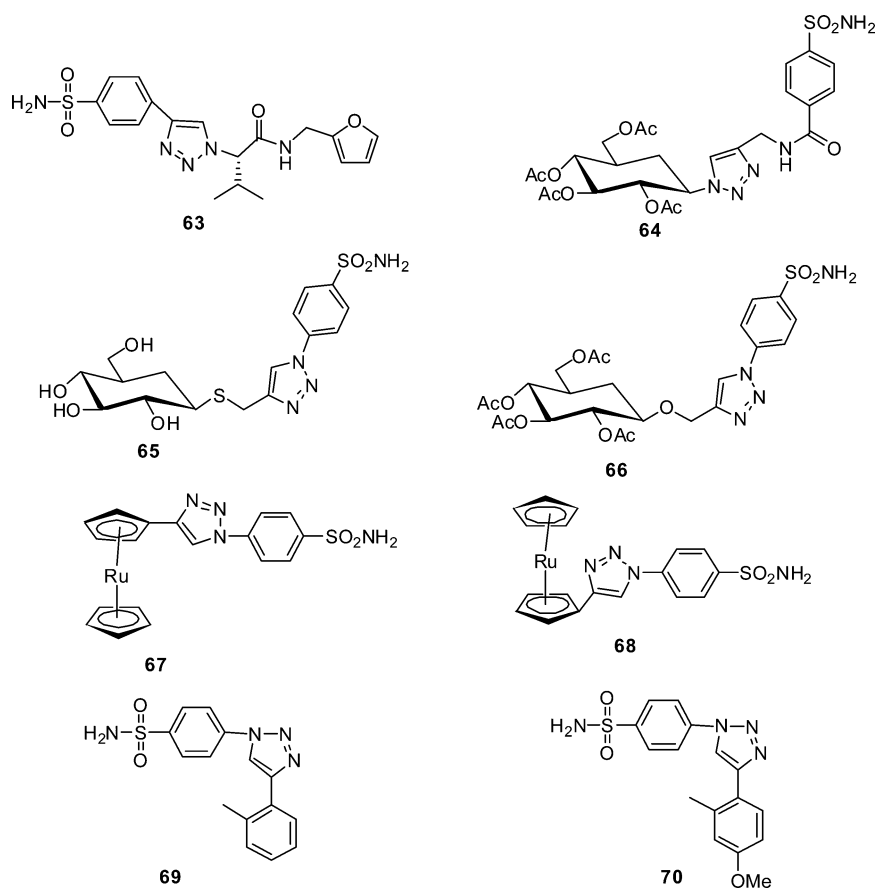


Figure 12. Chemical structures of carbonic anhydrase inhibitors explored via click chemistry.

showed good serine protease inhibition activity with $IC_{50} = 108.2 \mu M$.⁷⁹

Gil-Parrado and his co-worker developed the novel activity-based probe (ABP) for in-cell selectivity profiling of serine protease inhibitors. Probe **57** (Figure 10) was cell-permeable and achieved labeling of enzymes within living cells with efficiency similar to that observed for the corresponding lysate fraction with $IC_{50} = 4 \text{ nM}$ in cell and $IC_{50} = 14 \text{ nM}$ in lysate against serine protease. Several endogenous serine hydrolases whose activities were detected upon in-cell labeling were identified by two-dimensional gel and MS analyses. Cell-permeable inhibitors of an endogenous serine protease were assessed for their potency and specificity in competing for the in situ labeling of the selected enzyme.⁸⁰

3.2.7. Metalloproteinase Inhibitors. Matrix metalloproteinases (MMPs) are proteolytic enzymes that are involved in many physiological and pathological processes. The field of MMP research is very important due to the implications of the distinct paralogues in both human physiology and pathology. Overactivation of these enzymes results in tissue degradation, producing a wide array of disease processes such as rheumatoid arthritis, osteoarthritis, tumor growth and metastasis, multiple sclerosis, congestive heart failure, and others. Thus, MMP inhibitors are candidates for therapeutic agents to combat a number of diseases.^{81,82}

Ramos and his co-workers recently employed click chemistry for the synthesis of a new series of MMP2 (matrix metalloproteinase-2) inhibitors using fragment-based drug design approach. A click chemistry reaction was used to connect the azide to lipophilic alkynes selected to interact

selectively with the S1' subunit of MMP2. The most potent compounds **58** and **59** displayed an IC_{50} of 1.4 and 0.3 nM against MMP2, respectively, and showed negligible activity toward MMP1 (matrix metalloproteinase-1) and MMP7 (matrix metalloproteinase-7), two metalloproteinases that had a shallow S1' subsite. Compound **58** (Figure 11) also showed a promising selectivity profile against some antitarget metalloproteinases, such as MMP8 (matrix metalloproteinase-8), and considerably less activity against MMP14 (matrix metalloproteinase-14) ($IC_{50} = 65 \text{ nM}$) and MMP9 ($IC_{50} = 98 \text{ nM}$).⁸¹

Yao and co-workers reported a panel of 96 metalloprotease inhibitors assembled using click chemistry by reacting eight zinc-binding hydroxamate warheads with 12 azide building blocks. Screening of the bidentate compounds against representative metalloproteases provided discerning inhibition fingerprints, revealing compounds with low micromolar potency against MMP7. Compound **60** (Figure 11) inhibited MMP7 and MMP13 (matrix metalloproteinase-13) strongly with an IC_{50} value of 24 and 36 μM , respectively.⁸²

Forino and co-workers reported a small molecule MMP-click inhibitor library equipped with rhodanine as the zinc-binding scaffold. The inhibition assays revealed moderately potent inhibitors against MMP7 and MMP13 over other MMPs (compound **61**, Figure 11) ($IC_{50} = 6.5 \mu M$ against MMP7).⁸³

VIM-2 is an Ambler class B metallo- β -lactamase (MBL) capable of hydrolyzing a broad spectrum of β -lactam antibiotics. Hodder and his co-workers reported a compound library screening approach used to identify and characterize VIM-2 inhibitors from a library of pharmacologically active compounds as well as a focused "click" chemistry library. The four most

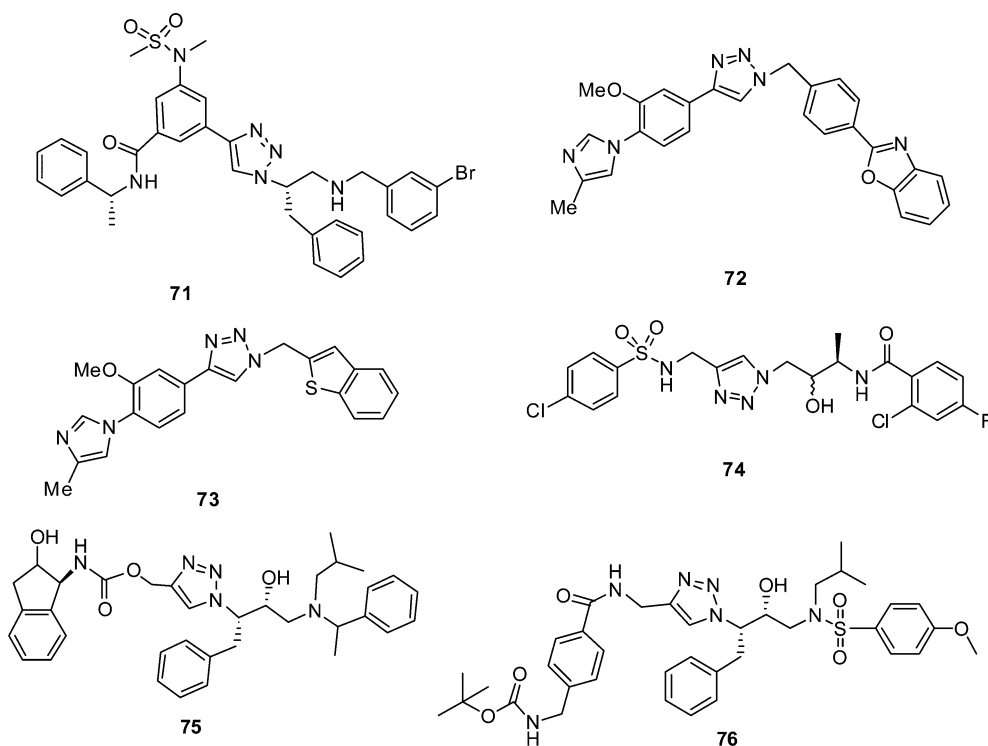


Figure 13. Chemical structures of aspartic protease inhibitors generated via click chemistry.

potent VIM-2 inhibitors resulting from a VIM-2 screen were characterized by kinetic studies to determine K_i and the mechanism of enzyme inhibition. Compound **62** (Figure 11) was found to be most potent inhibitor for VIM-2 with a reported $K_i = 0.41 \pm 0.03 \mu\text{M}$.⁸⁴

The zinc-containing enzymes carbonic anhydrases (CA) are very efficient catalysts for the reversible hydration of carbon dioxide to bicarbonate and hence play an important physiological role. Several of the 16 human isoforms are druggable targets considered as drug targets, and the design of selective inhibitors is a long-standing goal that has captured the attention of researchers for 40 years and has led to clinical applications against different pathologies such as glaucoma, epilepsy, and cancer. The clinical use of a highly active carbohydrate-based CA inhibitor, that is, topiramate, constitutes an interesting demonstration of the validity of this approach. Carbohydrate-based triazole compounds also demonstrate promising potential for the treatment of ophthalmologic diseases.⁸⁵

Aryl and heteroaryl sulfonamides (ArSO_2NH_2) are therapeutically used to inhibit the catalytic activity of carbonic anhydrases. Kolb and his co-workers employed click chemistry for the synthesis of carbonic anhydrase inhibitors using sulfonamide derivatives. Novel sulfonamide compounds were particularly active in inhibiting carbonic anhydrase (CA), and compound **63** (Figure 12) was identified as the most potent inhibitor of *hCA-II* and *hCA-IX* (h = human) with K_i values of 0.5 and 5.0 nM, respectively. These derivatives were useful for the development of *in vivo* positron emission tomography (PET) imaging agents for the diagnosis of diseases such as cancer.⁸⁵

Using a “click-tail” approach, a novel class of glycoconjugate benzene sulfonamides was synthesized that contains diverse carbohydrate–triazole tails. These compounds (**64–66**, Figure 12) were assessed for their ability to inhibit three human CA

isozymes *in vitro*: cytosolic *hCA-I*, *hCA-II*, *hCA-XII*, *hCA-XI*, and transmembrane, tumor-associated *hCA-IX* with $K_i = 4.3$ nM against alpha *hCA-XII* (**64**), $K_i = 7.0$ nM against alpha *hCA-I* (**65**), $K_i = 5.3$ nM against alpha *hCA-IIC* (**66**), and $K_i = 8.6$ nM against alpha *hCA-XI* (**66**). This isozyme was a minimal expression in normal tissue, but it was overexpressed in hypoxic tumors. The human CA isozymes’ inhibition is a current approach toward the development of a new drug in cancer therapies. The qualitative structure–activity for all derivatives demonstrated that the stereochemical diversity present within the carbohydrate tails effectively interrogated the CA active site topology, to generate several inhibitors that were potent and selective toward *hCA-IX*, an important outcome in the quest for potential cancer therapy applications based on CA inhibition.^{86–88}

A novel series of benzenesulfonamides that contain ferrocenyl or ruthenocenyl moieties were synthesized and investigated for their ability to inhibit the enzymatic activity of physiologically relevant carbonic anhydrase (CA) isozymes: *hCA-I*, *II* (h = human), and tumor-associated *IX*. These metallocene derivatives (**67,68**, Figure 12) were nanomolar inhibitors against *hCA-I*, *hCA-II*, and *hCA-IX* with inhibition in the range of 9.0–10.3 nM, respectively. Compound **67** showed $K_i = 9.0$ nM against alpha *hCA-I*, and compound **68** showed $K_i = 10.3$ nM against alpha *hCA-IX* and $K_i = 9.7$ nM against alpha *hCA-II*.⁸⁹

The mitochondrial membrane is impermeable to HCO_3^- . Mitochondrial CAs (isozymes VA and VB) provide HCO_3^- as substrate for the mitochondrial enzyme pyruvate carboxylase. Eventually, this biosynthetic pathway leads to the formation of citrate from pyruvate. Citrate is translocated from mitochondria to the cytoplasm, and through another biosynthetic pathway leads to *de novo* lipogenesis. A library of 10 novel benzenesulfonamides containing triazole-tethered phenyl “tail” moieties was synthesized by CuAAC (copper(I)-catalyzed

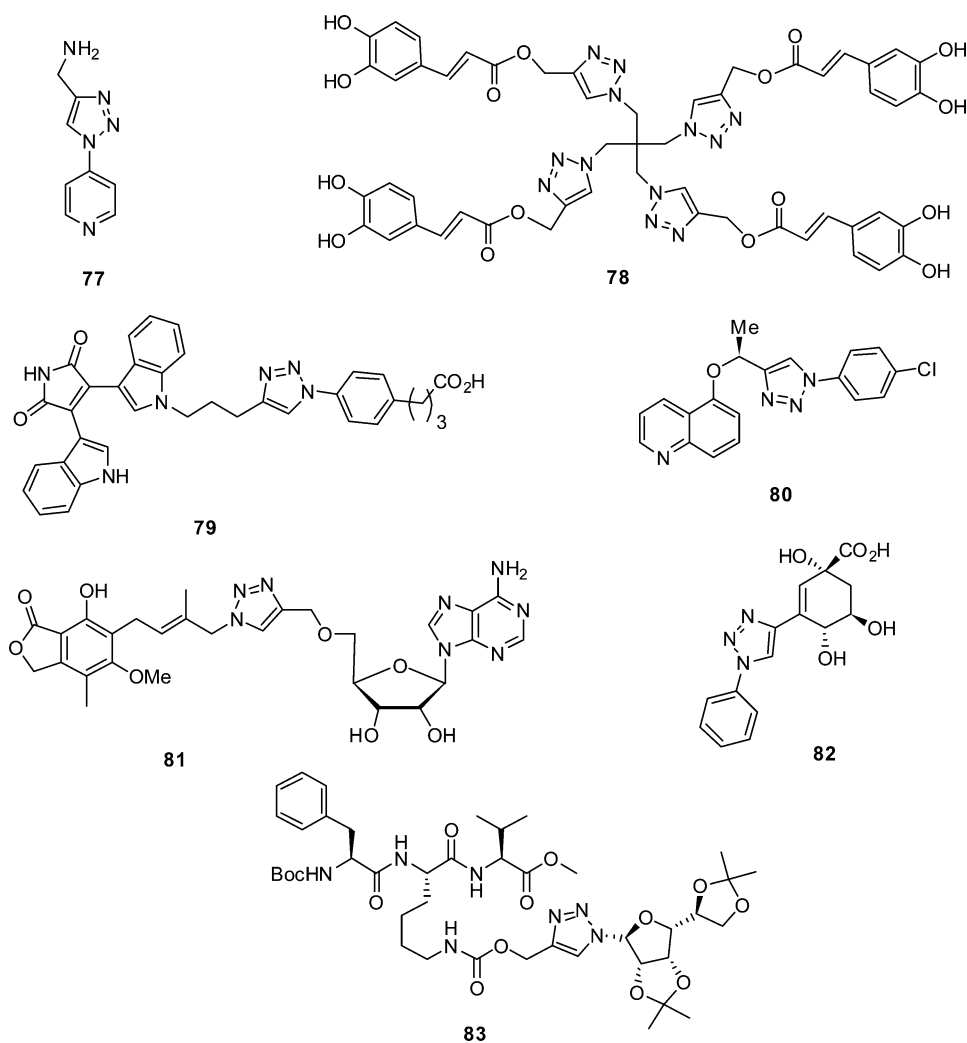


Figure 14. Chemical structures of oxidoreductase inhibitors synthesized via click chemistry.

azide–alkyne cycloadditions) reaction between 4-azido benzenesulfonamide and variously substituted phenyl acetylenes. These compounds (**69,70**, Figure 12) represent some of the first potent mitochondrial CAIs reported, and their inhibition profiles should prove valuable lead work in the discovery of isozyme selective CAIs targeting the mitochondrial CA isozymes with potential application as antiobesity agents.⁹⁰ Compound **69** showed $K_i = 7.7$ nM against alpha *hCA*-I and $K_i = 9.3$ nM against alpha *hCA*-VA. On the other hand, compound **70** showed $K_i = 10.5$ nM against alpha *hCA*-VB.

3.2.8. Aspartic Protease Inhibitors. Aspartic proteases constitute one of the major protease subclasses that share a common mechanism of catalysis. Aspartic proteases play important roles in several diseases such as AIDS (HIV protease), neoplastic disorders (cathepsin D and E), malaria (plasmepsins), and Alzheimer disease (β and γ secretase). Increased expression of human lysosomal cathepsin D is associated with a number of pathological conditions including neoplastic disorders and inflammatory diseases.^{91,92}

Carlier and his co-workers recently employed click chemistry for the preparation of β -site APP-cleaving enzyme 1 (BACE1) inhibitors from 120 reduced amide isostere inhibitors using a high-throughput in situ screening protocol. Compound **71** showed most potent inhibition of BACE1 when compared to the synthesized homologues with $IC_{50} = 2.0$ μ M.⁹¹

Fischer and his co-workers recently reported the synthesis, SAR, and evaluation of aryl triazoles as novel gamma secretase modulators (GSMs). 1,2,3-Caryl-triazoles were identified as a suitable replacement for gamma secretase modulators, which exhibited good modulation of γ -secretase activity, excellent pharmacokinetics, and good central lowering of A β 42 in Sprague–Dawley rats (Figure 13, compounds **72** and **73**) ($IC_{50} = 2.0$ μ M against A β 42 for compound **72**, $IC_{50} = 0.77$ μ M against A β 40 for compound **73**).⁹²

Yao and co-workers reported a click assembly of azido precursors of AfBPs of plasmepsins in malarial parasites with a library of aromatic azides, which led to the discovery of compound **74** (Figure 13), that showed good inhibition against all four PMs and parasite growth in infected RBCs with good membrane permeability and minimum cytotoxicity with $EC_{50} = 1.04$ μ M against aspartic protease.⁹³

Wong and co-workers employed click chemistry for the first time to generate inhibitors of HIV-1 protease. The researchers first synthesized two azides equipped with hydroxyethyl transition state analogues of aspartic proteases and subsequently click chemistry with a library of alkynes. Subsequent in situ screening in a microplate format revealed two potent inhibitors **75** and **76**, of HIV-1 protease (Figure 13) with $K_i = 1.7$ and 4.5 nM, respectively.^{94,95}

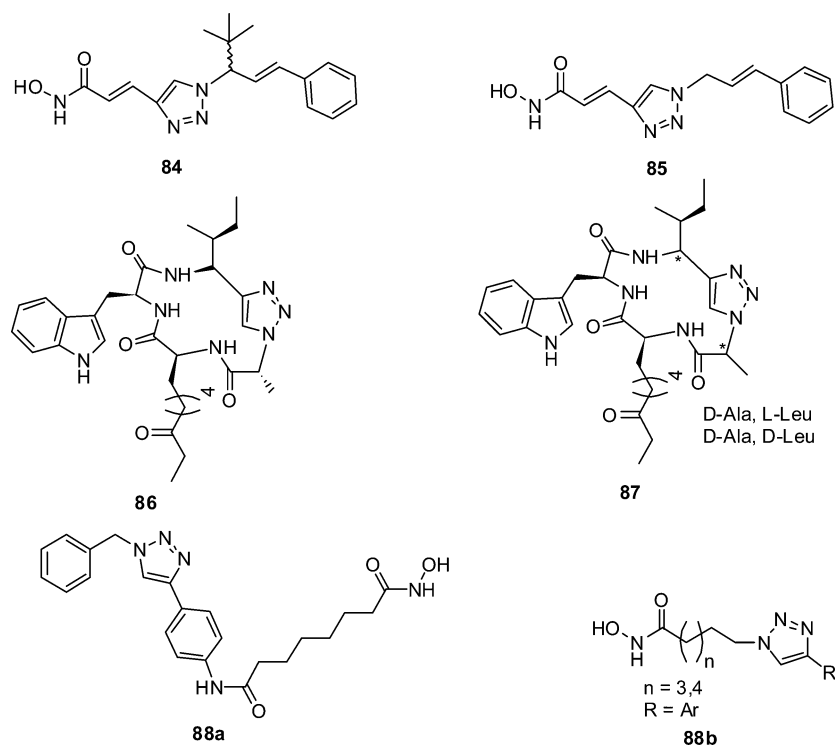


Figure 15. Chemical structures of histone deacetylase inhibitors generated via click chemistry.

3.2.9. Oxidoreductase Inhibitors. Zhu and his co-workers developed an efficient strategy for the fast construction of 108 compounds using click chemistry for monoamine oxidases-A/B inhibition. The fingerprint of inhibitory activity toward monoamine oxidases-A/B against this library was obtained, and four hit compounds were identified as selective inhibitors toward monoamine oxidases-A (MAO-A). Compound 77 (Figure 14) was the most potent inhibitor of MAO-A among the four hit compounds with IC_{50} of 0.83 μ M.⁹⁶

Novel cinnamoyl and caffeoyl clusters were synthesized by multiple Cu(I)-catalyzed [1,3]-dipolar cycloadditions, and their anti-5-lipoxygenase inhibitory activity was tested. Caffeoyl cluster showed an improved 5-lipoxygenase (LO-5) inhibitory activity as compared to caffeic acid, with caffeoyl tetramer 78 (Figure 14) showing the good LO-5 inhibitory activity with IC_{50} = 0.66 μ M.⁹⁷

Human lactate dehydrogenase-5 (*hLDH-5*) has emerged as a promising target for antiglycolytic cancer chemotherapy. Moses et al. reported the synthesis of a small library of bifunctional compounds using a fragment-based click chemistry approach, specifically designed to target *hLDH-5*. Promising lead structure 79 (Figure 14) was identified with impressive selectivity and activity against *hLDH-5* with IC_{50} = 14.8 ± 1.2 μ M against *hLDH-5* and IC_{50} = 10.0 ± 1.0 μ M against *rLDH-5* (rat lactate dehydrogenase-5). These ligands represent a new generation of bifunctional inhibitors specifically designed to target the *hLDH-5* isozyme with a means to interfering with tumor metabolism.⁹⁸

Cryptosporidium parvum is an important human pathogen and potential bioterrorism agent. This protozoan parasite cannot salvage guanine or guanosine and therefore relies on inosine 50-monophosphate dehydrogenase (IMPDH) for biosynthesis of guanine nucleotides and hence for survival. Because *C. parvum* IMPDH is highly divergent from the host counterpart, selective inhibitors could potentially be used to

treat cryptosporidiosis with minimal effects on its mammalian host. Cuny and co-workers synthesized a series of 1,2,3-triazole containing *Cp*IMPDH inhibitors using click chemistry reaction. Compound 80 (Figure 14) showed most efficient inhibitor for *Cp*IMPDH in BSA among the synthesized library with IC_{50} = 9 ± 1 nM against in (–) BSA and IC_{50} = 30 ± 1 nM in (+) BSA.⁹⁹

Nicotinamide adenine dinucleotide (NADa)-dependent inosine monophosphate dehydrogenase (IMPDH), which converts inosine monophosphate (IMP) into xanthosine monophosphate (XMP), is a key enzyme in the de novo synthesis of guanine nucleotides. Inhibition of IMPDH depletes the supply of guanine nucleotides that are required for the growth and proliferation of cells and constitutes a powerful strategy for the treatment of cancers and autoimmune diseases, as well as viral, protozoal, and bacterial infections. Chen et al. employed click chemistry for the synthesis of triazole-linked inhibitors of inosine monophosphate dehydrogenase from human and *Mycobacterium tuberculosis*. The synthesis and evaluation of these inhibitors led to identification of low nanomolar inhibitor 81 (Figure 14) of human IMPDH and more importantly the first potent inhibitor of IMPDH from *Mycobacterium tuberculosis* (*mt*IMPDH) with IC_{50} = 0.070 μ M against *h*IMPDH1 (human IMPDH1) and IC_{50} = 0.044 μ M against *h*IMPDH2 (human IMPDH2).¹⁰⁰

In the past year, there has been significant interest in the design and synthesis of type II dehydroquinase (DHQase II) inhibitors. This is due, in major part, to the operation of this enzyme in a number of pathogenic bacteria including *Mycobacterium tuberculosis* and *Helicobacter pylori*, the etiological agents of tuberculosis, and gastric ulcers and gastric cancer, respectively. It is therefore viewed as a potential target for the development of broad spectrum antibacterial agents. Payne and co-workers reported the design and synthesis of a novel series of triazole-based type II dehydroquinase inhibitors

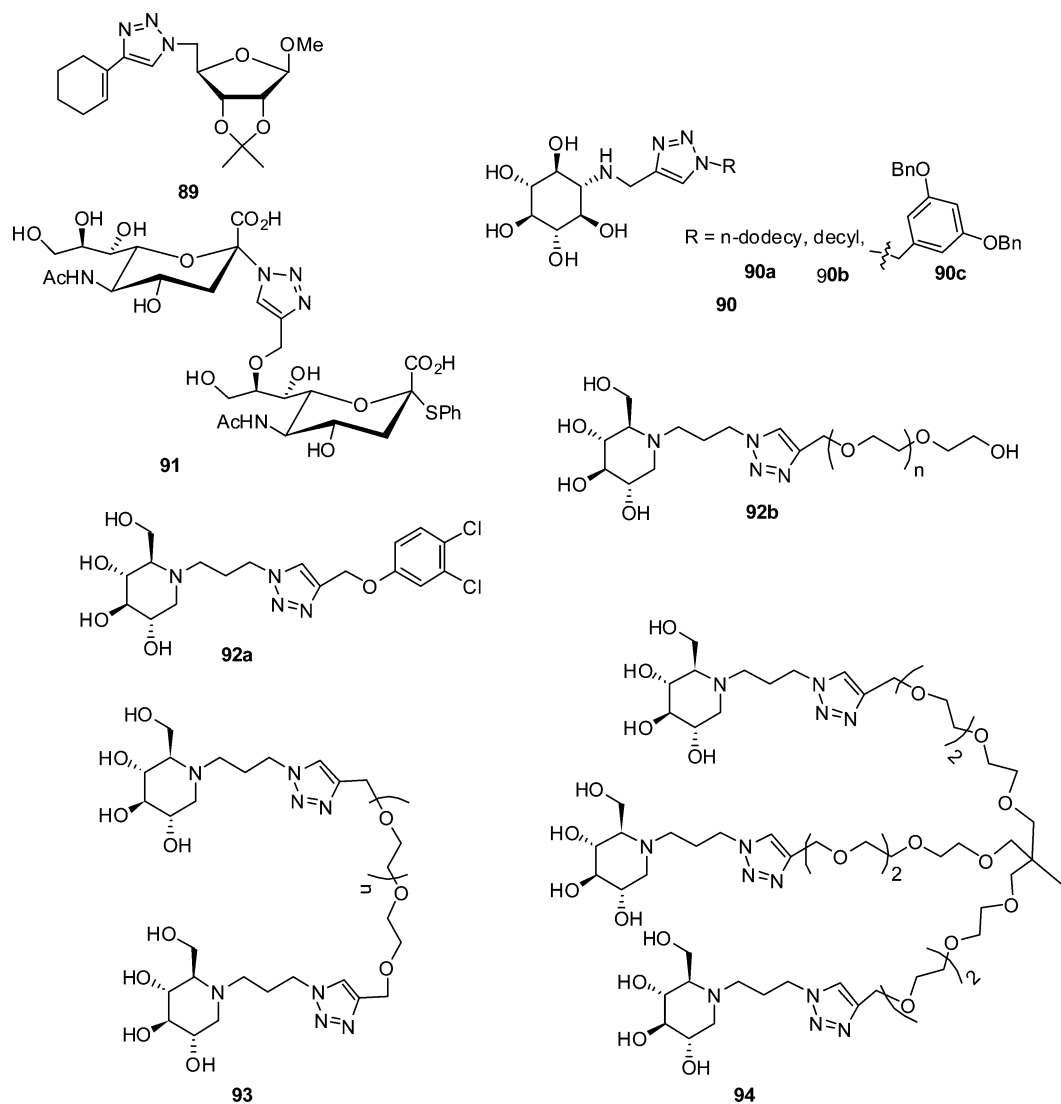


Figure 16. Chemical structures of glucocerebrosidase inhibitors synthesized via click chemistry.

using CuAAC reactions between a key quinate-derived ene-yne and a variety of aryl- and heteroaryl-azides. These were screened against *S. coelicolor*, *H. pylori*, and *M. tuberculosis* type II dehydroquinases (DHQase II). The majority of the compounds proved to be potent inhibitors of all three type II dehydroquinases (DHQase II) with inhibition constants in the low to mid nanomolar range. In particular, compound **82** (Figure 14) bearing terminal phenyl and 3-pyridyl rings directly linked to the triazole moiety represents the most potent inhibitor of the type II dehydroquinases (DHQase II) from *S. coelicolor*, *H. pylori*, and *M. tuberculosis* ever synthesized with $K_i = 5.7 \pm 0.9$ nM against *S. coelicolor* DHQase II, $K_i = 39 \pm 5$ nM against *M. tuberculosis* DHQase II, and $K_i = 225 \pm 51$ nM against *H. pylori* DHQase II.¹⁰¹

Sirtuins are NAD⁺-dependent deacetylases that modulate various essential cellular functions. The development of peptide-based inhibitors of Sir2 would prove useful both as pharmaceutical agents and as effectors by which downstream cellular alterations can be monitored. Click chemistry permits attachment of novel modifications onto the side chain of lysine. Balaran and his co-workers reported the synthesis of peptide analogues prepared using click reactions on *N*- ϵ -propargyloxycarbonyl protected lysine residues and their characterization as

inhibitors of *Plasmodium falciparum* Sirtuins-2 (Sir2) activity. The peptide-based inhibitor **83** (Figure 14) exhibited parabolic competitive inhibition with respect to acetylated-peptide substrate and parabolic noncompetitive inhibition with NAD⁺ (nicotinamide adenine dinucleotide) supporting the formation of E_{L2} (enzyme inhibitor) and E·NAD⁺·I₂ (enzyme inhibitor + nicotinamide adenine dinucleotide) complexes with $K_i = 58 \pm 7$ μ M against Sir2.¹⁰²

Histone deacetylase (HDAC) plays a critical role in the regulation of gene transcription by cleaving the acetyl groups from specific ϵ -amino acetylated lysine residues in nucleosomal histone tails and nonhistone proteins. Although the precise roles of HDAC isoforms in cellular function and tumorigenesis are not yet completely understood, the inhibition of HDAC activity has emerged as a promising approach in anticancer chemotherapy. An interesting family of nonribosomal cyclic-tetrapeptide natural products, including the apicidins, trapoxins, microcins, and chlamydocin, exerts potent cytotoxic activities against cancer cells by inhibiting HDACs. So HDACs' inhibitor plays a significant role in developing anticancer drugs.¹⁰³

A click chemistry-based approach to the synthesis of a novel series of cinnamyl derivatives of histone deacetylase (HDAC) inhibitors is discussed. Among the prepared compounds, *t*-butyl

derivative **84** (Figure 15) exhibited excellent potency against HDACs enzyme, with an IC_{50} value of 18 nM.¹⁰³

Wang et al. reported click chemistry-based approach for the synthesis of histone deacetylase inhibitors. Fourteen compounds were synthesized from the combination of two alkyne and seven azido precursors. The inhibition of HDAC1 and HDAC8 was then determined by in vitro enzymatic assays, after which the cytotoxicity was evaluated in the human cancer cell line screen. A lead compound **85** (NSC746457, Figure 15) was discovered that inhibited HDAC1 at an IC_{50} value of 104 ± 30 nM and proved quite potent in the cancer cell line screen with GI_{50} values ranging from 3.92 μ M to 10 nM.¹⁰⁴

Ghadiri and co-workers reported the synthesis of cyclic pseudotetrapeptides containing 1,4- or 1,5-disubstituted 1,2,3-triazoles analogues to a naturally occurring cyclic tetrapeptide inhibitor of HDACs called apicidin using click chemistry. The 1,4- and 1,5-substituted triazoles act as surrogates for trans and cis amide bonds, respectively, and the resultant molecules (**86** and **87**, Figure 15) provide useful for identifying the most bioactive conformation (cis–trans–trans) of the original cyclic-tetrapeptide inhibitor of HDAC with IC_{50} values of 25, 7, and 75 nM, respectively.¹⁰⁵

Kozikowski et al. employed click chemistry for the synthesis of triazole-based ligands, which were screened against a panel of pancreatic cell lines that consisted of BxPC-3, Hup T3, Mia Paca-2, Pan 04.03, and SU 86.86 cells and *Plasmodium falciparum* strains for their anticancer and antimalarial activity, respectively. The screening results showed that the nature of substitution on the phenyl ring plays a main role in their selectivity for HDAC1 versus HDAC6, with low to moderate selectivity (2–51-fold). In light of the valuable selectivity and potency that were identified for the triazolylphenyl ligand **88a** (Figure 15) in the inhibition of HDAC6 ($IC_{50} = 1.9$ nM) were significant anticancer and antimalarial activities.¹⁰⁶

Oyelere and co-workers synthesized a small library of SAHA-like hydroxamates using click chemistry. The amide bond in SAHA was replaced with a triazole ring. Both the linker chain length and the aromatic ring were varied, and series HDAC inhibitors were synthesized. Inhibition assays revealed several HDAC inhibitors (**88b**, Figure 15) with improved potency as compared to SAHA.¹⁰⁷

3.2.10. Glycosidase Inhibitors. Ferreira and his co-workers reported the synthesis of a series of 4-substituted 1,2,3-triazoles conjugated with sugars, including D-xylose, D-galactose, D-allose, and D-ribose. These compounds were screened for α -glucosidase inhibitory activity using yeast maltase (MAL12) as a model enzyme. Methyl-2,3-O-isopropylidene- β -D-ribofuranosides, such as the 4-(1-cyclohexenyl)-1,2,3-triazole derivative (compound **89**, Figure 16), were among the most active compounds, showing up to 25-fold higher inhibitory potency than the complex oligosaccharide acarbose with $IC_{50} = 3.8 \pm 0.5$ μ M.¹⁰⁸

New N-alkylaminocyclitols bearing a 1,2,3-triazole system at different positions of the alkyl chain were prepared as potential glucocerebrosidase pharmacological chaperones using click chemistry approaches. Among them, compound **90a** (Figure 16) ($K_i = 0.06$ μ M), with the shorter spacer ($n = 1$) between the alkyltriazolyl system and the aminocyclitol core, was the most active as glucocerebrosidase inhibitor, revealing a determinant effect of the location of the triazole ring on the activity.¹⁰⁹ Recently, the same research group developed new glucocerebrosidase inhibitors by diversity of N-substituted aminocyclitols using click chemistry and in situ screening. A

click chemistry approach based on the reaction between N-propargyl aminocyclitol and a series of azides was optimized for the synthesis and in situ screening of a variety of N-substituted aminocyclitols as glucocerebrosidase inhibitors. The highly aqueous content of the reaction media made possible the direct screening of the products by simple dilution of the crude reaction mixtures in the adequate buffer. The process was suitable for its implementation into a micro liter plate format and, hence, amenable to combinatorial protocols. Maximum diversity among the library members was secured by application of a proper selection algorithm from an initial collection of 343 compounds. Library members with IC_{50} values below 3.5 μ M were individually synthesized and tested as glucocerebrosidase inhibitors and also for their ability to induce enzyme thermal stabilization, an in vitro indication of their potential as pharmacological chaperones. Compounds **90b** ($K_i = 0.05$ μ M) and **90c** ($K_i = 0.06$ μ M) (Figure 16) with a linear aliphatic side chain showed the highest enzyme stabilization ratios and were promising candidates for further development.¹¹⁰

Linhardt and his co-workers reported that a small library of 1,2,3-triazole-linked sialic acid derivatives was synthesized using click chemistry. These novel sialic acid derivatives were then evaluated as potential neuraminidase inhibitors using a 96-well plate fluorescence assay. Compound **91** (Figure 16) showed potent inhibition activity against Neuraminidase with an IC_{50} value of 17 μ M.¹¹¹

Gouin and his co-workers recently developed an efficient click procedure to tether hydrophobic substituents to N-azidopropyl-1-deoxynojirimycin.¹¹² A set of 14 original iminosugars was synthesized and evaluated for inhibition of commercially available glucosidases. Most of the compounds were micromolar inhibitors of those enzymes. In vitro inhibition assays with the N370S β -GCase revealed that the sublibrary containing the derivatives with aromatic aglycons displayed the highest inhibitory potency. Chaperone activity of the whole set of synthetic compounds was also explored in mutant Gaucher cells. The most active compound (**92a**, Figure 16) gave a nearly 2-fold increase in enzyme activity at 20 μ M, a value significantly higher than the 1.33-fold recorded for the reference compound N-nonyl-1-deoxynojirimycin (N-nonyl-DNJ).¹¹² Compound **92a** showed $K_i = 9$ μ M against beta glucosidase (bovine liver), $K_i = 1$ μ M against beta glucosidase (almond), $K_i = 57$ μ M against alpha glucosidase, and $K_i = 16$ μ M against amyloglucosidase.

Kovensky et al. reported the synthesis of multivalent iminosugars from a click chemistry reaction between oligoethylene scaffolds and N-substituted DNJ derivatives.¹¹³ These series of compounds screened against glycosidase inhibitory activities and resultant compounds (**92b**, **93**, and **94**, Figure 16) showed good inhibition against glycosidase.¹¹⁴ Compound **92b** showed a K_i value of 47 ± 2 μ M against beta glucosidase when $n = 1$ (Figure 16) and $K_i = 95 \pm 5$ μ M against alpha galactosidase when $n = 4$ (Figure 16). The dimer version of compound **93** showed $K_i = 17 \pm 1$ μ M against amylogalactosidase when $n = 1$ in Figure 16 and $K_i = 55 \pm 2$ μ M against niringinase when $n = 4$ in Figure 16. Trimer version of compound **94** showed $K_i = 35 \pm 2$ μ M against alpha mannosidase.

Gouin and his co-workers recently developed an efficient click procedure to tether hydrophobic substituents to N-azidopropyl-1-deoxynojirimycin.¹¹⁴ A set of 14 original iminosugars was synthesized and evaluated for inhibition of commercially available glucosidases. Most of the compounds

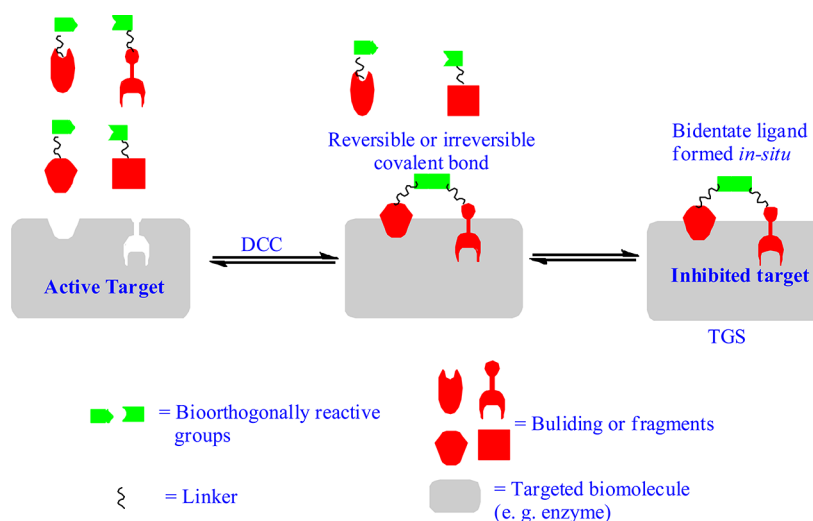


Figure 17. Schematic representation of in situ click chemistry used for the development of enzyme inhibitors.

were micromolar inhibitors of those enzymes. In vitro inhibition assays with the N370S β -GCase revealed that the sublibrary containing the derivatives with aromatic aglycons displayed the highest inhibitory potency. Chaperone activity of the whole set of synthetic compounds was also explored in mutant Gaucher cells. The most active compound (**94**, Figure 16) gave a nearly 2-fold increase in enzyme activity at 20 μ M, a significantly higher value than the 1.33-fold recorded for the reference compound *N*-nonyl-1-deoxynojirimycin (*N*-nonyl-DNJ) with $K_i = 35 \pm 2 \mu$ M.¹¹⁴

4. IN SITU CLICK CHEMISTRY

The conventional approach used by medicinal chemists in drug discovery consists of the synthesis of a collection of compounds and subsequent biological screening. The procedure would be shortened and optimized if the biological target could actively choose its best ligand. Indeed, the target would act as the ideal template to generate the perfect hit. In this specific context, it is therefore possible to envisage that, at room temperature, an enzyme could bring azide and alkyne containing molecules in close proximity so as to overcome the high energetic barrier allowing the click chemistry reaction to occur.¹¹⁵ In this manner, only compounds that fit correctly into the active site of the enzyme should react to give new potent ligands of the enzyme. The schematic pictorial representation of in situ click chemistry of enzyme inhibitor is shown in Figure 17.

A subset of the combinatorial enterprise that is highlighted here is target-guided synthesis (TGS), in which the biological target (protein or DNA) is directly involved in the choice of ligands assembled from a pool of smaller fragments. Two general forms of TGS had been tested, each involving incubation of the target with mixtures of reactive building blocks. The “equilibrium” or “thermodynamic” approach is frequently given the label “dynamic combinatorial chemistry” (DCC) and is distinguished by the reversible joining of pairs of blocks, and the sampling of those combinations by the target (Figure 17).¹¹⁶ Those molecules that bind most tightly are retained, skewing the equilibrium toward a different distribution than would be observed in the absence of the target. In the “nonequilibrium” or “kinetic” approach, the reaction that joins the building blocks was irreversible, and selectivity for one or more products over others was a function of differential acceleration of that reaction by the target. The simultaneous

binding of blocks to the target certainly contributes to that acceleration, increasing the local concentration of reactive blocks with respect to each other. As discussed below, however, other factors affecting the rate of the process can come into play. The compounds that are created by both styles of TGS are, at the very least, highly likely to bind to the target template with greater affinity than their individual components, because two- or multiple-point connections slow off-rates by virtue of the chelate effect. The use of the click chemistry reaction in TGS has been dubbed “click chemistry in situ”. Representative examples of in situ click chemistry are described below.

In principle, the “click chemistry” approach to drug design is applicable to almost any target. If it is possible to use a pure enzyme, the function of which can be measured easily, then the techniques are easier to apply. However, Finn stresses, “the in situ approach has the virtue of being potentially useful when these conditions were not met.” If everything works perfectly, one can even imagine administering a set of pieces of a drug to a patient and having the drug assemble itself at the desired site (e.g., a tumor) in response to the specific nature of the target (Figure 18) Further development work with enzyme inhibitors is now in progress in many research groups, on a variety of diseases including AIDS, cancer, anthrax, and Huntington’s disease.¹¹⁷

4.1. Mycobacterial Transcriptional Regulator

Tuberculosis is a major cause of morbidity and mortality worldwide. This infectious disease caused by *Mycobacterium tuberculosis* kills each year between 1.2 and 1.8 million people. Although the combined use of four first-line antibiotics (isoniazid, rifampicin, pyrazinamid, and ethambutol) known as directly observed treatment short-course (DOTS) claims to successfully treat 85% of the patients, multidrug-resistant strains of the mycobacteria rapidly emerge.¹¹⁸ Ethionamide, a second-line antibiotic, is one of the most widely used drugs for the treatment of multidrug-resistant tuberculosis; however, its use is hampered by severe side effects. Ethionamide (EthA) itself is inactive and requires activation by the mycobacterial mono-oxygenase EthA to active NAD-adduct that inhibits, in humans, the enoyl-ACP reductase involved in mycolic acid biosynthesis. The expression of *ethA* is controlled by the transcriptional repressor (EthR), a member of the TetR family of transcriptional regulators.^{119,120} Genetic inactivation of *ethR* logically

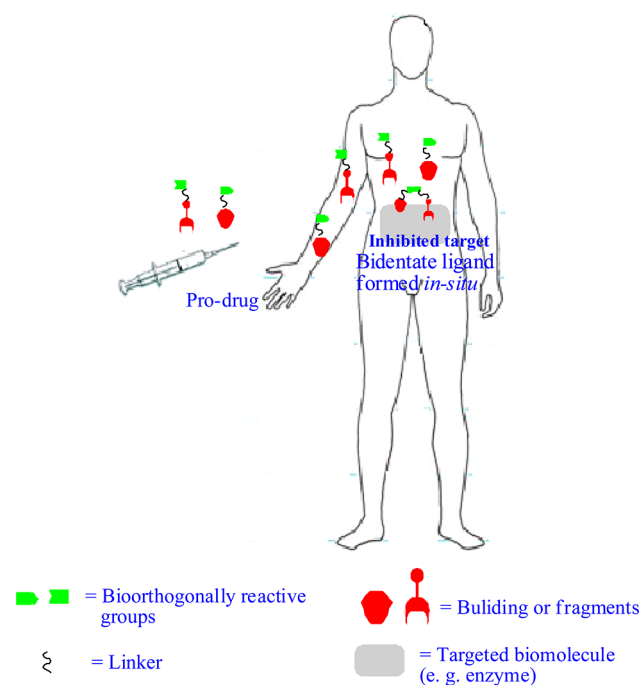


Figure 18. Schematic representation of in situ click chemistry used for drug development.

leads to overexpression of EthA and consequently to hypersensitivity of the mycobacteria to ethionamide. Deprez and his co-workers postulated that synthetic inhibitors of EthR would increase transcription of *ethA* and thus improve ethionamide bioactivation and efficacy. The first inhibitor of EthR, BDM14500, was identified through the screening of 131 compounds designed on the basis of the crystal structure of EthR. Hit-to-lead optimization was then performed via a rational design.¹²¹ During the hit-to-lead process, EthR binding of potent inhibitors was monitored by X-ray crystallography. Surprisingly, one compound (BDM31381) adopted a new orientation as compared to the initial hit by pointing its thieno acetyl substituent to the bottom of the pocket.¹²⁰ This observation stimulated one to design new analogues to explore the ligand binding pocket of the protein and experimentally probe its ability to adopt new conformations upon binding of more extended ligands.

Deprez and his co-workers successfully applied in situ click chemistry to probe the ligand binding domain of EthR, a mycobacterial transcriptional regulator known to control the sensitivity of *Mycobacterium tuberculosis* to several antibiotics.¹²² Specific protein-templated (EthR-template with or without BSA) ligands were generated in situ from one azide and six clusters of 10 acetylenic fragments using previous literature results. From LC-MS single ion monitoring, the formation of compounds **95** and **96** (Figure 19) via in situ click chemistry was confirmed, and the resultant compounds **95** and **96** showed most potent inhibition against EthR with IC_{50} values of 580 nM and 7.4 μ M. From the inhibition results, it is clear that 1,4-substituted triazole was the most potent inhibitor of EthR. Protein-directed in situ chemistry allows medicinal chemists to explore the conformational space of a ligand-binding pocket and is thus a valuable tool to guide drug design in the complex path of hit-to-lead processes.¹²²

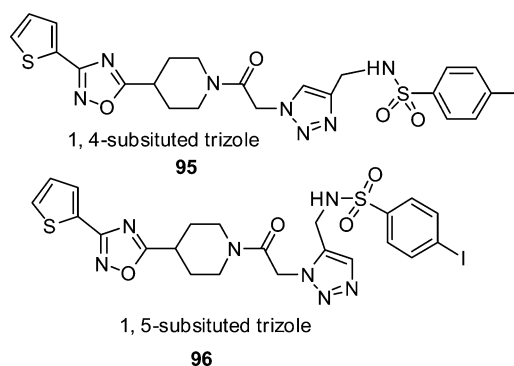


Figure 19. Chemical structures of EthR inhibitors synthesized via in situ click chemistry.

4.2. Histone Deacetylase Inhibitors

Histone deacetylase is a class of enzymes that remove acetyl groups from an ϵ -N-acetyl lysine amino acid on a histone. Its action is opposite of that of histone acetyl transferase. HDAC proteins are now also being referred to as lysine deacetylases (KDAC), as to more precisely describe their function rather than their target, which also includes numerous nonhistone proteins. HDAC inhibitors are attractive drug candidates for cancer, inflammation, and neurodegenerative disorders. HDAC inhibitors consist of a Zn-binding group (ZBG) that coordinates with the Zn ion in the active site, a capping region that interacts with residues on the rim of the active site, and a linker that connects the cap and ZBG at an appropriate distance.^{123,124}

Finn and his co-workers prepared two alkynes with hydroxamic acid and 15 alkyl azides as building blocks for in situ assembly screening.¹²⁵ In conventional in situ click chemistry, a mixture of an alkyne and an azide is incubated in the presence of the target. The convenient assay of HDAC was chosen to see if enough of an inhibitor could be generated by in situ assembly to measurably affect enzyme function. We incubated a mixture of each known alkyne ligand (at a concentration approximately equivalent to its IC_{50}) with each candidate azide (in large excess) in the presence of HDAC and subsequently carried out a fluorometric assay for HDAC activity directly on the reaction mixture. These experiments were conducted in parallel in 96-well microtiter plates using human recombinant HDAC8, which was shown separately to be stable under the incubation and assay conditions.

The experiment revealed that the syn-triazole isomer proved to be a better HDAC8 inhibitor **97** ($IC_{50} = 0.51 \mu$ M) than anti-3 **98** ($IC_{50} = 4.0 \mu$ M) (Figure 20). These factors suggested that the rapid and regioselective formation of anti-3 in the presence of HDAC8 was consistent with acceleration of the reaction by a small amount of enzyme containing Cu(I) instead of Zn(II).¹²⁵

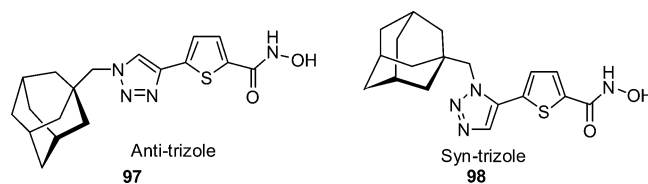


Figure 20. Chemical structures of histone deacetylase inhibitors synthesized via in situ click chemistry.

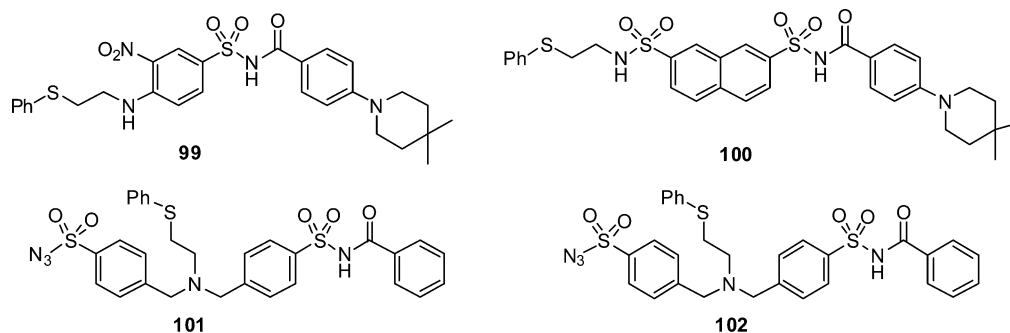


Figure 21. Chemical structures of protein–protein interaction modulators synthesized via in situ sulfo click chemistry.

4.3. Protein–Protein Interaction Modulators

Protein–protein interactions (PPIs) are central to a large number of vital biological processes and thus represent attractive targets for the development of novel therapies for a variety of diseases. The development of small molecules, which specifically modulate or disrupt a particular PPI, remains a challenging and risky undertaking. Commonly, protein–protein interfaces are large and flat and lack deep cavities that might serve as good binding sites for small molecules. Protein–protein interfaces bury 500–3000 Å² of total surface area, which exceeds the potential binding area of low-molecular-weight compounds. Wells and co-workers demonstrated that only a fraction of the amino acid residues at the protein–protein interface contributes to the major portion of the binding free energy,^{126,127} with the discovery of small molecules modulating or disrupting PPIs. Often, small molecule design is aimed at mimicking a peptide or a protein secondary structure in a truncated form.¹²⁸ Alternatively, fragment-based drug discovery strategies using biomolecular NMR, X-ray crystallography, or surface plasmon resonance (SPR) lead to the identification of fragments with good ligand efficiencies, which are further developed into potent protein–protein interaction modulators (PPIMs).^{126–128}

Manetsch and his workers recently employed kinetic target-guided synthesis (TGS) and in situ sulfo-click chemistry for the development of protein–protein interaction modulators.¹²⁹ In kinetic TGS and in situ click chemistry, the target is directly involved in the assembly of its own potent, bidentate ligand from a pool of reactive fragments.¹²⁹ Use and validation of kinetic TGS based on the sulfo-click reaction between thio acids and sulfonyl azides was screened. Starting from a randomly designed library consisting of 9 thio acids and 9 sulfonyl azides leading to 81 potential acylsulfonamides, the target protein, Bcl-XL, selectively assembled four PPIMs, acylsulfonamides (compounds **99–102**, Figure 21), which were shown to modulate Bcl-XL/BH3 interactions. Compound **99** (Figure 21) showed a nanomolar PPIM activity with K_i value of 37.5 ± 5.0 nM. Remaining compounds (**100–102**) showed micromolar PPIM activity with K_i values of 11.5 ± 1.4 , 11.6 ± 1.6 , and 14.6 ± 1.0 μ M, respectively. To further investigate the Bcl-XL templation effect, control experiments were carried out using two mutants of Bcl-XL. In one mutant, phenylalanine Phe131 and aspartic acid Asp133, which were critical for the BH3 domain binding, were substituted by alanines, while arginine Arg139, a residue identified to play a crucial role in the binding of ABT-737, a BH3 mimetic, was replaced by an alanine in the other mutant. Incubation of these mutants with the reactive fragments and subsequent LC/MS-SIM analysis confirmed that these building block combinations

yield the corresponding acylsulfonamides at the BH3 binding site, the actual “hot spot” of Bcl-XL. These results validate kinetic TGS using the sulfo-click reaction as a valuable tool for the straightforward identification of high-quality PPIMs.¹²⁹

4.4. Antibody-like Protein-Capture Agents

Most protein-detection methods rely upon antibody-based capture agents. A high-quality antibody exhibits high affinity and selectivity for its cognate protein. However, antibodies are expensive and can be unstable toward chemical and biochemical processes. Several alternative protein-capture agents, including oligonucleotide aptamers and phage-display peptides, were reported, each of which had advantages as well as significant limitations.¹³⁰

Heath and his co-workers recently reported accurate MALDI-TOF/TOF sequencing of one-bead-one-compound peptide libraries to the identification of multiligand protein affinity agents using in situ click chemistry screening.¹³⁰ Semiautomated sequencing algorithm was used for the accurate use of MALDI-TOF/TOF for the sequencing of peptides cleaved from single TentaGel beads. The initial 44% sequencing success rate of the standard de novo sequencing software was improved to nearly 100%. The MS/MS approach was validated in two ways. First, single beads, randomly chosen from a comprehensive OBOC 5-mer peptide library, were split in half and sequenced using both the MS/MS approach and Edman degradation. Excellent agreement was found between the two methods. Second, the sequencing approach was utilized to successfully identify two biligand affinity agents against bCAII through the approach of in situ click/OBOC screening. On the basis of this screening, two triazole-coupled peptide biligands were synthesized in bulk, and their binding affinities against bCAII were characterized using SPR. Note that the best of these biligands exhibited an affinity for bCAII in the 0.5–5 μ M range, which was as good as those of the biligands identified previously through the use of in situ click/OBOC library screening (compound **103**, Figure 22a). The sequencing approach and algorithm reported here should provide a valuable tool for making the approach of sequential in situ click/OBOC screening a high-throughput approach toward the identification of high-affinity, high-selectivity protein-capture agents.

The same research group again reported a poly peptide-based multiarmed capture agent for proteins. The researchers used the in situ click chemistry approach toward the construction of multiligand protein-capture agents and triligand capture agent evaluated against human bovine carbonic anhydrase II (h(b)CAII) as a model system.^{131a} Standard methods for the bead-based combinatorial synthesis of oligopeptides were

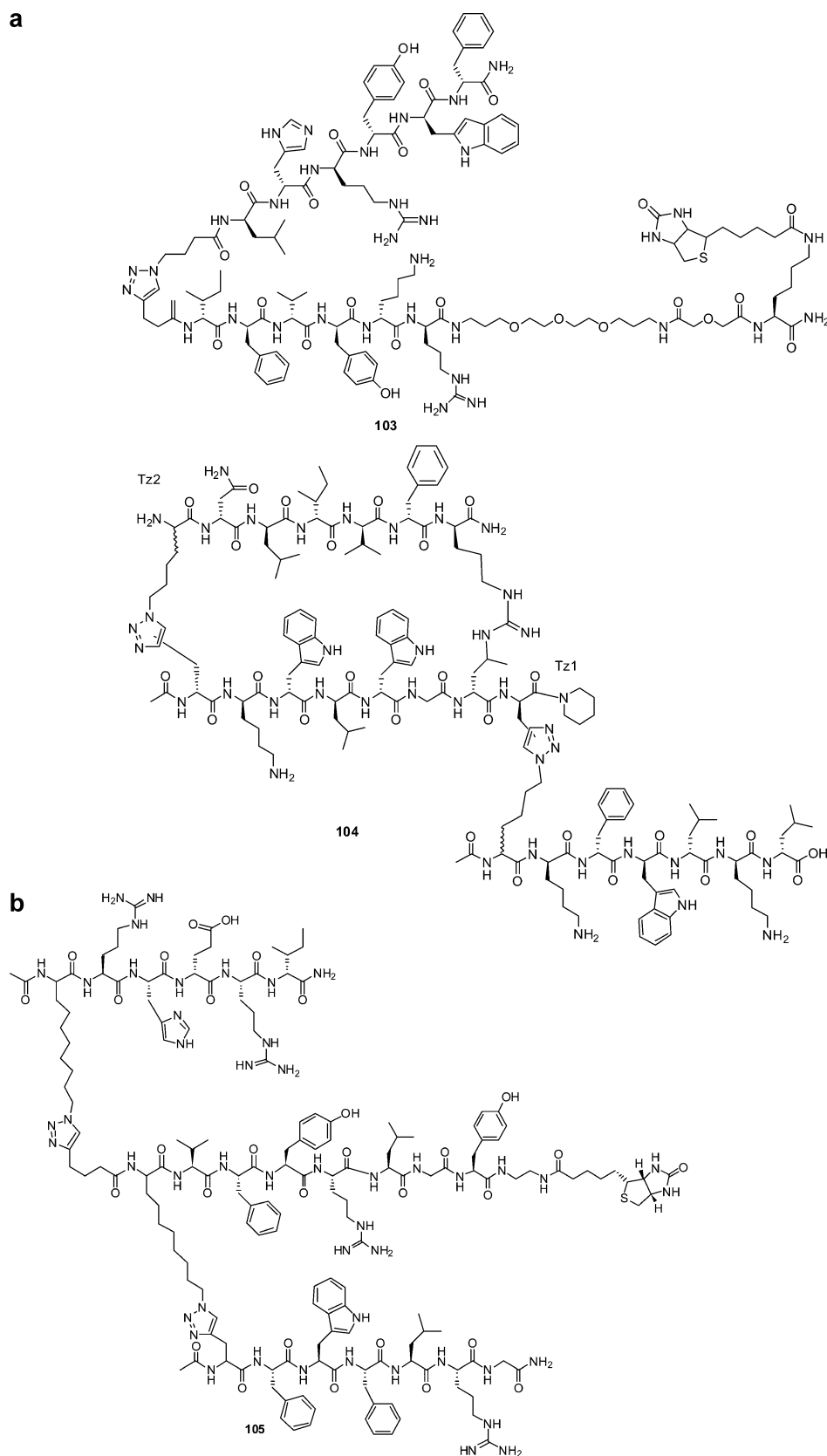


Figure 22. (a) Chemical structures of antibody-like protein-capture agents synthesized via click chemistry: Triligand capture agent for the protein b(h)CAI. **104**: The triazoles (Tz1, Tz2) can be either 1,4 (anti) or 1,5 (syn) isomers. (b) **104**: Structure of the biotinylated Akt triligand.

employed, with the installation of an alkyne group at the terminus of each library member. An initial hexa peptide anchor structure was identified by determining which beads bound the

protein most strongly, followed by Edman sequencing. The dissociation constant of this peptide was approximately $500 \mu\text{M}$, but this interaction was enough to allow for an in situ

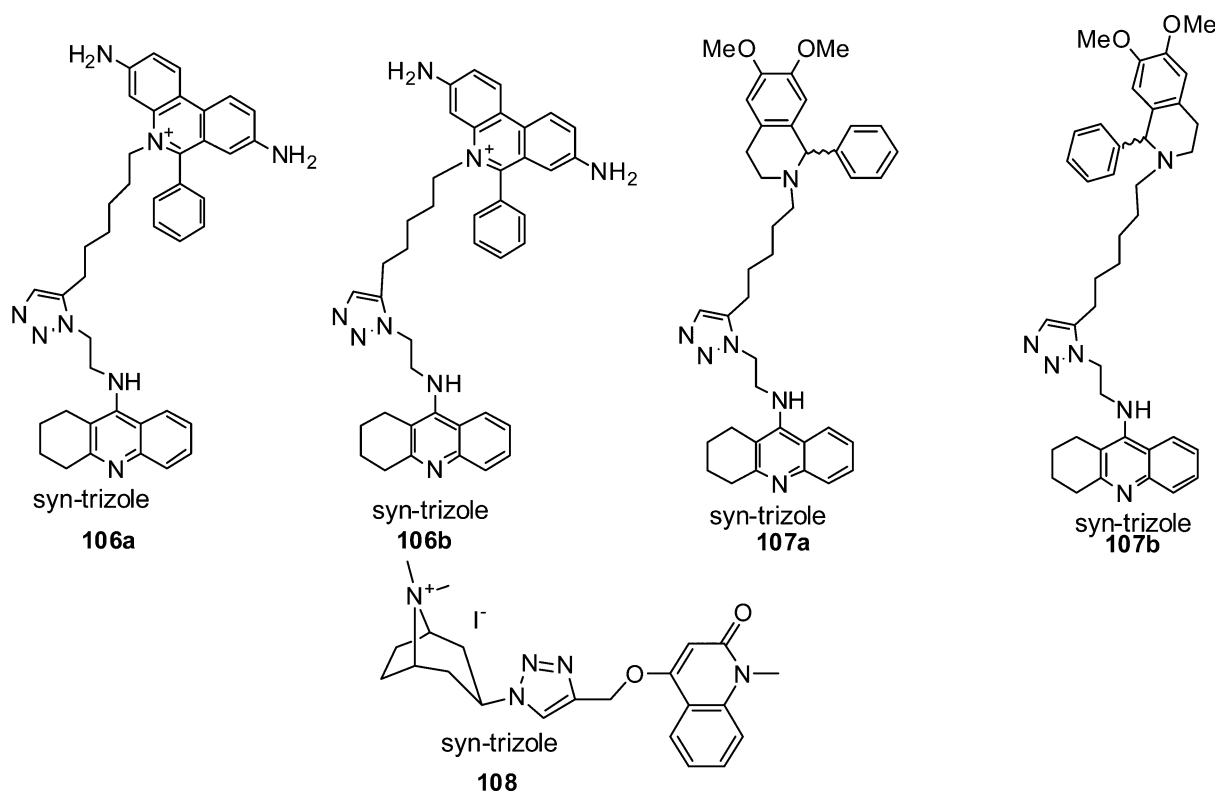


Figure 23. Chemical structures of acetylcholinesterase inhibitors synthesized via in situ click chemistry.

assembly of a triazole-linked bivalent ligand incorporating a second hexapeptide from a large library of combinatorial possibilities. The biligand exhibited a $3 \mu\text{m}$ binding affinity for bCAII, as measured by surface plasmon resonance (SPR). The process was repeated a second time, giving structure **104** (Figure 22a), which contained 18 amino acids and two triazoles. Triligand capture agent **104** exhibited 64 and 45 nm binding affinities against bCAII and hCAII, respectively, as determined by SPR.

Heath and his co-workers reported in situ click chemistry for the development of Akt-specific branched peptide triligand (compound **105**, Figure 22b) that was a drop-in replacement for monoclonal antibodies in multiple biochemical assays. Each peptide module in the branched structure makes unique contributions to affinity and/or specificity resulting in a $K_d = 200 \text{ nM}$ affinity ligand that efficiently immunoprecipitates Akt from cancer cell lysates and labels Akt in fixed cells.^{131b}

4.5. Acetylcholinesterase Inhibitors

AChE catalyzes the hydrolysis of neurotransmitter acetylcholine at the synaptic cleft, facilitating nerve impulse transmission across the synaptic gap. Alzheimer's disease (AD) is a progressive, degenerative disorder of the brain and is the most common form of dementia among the elderly especially in industrialized countries. According to the cholinergic hypothesis, the decreased levels of acetylcholine in the brain areas dealing with learning, memory, behavior, and emotional responses (neocortex and hippocampus) are of critical importance in AD. The reduced levels of neurotransmitter acetylcholine are due to its rapid hydrolysis by an enzyme, acetylcholinesterase (AChE). There were several reports showing that the enzyme AChE plays a key role in the development of the senile plaques by accelerating amyloid- β deposition. Thus, AChE inhibition plays a significant role as a

critical target for the effective management of AD by an increase in the availability of acetylcholine in the brain regions and decrease in the deposition of β -amyloid.^{132–134} The first target used for in situ click chemistry was the enzyme acetylcholinesterase (AChE), selected for its biological importance as a key component of neurological function and therefore a drug target, and for the structure of its active site. AChE has two distinct binding sites in close proximity to each other, at either end of an active site “gorge” lined by 14 conserved amino acid residues. Several site-specific ligands have been developed that inhibit the catalytic cycle by binding to the catalytic site at the bottom of the gorge as well as peripheral site at the top. Bivalent ligands synthesized to address both sites simultaneously were found to be effective. Sharpless and co-workers applied in situ click chemistry, for the first time, via mixing 49 building block combinations of tacrine molecules equipped with alkyl azides and phenanthridinium molecules equipped with alkyl acetylenes in the presence of the enzyme. The researchers found that only one product, *syn*-TZ2PA6, which was a femtomolar inhibitor, was chosen by the enzyme.¹³²

Kolb and co-workers further optimized this approach with the help of liquid chromatography–mass spectrometry in selected ion mode (LC–MS–SIM).¹³³ The same group, in a subsequent report, employed a tacrine azide as an anchor molecule at concentrations sufficient to saturate the active site, and this enzyme–inhibitor complex was found to recruit the most preferred peripheral binding group from a mixture of alkynes, leading to the identification of four compounds **106a–107b** (Figure 23), which were the most potent noncovalent inhibitors of AChE.^{134a} Compounds **106a** and **106b** (Figure 23) of the *syn*-triazole derivatives showed good binding affinity to AChE with K_d values of 99 and 100 nM, respectively, whereas compound **107a** (Figure 23) of the *R*- and *S*-isomers of *syn*-

triazole was exhibiting even lower nanomolar affinity to AChE with K_d values of 33 (for *S*-isomer) and 36 nM (for *R*-isomer). Finally, compound **107b** showed moderate binding affinity toward AChE with $K_d = 96$ nM.

Fokin et al. reported successfully the combination of CuAAC and in situ click chemistry for the synthesis of a highly potent and selective ligand (compound **108**, Figure 23) for *Lymnaea stagnalis* acetylcholine binding protein (AChBPs). The researchers compared the preference of anti and syn regioisomer formation on acetylcholinesterase with the equilibrium affinities of the respective triazoles. The syn regioisomer of the triazole showed higher affinity to AChBPs due to an induced change in conformation that enhanced aromatic π - π association at the peripheral site, whereas a change in conformation did not occur in the anti-isomer with the lower affinity ($K_d = 0.96$ nM) against *Lymnaea stagnalis* AChBPs. The researchers used homomeric AChBPs from *Lymnaea* and *Aplysia* snails as in situ templates for the generation of novel and potent ligands that selectively bind to these proteins. The researchers successfully demonstrated that the in situ click reaction can take place at the subunit interfaces of an oligomeric protein and can thus be used as a tool for identifying a novel candidate for nicotinic acetylcholine receptor ligands. The crystal structure of one of the in situ-formed triazole-AChBP complexes showed binding poses and molecular determinants of interactions predicted from structures of known agonists and antagonists.^{134b}

4.6. HIV Protease Inhibitors

The aspartic protease of HIV-1 is a major therapeutic target in the fight against AIDS. The high rate of mutational adaptation by the virus to drug challenge makes methods for the discovery of new inhibitors of protease (and other viral enzymes or necessary functions) a high priority.¹³⁵

Sharpless et al. prepared two focused libraries of 50 compounds each, based on hydroxyethylamine peptide isosteres. Azide-bearing scaffolds were united via the new copper-catalyzed process with acetylenes, for library production. These libraries, which were already in aqueous solution from the synthesis step, were used directly, for screening against wild type HIV-1 protease and three mutants (G48 V, V82F, V82A). As was predicted by molecular modeling, two of these compounds strongly inhibited all four proteases tested, with activities in the low nanomolar range (purified compounds). Especially compound **109** (Figure 24) showed most potent inhibition against HIV protease in the series with $K_i = 1.7$ nM.¹³⁶

4.7. Chitinase Inhibitors

Chitinases catalyze the hydrolysis of chitin, a linear homopolymer of *N*-acetyl-D-glucosamine (GlcNAc), which is present in a wide range of organisms, including bacteria, fungi, insects, viruses, higher plants, and animals. Chitin is found in

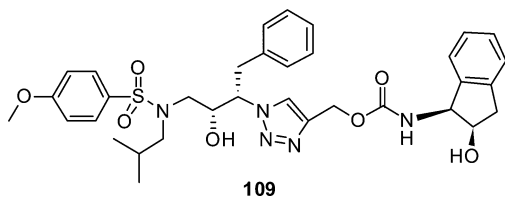


Figure 24. Chemical structures of HIV protease inhibitors synthesized via in situ click chemistry.

fungal cell walls, the exoskeletons of crustaceans and insects, and the microfilarial sheaths of parasitic nematodes, making chitinases potential targets for antifungal, insecticidal, and antiparasitic activity. Chitinase inhibitors identified as potential anti-inflammatory agents against asthma and allergic diseases, including atopic dermatitis and allergic rhinitis.¹³⁷

Omura and co-workers reported a chitinase templated formation of a potent triazole inhibitor marrying a biologically active azide-containing compound with structurally unrelated alkyne fragments.¹³⁷ Compound **110** based on a motif excised from a natural cyclic peptide binder of blowfly and *Serratia marcescens* chitinases (SmChi) was used as an anchor molecule for in situ click reactions with a library of alkynes, each in the presence of a mixture of three SmChi subtypes. Syn-triazole **110** (Figure 25) displayed high inhibitory activity against SmChiB

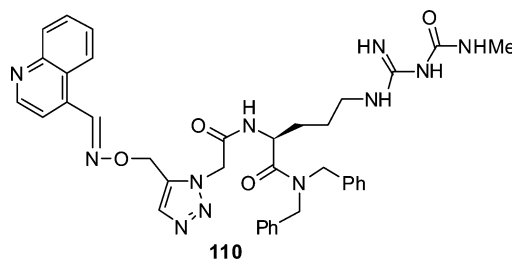


Figure 25. Chemical structures of chitinase inhibitors synthesized via in situ click chemistry.

(IC_{50} value of 0.022 μ M), which is approximately 30-fold stronger than that of the precursor (approximately 300-fold potency as compared to natural product precursor). Syn-anti selection for the in situ screening by LCMS-SIR revealed that a combination of azide and alkyne had led to the accelerated formation of syn-triazole in the presence of pure (His) 6-SmChiB in an enzyme-dose-dependent manner, thereby validating syn-50 as an in situ “hit” and confirming that its formation required the enzyme active site to be accessible.^{137,138}

4.8. Carbonic Anhydrase Inhibitors

Carbonic anhydrases (CA) are a family of metalloenzymes that catalyze the interconversion of HCO_3^- and CO_2 . They play essential roles in respiration, pH balancing of blood and other tissues, transport of CO_2 and protons, tumorigenicity, etc. Most of the CA contain a zinc ion at the active site, and the majority of inhibitors for this class of enzymes are aromatic or heteroaromatic sulfonamides, which act by coordinating to the zinc ion.¹³⁹

Kolb and his co-workers employed the in situ click chemistry with acetylenic benzenesulfonamide as the reactive scaffold and 24 different azides to identify potent inhibitors of CA. The in situ click experiments were performed in a 96-well micro liter plate with each well containing a mixture of bovine CA II (bCA II), an acetylenic benzenesulfonamide at a concentration enough to saturate the enzyme active site, and an azide. Analysis of the crude reaction mixture with LCMS-SIM revealed that 12 out of the 24 reagent combinations led to triazole formation (compound **111**, Figure 26) and all of the observed triazoles were of an anti-regiochemistry, which is a consequence of the inhibitor selection by the enzyme active site with a K_i value of 0.2 ± 0.3 nM.¹⁴⁰

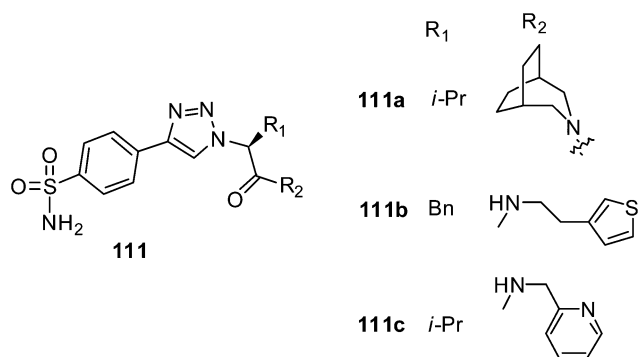


Figure 26. Chemical structures of carbonic anhydrase binders and inhibitors synthesized via in situ click chemistry.

4.9. Cell Imaging

Protein prenylation is a common post-translational modification present in eukaryotic cells. Many key proteins involved in signal transduction pathways are prenylated, and inhibition of prenylation can be useful as a therapeutic intervention. Significant progress was made in understanding protein prenylation in vitro, by researchers interested in studying this process in living cells. This modification involves the addition of a C15 (farnesyl) or C20 (geranylgeranyl) isoprenoid moiety onto a cysteine residue near the C-terminus of proteins that bear a “CAAX” box motif, catalyzed by either the farnesyltransferase or the geranylgeranyltransferase enzyme. This natural modification serves to direct a protein to the

plasma membrane of the cell. A recently discovered application of prenylated peptides is that they have inherent cell-penetrating ability, and are hence termed cell-penetrating prenylated peptides. These peptides are able to efficiently cross the cell membrane in an ATP independent, nonendocytotic manner, and it was found that the sequence of the peptide does not affect uptake, so long as the geranylgeranyl group is still present.¹⁴¹ This information may be useful for applications utilizing cell-penetrating peptides to deliver cargo across membranes. The nonendocytotic mechanism that functions in the uptake of these peptides may also prove to be useful because it avoids potential endosomal localization/degradation of cargo.¹⁴¹

Distefano and his co-workers recently reported evaluation of a cell-penetrating prenylated peptide using fluorophore via in situ click reaction for cell imaging applications.¹⁴² The cell-penetrating prenylated peptide was synthesized using standard Fmoc coupling conditions on an automated synthesizer with rink-amide resin to afford the C-terminal amide peptides. The N-terminal lysine side chain was acetylated, followed by acylation with an alkyne-containing acid (4-pentynoic acid) on the amino group to give the resulting N-terminal alkyne. Geranylgeranylation of that peptide was performed in solution using acidic Zn(OAc)₂ coupling conditions to afford peptide 112a. Peptide 112b (Figure 27) was prepared in an analogous manner except that the ϵ -amino group of the N-terminal lysine was acylated with 5-Fam. Thus, peptide 112a contains an alkyne but no fluorophore, whereas peptide 112b contains both an alkyne and a fluorophore.

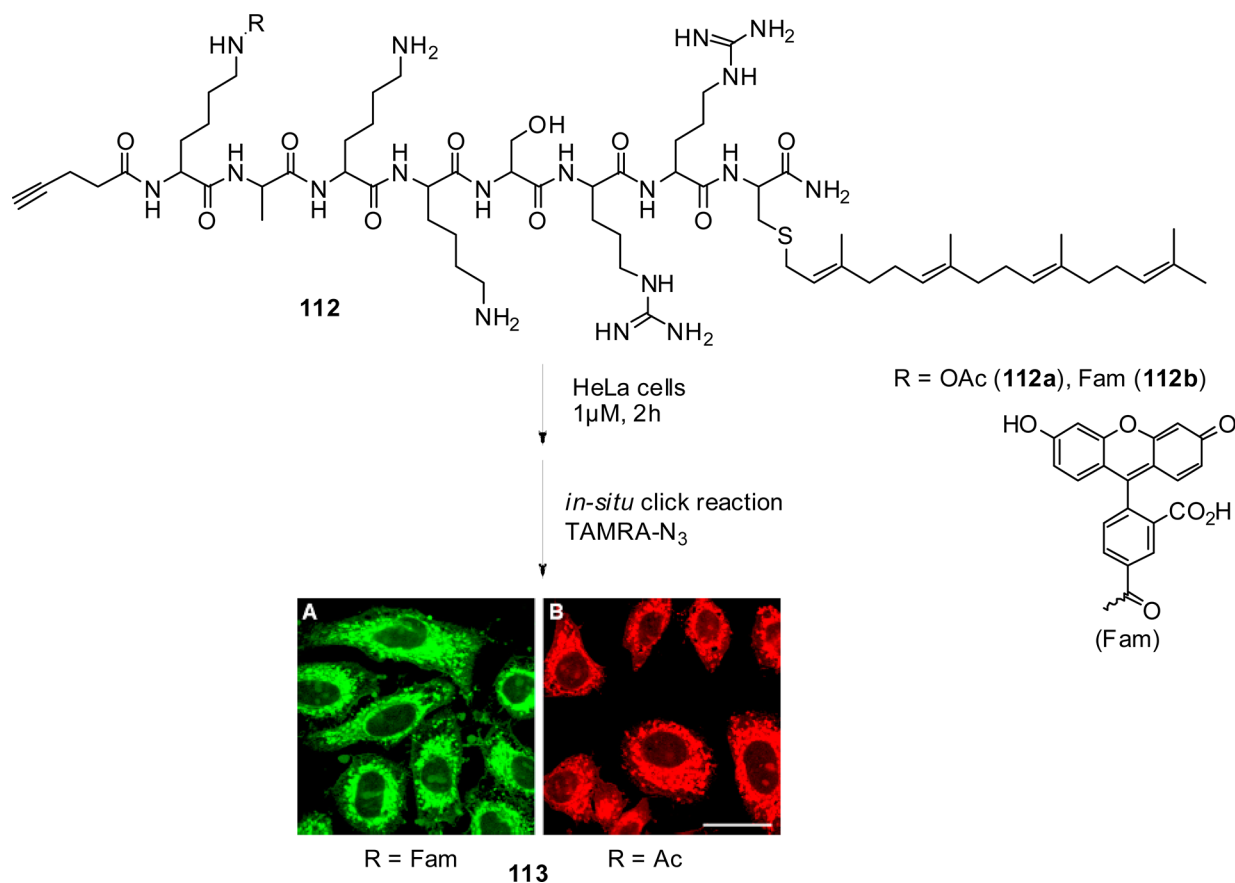


Figure 27. HeLa cells incubated with peptide 112 for 1 μM for 2 h. (A) Peptide 112 visualized by click reaction with 5-Fam-PEG-N₃ on fixed cells. (B) Peptide 112 visualized by click reaction with TAMRA-N₃ on fixed cells.

The ability of both of these peptides to enter cells was first established using confocal laser scanning microscopy (CLSM). Because peptide **112b** contains the 5-Fam fluorophore, visualization after uptake in HeLa cells is easily accomplished after a 2 h incubation of the peptide at 1 μM . A copper-catalyzed click reaction was then conducted using tetramethylrhodamine azide (TAMRA- N_3) to form a covalent triazole linkage between the peptide-alkyne and the tetramethylrhodamine (TAMRA) fluorophore; when **112a** enters cells, it could be visualized through the TAMRA fluorophore using CLSM (Figure 27), while control experiments in which HeLa cells were treated with TAMRA- N_3 (without prior peptide treatment) manifested no background labeling. Incubation of **112b** with HeLa cells and subsequent click reaction to TAMRA- N_3 resulted in strong colocalized fluorescence in the cells (yellow color, **113A**, Figure 27); this observation also confirmed that little background reaction occurs in the TAMRA- N_3 labeling process because the red TAMRA fluorophore is only present where the green 5-Fam of the peptide was observed.

The incorporation of bulky, hydrophobic fluorescent groups inevitably perturbs the chemical and physical properties of the molecules under study and hence complicates structure/function analysis. For example, the addition of the 5-Fam fluorophore to a lysine residue alters the calculated partition coefficient ($c \log P$) by 3 units, illustrating a large change in the hydrophobic properties of the parent molecule (**113B**, Figure 27). The method reported here provides a simple solution to this problem. The incorporation of a small alkyne-containing moiety into the peptide results in minimal alteration of the properties of the parent peptide. The $c \log P$ value of Lys(5-Fam) with either an acetylated N-terminus or an N-terminal alkyne differs by only approximately 0.5 units, indicating the addition of the alkyne is a rather benign change to the hydrophobicity of the peptide. However, the presence of the alkyne allowed for facile visualization via click-mediated fluorescent labeling.

5. SYNTHETIC UTILITY OF CLICK CHEMISTRY IN RECEPTOR–LIGAND BINDING STUDIES

The early pioneers of the receptor concept, notably Langley and Ehrlich, and later Clark, clearly recognized the importance of receptors in understanding diverse biological phenomena, and with great insight, they also anticipated its potential for pharmacotherapy. Receptors that couple to G-proteins communicate signals from a large number of hormones, neurotransmitters, chemokines, and autocrine and paracrine factors. G-proteins play a significant role in signaling pathways. It regulates important cellular components, such as metabolic enzymes, ion channels, and the transcriptional machinery. The resulting alterations in cellular behavior and function are manifested in many critical systemic functions, including embryonic development, learning and memory, and organismal homeostasis.¹⁴³ This results in the propagation of regulated activities through increasingly complex layers of organization to serve as the basis of integration at the systemic level. Among the many receptors, GPCRs in humans are all potentially very important drug targets. For example, glucagon and glucagon-like peptide receptors are involved in glucose metabolism; calcitonin and parathyroid hormone receptors regulate calcium homeostasis; and the CRF₁R receptor is a key regulator of the hypothalamic-pituitary-adrenal axis. All class B GPCRs bind endogenous large peptide hormones (30–40 amino acid residues) and are characterized by relatively long (up to

~160 residues) extracellular N-terminal tail domains (NTDs). Their helical trans membrane domains (TMDs) have very little primary structural conservation with respect to the more widely “drugged” class A, or rhodopsin-like, family of GPCRs. Therefore, G protein-coupled receptors (GPCRs) are the largest single class of molecular targets for therapeutic agents. However, developing synthetic ligands for one particularly attractive class of GPCRs, class B (also known as the secretin-like family of GPCRs), has been surprisingly challenging.^{144–146}

CRF₁R receptor is taken as model receptor to explain the ligand–receptor interactions and ligand generated via click chemistry reactions. Two decades of structure–activity studies of class B GPCRs and their peptide agonist ligands have led to a model in which the C-terminal region of the ligand binds to the NTD of the receptor with high affinity. This primary docking step allows the N-terminal region of the ligand to interact with the TMD of the receptor so as to facilitate some type of conformational change in the receptor, leading to activation. One interesting approach used to demonstrate the independence of the functional domains involved “tethered ligands”,⁵ which were expressed as fusion proteins with a single transmembrane helix linked to a peptide hormone fragment.¹⁴⁷

Although the structures of several class B receptor NTDs in complex with ligands or analogues have been solved, either by NMR or by X-ray crystallography, the situation is complex. For two class B receptors, the calcitonin receptor and calcitonin receptor-like receptor, ligand specificity is defined by the heterodimerization of the NTD with one of three receptor activity-modifying proteins (RAMPs). The key point, however, is that the NTD of class B GPCRs can generally fold independently and bind ligand, even in the absence of its TMD.^{144–146}

To exploit the apparently independent nature of the binding and activation domains of CRF, Perez-Balderas et al. separately prepared two peptidic constructs. One represented the basic binding domain and contained an azide group, and the second represented the activation domain and contained a complementary alkyne.¹⁴⁷ The “click” chemistry, of course, worked; but, more importantly, the resulting peptide–peptide conjugate CRF analogue was active in cell-based receptor activation assays. Not only did the purified conjugates achieve this, but crude preparations made from libraries of “variable probe” activation domain fragments did as well, once the copper catalyst from the click step was diluted out. This approach allowed efficient structure–activity relationship studies on the activation domain that showed that Ser6 and Asp8 were essential for activation. The idea behind these experiments was to design a ligand with enhanced agonist properties, and this exercise was so spectacularly successful, first with three substitutions, and then with an additional three, that a hexasubstituted full-agonist peptide was produced with low nanomolar efficacy. Of note is that five of the six substitutions involved hydrophobic, unnatural amino acids. Strikingly, the optimized activation domain analogue worked even in the absence of a coupled binding domain: no further increase in potency was observed when the high-affinity carrier was restored (Figure 28).

This observation alone is interesting because it has been suggested that click chemistry is an emerging power tool for the development of ligands for the receptor activation and binding studies.

Several research groups used the click chemistry reaction for the development of selective agonist, antagonist, and efficient

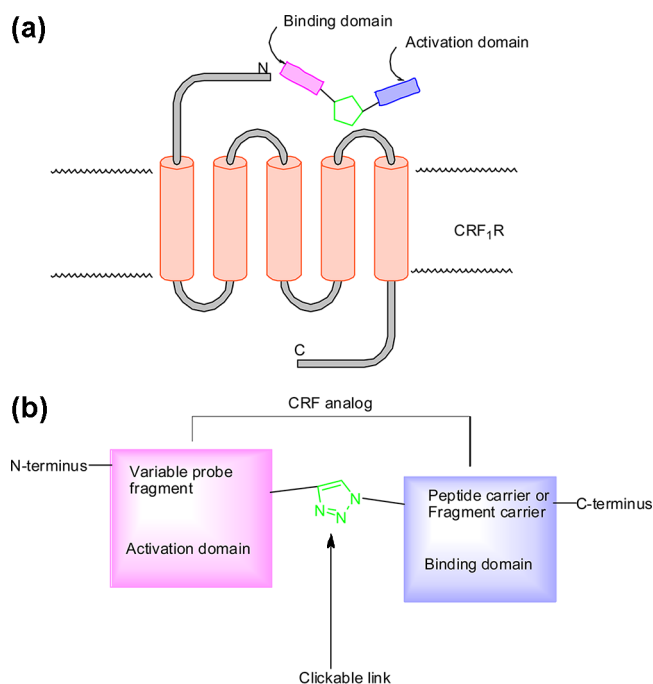


Figure 28. Peptide–peptide conjugates bind to and activate the corticotropin-releasing-factor receptor 1 (CRF1R). (a) The C-terminal binding domain of the CRF analogue ligand interacts with the extracellular N-terminal domain of CRF1R, whereas the N-terminal activation domain causes receptor activation by interacting with its helical bundle region. (b) A “clickable” link is introduced between two independent functional units of the CRF analogue, which facilitates optimization of agonist activity of the N-terminal activation domain.

binding ligands for various GPCR receptors. These developments of the new agonist, antagonist, and efficient binding ligands are very useful in the new drug discovery for uncured diseases. Here, we are presenting some of the click chemistry literature used in selective agonist, antagonist, and efficient binding ligands development.

5.1. Selective Agonists

The adenosine receptor (AR) is a G protein-coupled receptor, found in myocytes, astrocytes, neurons, neutrophils, eosinophils, and other cell types. Both A_3 AR agonists and antagonists are proposed for the treatment of cancer and inflammatory diseases. An antiischemic effect of A_3 AR agonists also suggests their use in the protection of skeletal muscle and cardiac muscle.¹⁴⁸

Calenbergh and his workers explored click chemistry to synthesize two series of 2-(1,2,3-triazolyl)adenosine derivatives. Binding affinity at the human A_1 , A_2 , and A_3 ARs (adenosine receptors) and relative efficacy at the A_3 AR of these compounds were determined. Some triazol-1-yl analogues showed A_3 AR affinity in the low nanomolar range, with a high ratio of A_3/A_2A selectivity, and a moderate-to-high A_3/A_1 ratio. The 5'-OH ethyluronamide analogues showed increased A_3 AR affinity and behaved as full agonists, that is, compound **114** (Figure 29), with 910-fold A_3/A_1 selectivity with $K_i = 1.8 \pm 0.6$ nM.¹⁴⁸

Jacobson et al. employed click chemistry for the synthesis of 2-dialkynyl derivatives of *N*-methanocarba triazole nucleosides for A_3 adenosine receptor-selective agonists' development. The most potent and selective novel compound was a 1-adamantyl derivative **115** ($K_i = 6.5$ nM, Figure 29), which suggested the

existence of a hydrophobic binding pocket in this region of the receptor. Curiously, this compound proved to be a partial agonist of the A_3 AR with only 27.8% of the maximal efficacy in comparison to 5'-*N*-ethylcarboxamidoadenosine.¹⁴⁹

The same research group also developed a series of potent and selective A_3 adenosine receptor (AR) agonists (north-methanocarba nucleoside 5'-uronamides) containing dialkyl groups on extended adenine C2 substituents. Polyamidoamine (PAMAM) dendrimer triazole conjugate series was prepared using click chemistry reaction of alkyne of a 2-octadiynyl nucleoside and azide-derivatized G4 (fourth-generation) PAMAM dendrimers. A_3 AR activation was preserved in these multivalent conjugates, which bound with an apparent K_i of 0.1–0.3 nM. A bifunctional conjugate **116** (Figure 29) activated both A_3 and A_1 with selectivity in comparison to other ARs receptors.¹⁵⁰

Ten 1,4-disubstituted 1,2,3-triazoles were prepared and tested for their ability to increase oleic acid oxidation in human myotubes using a high-throughput multiwell assay. Compound **117** (Figure 29) exhibited potent agonist activities with peroxisome proliferator-activated receptors (PPAR). Compound **117** exhibited dual agonist effects for both PPAR α and PPAR δ in a luciferase-based assay with an EC_{50} value of 0.85 nM.¹⁵¹

A series of new 1-aryl-3-benzazepine derivatives containing an arylpiperazinyl function as the N3 substituent were synthesized by combining a D1 receptor agonistic pharmacophore and a 5HT $_{1A}$ receptor pharmacophore through click reaction. Compound **118** (Figure 29) showed the highest affinity at the 5HT $_{1A}$ receptor with a K_i value of 85 nM. Functional assays indicated that compound **118** showed full agonistic activity with 5-HT $_{1A}$ receptor.¹⁵²

The cytokine MIF is involved in inflammation and cell proliferation via pathways initiated by its binding to the trans membrane receptor CD74. MIF also promotes AMPK (adenosine monophosphate-activated protein kinase) activation with potential benefits for response to myocardial infarction and ischemia-reperfusion. Jorgensen and his co-workers reported the design and synthesis of agonists for MIF-CD74 receptors using click chemistry. The three compounds (**119a**, **119b**, and **119c**, Figure 29) showed full agonist effect with MIF-CD74 receptor.¹⁵³

The 41-amino acid peptide corticotropin releasing factor (CRF) is a major modulator of the mammalian stress response. Upon stressful stimuli, it binds to the corticotropin releasing factor receptor 1 (CRF1R), a typical member of the class-B G-protein-coupled receptors (GPCRs) and a prime target in the treatment of mood disorders.^{147,154}

Hausch and his co-workers employed click chemistry for the development of peptide–peptide conjugates ligand synthesis for full activator of CRF1R using a high-throughput approach. An acetylene-tagged peptide library was synthesized and conjugated to an azide-modified high-affinity carrier peptide derived from the CRF C-terminus using copper-catalyzed dipolar cycloaddition. The resulting conjugates reconstituted potent agonists and were tested in situ for activation of the CRF1 receptor in a cell-based assay. Compound **120** (Figure 29) showed good activation and binding affinity toward CRF1 receptor. Some unnatural amino acid peptide–peptide conjugates also were synthesized using click chemistry, and these unnatural amino acid peptide–peptide conjugates showed good binding affinity and activation with CRF1 receptor with IC_{50} values of 1.6 ± 1.0 nM. By use of this approach, researchers

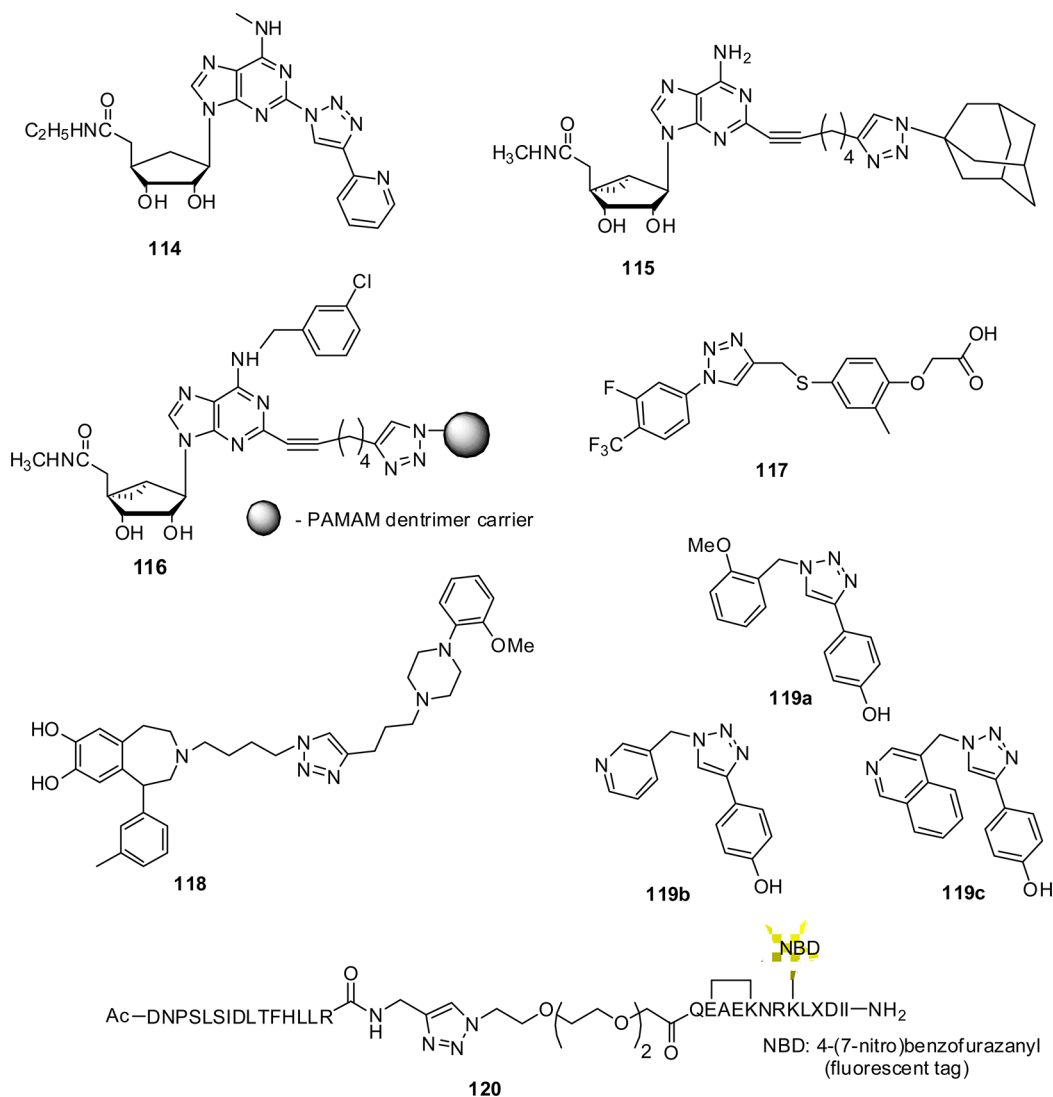


Figure 29. Chemical structures of agonist effect on various receptors synthesized via click chemistry.

achieved the following outcomes: (i) defined the minimal sequence motif that is required for full receptor activation, (ii) identified the critical functional groups and structure–activity relationships, (iii) developed an optimized, highly modified peptide probe with high potency ($EC_{50} = 4$ nM) that is specific for the activation domain of the receptor, and (iv) probed the behavioral role of CRF receptors in living mice.¹⁵⁴

5.2. Selective Antagonists

Jacobson and his co-workers prepared GPCR ligand–dendrimer (GLiDe) conjugates from a potent adenosine receptor (AR) antagonist for treating Parkinson’s disease, asthma, and other diseases. Xanthine amine congener (XAC) was appended with an alkyne group on an extended C8 substituent for coupling by Cu(I)-catalyzed click chemistry with azide-derivatized G4 (fourth-generation) PAMAM dendrimers to form triazoles. These conjugates also contained triazole-linked PEG groups (8 or 22 moieties per 64 terminal positions) for increasing water-solubility and optional prosthetic groups for spectroscopic characterization and affinity labeling. Human AR binding affinity increased progressively with the degree of xanthine substitution to reach K_i values in the nanomolar range. The order of affinity of each conjugate was $hA_2AR > hA_3AR > hA_1AR$, while the corresponding monomer was ranked hA_2AR

$> hA_1AR \geq hA_3AR$. The antagonist activity of the most potent conjugate **121** (Figure 30) (34 xanthines per dendrimer) was examined at the G_i -coupled A_2AR , and it showed significant binding affinity toward A_2AR at low nanomolar concentration. Conjugate **122** (Figure 30) showed most potent antagonist activity toward A_2AR with a K_i value of 6.2 ± 0.9 nM.¹⁵⁵

“Click chemistry” was explored to synthesize two series of 2-(1,2,3-triazolyl)adenosine derivatives. Binding affinity at the human A_1 , A_2 , and A_3ARs (adenosine receptors) and relative efficacy at the A_3AR were determined. 2-Triazole analogues with an unmodified ribose moiety **123** (Figure 30) showed good antagonist activity at the A_3AR .¹⁴⁸

Chaiken and his co-workers explored click chemistry for the synthesis of high-affinity dual antagonist for HIV-1 envelope glycoprotein gp120. The peptide **124** (Figure 30) of (2*S*,4*S*)-4-(4-phenyl-1*H*-1,2,3-triazol-1-yl)pyrrolidine-2-carboxylic acid ($K_i = 12.7$ nM) at residue position 6 was binding to gp120 with an affinity 2 orders of magnitude greater than that of the parent peptide and strongly inhibits the interaction of gp120 with both CD4.¹⁵⁶

A series of peptide conjugates was constructed via click reaction of both aryl and alkyl acetylenes with an internally incorporated azidoproline derived from the parent peptide.

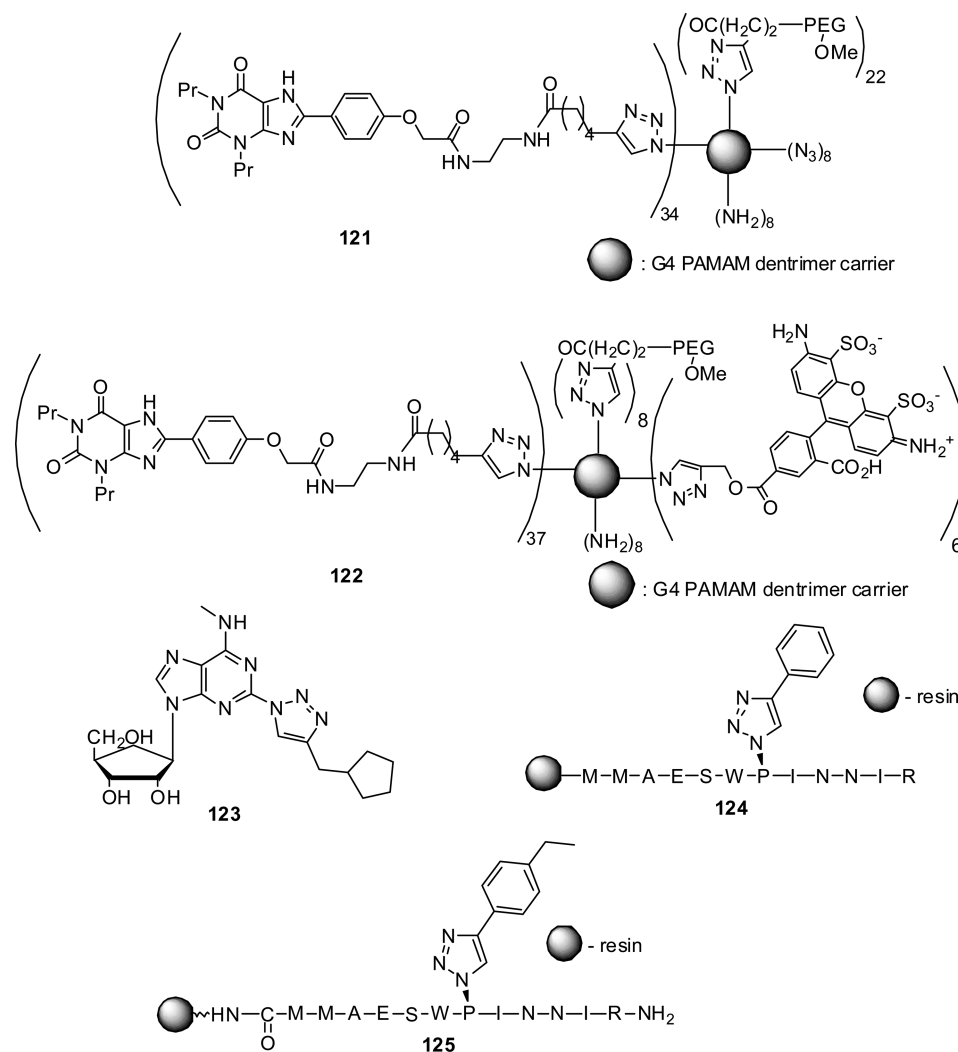


Figure 30. Chemical structures of antagonist effect on various receptors synthesized via click chemistry.

These conjugates (compound **125**, Figure 30) were found to exhibit several orders of magnitude increase in both affinity for HIV-1 gp120 and inhibition potencies at both the CD4 and the coreceptor binding sites of gp120 with $K_d = 9$ nM. Structural factors in the added triazole grouping were responsible for the increased binding affinity and antiviral activity of the dual inhibitor conjugates. Peptide conjugate potencies were measured in both kinetic and cell infection assays. High affinity was sterically specific, being exhibited by the *cis*- but not the *trans*-triazole. The results demonstrated that aromatic, hydrophobic, and steric features in the residue 6 side-chain are important for increased affinity and inhibition (compound **125**, Figure 30).¹⁵⁷

De novo design of small molecules to bind to the MIF tautomerase active site was carried out using the program BOMB (biochemical and organic model builder) and aryl-1,2,3-triazole derivatives were discovered that also showed 1 μ M potency in inhibiting the binding of MIF to its receptor CD74. Compound **126** (Figure 31) showed antagonist effect with CD74 receptor with $IC_{50} = 0.9$ μ M.¹⁵³

Gmeiner and his co-workers employed click chemistry for the synthesis of 1,1'-substituted ferrocene triazole derivatives for the development of novel antagonist for dopamine receptor. The 1,1'-substituted ferrocene triazole derived appendages were used for the fine-tuning of biological activity and for the

attachment of linker units generating bivalent GPCR ligands. Receptor binding was evaluated by radio-ligand displacement experiments, revealing super affinity with sub- to single-digit nanomolar K_i values for particular test compounds. As a neutral antagonist at the dopamine receptors D3 and D4 and a potent partial agonist at the D2 subtype (intrinsic activity = 57%, $EC_{50} = 2.5$ nM), the bifunctional ferrocene **127** (Figure 31) revealed a novel and unique activity profile.¹⁵⁸

Dopamine D2 receptor homo dimers might be of particular importance in the pathophysiology of schizophrenia and, thus, serve as promising target proteins for the discovery of typical antipsychotics. A highly attractive approach to investigate and control GPCR dimerization may be provided by the exploration and characterization of bivalent ligands, which can act as molecular probes simultaneously binding two adjacent binding sites of a dimer. The synthesis of bivalent dopamine D2 receptor ligands was described, incorporating the privileged structure of 1,4-disubstituted aromatic piperidines/piperazines (1,4-DAPs) and triazolyl-linked spacer elements. Radioligand binding assays revealed that the bivalent ligands exhibited a distinct binding profile as compared to monovalent analogues containing capped spacer and asymmetric "dummy ligands" incorporating one original pharmacophore, while the second pharmacophore is replaced by a structurally similar nonbinding motif. Bivalent ligands **128** and **129** (Figure 31) revealed a

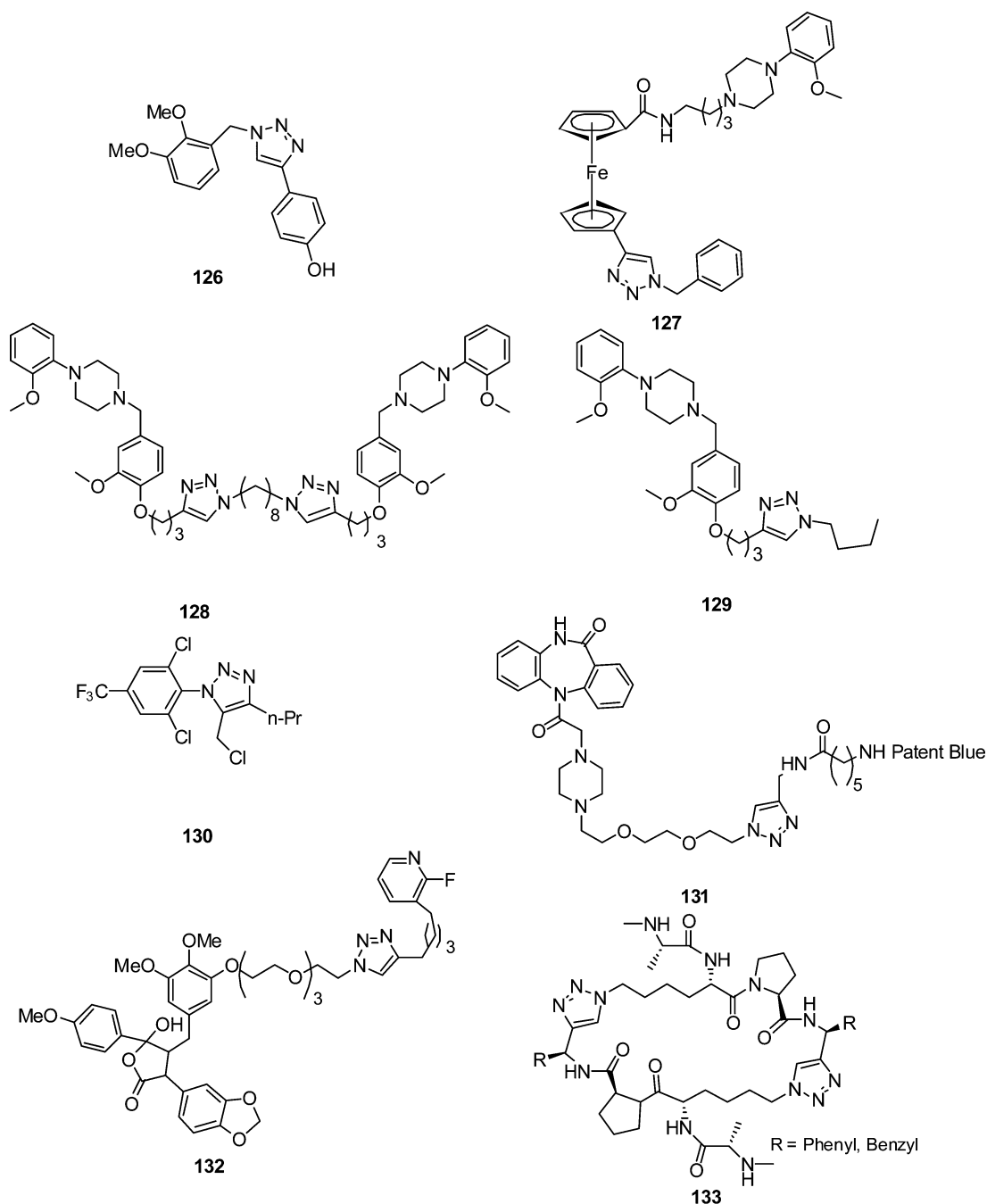


Figure 31. Chemical structures of antagonist effect on various receptors synthesized via click chemistry.

most potent binding affinity toward the D2 receptors with $K_i = 22 \pm 2.4$ and 67 ± 12 nM binding affinity toward hD_{2long} .¹⁵⁹

Ozoe and his co-workers recently reported the synthesis and docking studies of 1-phenyl-1*H*-1,2,3-triazoles as selective antagonists for β_3 over $\alpha_1\beta_2\gamma_2$ GABA receptors. Among all tested triazole compounds, the 4-*n*-propyl-5-chloromethyl analogue of 1-(2,6-dichloro-4-trifluoromethylphenyl)-1*H*-1,2,3-triazole (compound **130**, Figure 31) showed the highest level of affinity for both β_3 over $\alpha_1\beta_2\gamma_2$ receptors, with K_i values of 0.659 and 266 nM, respectively.¹⁶⁰

Tagged biologically active molecules represent powerful pharmacological tools to study and characterize ligand receptor interactions. Click chemistry was used as a tool to facilitate the access to labeled novel pirenzepine derivatives. The incorpo-

ration of a fluorophore (Lissamine Rhodamine B), a non-fluorescent dye (Patent Blue VF), or biotin into a muscarinic antagonist scaffold was derived from pirenzepine using click chemistry. The affinity of the compounds for the *human* M1 muscarinic receptor fused to EGFP (enhanced green fluorescent protein) was checked under classical radioligand and FRET (fluorescence resonance energy transfer) binding assays. The pirenzepine constructs (**131**, Figure 31) displayed a nanomolar affinity ($K_i = 16.3$ nM) for the M1 receptor. In addition, both dye-labeled derivatives behave as potent acceptors of energy from excited EGFP with a very high quenching efficiency.¹⁶¹

The expression and function of endothelin (ET) receptors are abnormal in cardiovascular diseases, tumor progression, and

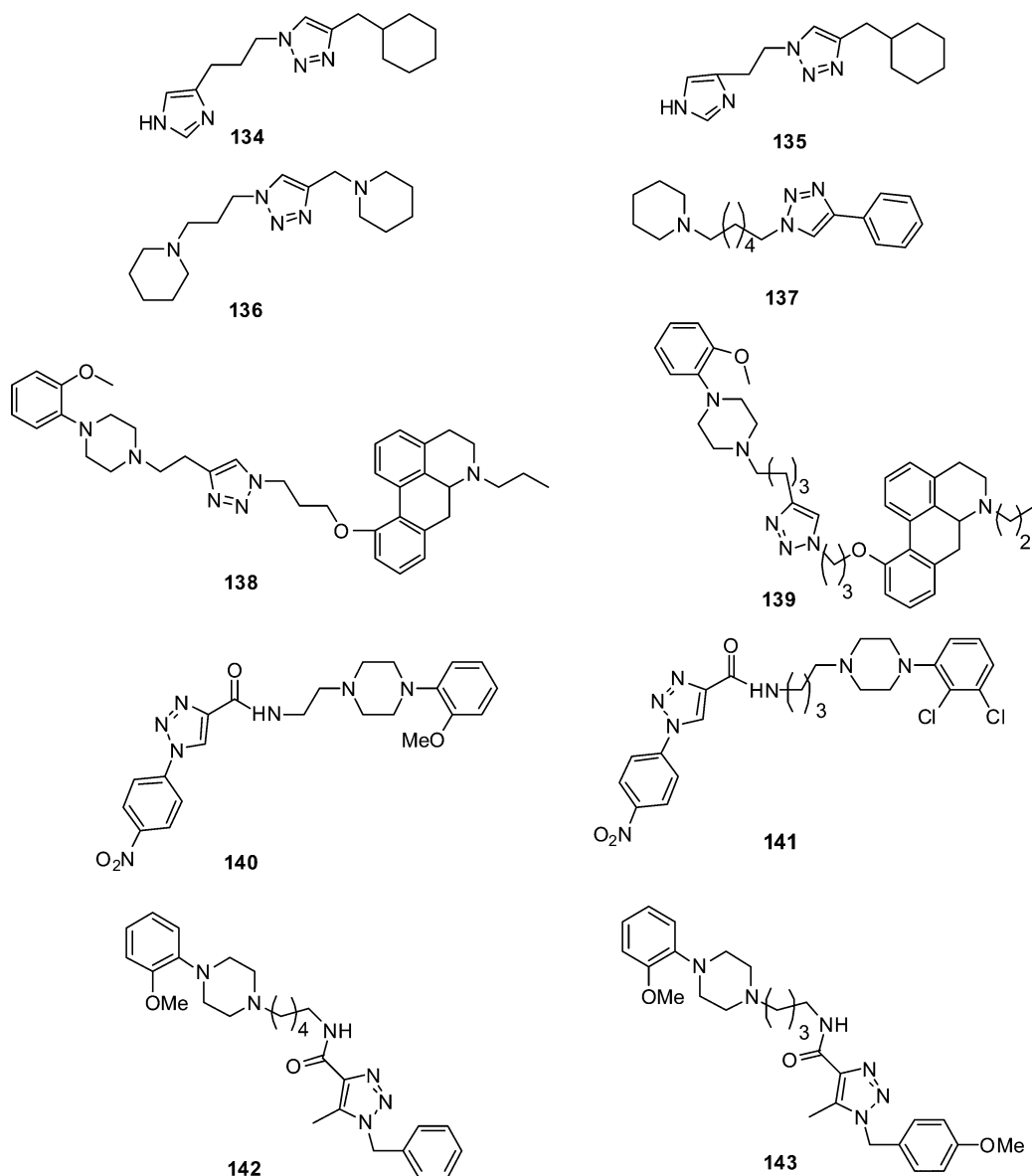


Figure 32. Chemical structures of receptor-selective binding ligands explored via click chemistry.

tumor metastasis. Michel and his co-workers explored click chemistry for the synthesis of new high affinity ET_A selective receptor ligands with $c \log D$ values ranging from 1.50 to 3.90, which allow systematic investigations of pharmacokinetic properties and metabolic stability. The compound **132** (Figure 31) showed good selectivity toward ET_B/ET_A with $K_i = 37 \pm 22$ nM for ET_B and $K_i = 3.5 \pm 2.4$ nM for ET_A .¹⁶²

Wang and his co-workers employed click chemistry for the synthesis of cyclopeptidic Smac (second mitochondria-derived activator of caspase) mimetics. These two compounds (**133**, R = Ph, Bz) bind to XIAP (X-linked inhibitor of apoptosis protein) and cIAP-1/2 (Cellular Inhibitor of Apoptosis-2) with low nanomolar affinities, and restore the activities of caspase-9 and caspase-3/-7 inhibited by inhibitors of apoptosis proteins (XIAP). Compound **133** (Figure 31) ($IC_{50} = 0.43$ nM antagonist effect with XIAP4 (R = phenyl), $IC_{50} = 1.3$ nM antagonist effect with XIAP4 (R = benzyl)) potently inhibits cancer cell growth and is 5–8 times more potent than the initial lead compound.¹⁶³

5.3. Selective Binding Ligands

The histamine H_3 (H_3R) and H_4 (H_4R) receptors attract considerable interest from the medicinal chemistry community. It is playing an important role in inflammation and immune responses with possible applications in diseases such as inflammatory bowel disease, allergic asthma, and pruritis. Interrogated H_4R/H_3R selectivities use ligands with a triazole core. Wijtman and co-workers employed Cu(I)-assisted “click chemistry” to assemble diverse triazole compounds containing a peripheral imidazole group. The imidazole ring posed some problems in the click chemistry putatively due to Cu(II) coordination, but Boc protection of the imidazole and removal of oxygen from the reaction mixture provided effective strategies. Pharmacological studies of triazole scaffold proved remarkably sensitive H_4R affinities. With subtle changes in the aliphatic group, **134** and **135** (Figure 32) were obtained, which boosted high H_4R affinity ($pK_i = 8.08$ and 7.12) and a good H_4R/H_3R selectivity of 15 and 10 noteworthy for a mono-substituted imidazole compound. In contrast, a replacement of both peripheral groups by piperidines led to compound **136**

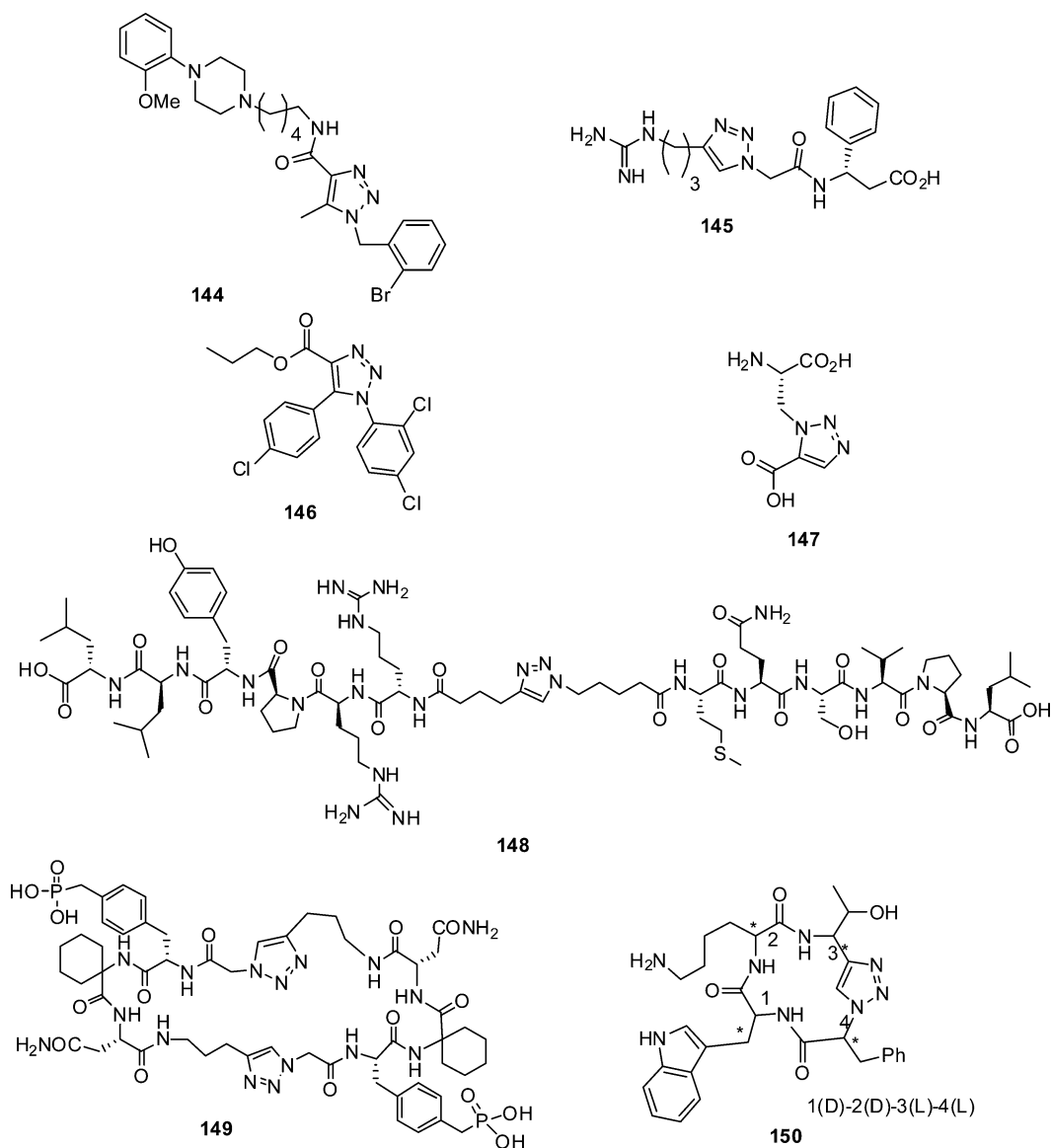


Figure 33. Chemical structures of efficiently receptor binding ligands synthesized via click chemistry.

with good H_3R affinity ($pK_i = 6.92$) and excellent H_3R/H_4R selectivity (320).¹⁶⁴

Human histamine H_3 receptors (hH_3R) in the central nervous system (CNS) are auto- and heteroreceptors modulating the synthesis and the release of histamine as well as the liberation of various other neurotransmitters. Hence, histaminergic neurons, which spread from the tuberomammillary nucleus into most parts of the brain, influence the neurotransmitter balance in the respective compartments in the dependence of colocalized neurons. Central functions like vigilance, attention, and learning are affected. Modulation of this neuronal interplay by hH_3R antagonists/inverse agonists might be an effective approach in the therapy of neuronal diseases, for example, cognitive impairment, sleep/wake disorders, epilepsy, and obesity. The diversity of potential indications gives a hint of the complexity of hH_3R modulation. Stark and his co-worker employed click chemistry for the synthesis of human histamine H_3 receptor (hH_3R) binding ligands using ω -piperidinylalkyl azide derivatives. Compound 137 (Figure 32) ($pK_i = 6.6$) showed the most binding affinity

toward hH_3R within this series, showing receptor binding affinity in the nano- and subnanomolar concentration range.¹⁶⁵

Dopamine (DA) D_3 receptor belongs to the D_2 -like subfamily of dopamine receptors, including D_2 , D_3 , and D_4 , functionally distinct from the D_1 -like subfamily (D_1 and D_5). D_3 receptor is implicated in a variety of brain functions and proposed as a promising therapeutic target for a number of neurological and psychiatric disorders, including schizophrenia, depression, drug abuse, Parkinson's disease, and restless leg syndrome. Zhang and co-workers explored click chemistry for the synthesis of a series of new aporphine analogues (aporphines) prepared from appropriate precursors and aryl piperazines. Compound 138 (Figure 32) displayed good to high affinity at the D_3 receptor, and low or no affinity at the D_1 and D_2 receptors with $K_i = 1.14$ nM against D_3 receptor. Compound 139 (Figure 32) was identified as the most potent at the D_1 and D_2 receptors among our newly synthesized analogues with K_i values of 1.9 and 0.206 μ M against D_1 and D_2 receptor, respectively.¹⁶⁶

Gmeiner et al. successfully applied click chemistry for a parallel synthesis of dopaminergic phenyltriazoles utilizing the

triazolylmethylcatechol (TMC) resin. A focused model library of 20 test compounds revealing three points of diversity was generated by a three-step SPOS (solid-phase organic synthesis) approach. Product purification was performed employing a solid-supported carboxylic acid anhydride as a scavenger. GPCR-ligand binding screening revealed dopamine D₃ ligand (**140**, Figure 32) with K_i values in the single digit nanomolar range. Also, compound **141** showed good binding affinity toward $\text{P}\alpha 1$ with a K_i value of 6.5 nM.¹⁶⁷

Gmeiner and his research group employed click chemistry for a parallel solid-supported synthesis of formylaryloxymethyl-triazole (FAMT) resins. A library of 60 test compounds revealing three points of diversity was generated by a four-step BAL-based strategy including reductive amination, acylation, 1,3-dipolar cycloaddition, and TFA-induced cleavage. The target compounds were screened for neuroreceptor binding employing eight different GPCRs, whereas high-affinity dopamine D₃ and $\alpha 1$ -receptor binders were identified. The library members **142**, **143**, and **144** (Figures 32 and 33) revealed K_i values ($K_i = 56$ pm for compound **142**, $K_i = 58$ pm for compound **143**, and $K_i = 58$ pm for compound **144**) for the $\text{P}\alpha 1$ receptor in the medium picomolar range.¹⁶⁸

Integrin receptors constitute a large family of proteins with structural characteristics of noncovalent heterodimeric glycoproteins formed of α and β subunits. One important recognition site for many integrins is the arginine-glycine-aspartic acid (RGDa) tripeptide sequence, found in a series of peptide-based ligands such as vitronectin, fibronectin, and osteopontin. Regarding RGD-dependent integrins, $\alpha_v\beta_3$ and $\alpha_v\beta_5$ receptors have received increasing attention as therapeutic targets, as they are expressed in various cell types and are involved in inflammatory and tumor-related processes. $\alpha_v\beta_3$ integrin expression is up-regulated in many solid tumors and contributes to the mechanisms involved in tumor growth and metastatic dissemination. During the progression from a benign melanocytic disease to a metastatic malignant melanoma, melanocytes undergo a series of changes in the expression of cell-surface molecules, including $\alpha_v\beta_3$ integrin. Guarna and his co-workers employed click chemistry for the discovery of triazole-based arginine-glycine-aspartate (RGD) mimetics, which showed binding affinity properties toward $\alpha_v\beta_3/\alpha_v\beta_5$ integrins. Biological assays showed compound **145** (Figure 33) capable of binding $\alpha_v\beta_3$ integrin with nanomolar affinity ($K_i = 1.35 \pm 0.25$ nM binding affinity toward $\alpha_v\beta_3$ and $K_i = 1.02 \pm 0.12$ nM binding affinity toward $\alpha_v\beta_5$) according to a two-sites model, and molecular modeling studies revealed a peculiar π -stacking interaction between the triazole ring and Tyr178 side chain. Accordingly, compound **145** inhibited the adhesion of integrin-expressing human melanoma cells to RGD-containing proteins of the extracellular matrix, such as vitronectin, fibronectin, and osteopontin, and also angiogenesis in the in vitro and in vivo experimental models. The relevant biological effects exerted by compound **145** suggest its potential application as an antiangiogenic agent in the diagnosis and therapy of tumors where $\alpha_v\beta_3$ integrin expression is up-regulated.¹⁶⁹

The wide range of pharmacological effects of cannabinoid and endogenous cannabinoid ligands is mediated by two subtypes of transmembrane G-protein coupled receptors: CB1 and CB2. CB1 receptors are expressed in the central nervous system (CNS) with high density in the cerebellum, hippocampus, and striatum. CB1 receptors are found in some peripheral tissues (urinary bladder, testis, and ileum) as well.

CB2 receptors are predominantly located in the immune system (tonsils, spleen, and immune cells) with very low concentration in the CNS.⁶ CB1 agonists have potential therapeutic applications in developing drugs for pain, nausea, glaucoma, stroke, cancer, and neurological disorders such as multiple sclerosis and Parkinson's disease. The potential applications of CB1 antagonists include the therapeutic treatment of obesity and related metabolic disorders as well as medications for drug addiction. Trudell and his workers employed click chemistry for the synthesis of a series of 4-alkoxycarbonyl-1,5-diaryl-1,2,3-triazoles and evaluated them as a novel class of potent cannabinoid receptor ligands. The *n*-propyl ester **146** ($K_i = 4.6$ nM, Figure 33) exhibited the most potent binding affinity toward cannabinoid receptor of the series.¹⁷⁰

AMPA receptors are heterotetrameric combinations of GluR1–4 subunits that provide the major fast excitatory inputs in the CNS. Regulation of AMPA receptor number at the post synaptic membrane contributes to changes in synapse strength and to synaptic plasticity. Such regulation requires a synaptic infrastructure that controls the trafficking and localization of receptors, such as through the interaction of receptors with synaptic scaffolding proteins. The central nervous system glutamate receptors are an important target for drug discovery. Abell and his co-workers reported the synthesis and glutamate receptor activity of 1,4- and 1,5-disubstituted 1,2,3-triazolyl amino acid glutamate homologues. In vitro screening indicated selective binding for **147** (Figure 33) at AMPA receptors of the series with an IC_{50} value of 49 μM .¹⁷¹

Neurotensin (NT) is an amino acid containing neuro peptide expressed within the central nervous system and in peripheral tissues like the gastrointestinal tract system. NT binds to the neurotensin receptor (NTR) where three different subtypes, NTR1, NTR2, and NTR3, are characterized. NTR1 and NTR2 belong to the family of G-protein coupled receptors, and their internalization mechanism via receptor-mediated endocytosis is well described by Mazella et al.^{172a} In the past decade, numerous studies described NTR as a promising target for cancer diagnosis and therapy. Wuest and co-workers employed click chemistry for the synthesis of neurotensin containing peptide heterodimers analogues. Neurotensin-containing peptide dimers analogues were used in an in vitro binding assay to determine binding affinity toward the neurotensin receptor-1 (NTR1). The determined IC_{50} values of 0.7 μM indicated only very low binding affinity of the neurotensin (compound **148**, Figure 33)-containing peptide hetero dimer toward the NTR1.^{172b}

The growth factor receptor-bound protein 2 (Grb2) is an SH2 domain-containing signal transducer that represents an attractive therapeutic target. For Grb2 SH2 domains, where open-chain "pTyr-Xxx-Asn" sequences are preferentially recognized in type-I β -turn conformations, induction of turn geometries through macrocyclization using ring-closing olefin metathesis2 (RCM) has resulted in a number of potent binding inhibitors. Burke and his workers employed click chemistry for the synthesis of triazole-containing macrocycles based on the Grb2 SH2 domain-binding motif, "Pmp-Ac6c-Asn", where Pmp and Ac6c stand for 4-phosphonomethylphenylalanine and α -amino cyclohexane carboxylic acid, respectively. In Grb2 SH2, domain-binding assays revealed that compound **149** (Figure 33) showed the most binding affinity toward Grb2 SH2 of the series with $K_{d1} = 1.8$ nM and $K_{d2} = 4.0$ nM.¹⁷³

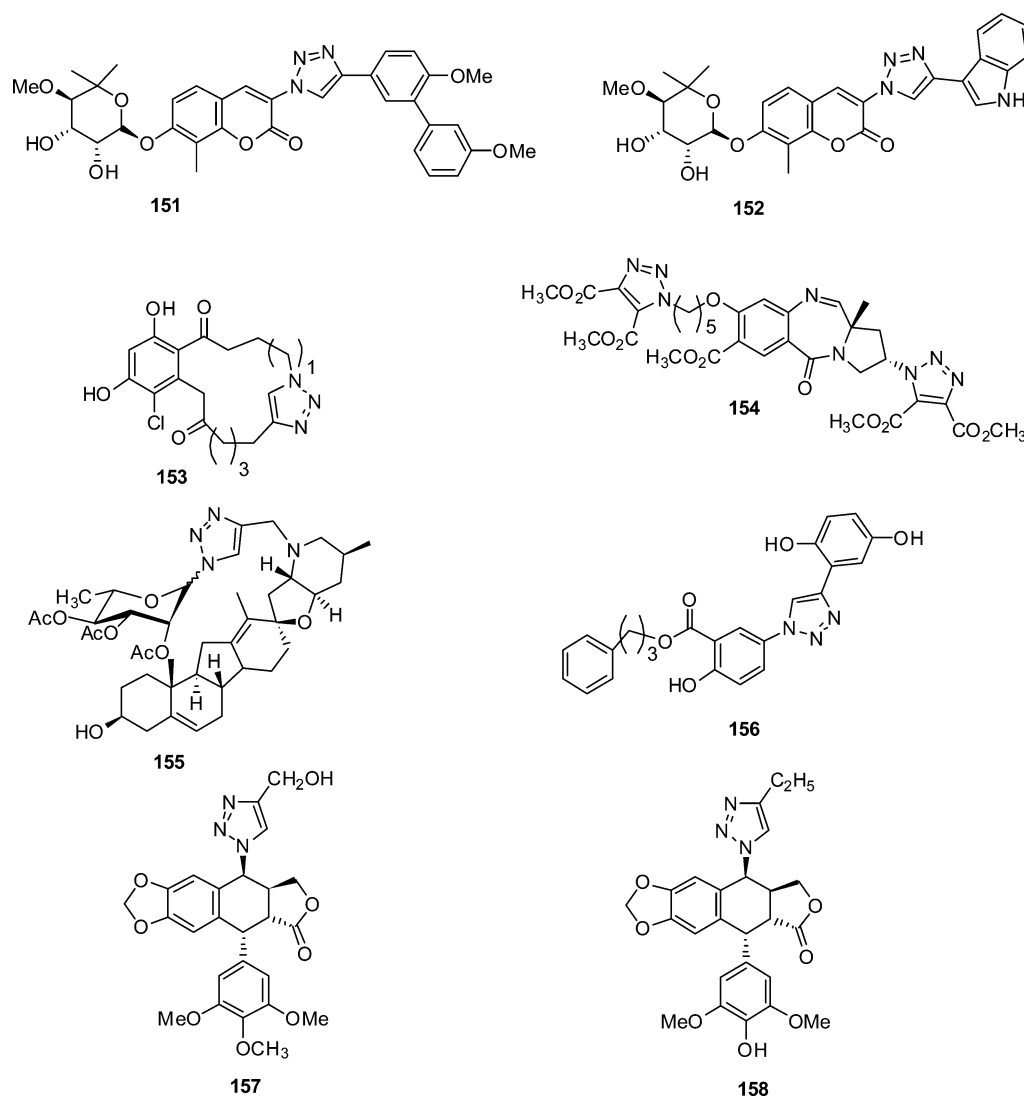


Figure 34. Chemical structures of anticancer drugs constructed via click chemistry.

Ghadiri and co-workers also reported 1,4-substituted triazole-based peptidomimetics as ligands for the somatostatin receptor (SSTR). Here, the triazole was used to mimic a *trans*-peptide bond within a tetrapeptide. Sixteen stereoisomeric peptidomimetics were synthesized by CuAAC, using the ligand TBTA to suppress competing homodimer formation (compound **150**, Figure 33). NMR analysis showed that all compounds existed in a single conformation on the NMR time scale. The compounds exhibited diverse selectivity against the five human SSTR subtypes 1–5. In an attempt to define the three-dimensional pharmacophoric requirements for receptor binding, the most potent human SSTR subtype 4 peptidomimetic was overlaid with all of the other peptidomimetics. Three ligand groups were thus identified: selective ligands, broad spectrum binders, and low affinity ligands. Compound **150** displayed a IC_{50} value of 67 ± 30 nM binding affinity toward *hSSTR*₃ (human somatostatin receptor-3).¹⁷⁴

6. CLICK CHEMISTRY IN DRUG DEVELOPMENT USING FRAGMENT-BASED DRUG DISCOVERY

The main target in medicinal chemistry is to synthesize compounds or libraries of compounds during the process of drug discovery or lead optimization, and for this reason, this

field is particularly attracted to synthetic methodologies that allow rapid construction of molecules. The identification of such rapid synthetic strategies should allow the medicinal chemist to assemble a large number of biologically active compounds in a very short period of time, speeding up the process of discovery and lead optimization. Click chemistry is one of the powerful tools to synthesize many drugs using fragment-based drug screening methods.^{175,176} This click-FBDD-based screening allows for more efficient lead identification and lead optimization procedures in medicinal chemistry. In this context, it is easy to predict the usefulness of this reaction in fragment-based ligand design. Triazole peptidomimetic fragments are generated, and these could act as building blocks to be used in the fragment-based approach to drug discovery, thereby rendering this technique feasible in drug discovery. Hence, we are describing some potential applications of the click chemistry reaction found in the literature toward novel drug development for many incurable diseases such as anticancer, anti-TB, etc.^{175–178}

Blagg and his co-workers employed click chemistry for the synthesis of a series of triazole-containing novobiocin analogues. These compounds contain a triazole ring in lieu of the amide moiety present in the natural product. The

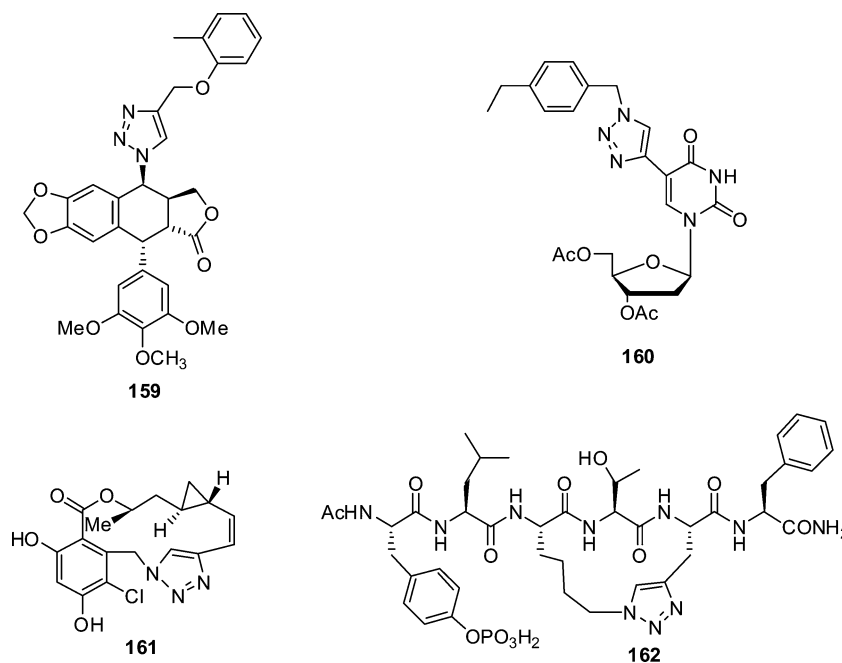


Figure 35. Chemical structures of anticancer drugs generated via click chemistry.

antiproliferative effects of these compounds were evaluated against two breast cancer cell lines (SKBr-3 and MCF-7), and manifested activities similar to those of their amide-containing counterparts. In addition, Hsp90-dependent client protein degradation was observed via Western blot analyses, supporting a common mode of Hsp90 inhibition for both structural classes. Compounds **151** and **152** showed most potent inhibition against SKBr-3 and MCF-7 among homologous series with $IC_{50} = 13.16 \pm 3.85 \mu\text{M}$ against MCF-7 and $IC_{50} = 21.22 \pm 5.99 \mu\text{M}$ against SKBr-3 for compound **151**. Compound **152** exhibited a IC_{50} value of $18.33 \pm 4.67 \mu\text{M}$ against MCF-7 and $IC_{50} = 8.17 \pm 0.11 \mu\text{M}$ against SKBr-3.¹⁷⁹

A series of benzo-macrolactone derivatives were prepared by click chemistry reaction and evaluated as inhibitors of heat shock protein 90 (Hsp90), an emerging attractive target for novel cancer therapeutic agents. A new synthesis of these resorcylic acid macrolactone analogues of the natural product radicicol is described in which the key steps are the acylation and ring-opening of a homophthalic anhydride to give an isocoumarin, followed by a ring-closing metathesis to form the macrocycle. The novel triazole-macrocyclic lactones were evaluated for Hsp90 inhibition in two Hsp90 binding assays: the fluorescence polarization (FP) assay and the TR-FRET assay. Their growth inhibitory potency in HCT116 human colon cancer cell line, as measured by the SRB assay, was also determined. Compound **153** (Figure 34) showed good inhibition of Hsp90 in the FP assay in the series with $IC_{50} = 2.7 \pm 1.3 \mu\text{M}$.¹⁸⁰

1,2,3-Triazole-based molecules are useful pharmacophores for several DNA-alkylating and cross-linking agents. A series of A/C8, C/C2, and A/C8-C/C2-linked 1,2,3-triazole-pyrrolo-[2,1-c][1,4]benzodiazepines (PBD) conjugates was synthesized by employing “click” chemistry. These molecules exhibited promising DNA-binding affinity and were evaluated for their *in vitro* anticancer activity in selected human cancer cell lines of breast (Zr-75-1, MCF7), oral (KB, DWD, Gurav), ovary (A2780), colon (Colo205), lung (A549), prostate (PC3), and cervix (SiHa) by using the sulforhodamine B (SRB) method.

Especially, compound **154** (Figure 34) showed good inhibition ($GI_{50} = 0.15 \mu\text{M}$ against DWD, $GI_{50} = 0.16 \mu\text{M}$ against A2780, $GI_{50} = 0.17 \mu\text{M}$ against PC3, and $GI_{50} = 0.12 \mu\text{M}$ against SiHa) against various cancer cells such as oral, ovary, colon, lung, prostate, and cervix.¹⁸¹

Chang and his co-workers employed click chemistry for the synthesis of a library of carbohydrate–cyclophosphamide conjugates. The synthetic protocol is suitable for generating cyclophosphamide derivatives with various structural motifs for exploring the desired activity. From this initial library, we have observed one derivative that exhibits improved activity against lung cancer cell as compared to cyclophosphamide. Compound **155** (Figure 34) expressed potent activity against lung cancer cell lines with IC_{50} value of $33 \mu\text{M}$.¹⁸²

Ryu and his co-workers developed click fragment-based approach for rapid synthesis of Lavendustin-mimetic small molecules modifying the linker $-\text{CH}_2-\text{NH}-$ with a 1,2,3-triazole ring. Two pharmacophoric fragments of lavendustin were varied to investigate chemical space, and the auxophoric $-\text{CH}_2-\text{NH}-$ was altered to a 1,2,3-triazole for rapid click conjugation. The small molecules were evaluated against HCT116 colon cancer and CCRF-CEM leukemia cell lines. Among 28 analogues, 3-phenylpropyl ester **156** (Figure 34) inhibited CCRF-CEM leukemia cell growth with a GI_{50} value of $0.9 \mu\text{M}$.¹⁸³

A series of 4β -[(4-alkyl)-1,2,3-triazol-1-yl] podophyllotoxin derivatives were synthesized by employing the click chemistry approach and were evaluated for cytotoxicity against a panel of human cancer cell lines (SF-295, A-549, PC-3, Hep-2, HCT-15, and MCF-7). The majority of the compounds proved to be more potent than etoposide, and select compounds **157** and **158** (Figure 34) exhibited significant anticancer activity with IC_{50} values in the range of 0.001 – $1 \mu\text{M}$. DNA fragmentation and flow-cytometric results reveal that 4β -[(4-alkyl)-1,2,3-triazol-1-yl] podophyllotoxin derivatives induce dose-dependent apoptosis. Docking experiments showed a good correlation between their calculated interaction energies with the

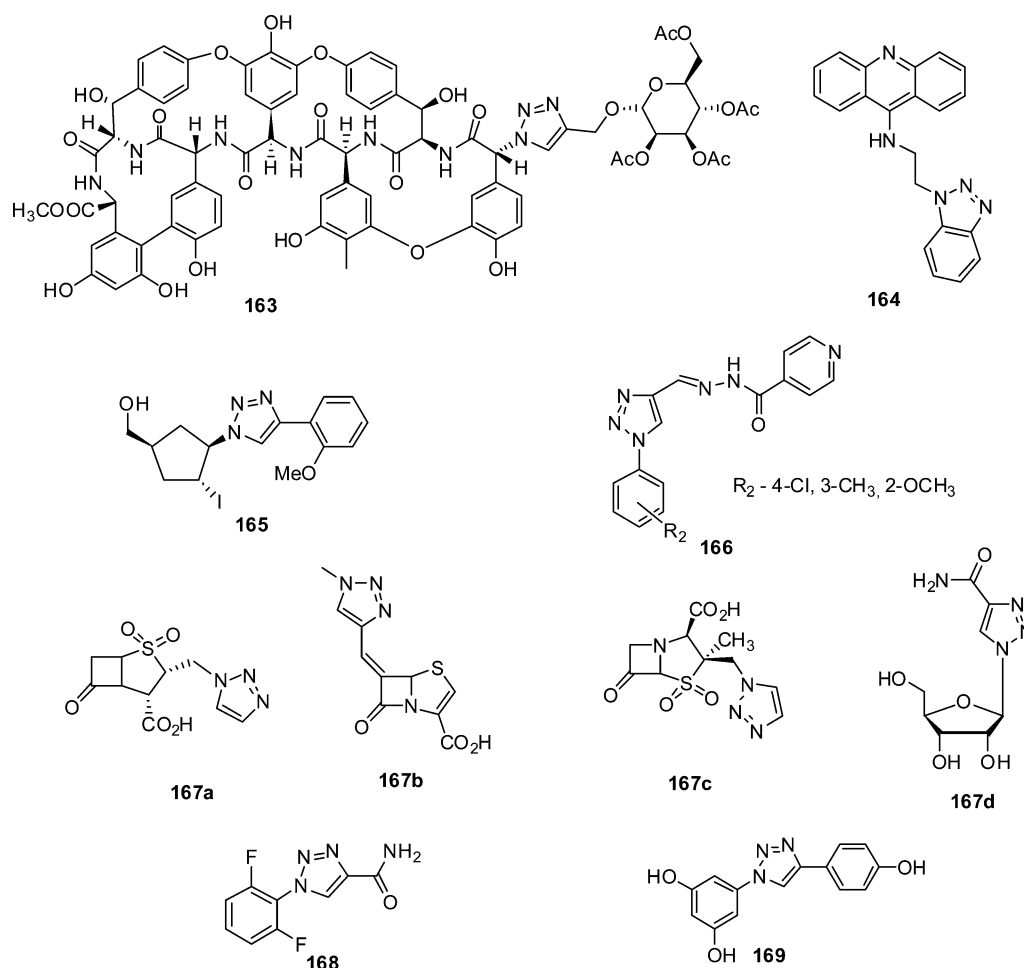


Figure 36. Chemical structures of antimicrobial, antibiotic, and some other drugs constructed via click chemistry.

topoisomerase-II and the observed IC_{50} values of all of these compounds.¹⁸⁴

Kumar and co-workers reported the synthesis of a series of novel 4 β -[(4-substituted)-1,2,3-triazol-1-yl]podophyllotoxin derivatives by employing CuI-catalyzed click chemistry and evaluated for their anticancer activity against a panel of seven human cancer cell lines (HT-29, HCT-15, S02713, HOP-62, A-549, MCF-7, and SF-295). Compound **159** (Figure 35) showed significant cytotoxic activities especially against HT-29, HCT-15, S02713, and HOP-62 cell lines with IC_{50} = 0.34 μ M against HT-29, IC_{50} = 0.53 μ M against HCT-15, IC_{50} = 0.32 μ M against S02713, and IC_{50} = 0.5 μ M against HOP-62.¹⁸⁵

Kim and his co-workers employed click chemistry for the synthesis of C5-modified nucleosides from 5-iodo-2'-deoxyuridine and their activity against six types of human cancer cell lines (HCT15, MM231, NCI-H23, NUGC-3, PC-3, ACHN). Researchers synthesized several azides from benzylic bromides, and their click reactions with 5-ethynyl-2'-deoxyuridine provided triazole derivatives. Compound **160** (Figure 35) revealed good inhibition against lungs cancer lines (NCI-H23) with IC_{50} = 77.2 μ M.¹⁸⁶

Danishefsky et al. employed click chemistry for the synthesis of novel heat shock protein 90 (Hsp90)-based anticancer agent, triazole-cycloproparadicol derivative. The key step involved an efficient cross coupling reaction using a "click" type construction. Preliminary biological evaluations revealed triazole-cycloproparadicol **161** (Figure 35) as a potent

inhibitor of Hsp90, with IC_{50} = 400 nM. Triazole-cycloproparadicol **161** also displayed significant in vitro inhibitory activity against the leukemia cell line Kasumi-1 (IC_{50} = 650 nM).¹⁸⁷

STAT3 (signal transducers and activators of transcription 3) is a promising molecular target for the design of new anticancer drugs. Wang and co-workers reported the synthesis of conformationally constrained macrocyclic peptidomimetic analogues via click chemistry. Compound **162** (Figure 35) was revealed to bind to STAT3 with a K_i value of 7.3 μ M in a competitive fluorescence-polarization-based binding assay, representing a promising initial lead compound.^{188,189}

Herczegh and his co-workers employed click chemistry for the synthesis of sugar derivatives of ristocetin from azido-ristocetin aglycon and various propargyl glycosides. Some of the sugar derivatives were found active against Gram-positive bacteria and showed favorable antiviral activity against the H1N1 subtype of influenza A virus. Compound **163** (Figure 36) showed good inhibition activity against H1N1 subtype of influenza A virus with an EC_{50} value of 4.0 μ M.¹⁹⁰

DNA intercalators have found great utility as antitumor agents, from natural products such as doxorubicin and actinomycin D to synthetic agents such as mitoxantrone and amsacrine. Amsacrine is an acridine that binds to DNA and inhibits the enzyme topoisomerase. A small set of 9-aminoacridine-3- and 4-carboxamides were synthesized efficiently using benzyne/azide click chemistry. The synthesis of

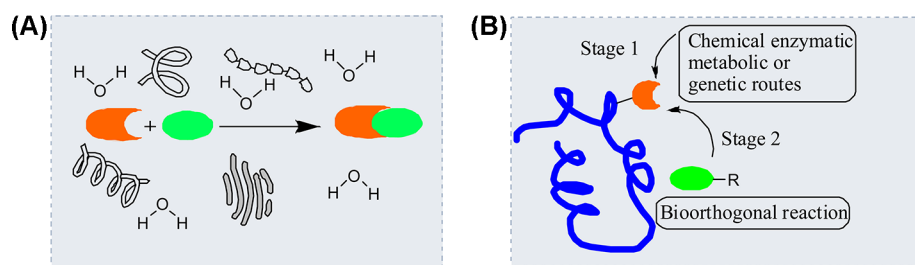


Figure 37. (A) Bioorthogonal reactions: full selectivity and inert to surrounding functionality. (B) Bioconjugation employing bioorthogonal chemistry.

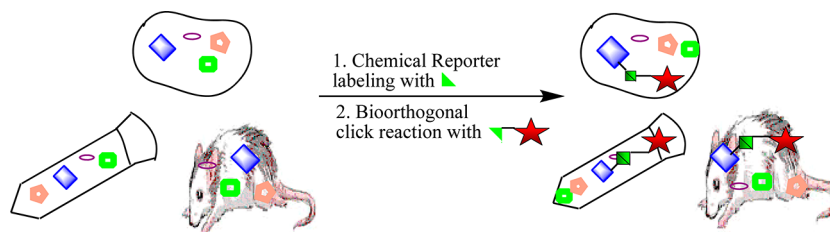


Figure 38. Bioorthogonal-click chemistry reporter strategy. (1) Target biomolecules (blue square) are labeled in the presence of nontarget biomolecules (green triangle) in vitro or in vivo with a chemical reporter (triangle). (2) The chemical reporter is then detected using bioorthogonal click chemistry to append a functional probe of interest (star).

threading intercalators was bound to DNA with reasonable affinity and had up to low micromolar antitumor activity. Compound **164** (Figure 36) revealed good antitumor activity with HL60 cell line with $IC_{50} = 5.4 \mu\text{M}$.¹⁹¹

Caamaño et al. reported the synthesis and biological evaluation as antiviral agents of a series of racemic 4-aryl-1,2,3-triazolo-2',3'-dideoxy-2'-iodocarbanucleosides and 4-aryl-1,2,3-triazolo-2',3'-dideoxy-2',3'-didehydrocarbanucleosides using the click chemistry reaction. These compounds were evaluated for their inhibitory activities against cytomegalovirus (CMV Davis strain) and varicella-zoster virus (TK⁺VZV, thymidine kinase positive strain, and TK⁻VZV, thymidine kinase deficient strain) in human embryonic lung (HEL) cells. Compound **165** (Figure 36) exhibited specific inhibitory potential against TK⁺VZV ($EC_{50} = 4.5 \mu\text{g}/\text{mL}^{-1}$).¹⁹²

Boechat and co-workers reported the synthesis of 4-substituted *N*-phenyl-1,2,3-triazole derivatives using click chemistry. The derivatives were screened in vitro for antimicrobial activity against *Mycobacterium tuberculosis* strain H37Rv (ATCC 27294) using the Alamar Blue susceptibility test. The activity was expressed as the minimum inhibitory concentration (MIC) in $\mu\text{g}/\text{mL}$ (μM). Derivatives of isoniazid (INH), (*E*)-*N'*-[(1-aryl)-1*H*-1,2,3-triazole-4-yl]methylene] isonicotinoyl hydrazides (**166**, Figure 36), exhibited significant activity with MIC values ranging from 2.5 to 0.62 $\mu\text{g}/\text{mL}$. In addition, they displayed low cytotoxicity against liver cells (hepatoma HepG2) and kidney cells (BGM), thereby providing a high therapeutic index.¹⁹³

Among the best-known examples of triazole-containing structures is tazobactam, a β -lactamase inhibitor that is marketed in combination with the broad spectrum antibiotic piperacillin. Tazobactam (**167a**) and related triazole-containing compounds (**167b** and **167c**; Figure 36) turned out to be potent β -lactamase inhibitors with higher potency than clavulanic acid and sulbactam, and the triazole ring appears to play a pivotal role for its potency.¹⁹⁴

Epilepsy is a neurological disorder characterized by unprovoked seizures affecting at least 50 million people

worldwide. There is a continuing demand for new anti-convulsant agents as it has not been possible to control every kind of seizure with the currently available antiepileptic drugs. Compound **168** (Figure 36) exhibiting antiepileptic activity was generated via click chemistry.^{195a}

Genazzani et al. employed click chemistry to generate triazole-substituted resveratrol analogues. Resveratrol possesses numerous therapeutic actions including cytotoxic activity, and therefore the rapid synthesis of these triazole-containing resveratrol analogues was utilized to generate an enormous chemical database for preliminary screening of analogues with an antitumoral potential. Some of the compounds screened were found to be more potent (compound **169**, Figure 36) than resveratrol as cytotoxic/antiproliferative agents.^{195b}

7. CLICK CHEMISTRY AND BIOORTHOGONAL CHEMISTRY

Understanding many biological structures and functions in the living system is essential for uncovering the secrets of biology, but it remains extremely challenging because of the high complexity of biological processes networks and their wiring. The daunting task of elucidating these interconnections requires the concerted application of methods emerging from different disciplines. Chemical biology integrates chemistry, biology, and pharmacology and has provided novel techniques and approaches to the investigation of biological processes. Among these, site-specific protein labeling with functional groups such as fluorophores, spin probes, and affinity tags has greatly facilitated both in vitro and in vivo studies of protein structure and function.¹⁹⁶

The ability to achieve high selectivity in the modification of a protein or cell that exists within a complex sample represents an extremely advantageous skill needed for studies conducted in a broad range of chemical and biological systems. In particular, the selective derivatization of biomolecules long presented a significant barrier due to the vast array of functionality present in biological systems, rendering side reactions and nonspecific labeling all but unavoidable. Recently, a series of chemical

reactions that are orthogonal to functional groups present within biological systems have revolutionized this field through the unprecedented selectivity they exhibit in the tagging of biological targets within complex samples (Figure 37).¹⁹⁷

A prime example of the advantages of orthogonal reactivity is presented by a family of reactions collectively termed “click chemistry”. The attributes of these transformations render them particularly advantageous for achieving the selective coupling of molecules within a complex biological environment. This ability has opened the door to a range of applications in chemical biology that have greatly enhanced the efficiency of biological studies aimed at understanding natural systems. This current topic provides an introduction to the profound effects that click chemistry and bioorthogonal reactions had on state-of-the-art biological applications, including biomolecule labeling and imaging, and activity-based protein profiling.^{196–198}

The bioorthogonal nature of click chemistry components lends these reactions as valuable tools for the selective labeling and detection of biological molecules in complex samples such as cellular extracts and ultimately in vivo (Figure 38). Such studies are necessary to understand the complex nuances of spatial and temporal aspects of biomolecule localization and function within the cell. The Staudinger ligation and azide–alkyne cycloadditions have both proven to be effective for these challenging tasks and have now been employed for selective derivatization of a wide range of biomolecules, including proteins, viruses, sugars, DNA, RNA, and lipids (Figure 38).¹⁹⁸

Bioorthogonal chemistry encompasses a broad arena of science at the interface between molecular biology and chemistry. Bioorthogonal chemistry techniques generally involve the covalent attachment of synthetic labels to a biomolecular framework. Examples include the modification of proteins and nucleic acids by incorporation of fluorophores, ligands, chelates, radioisotopes, and affinity tags, or modifications such as fusing two or more proteins together or linking a complex carbohydrate with a peptide. The power of bioorthogonal chemistry extends to the labeling of biomolecules in vivo. The bioorthogonal chemical reporter technique has been employed to probe enzymes in living systems as a function of their catalytic activity. Standard biochemical techniques such as in situ hybridization, which probes for mRNA, or antibody staining, cannot distinguish between active and inactive pools of enzymes. Yet, knowledge of when a particular enzyme was active could be critical to understanding physiological processes as diverse as cancer, apoptosis, and inflammation. Cravatt has pioneered the use of activity-based protein profiling (ABPP), a technique in which enzymes were covalently labeled with a mechanism-based inhibitor derivatized either directly with an affinity tag or fluorophore or with a bioorthogonal chemical reporter. In the latter case, a second step, the bioorthogonal click reaction, was employed to append the desired biophysical probe (Figure 39).^{199–203}

Azide or alkyne tags are often easily introduced into small molecules via chemical synthesis, the site-specific introduction of these labels into more complicated structures; particularly site-specific labeling proteins is significant challenge.^{204–206} One approach developed by Tirrell and co-workers exploited the inability of certain tRNA synthetases employed for protein biosynthesis to differentiate between natural amino acids and analogues with closely related structures. Click chemistry was used to improve the efficiency of this method by screening the extent of unnatural amino acid incorporation by mutant tRNA synthetases through post-translational modifications.²⁰⁷

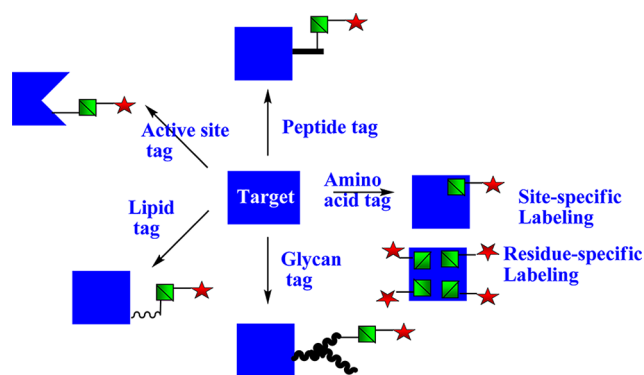


Figure 39. Strategies for labeling biomolecules with chemical reporters in vitro and in vivo. (Clockwise from top left) Enzymes that are catalytically active can be specifically labeled with activity-based probes bearing chemical reporters. Proteins can be labeled with a chemical reporter by enzymatic modification of a short peptide sequence. Individual amino acids within proteins can be replaced, either in a site-specific or residue-specific manner, with unnatural amino acids bearing chemical reporters. Glycans can be metabolically labeled with chemical reporters using unnatural monosaccharide precursors. Lipids can be metabolically labeled with chemical reporters using unnatural lipids.

Schultz and co-workers applied a site-specific incorporation used for codon-reassignment of the amber stop codon UAG and its corresponding tRNA (called the amber suppressor) in combination with an orthogonal aminoacyl-tRNA synthetase to place a noncanonical amino acid at precisely one position in the selective modification protein (Figure 40a).²⁰⁴ A number of noncanonical amino acids incorporated into nascent proteins as many mutants were generated using high-throughput screening for the directed evolution of these enzymes. The amber suppressor methodology requires substantial genetic manipulations and, therefore, might be not readily applicable to complex cellular systems or in vivo approaches. Schultz and co-workers developed a powerful technique for site-specific installation of unnatural amino acids by reengineering protein synthesis. An orthogonal tRNA/mutant tRNA synthetase pair was exploited to introduce a noncanonical amino acid at a prescribed location. This was initially performed in *Escherichia coli* and then subsequently expanded to eukaryotic and mammalian cells by harnessing the amber codon in concert with suppressor tRNA synthetases that were genetically engineered to accept unnatural amino acids as substrates. Using this strategy, an impressive array of amino acid derivatives bearing various reactive or reporter groups, including and bearing azide and alkyne tags, respectively, was site-specifically incorporated into protein targets, the latter of which can be subsequently modified via click chemistry.^{200,204,205}

Residue-specific replacement of natural amino acids with a functionalized noncanonical surrogate is much simpler (Figure 40b). Key to this methodology is the recognition of noncanonical amino acid surrogates by its corresponding amino acyl tRNA synthetase (AARS), which guarantees the fidelity of amino acid incorporation during translation, as the ribosomes do not exert any quality control toward the charged amino acid. Tirrell and co-workers showed that the methionyl tRNA synthetase (MetRS) was promiscuous in accepting the conservatively modified noncanonical amino acids azido-homalanine (AHA) and homopropargylglycine (HPG) in place of methionine. AHA-charged or HPG-charged methionyl

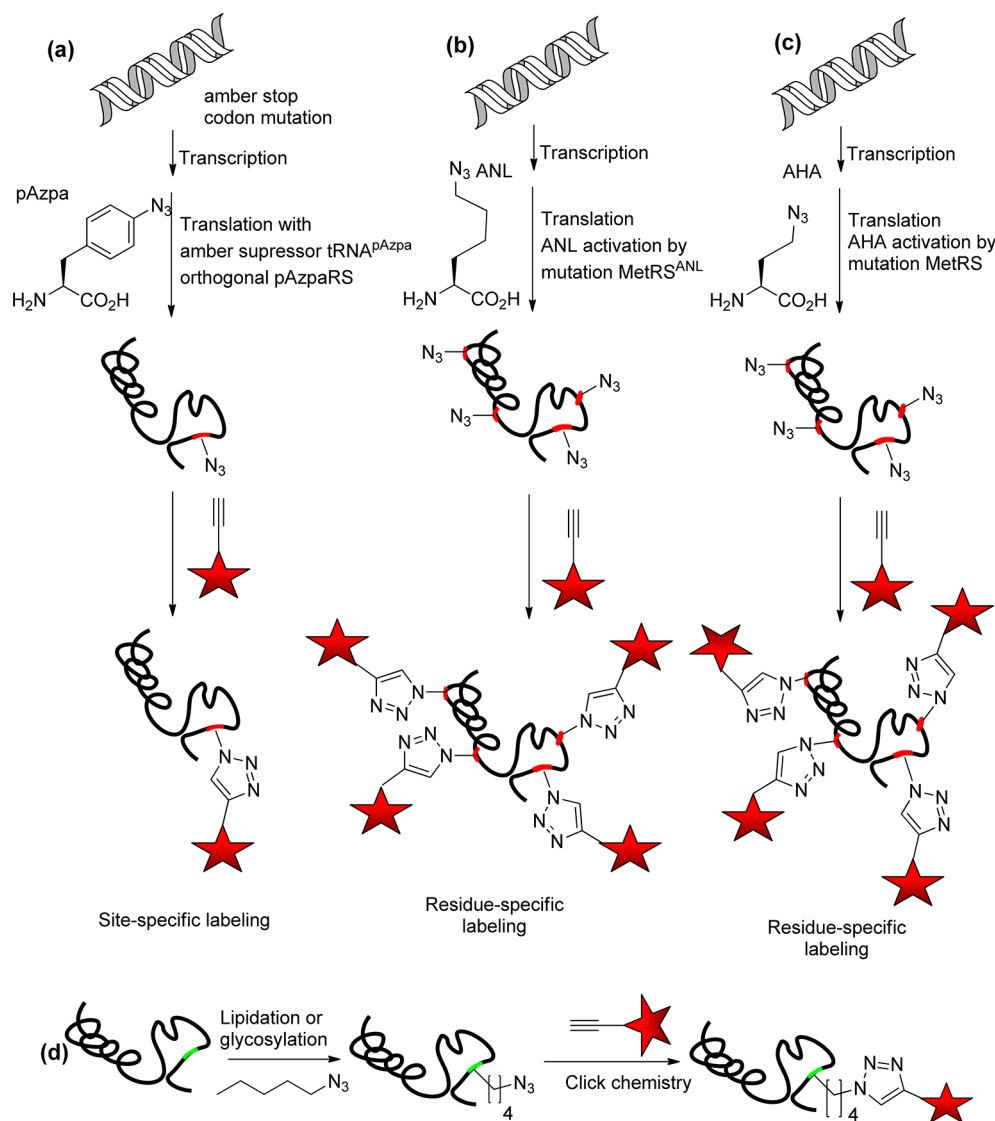


Figure 40. Strategies for labeling biomolecules with chemical reporters in vitro and in vivo using click chemistry reaction. (a) Incorporation of noncanonical amino acids during translation using site-specific labeling. (b) Incorporation of noncanonical amino acids (ANL) during translation using residue-specific labeling. (c) Incorporation of noncanonical amino acids (AHA) during translation using residue-specific labeling. (d) Post-translational incorporation of noncanonical lipids and glycans.

tRNAs were used by ribosomes for translation in the absence of the competing natural substrate methionine with this residue-specific incorporation technology. Tirrell and co-workers successfully labeled overexpressed proteins in *Escherichia coli*. Later, this technology was expanded by the laboratories of Schuman and Tirrell with the introduction of BONCAT (bioorthogonal noncanonical amino acid tagging) to monitor global de novo protein translation in different cell types and culture systems with high specificity. During metabolic labeling (that is very similar to traditional labeling with radioactive methionine or cysteine), proteins were endowed with a novel azide or alkyne functionality that serves to distinguish them from the pool of pre-existing proteins. Employing either copper-catalyzed azide–alkyne ligation (commonly referred to as “click chemistry”) or strain-promoted cycloaddition, the reactive azide group of AHA is covalently coupled to an alkyne bearing tag in the second step, enabling subsequent imaging, affinity purification, and MS identification procedures of tagged proteins.^{206–208}

Tirrell and Schuman refined the residue-specific incorporation of non-natural methionine surrogates to exclusively target specified prokaryotic cells in a complex cellular mixture (Figure 40c). Expression of a mutant MetRS and using the noncanonical amino acid azidonorleucine (ANL), which is excluded by the endogenous MetRS due to its long side-chain, restricted the visualization of de novo synthesized proteins to cells expressing the mutant MetRS only.²⁰⁸

Metabolic labeling of proteins using bioorthogonal chemical reporters was not restricted to monitor global de novo protein synthesis as analogous techniques capitalize on the manifold potential of alkynes and azides to target other classes of biomolecules such as glycans and lipids (Figure 40d). Bioorthogonal chemical reporters in combination with azide–alkyne ligation have been applied to track lipid-containing molecules via azido lipid precursors tackling *N*-myristoylation, *S*-palmitoylation, or farnesylation in living systems. Palmitoylation was the most frequently observed lipid modification for neuronal proteins and occurs with a few exceptions at cysteine

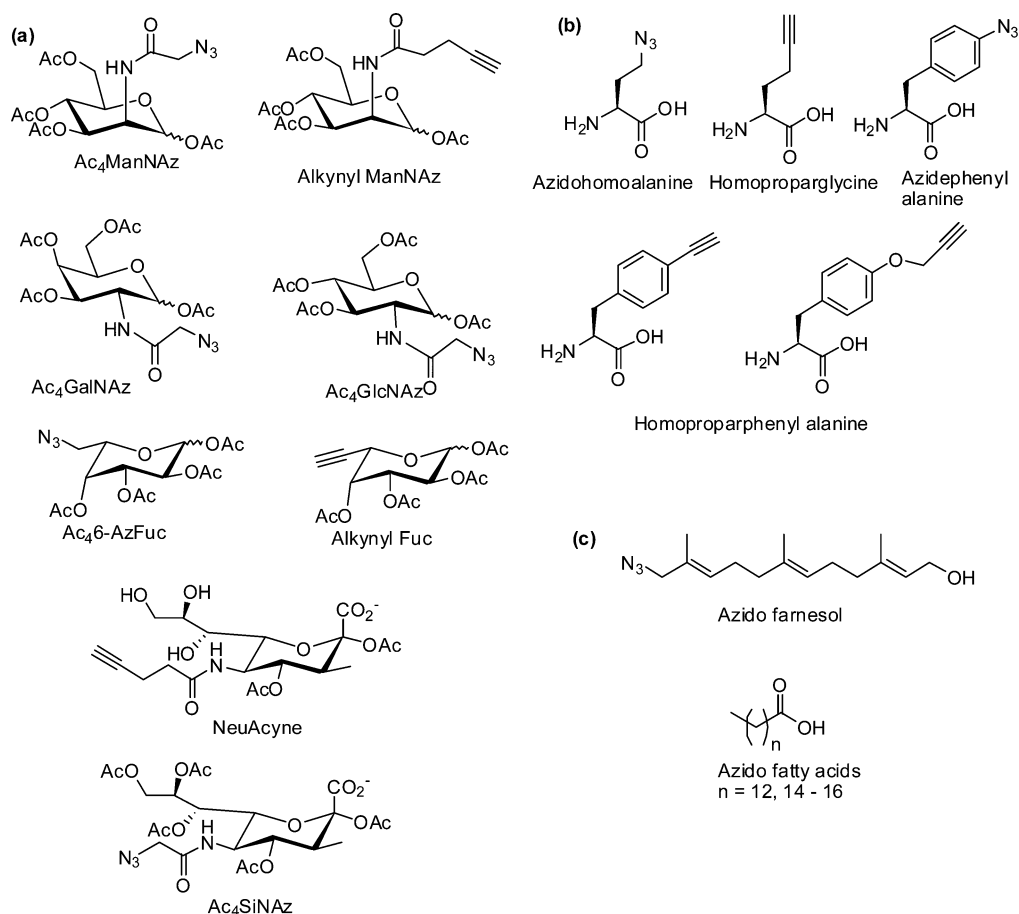


Figure 41. Azide- and alkyne-bearing substrates for metabolic labeling of glycans, proteins, and lipids. (a) Azido and alkynyl monosaccharide precursors for labeling glycans. (b) Unnatural amino acids bearing azides and alkynes for residue-specific protein labeling. (c) Azido lipid substrates for probing protein lipidation.

residues via the formation a labile thioester bond with saturated palmitic acid. With the use of the palmitic analogue 17-octadecynoic acid in a bioorthogonal metabolic labeling approach, a total of 125 palmitoylated proteins were identified in Jurkat cells, and the corresponding approaches were described for myristoylated or farnesylated proteins as well.²⁰⁹

The basis of metabolic incorporation using unnatural sugar analogues relies on the finding that certain metabolic pathways were shown to tolerate minimally modified sugar precursors (Figure 41). This was originally reported by Reutter and co-workers, who successfully demonstrated the incorporation of chemically synthesized *N*-propanoyl-*D*-mannosamine into membrane and serum glycoproteins. Bertozzi and co-workers adopted this approach with a ketone-modified *N*-acetylmannosamine. They showed the unnatural sugar was efficiently taken up by mammalian biosynthetic pathways and incorporated into sialic acid, which was eventually incorporated into glycoproteins. The unnatural sugar bearing glycoconjugates on the cell surface was subsequently labeled by a biotin-derivatized hydrazide. Bertozzi's group further refined this strategy by utilizing the azide-modified *N*-acetylmannosamine, and selective labeling of the azide-modified cell surface glycoconjugates was observed with a modified Staudinger ligation using a biotinylated triarylphosphine.^{197,198}

7.1. Site-Specific Labeling of Cells, Live Organisms, and Proteins

The recent development of bioorthogonal click chemistry has led to an explosion of interest in the selective covalent labeling of biomolecules in cells and living organisms. In these labeling reactions, one of the two bioorthogonal functional groups is first incorporated into target biomolecules via genetic or metabolic approaches. A biophysical probe, functionalized in a complementary fashion, is introduced in the second step, allowing detection or isolation of the target of interest. To minimize perturbations to the physiological state of the cells or organisms probed, an ideal ligation reaction must proceed in water at neutral pH and at temperatures between 25 and 37 °C without any cytotoxic effects. Further, the reactive partners participating in this transformation must be inert to the native functional groups present in the biological system. Many research groups developed site-specific labeling methods for labeling of cells, live organisms, and proteins.^{210–216} Some recent examples are presented below.

A major advance in chemo-selective ligation on virus surfaces used copper(I)-catalyzed azide–alkyne [3 + 2] cycloaddition (CuAAC or click chemistry), where both virus nano particles and the desired substrate can be specifically coupled in an orthogonal manner without the use of protecting groups. One particularly striking application of click chemistry was reported by Finn et al., in their studies on the conjugation of fluorescein dye molecules onto the cowpea mosaic virus. The virus itself

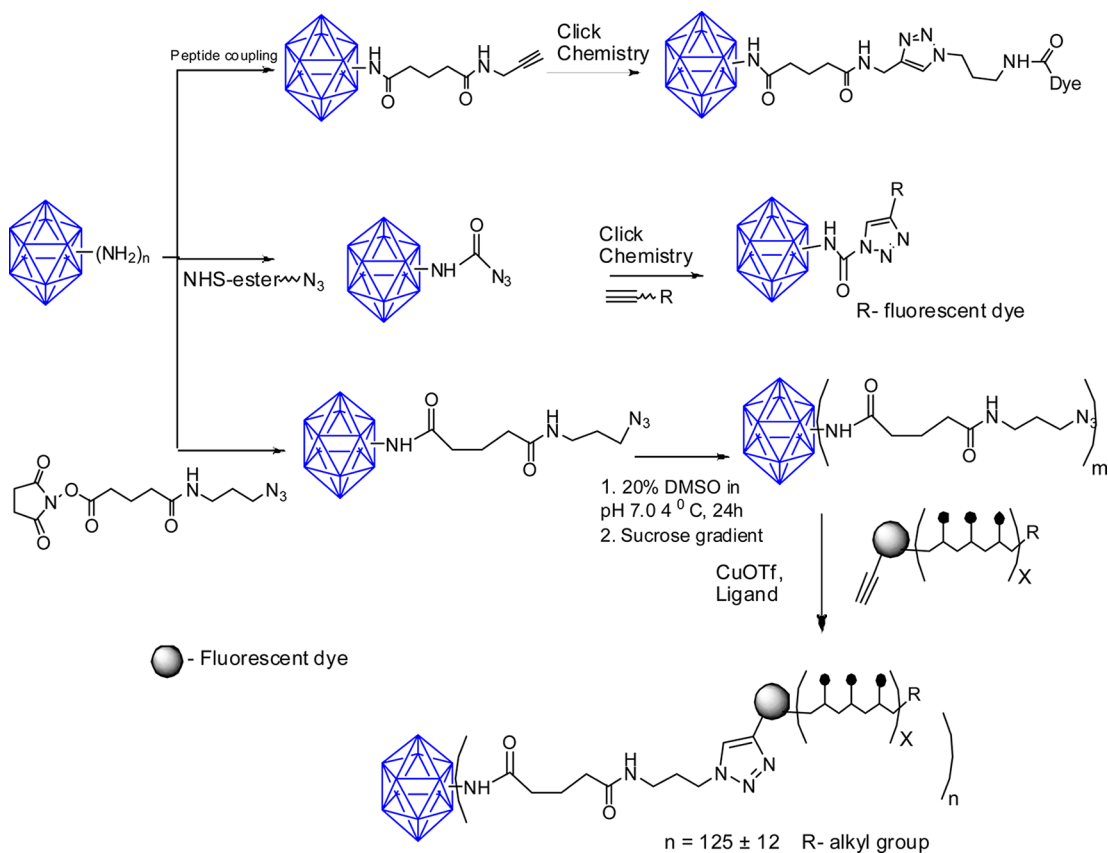


Figure 42. Common strategies involved for chemical modification of viral nanoparticles (VNPs) using click chemistry reaction.

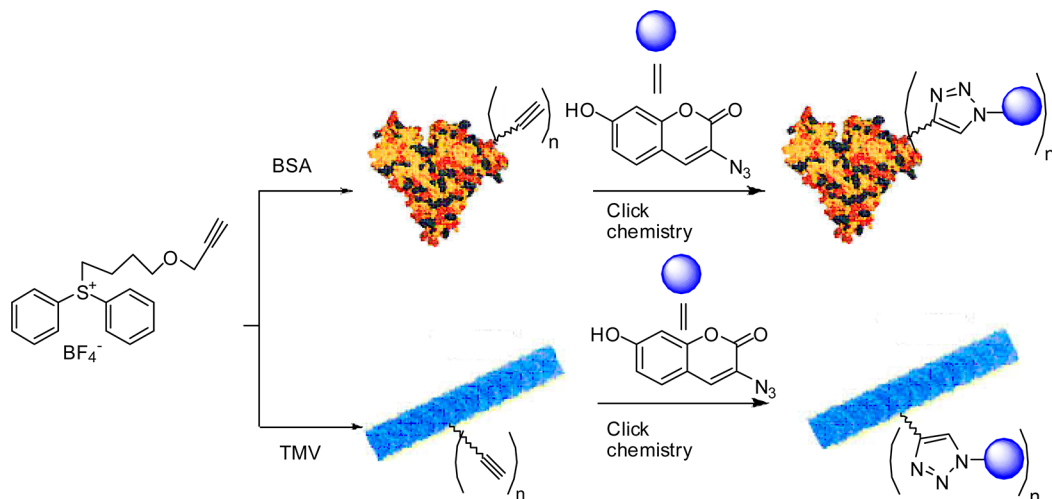


Figure 43. Surface modification of proteins and tobacco mosaic virus of BSA and TMV to give fluorescent labeling products using click chemistry reaction.

resembles a cage-like molecule, formed from 60 identical copies of a two-protein asymmetric unit, which surrounds the genetic information in the core. The virus particle presented functionality on its exterior surface, including the free amines found in lysine, and thiols found in cysteine residues. The virus particle was decorated with azide and alkyne functionality, via peptide coupling (Figure 42) and thio-ether formation.^{210–212}

The same research group again developed click chemistry-based site-specific labeling of virus-like particle using NHS-ester (aminothioester functional group) azide and fluorescein alkyne. The polyvalent azide-decorated capsid was prepared by

acylation of surface lysine and N-terminal amine groups (4 per subunit; 720 per particle) with a large excess of 5-(3-azidopropylamino)-5-oxopentanoic acid NHS ester. Subsequent click reaction of VNP (virus nano particle)-azides (1 mg mL⁻¹ protein, 0.4 μm in particles, approximately 280 nm in azide) with only 2 equiv of fluorescein alkyne 13 per azide (250 μM CuSO₄, 1.25 mM 3, 5 mm aminoguanidine 4, 5 mm sodium ascorbate, pH 7 phosphate buffer) for 1 h gave an excellent yield of particles bearing an average of 630 dyes per capsid, determined by MALDI-TOF.^{210,211,212a} The researchers initially measured the mass of TMV surface-modified acetylenes

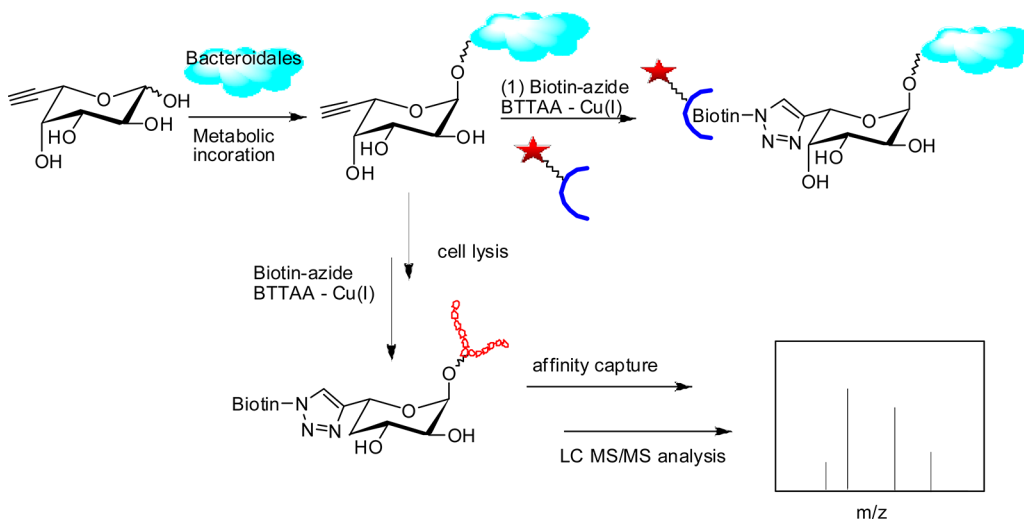


Figure 44. Detection of fucosylated glycoproteins in *Bacteroidales* species. A chemical strategy for the detection and enrichment of fucosylated glycoproteins in *Bacteroidales* species.

with m/z value of 17 664. After the click chemistry reaction, TMV surface-modified trizoles exhibited the m/z range of 17 804–18 894.^{212b}

Alkyl sulfonium salts (ASS) can act as powerful alkylating agents for biomolecules. Few studies have addressed the application of sulfonium salts to the modification of biomolecules such as nucleic acids and proteins. Xi and co-worker developed a tandem method of sulfonium alkylation and click chemistry for modification of biomolecules like cowpea mosaic virus and BSA. Fluorescent labeling of proteins and virus was successfully performed after simple incubation of biomolecules with sulfonium salts followed by azido-containing compound at room temperature. The mild and biocompatible conditions of sulfonium alkylation followed by click chemistry reactions used efficiently bioconjugate and a wide range of compounds and/or functional groups to the surface of proteins and virus (Figure 43).²¹³

Members of the *Bacteroidales* order are among the most abundant gram-negative bacteria of the human colonic microbiota. These species decorate their cell-surface glycoproteins with fucosylated glycans, which are believed to play important roles in host intestinal colonization. Baughn and his co-workers applied click chemistry for the chemical approach directed toward labeling and detecting fucosylated glycoproteins from cultured *Bacteroidales* species, *Bacteroides fragilis* and *Parabacteroides distasonis*. These bacteria were treated with an alkyne-bearing fucose analogue, which was metabolically integrated into the bacterial surface fucosylated glycoproteins. FucAl, an alkynyl analogue of fucose, was metabolized by *Bacteroidales* species and incorporated into the cell-surface glycoproteins. The alkyne-tagged glycoproteins reacted with azide-bearing biophysical probes via bioorthogonal click chemistry for detection or glycol-proteomic analysis using LC–MS analysis or fluorescent assay analysis (Figure 44).²¹⁴

Finn and his co-workers employed click chemistry for rapidly label of mammalian cells in culture with no loss in cell viability in biological molecules in aqueous buffers.²¹⁵ Metabolic uptake and display of the azide derivative of *N*-acetylmannosamine developed by Bertozzi,^{197,198} followed by CuAAC ligation using sodium ascorbate and the ligand tris(hydroxypropyltriazolyl)methylamine (THPTA), gave rise to abundant covalent attachment of dye-alkyne reactants. The toxicity commonly

attributed to copper results from the production of reactive oxygen species by Cu, ascorbate, and atmospheric oxygen. The important features of the cell labeling protocol were the use of a water-soluble accelerating ligand (THPTA) that also acts as a sacrificial reductant for oxidative species as they are produced in the coordination sphere of the metal and aminoguanidine to intercept strongly electrophilic byproducts of dehydroascorbate. THPTA serves both to accelerate the CuAAC reaction and to protect the cells from damage by oxidative agents produced by the Cu-catalyzed reduction of oxygen by ascorbate, which was required to maintain the metal in the active +1 oxidation state (Figure 45a). The various fluorescent dyes were used to label glycol proteins shown in Figure 45b. This procedure was extended for the application of this fastest of azide-based bioorthogonal reactions to the exterior of living cells.²¹⁵

Wu and his workers applied click chemistry for in vivo imaging of glycans using zebrafish early embryogenesis²¹⁶ (Figure 45c). The Cu(I)-catalyzed azide–alkyne cycloaddition (CuAAC) is the standard method for bioorthogonal conjugation. However, current Cu(I) catalyst formulations are toxic, hindering their use in living systems. The researchers employed a tris(triazolylmethyl)amine-based ligand (BTTEs) for Cu(I), which promotes the cycloaddition reaction rapidly in living systems without apparent toxicity that allows the imaging of glycan biosynthesis during zebrafish early development. This catalyst was used for the first time, in noninvasive imaging of fucosylated glycans during zebrafish early embryogenesis. The researcher microinjected embryos with alkyne bearing GDP-fucose at the one-cell stage and detected the metabolically incorporated unnatural sugars using the biocompatible click chemistry. Robust labeling, which requires 1 h of reaction time when using cyclooctyne-based copper-free click chemistry, was achieved within minutes. Labeled glycans were imaged in the enveloping layer of zebrafish embryos between blastula and early larval stages (Figure 45c). The BTTEs-Cu(I) catalyst, combined with yolk-cell microinjection, allowed for the rapid imaging of fucosylated glycans in the enveloping layer of zebrafish embryos as early as 2.5 h post fertilization. This new method paves the way for rapid, noninvasive imaging of biomolecules in living organisms.²¹⁶

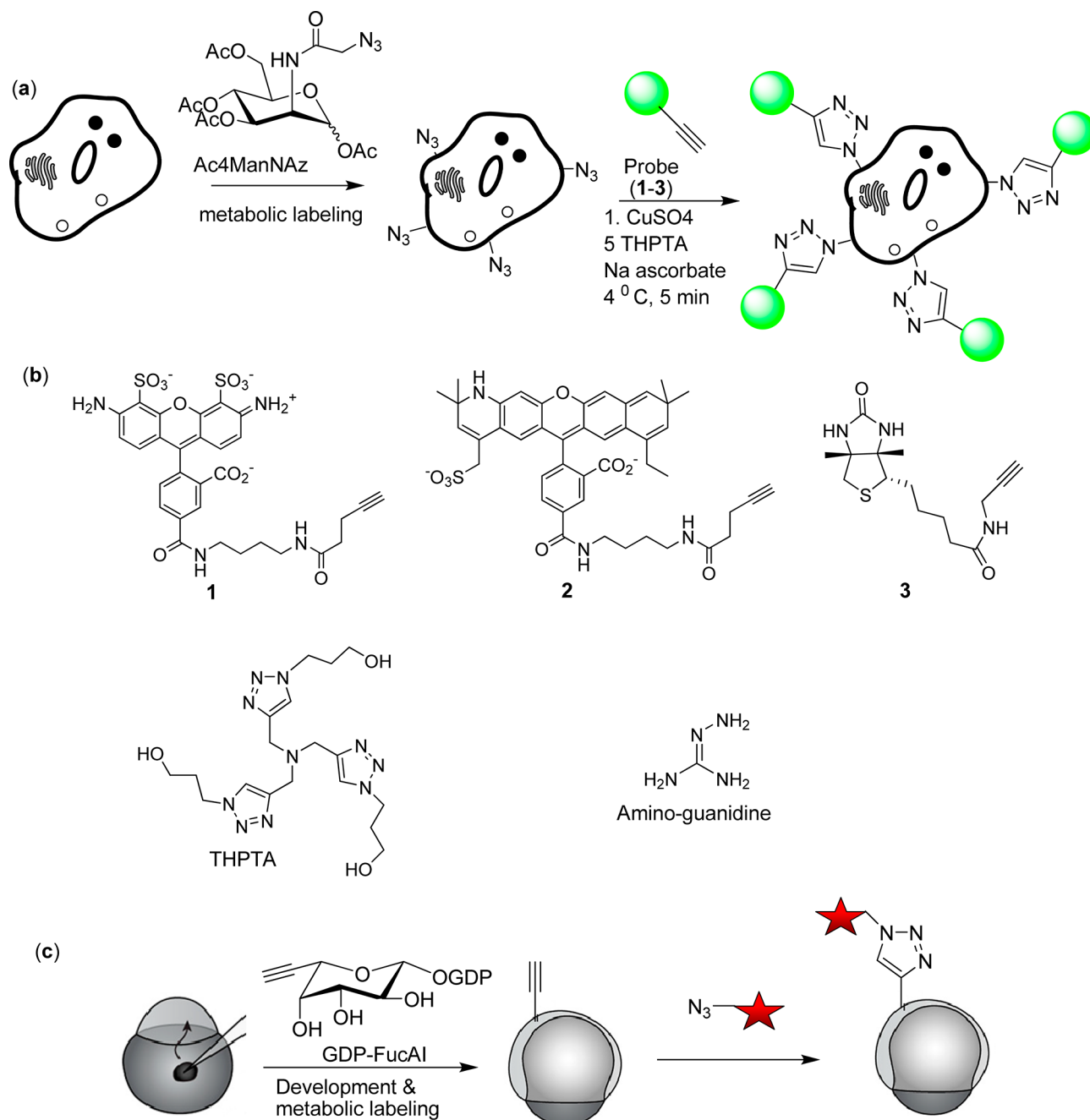


Figure 45. Chemical strategies involved in the labeling of living cells using click chemistry reaction. (a) Cell labeling steps. (b) Alkynyl probe reagents and catalyst additives. (c) Microinjection combined with the BTTEs-Cu(I)-catalyzed click chemistry enables the labeling of fucosylated glycans in zebrafish embryos. Zebrafish embryos were microinjected with a single dose of GDP-FucAl and allowed to develop to 10 hpf.

7.2. Site-Specific *In Vitro* and *In Vivo* Incorporation of Molecular Probes To Study G-Protein-Coupled Receptors

Over the past decade, advances in the structural biology of GPCRs and their signaling partners have provided significant information about the molecular mechanism of trans membrane signaling by GPCRs. However, although a crystal structure provides invaluable information, it represents only one particular conformation of one component of a complex allosteric machine. To further understand with chemical precision the molecular pharmacology and dynamics of GPCR signaling, a tool kit of molecular approaches is required to incorporate informative probes that allow for monitoring

receptor activation and real-time interrogation of active signaling complexes.^{217,218}

Unnatural amino acid (UAA) mutagenesis is now widely used to introduce unique chemical handles into a protein of interest. In site-directed UAA mutagenesis, a “blank codon”, typically the amber stop codon, UAG, is introduced into the gene of interest. In one formulation of the UAA mutagenesis strategy, an engineered suppressor tRNA is synthetically amino acylated and microinjected into *Xenopus* oocytes, a method that was originally developed by Dougherty and colleagues to perform whole-cell electrophysiology on ion channels.²⁰⁵ This technique facilitated the introduction of fluorinated aromatic amino acids into the agonist binding pockets of M2 muscarinic

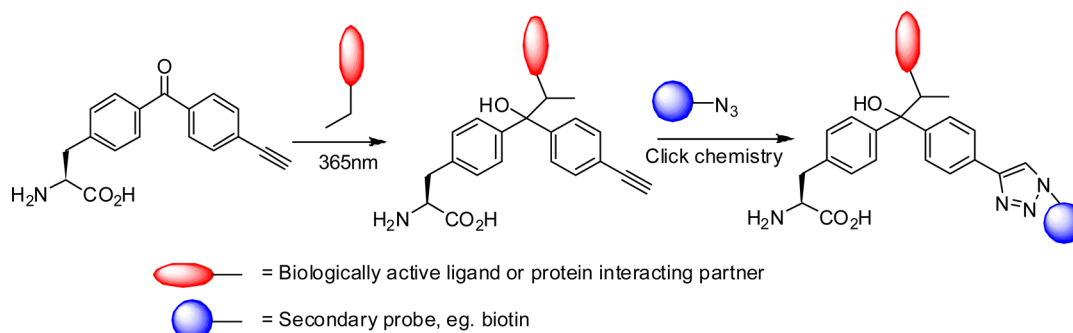


Figure 46. Click chemistry used in GPCR structure–function studies. Unnatural amino acid (UAA) was incorporated into GPCRs using click chemistry reaction. *p*-Ethynylbenzoyl-*L*-phenylalanine (E-BzF) is the clickable group allowed to form a cross-linked labeled product with an azido-containing probe (functionalized GPCR).

acetylcholine receptor and D2 dopamine receptor to study cation– π interactions.^{219,220}

Chemical modification of proteins has a rich history in biochemistry and chemical biology. However, studies of membrane protein function, especially in cases where functional expression is low and purification and reconstitution are not feasible, present unique challenges. Heptahelical G-protein-coupled receptors (GPCRs) are a particularly important class of cell-surface receptors that represent targets of more than a quarter of all therapeutic drugs. Understanding with chemical precision how GPCRs function in biological membranes remains a central problem in biology. Recently, a number of creative strategies have been developed that allow site-specific attachment of chemical probes or tags directly on expressed receptors or on biologically active peptide ligands or substrates. One particularly important advance was the genetic encoding of unnatural amino acids (UAAs) with unique small bioorthogonal tags using amber codon suppression in mammalian cells. This method should allow site-specific labeling of GPCRs with various molecular probes to facilitate cell-based studies of protein–protein or protein–ligand interactions and the visualization of conformational changes using fluorescence spectroscopy or single-molecule imaging (Figure 46).²²⁰

7.3. Activity-Based Protein Profiling versus Affinity-Based Protein Profiling

Activity-based protein profiling (ABPP) has been emerging as a powerful chemical proteomic method toward the analysis of functional states of proteins in a complex proteome. ABPP is a chemical method that employs active site-directed probes to tag proteins and monitor their expression levels and function in complex proteomes; however, the bulky reporter tags used require cell homogenization before analysis, thereby preventing measurements in living organisms.²²¹ Activity-based protein profiling (ABPP), originally developed by Cravatt and co-workers, is a novel technique that enables one to selectively target and elucidate the functional state of one particular enzyme or enzyme class from a crude proteome, in an activity-based manner, by using the so-called activity- or affinity-based small molecule probes (ABPs).²²² This strategy was developed as a complementary method to conventional comparative proteomic methods such as two-dimensional gel electrophoresis coupled with mass spectrometry (2DE-MS) as the latter could provide only information about protein abundance. The general designs of activity-based probes (ABPs) contain three parts (Figure 47): active site-targeting reactive group (e.g., warhead or WH) that directs the probe to the active site

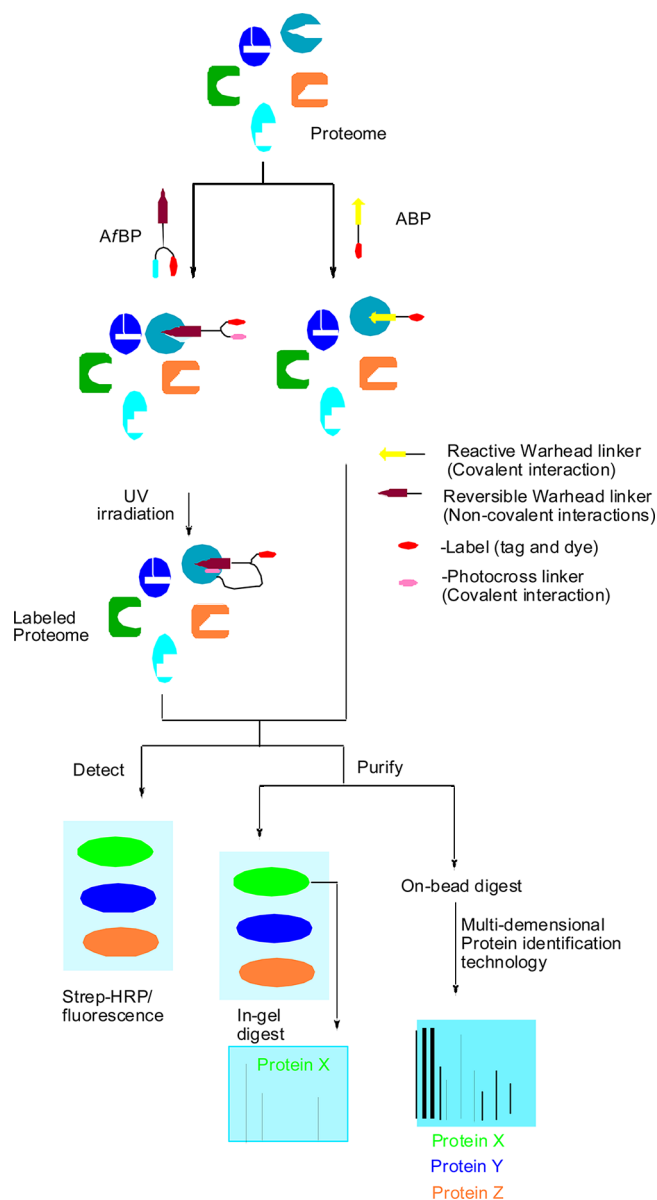


Figure 47. Schematic of ABPP showing two different approaches using ABPs (activity-based probes) or A/BPs (affinity-based probes).

and causes covalent reaction with the protein; (2) a reporter unit, which is typically a fluorophore or biotin for the direct readout of the protein's activity; and (3) a linker/spacer, which

Table 1. Advantages and Disadvantages of Using AfBPs and ABPs

technique	advantages	disadvantages
affinity-based probes (AfBPs)	can screen complex samples—simple procedure; generalizable method	low abundance proteins difficult to detect; time consuming; nonspecific binding to resin; immobilization may affect binding or pharmacological properties
activity-based probes (ABPs)	accesses enzyme activity directly—high sensitivity; applicable to in vivo studies	requires nucleophile in active site of protein; limited coverage of proteome; indirect read-out of drug–target interactions

minimizes the possible disruption from the reporter tag in the protein reactivity/recognition of the reactive unit, or in some cases serves as an additional recognition element.^{32,221,222} In this approach, a crude proteome was treated with the activity-based probe, which bears a reactive group or warhead (W, shown in yellow) and the reporter unit (R, shown in red). The probe covalently reacts with the active site of the target protein, and the labeling is visualized by in-gel fluorescence scanning following separation of proteins on SDS-PAGE. The range of proteins that can be detected by ABPP is quickly expanding with the development of novel probes. Probes have been generated for proteases, lipases, methylsterases, glycosidases, kinases, phosphatases, cytochrome P450s, histone deacetylases, and many other protein families.^{32,223}

Affinity-based probes (AfBPs) is a useful technique for elucidating direct protein binders of bioactive small molecules. Yao's group achieved labeling by binding at a specific site on a protein (not necessarily an enzyme active site) followed by a nonspecific covalent bond-forming event, for example, photochemical cross-linking or spontaneous trapping of a nearby (noncatalytic) protein functional group.²²⁹ Careful design of an AfBP could result in the generation of a functional ABP, for example, a substrate mimic that binds preferentially to a well-formed active site coupled to a photoactivated linker. The distinction resides in the need for a catalytically active enzyme: if a catalytic site residue that is essential for enzyme chemistry but nonessential for substrate recognition is inactivated (e.g., by mutation), an AfBP may be able to function as normal. However, an ABP would not, as labeling relies on the specific chemistry that the enzyme performs for its activation. AfBPs lie largely outside the scope of this Review, but they can be potent tools for the identification/validation of the targets (and off-targets) of drugs and inhibitors, and for general protein-labeling. In this approach, the crude proteome was treated with an AfBP whose warhead (W, shown in brown) first recognizes the target protein's active site via noncovalent interactions. Subsequently upon UV irradiation, a reactive intermediate generated from the photoreactive unit (depicted as pink oval) covalently reacts with suitable residues near the active site. The labeled protein is separated by SDS-PAGE and visualized by in-gel fluorescent scanning.^{224,225} The advantages and disadvantages of activity-based probes and affinity-based probes are tabulated in Table 1.

ABPs and AfBPs Used for Targeting Various Protein Classes in Conjunction with Click Chemistry Bioorthogonal Labeling. Chemical probes appended with detection tags are providing new opportunities to analyze complex proteomes and characterize small molecule inhibitor specificities. The attachment of detection tags (radioactive isotope, affinity tag, or fluorophore) onto covalent inhibitors or photoaffinity agents has enabled the analysis of discrete protein families in complex mixtures. To target specific protein families selectively, chemical probes typically contain a reactive functional group for covalent labeling of proteins and a unique chemical scaffold to confer binding affinity to subsets of proteins.²²³

The direct visualization of small molecule–protein interactions with chemical probes has provided new tools to accelerate drug discovery. Certain small molecule–protein interactions might require factors only present in living systems that are not preserved in cell lysates. Detection tags such as biotin or fluorophores, however, can influence the specificity of chemical probes and also limit their utility in living cells. The emergence of two chemo-selective reactions that function under physiological environments of click chemistry (Figure 47) has enabled the installation of detection tags after chemical probes have reacted with target proteins. Herein, we survey the union of chemical probes with bioorthogonal labeling methods, which has yielded new chemical probes with enhanced selectivity and improved pharmacological properties for selective labeling of protein targets in living cells.^{221–223}

Several azide/alkyne-modified chemical probes were developed to target γ -secretase, cysteine proteases, glycosidases, metalloproteases, histone deacetylases, methionine aminopeptidases, kinases, as well as a variety of other protein classes (Table 2). Of note, the decoupling of detection tags from chemical probes alters and often improves the specificity of protein labeling as compared to directly modified chemical probes, which is readily apparent with cysteine proteases, metalloproteases, kinases, and methionine aminopeptidases. The diversity of azide/alkyne-modified chemical probes listed above highlights the utility of this two-step labeling approach for targeting various protein classes.

7.4. Labeling and Sequencing of DNA

The discovery and development of the “click reaction” in water, the potential for facile introduction of varying functionality into the biomolecular environment, has been realized. As a result, numerous biomolecules including DNA, peptides proteins, oligosaccharides, and glycoconjugates were labeled with various appendages using click chemistry reaction. Many of these new molecular entities were proved extremely useful in the study of biological systems.²⁵³ Bioorthogonal labeling methods are valuable tools in nucleic acid research to study their cellular behaviors, in particular, recent bioorthogonal assays developed to measure DNA and RNA syntheses inside cells. Bioorthogonal labeling methods rely on chemical or photochemical strategies to study DNA modification and interactions involving nucleic acids. In eukaryotes, the genomic information is encoded by the primary DNA sequence. The DNA modification has a greater impact with a broad range of biological functions, including gene expression, maintenance of genome integrity, parental imprinting, X-chromosome inactivation, regulation of development, aging, and cancer (Figure 48).^{253–257}

High density functionalization of modified DNA was carried out by many research groups, wherein the “click reaction” was used to postsynthetically decorate alkyne-modified DNA. The DNA was synthesized by standard means using phosphoramidite chemistry, but with the incorporation of the modified nucleosides (Figures 49 and 50). The fluorescent labeled

Table 2. Survey of Chemical Probes Used for Targeting Various Protein Classes in Conjunction with Bioorthogonal Labeling

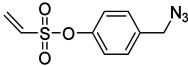
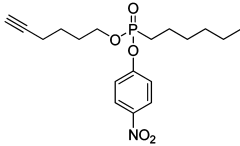
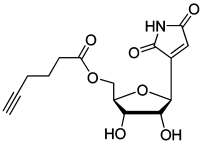
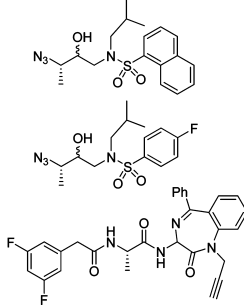
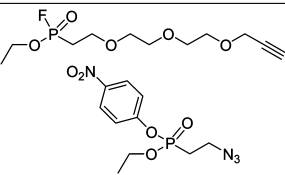
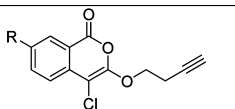
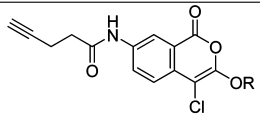
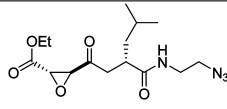
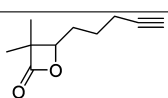
Chemical probe	Protein targets	References
	protein tyrosine phosphatase ^a	226
	lipases ^a	227
	UDP- <i>N</i> -acetylglucosamine 1-carboxyvinyltransferase ^a	228
	γ -secretase ^b	229 230
	Serine hydrolases ^a	231,232
 R = NO ₂ , H, NH ₂ , NHBz, NH-CO-CH ₂ NH ₂ , NH-CO-CH ₂ NH-C(NH)-NH ₂	serine proteases ^a	233
 R = Me, CH ₂ CH ₂ Ph, CH ₂ CHBr, CH ₂ CH ₂ -S-C(NH)-NH ₂	serine proteases ^a	233
	Cysteine proteases (cathepsins) ^a	234
	Serine and cysteine hydrolases ^a	235

Table 2. continued

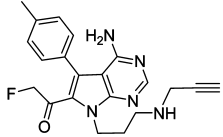
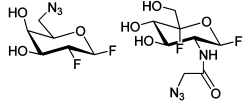
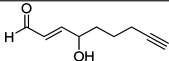
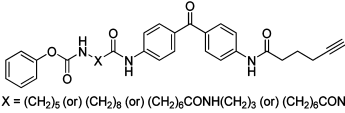
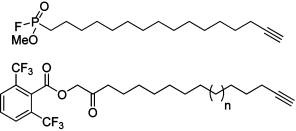
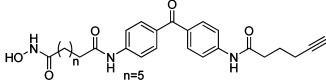
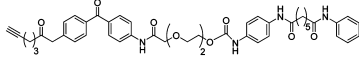
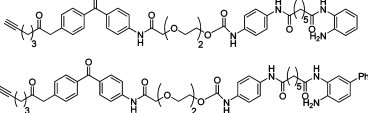
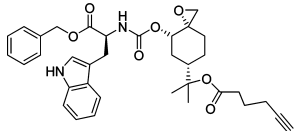
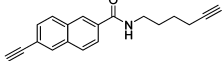
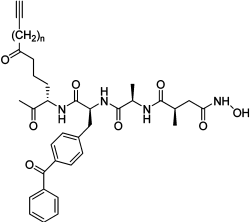
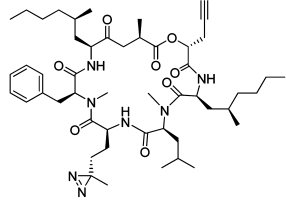
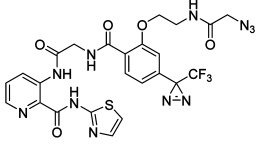
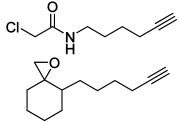
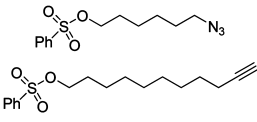
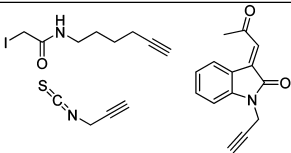
Chemical probe	Protein targets	References
	Kinases ^a	236
	Glycosidases ^a	237
	Oxidoreductases ^a	238
 X = (CH ₂) ₅ (or) (CH ₂) ₈ (or) (CH ₂) ₈ CONH(CH ₂) ₃ (or) (CH ₂) ₈ CONH(CH ₂) ₆	Fatty acid amide hydrolase ^a	239
	Fatty acid associated proteins ^a	240
	Histone deacetylases ^a	241-243
		
		
	Glycolytic enzyme: phosphoglycerate mutase-1 ^a	244
	Cytochrome P450 monooxygenases ^a	245
	Metalloproteases ^b	246

Table 2. continued

Chemical probe	Protein targets	References
	Protein transporter ^b	247
	Methionine amino peptidase ^b	248
	Disparate proteome reactivity ^a	249
	Multiple enzymes: transferases, dehydrogenases, hydratases ^a	250-251
	Cysteine residues ^a	252

^aActivity-based protein profiling (ABPP). ^bAffinity-based probes (AfbPs).

modified DNA was extremely useful to study many functions of nucleic acids and intercellular processes.

The labeling of both DNA and RNA using bioorthogonal chemistry was successfully performed by several research groups.²⁵³ DNA alkylation has also been probed through click derivatization of an alkynyl nucleotide cofactor analogue. Modified nucleotide analogues were developed containing a propargyl group introduced onto the uracil and other nitrogen bases moiety. These nucleotide derivatives were effectively incorporated into DNA and RNA biosynthesis, respectively, and subsequently labeled with fluorescent tags via click chemistry to achieve optical detection and sequencing of DNA and RNA.

7.5. Analysis of G-Quadruplex Structure Using Click Chemistry and G-Quadruplex Stabilizing Ligands

Guanine-rich (G-rich) stretches of DNA have a high propensity to self-associate into planar guanine quartets (G-quartets) to give unusual structures called G-quadruplexes. The association of G-quartets could also happen in solution by stacking the planar tetramers on top of each other.

G-quadruplex DNA plays an important role in telomere maintenance and is a potential tumor-selective target for chemotherapy in cancer.²⁵⁸

With the advance methods of X-ray crystallography, nuclear magnetic resonance spectroscopy (NMR), and other powerful technologies, the structures of many G-quadruplexes were resolved. The common structural characteristic of G-quad-

ruplexes was that the G-rich nucleic acid sequences tend to adopt the G-quadruplex conformation, which is a structure consisting of flat G-quartets of hydrogen-bonded guanines. Recent structural studies of various G-quadruplexes revealed the conformational polymorphism of these structures. For example, human telomeric sequences in physiological ion (K^+ or Na^+) solution have been found to fold into different quadruplex conformations.²⁵⁹

Komiyama and his co-workers successfully applied click chemistry for identification of many G-quadruplex structures, and they discovered the existence of DNA–RNA G-quadruplex.²⁶⁰ The researchers used differently modified nucleotides bearing azide and alkyne functional groups.

CuAAC reaction of a 5'-alkyne with a 5'-azide, of a 3'-alkyne with a 3'-azide, and of a 5'-alkyne with a 3'-azide can form different types of G-quadruplex structures. This method was used to probe the structures of G-quadruplexes, the most important finding being that a DNA–RNA hybrid G-quadruplex structure formed from human telomeric DNA and RNA sequences. The isolation of "all-DNA" and "all-RNA" quadruplexes was avoided by using alkyne-labeled RNA and azide-labeled DNA in the reaction. The advantage of the click reaction in this context is that it can trap a particular species, or produce a snapshot of the various interconverting structures that are present in a complex solution. Click method enables a snapshot to be taken of the existing species in solution. The species trapped by the click reaction can be separated and

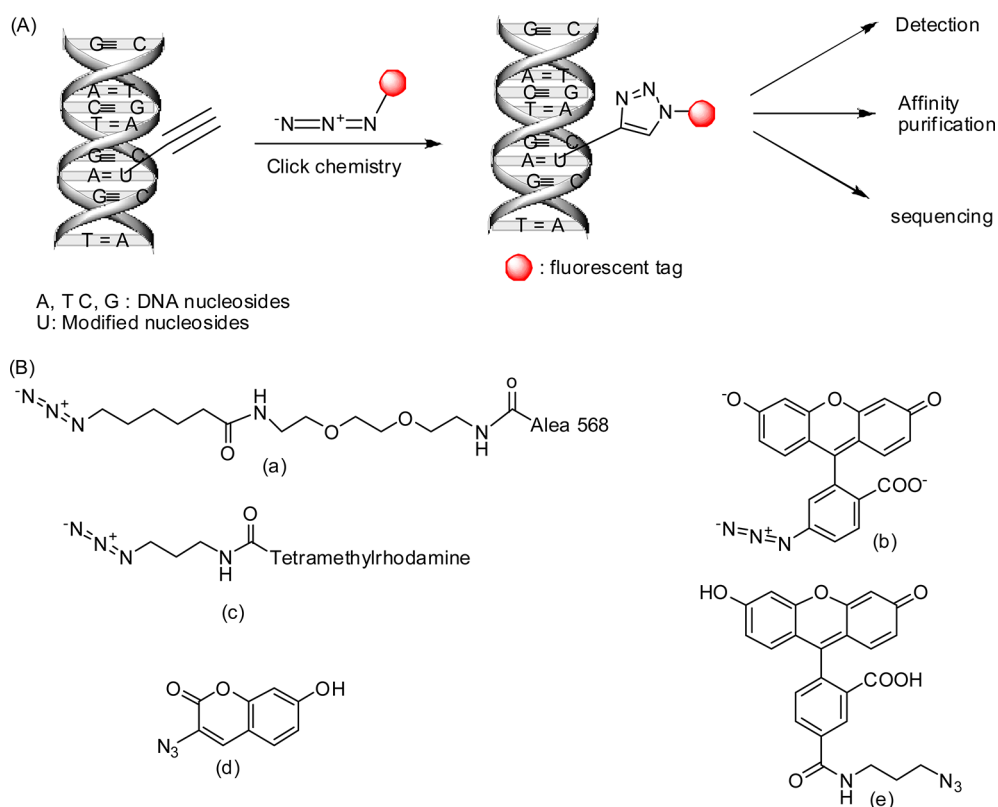


Figure 48. Use of modified nucleosides to label DNA in cells. (A) Schematic of the click reaction for detecting modified nucleosides incorporated into cellular DNA. The terminal alkyne group, exposed in the major groove of the DNA helix, readily reacts with an organic azide (R can be any fluorophore, hapten, electron-dense particle, quantum dot, etc.) in the presence of catalytic amounts of Cu(I). (B) Structures of the fluorescent azides used for detection of DNA.

analyzed. This approach is greatly facilitating G-quadruplex analysis in solution under various conditions (Figure 51).

The researchers initially investigated the telomere RNA G-quadruplex structures using the click chemistry reaction. The two possible structures of RNA G-quadruplex are shown in Figure 51: (a) the parallel dimeric telomere RNA G-quadruplex formed by 12-mer telomere RNA, and (b) the antiparallel dimeric G-quadruplex formed by the 12-mer *Oxytricha nova* sequence d(G4T4G4).

The researchers prepared the 12-mer 2'-OMe oligoribonucleotides (ORNs) ORN-1, with a 5'-alkyne, and ORN-2, with a 5'-azido group (Figure 52a), for structural analysis of parallel dimeric telomere RNA G-quadruplex. The RNA G-quadruplex was formed from 5'-alkyne and 5'-azido of modified oligoribonucleotides using the click chemistry reaction in the presence of CuSO₄/sodium ascorbate. The formation of RNA G-quadruplex confirmed gel electrophoresis and MALDI-TOF MS spectral analysis. This result indicates clearly that the formation of the G-quadruplex promotes the click reaction by bringing the 5'-alkyne and 5'-azido reaction partners into close proximity to one another.

Antiparallel G-quadruplex formed by an *Oxytricha nova* sequence was investigated using click chemistry reactions. The 5'-alkyne- and 3'-azido-labeled 12-mer oligodeoxyribonucleotide (ODN) ODN-5 was used for the synthesis of antiparallel G-quadruplex using Cu(I)-mediated click chemistry cycloaddition. The formation of antiparallel G-quadruplex was confirmed from gel gel electrophoresis and MALDI-TOF MS analysis (Figure 52b).

Next, the researchers applied click chemistry for establishing DNA G-quadruplexes structures. Two possible G-quadruplex structures are (i) (3 + 1) dimeric DNA G-quadruplex formed by 16-mer and 6-mer human telomeric and (ii) a DNA–RNA hybrid G-quadruplex formed by 12-mer human telomere DNA and 12-mer human telomere RNA sequences (Figure 53).

The researcher synthesized the 5'-alkyne- and 3'-azido-labeled 16-mer oligonucleotide ODN-7, and the 5'-azido- and 3'-alkyne-labeled 6-mer oligonucleotide ODN-8. A click reaction between ODN-7 and ODN-8 was performed in the presence of KCl and analyzed by polyacrylamide gel electrophoresis. When the copper catalyst was added, a new product, likely to be the circular oligonucleotide derived from the two linear precursors, was generated from the click reaction. This result indicates that the formation of a (3 + 1) dimeric DNA G-quadruplex between ODN-7 and ODN-8 promotes the click reaction to form the circular oligonucleotide. The formation of (3 + 1) dimeric DNA G-quadruplex was further confirmed by using a photo cleavable linker with gel electrophoresis analysis (Figure 54).

The researcher believed that click chemistry is a powerful emerging tool for analyzing and detecting a DNA–RNA hybrid G-quadruplex. So the researcher designed a click reaction in which only the DNA–RNA hybrid G-quadruplex could undergo an azide–alkyne cycloaddition, even in the presence of the corresponding DNA–DNA or RNA–RNA dimeric G-quadruplex. A 5'-azido ODN, ODN-12, and a 5'-alkyne-labeled ORN, ORN-1, were prepared as substrates for the click reaction. In the gel electrophoresis analysis, a new band appeared with a mobility shift between that of the 20-mer

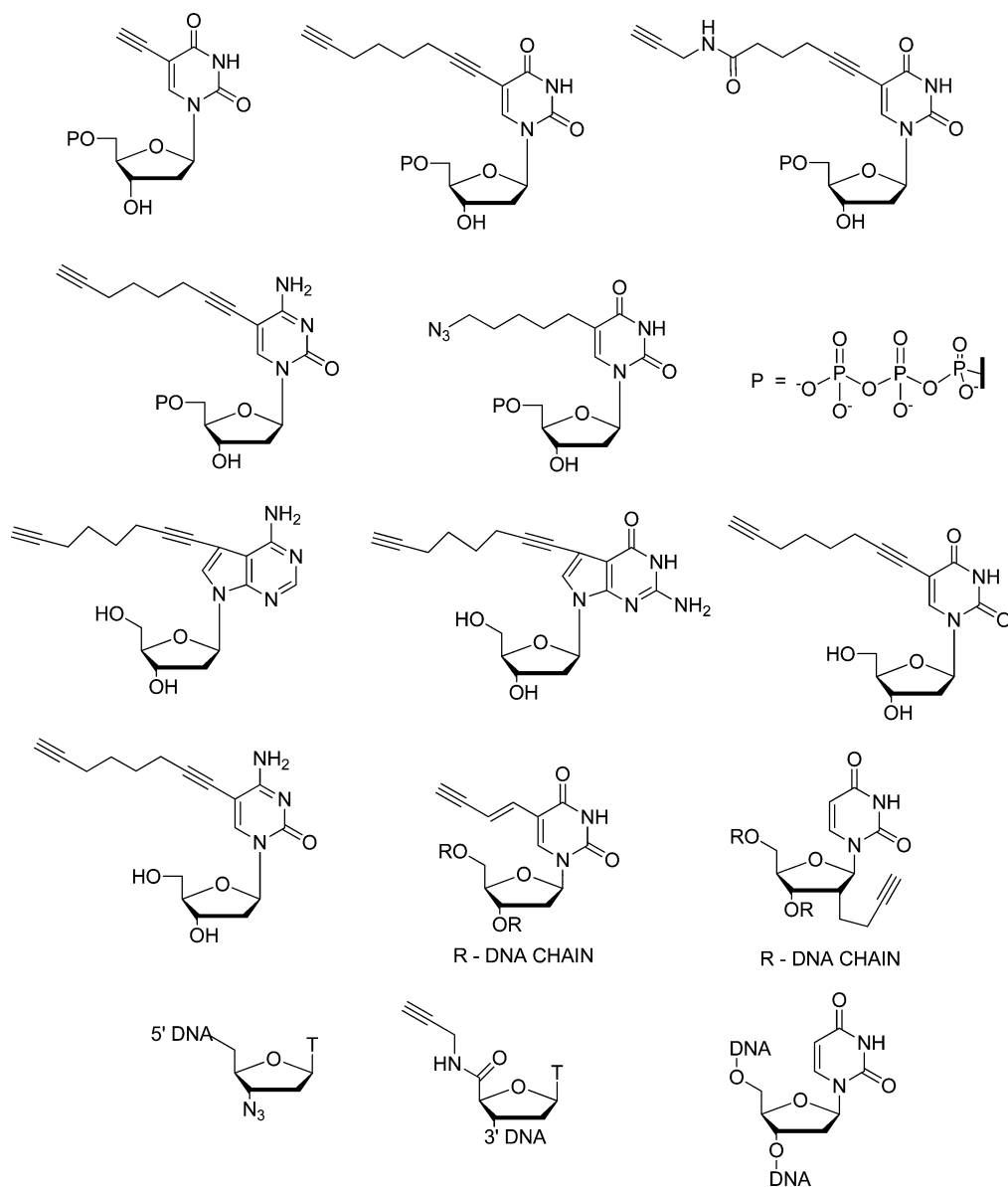


Figure 49. Azide- and alkyne-modified nucleosides used for DNA and RNA functionalization via click chemistry reaction.

oligonucleotide marker and that of the 30-mer marker in presence of CuSO_4 /sodium ascorbate solution. This band confirmed the formation product of a click reaction between the 5'-alkyne-labeled RNA and the 5'-azido DNA in a DNA–RNA hybrid G-quadruplex. Moreover, the 5'-alkyne-labeled 12-mer ORN-4 without the telomere sequence and 5'-azido ODN-12 were subjected to the same reaction conditions; no reaction occurred, which suggests that DNA–RNA G-quadruplex formation is required for the click reaction. This result indicates strongly that human telomere 12-mer DNA and 12-mer RNA could form a hybrid-type DNA–RNA G-quadruplex (Figure 55).

The conformations of G-quadruplexes provide selective recognition sites for small molecules, and thus these structures have become important drug-design targets for the treatment of various human disorders like viral infections and cancer. Many research groups developed G-quadruplexes stabilizing ligands. Click chemistry is also a powerful tool for generating G-quadruplexes stabilizing ligands.

Balasubramanian and co-workers employed click chemistry for the synthesis of novel 1,2,3-triazole-linked diethynylpyridine amides and trisubstituted diethynylpyridine amides as promising G-quadruplex binding ligands.²⁶¹ The researchers studied the binding properties of the ligands with four distinct G-quadruplexes found in the promoter regions of the proto-oncogenes *k-ras*, *c-myc*, and *kit*. These results reveal significant correlations between structural features and binding aptitudes of these ligands. Ligands of the trisubstituted series were found to be strong stabilizers and tight binders. All ligands showed excellent selectivity for quadruplexes over duplex DNA and some diversity in G-quadruplex recognition with K_d (quadruplex) values varying from 120 nM to 19 μM (2-fold to 50-fold specificity). Compound 170 showed the most potent stabilizing ligand in the triazole series with high binding affinity toward the *c-myc* and *c-kit2* quadruplexes with submicromolar equilibrium dissociation constants (K_d) of 200 and 350 nM, respectively (Figure 56).

Moses and co-workers explored click chemistry for the synthesis of highly selective stabilization of G-quadruplex ligand

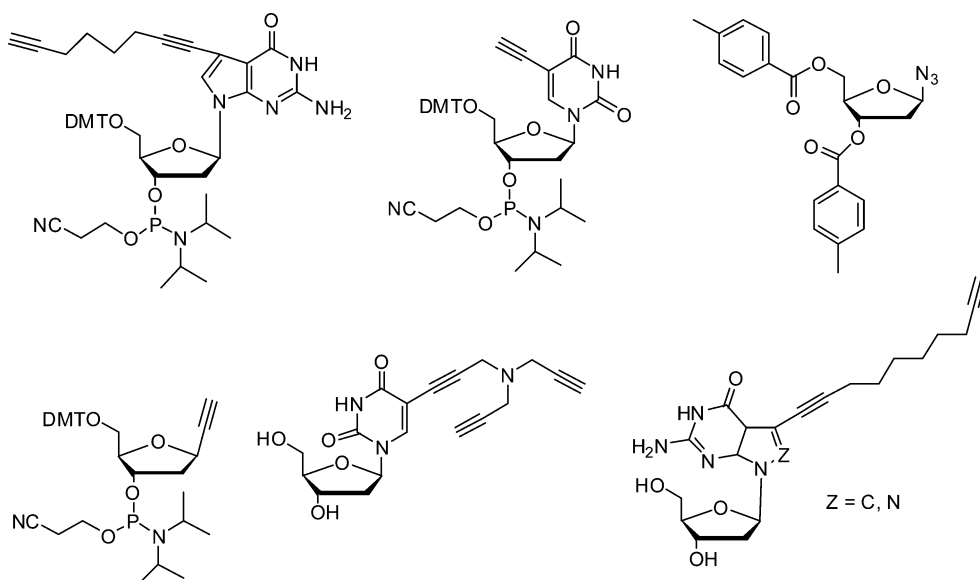


Figure 50. Azide- and alkyne-modified nucleosides used for DNA and RNA functionalization via click chemistry reaction.

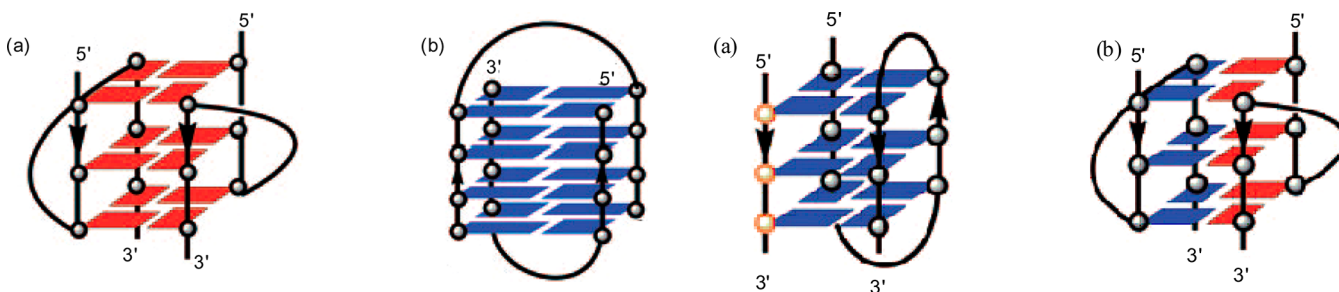


Figure 51. Schematic representation of possible human telomeric RNA G-quadruplex structures. (a) The parallel dimeric telomere RNA G-quadruplex formed by 12-mer telomere RNA. (b) The antiparallel dimeric G-quadruplex formed by the 12-mer *Oxytricha nova* sequence d(G4T4G4).

Figure 53. Schematic representation of two possible DNA G-quadruplex structures: (a) A (3 + 1) dimeric DNA G-quadruplex formed by 16-mer and 6-mer human telomeric sequences; and (b) a DNA–RNA hybrid G-quadruplex formed by 12-mer human telomere DNA and 12-mer human telomere RNA.

from 1,3-diethynylbenzene precursors.²⁶² First generation of synthesized compounds showed excellent affinity and selectivity

for the G-quadruplex. The ability of these compounds to stabilize G-quadruplex DNA was investigated using a high-

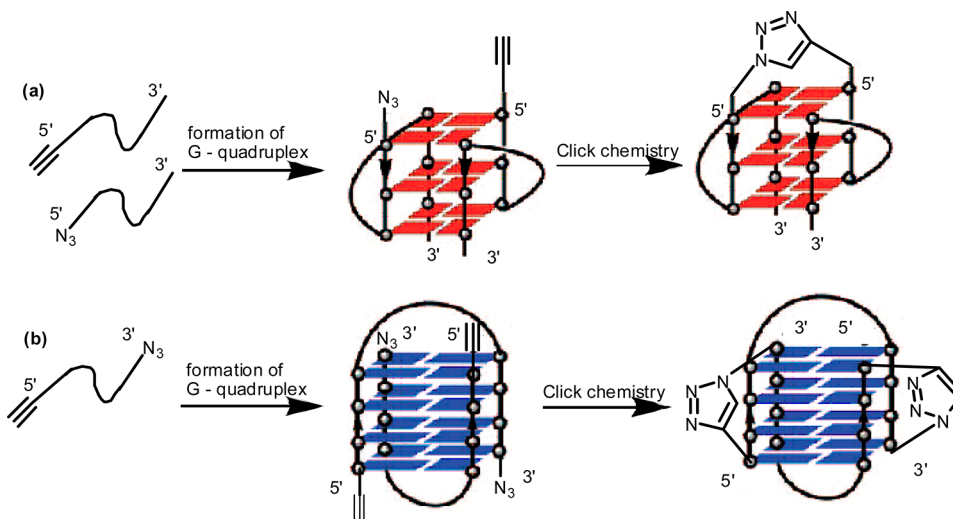


Figure 52. Click chemistry reaction of RNA G-quadruplex formation. (a) Parallel dimeric telomere RNA G-quadruplex formed by 12-mer telomere RNA using click chemistry reaction. (b) Antiparallel dimeric G-quadruplex formed by the 12-mer *Oxytricha nova* sequence d(G4T4G4) using click chemistry reaction.

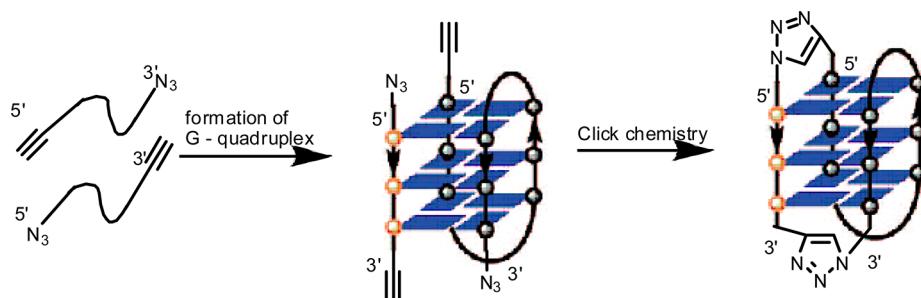


Figure 54. Confirmation of the formation of a (3 + 1) dimeric DNA G-quadruplex by a click reaction in a solution containing K^+ ions. Click reactions between the 5'-alkyne and the 5'-azido group and between the 3'-azido group and the 3'-alkyne lead to a 22-mer circular oligonucleotide.

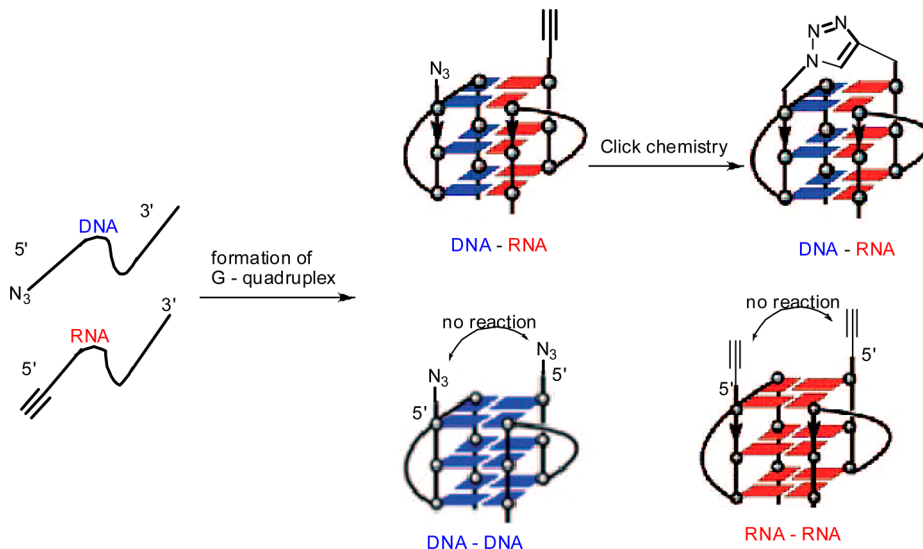


Figure 55. Schematic depiction of the detection of the DNA–RNA G-quadruplex. The use of 5'-azido-labeled DNA and 5'-alkyne-labeled RNA may result in a mixture of three types of G-quadruplex. Only the DNA–RNA G-quadruplex brings the alkyne and the azido group into close proximity to give the product of an azide–alkyne cycloaddition.

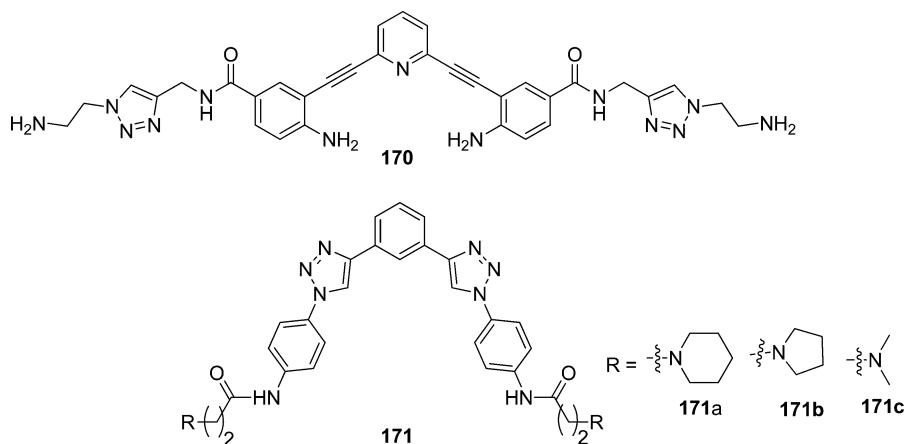


Figure 56. Chemical structures of G-quadruplex stabilizing ligand generated via click chemistry.

throughput FRET (fluorescence resonance energy transfer)

assay. Using this assay, compounds **171a**, **171b**, and **171c**

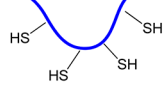
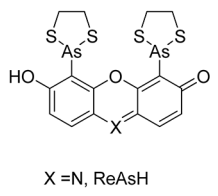
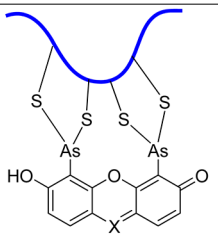
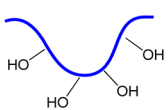
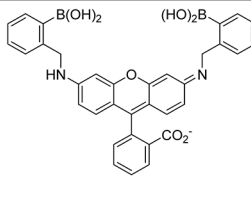
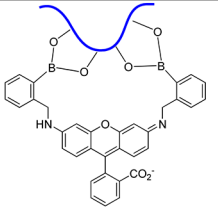
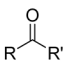
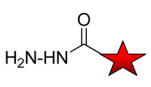
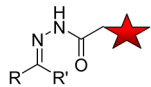
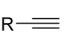

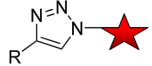
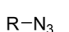

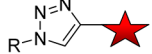
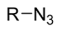
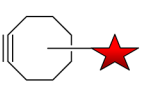
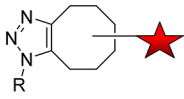
showed high activity with $^{tel}EC_{50}$ values of 13.3, 17.1, and 23.5

μM , respectively (Figure 56).

8. COPPER-FREE CLICK CHEMISTRY REACTIONS FOR BIOLOGICAL SYSTEMS

Cells and organisms are highly dynamic entities involving a very diverse array of biomolecules to conduct intercellular and intracellular processes throughout life. To monitor and understand these cellular process both in time and in space has sparked tremendous interdisciplinary developments in biology, chemistry, and physics. Chemical labeling is one of

Table 3. Chemical Reporters, Probes, and Reactions Used in Imaging Approaches^a

Chemical receptor	Probe	Bioconjugation product	Reaction type, covalent or non-covalent binding target
	 X = N, ReAsH		Arsenic-thiol interaction, non-covalent attachment proteins
			Boronate esterification, Covalent attachment of proteins
			Hydrazone formation Covalent attachment of proteins and glycan
			Click chemistry Covalent attachment of proteins, lipids and glycan
			Click chemistry Covalent attachment of proteins, lipids and glycan
			Strain promoted click chemistry Covalent attachment of proteins, lipids and glycan

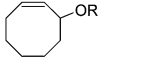
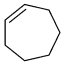
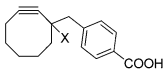
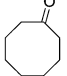
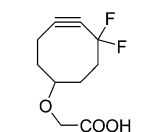
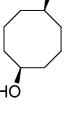
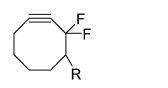
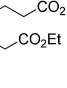
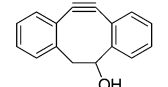
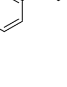
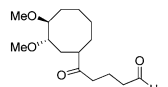
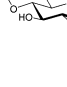
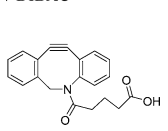
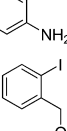
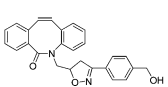
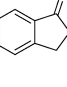
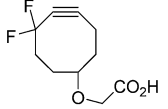
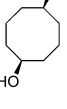
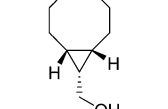
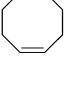
^aRed stars depict fluorescent tag moieties.

the powerful emerging tools for monitoring biological process in the living systems. Their many types of chemical labeling processes are reported in the literature. Click chemistry is one of the best reactions to label the biomolecules in and outside the living systems (Table 3).^{200,263,264}

The main feature of all chemical labeling approaches is the introduction of a small and unique, noncanonical reporter group that provides a molecular “handle” in subsequent bioconjugation reactions with a probe to follow the fate of

the tagged biomolecule in downstream visualization or affinity purification applications. In the design of chemical reporters and labeling probes, the following prerequisites have to be considered to achieve a “true” bioorthogonality (bioorthogonal meaning “noninteracting but compatible with biology”): minimal invasiveness to avoid perturbations of the particular biomolecule in its cellular environment, high reactivity, as well as high chemo-selectivity and biocompatibility of the bioconjugation reaction for intracellular and extracellular

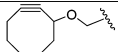
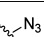
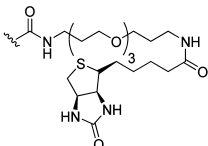
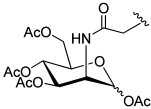
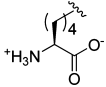
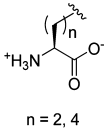
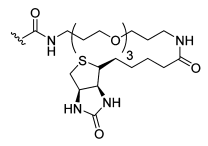
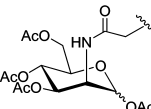
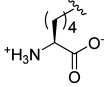
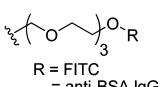
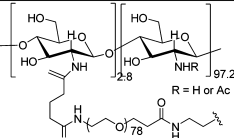
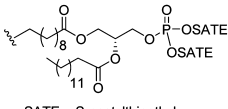
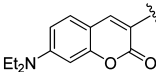
Table 4. Overview of Cyclooctyne Probe Synthesis and Their Reactivities toward [3 + 2] Cycloadditions with Azides

Azidophile	Starting material	$^{\circ}\log P$	No. of synthetic steps	Yield [%]	$k^{[a]}$ [$\times 10^{-3}$ $\text{m}^{-1} \text{s}^{-1}$]	Solvent	Ref.
1 OCT AND ALO  R = $\text{CH}_2\text{PhCO}_2\text{H}$ (OCT) R = $\text{CH}_2\text{CO}_2\text{H}$ (ALO)		OCT: 4.23 ALO: 2.30	4 5	52 36	2.4 1.3	CD_3CN	270, 271
2 MOFO, NOFO  R = H (NOFO) R = F (MOFO)		NOFO: 5.31 MOFO: 4.79	4 5	12 15 4.3	1.2	CD_3CN	271
3 DIFO3 		1.93	10	1.2	76	CH_3CN	272
4 DIFO2 AND DIFO3  R = $\text{CH}_2\text{PhCO}_2\text{H}$ (DIFO2) R = $\text{CH}_2\text{CO}_2\text{H}$ (DIFO3)		DIFO2: 5.17 DIFO3: 2.59	8 10	27 21	42	CH_3CN	273
5 DIBO 		3.90	5	10	170 120	CH_3CN CD_3OD	274
6 DIMAC 		1.12	11	5	3	CH_3CN	275
7 DIBAC 		4.07	9	41	310 360 ^(b)	CD_3OD D_2O	276
8. BARAC 		3.9	6	18	960	CD_3CN	277
9. DIFO 		1.3	4	-	76	CD_3CN	278
10. BCN 		1.2	3	61	140	CD_3OD : D_2O (3:1)	279

^aSecond-order reaction rate constant determined with benzyl azide as model, unless otherwise indicated. ^b2-Azidopropanoic acid used as azide to determine reaction kinetics.

biomolecules. Endowed with these features, bioorthogonal labeling strategies possess characteristics of chemical reactions

Table 5. Use of 3-Alkoxyoctyne Conjugates and Azides for Bioorthogonal Labeling

			Purpose(s)	Detection	Ref.
1.			as above, in Jurkat cell-surface glycoproteins	avidin-FITC, flow cytometry	270
2			incorporation of azidomethyl amino acid in dihydrofolate reductase (DHFR)	Western blot (a-biotin-HRP)	270
3			aminoacyl-tRNA synthetase activity monitoring from cell-surface display of noncanonical amino acids	avidin-Alexa Fluor 488, then flow cytometry and cell sorting	280
4			metabolic conversion of Ac4ManNAz into SiaNAz and detection in Jurkat cell surface glycoproteins	avidin-FITC, flow cytometry	270
5			incorporation in dihydrofolate reductase (DHFR)	Western blot (a-biotin-HRP)	270
6			development of stable polymeric carriers for drug delivery	DLS, Dot Blot and confocal fluorescence microscopy of nanoparticles	281
7			labeling of lipids in RAW macrophages ^[a]	fluorescence microscopy of living cells	282

^aThe cyclooctyne–lipid conjugate is mixed with living cells; detection was achieved with an azide-containing probe.

and a highly versatile “platform” principle enabling a wide range of different probes to be assigned to different classes of biomolecules.²⁶⁵

Bioorthogonal chemical reactions, those that do not interact or interfere with biology, have allowed for the exploration of numerous biological processes that were previously difficult to study. A widely used bioorthogonal functional group is the

Table 6. Use of 3-Alkylcyclooctyne Conjugates and Azides for Bioorthogonal Labeling^a

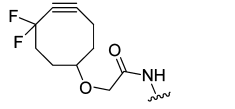
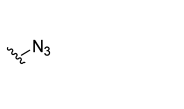
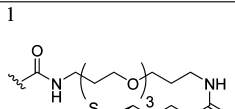
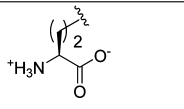
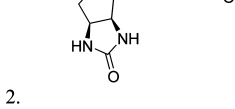
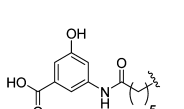

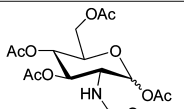
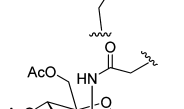
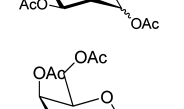
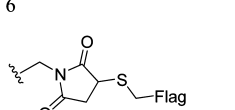
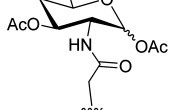

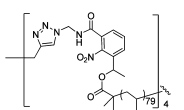
			Purpose(s)	Detection	Ref.
1.			metabolic conversion of Jurkat cell-	avidin-FITC flow cytometry	270
2.			ligation of azido-octanoic acid to fusion protein containing a LpIA acceptor peptide	fluorescence microscopy	283
3.	X = H NH-Ala-PG-OH NH-Gly-Pro-Leu-Gly-Val-Arg-PG-OH PG = Propargylglycine		sequential labeling of peptide substrate for MMP-2 with different fluorophores	FRET	284
4.			dual loading of silica nanoparticles	FRET	284
5.	X = H 		metabolic conversion of Ac4ManNAz to SiaNAz and detection in CHO glycoproteins	confocal luminescence imaging	285
6.	X = H 		incorporation of azido-homoalanine in newly synthesized proteins (PYP, E. coli)	tryptic digest, mass spectrometry	286-288
7.			chemical cross-linking of cytochrome c	tryptic digest, mass spectrometry	287
8.	X = F 		in situ cross-linking of photodegradable star polymers	time-resolved FTIR spectroscopy, size-exclusion chromatography	289

^aA cyclooctyne-biotin conjugate without the lipophilic phenyl ring was also applied (not shown).

azide, which can be incorporated into myriad biological molecules by feeding cells or organisms azide-functionalized metabolic substrates. The abundance, location, and dynamics of the azide-labeled biomolecules were monitored by chemical

ligation with probes bearing complementary functionality. The copper-catalyzed click reaction between azides and terminal alkynes is ideal for many applications, but copper(I) has the undesirable side effect of being cytotoxic at low concentrations.

Table 7. Use of the First-Generation DIFO and Azides for Bioorthogonal Labeling

			Purpose(s)	Detection	Ref.
1			incorporation of azido-homoalanine in dihydrofolate receptor	SDS-PAGE, then silver staining	272
2.			identification of catalytically active adenylation domains of NRPS	Western blot streptavidin pull-down and E. coli infection by phages	290
			labeling of azido glycans in Jurkat cells, time-lapsed and multicolor imaging of glycans in CHO cells	fluorescence microscopy	272
	2 R = Alexa Fluor 488		in vivo labeling of glycans in developing zebrafish		291
	3 R = Alexa Fluor 568		in vivo labeling of glycans in C. elegans		292
6			in vivo labeling of glycans in mice, isolation of splenocytes	anti-FLAG-FITC antibody, flow cytometry	272
7			in situ cross-linking of photodegradable star polymers	time-resolved FTIR spectroscopy, size-exclusion chromatography	289

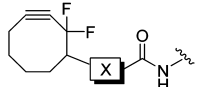
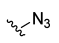
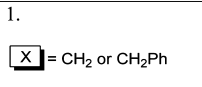
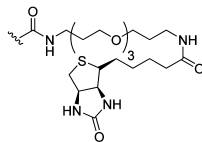
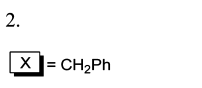
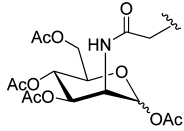
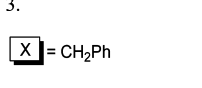
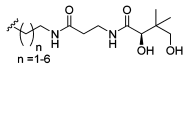
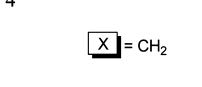
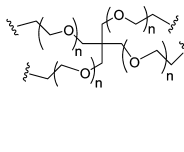
The reaction of azides with strained alkynes, such as cyclooctynes, relieves that burden by readily forming a triazole product without a toxic catalyst. Such reactions, in addition to other select cycloadditions, are now being referred to as Cu-free click chemistries.^{266,267}

Cycloadditions were viewed as ideal reactions because of tunable electronics and their intrinsic selectivity. Huisgen developed the [3 + 2] cycloaddition between an azide and an acyclic alkyne, but this reaction required a good deal of heat to overcome the activation barrier of deforming the alkyne's bond angle to form the triazole.^{263a} Sharpless and co-workers developed a Cu-catalyzed rendition of this reaction using terminal alkynes as substrates, but the metal's cytotoxicity limits its use in living systems.^{263b} To increase the rate of the cycloaddition without the need of a catalyst, researchers took a page out of old physical organic literature and looked at ring-strain as a way to overcome the sluggish reactivity of alkynes with azides. Upon reading that cyclooctyne reacts with phenylazide "explosionsartig" (like an explosion), we decided to investigate this class of molecules. The bond angle of the sp²-hybridized carbons in cyclooctynes is B1601, which is distorted toward the transition state of the cycloaddition reaction, resulting in a dramatic rate acceleration.^{263c}

8.1. Design and Synthesis of Bioorthogonal Reagents

The potential for application of CuAAC in (bio)materials and living systems is very limited, due to the toxicity of copper. For in vitro and in vivo applications in particular, the development of copper-free or preferably metal-free-ligation chemistries is very much helpful. The azide and strained cycloalkane promoted cycloaddition reaction only plays a significant role in developing potential application in the living system. The majority of papers dealing with copper-free procedures focused on the chemistry of azides with strained alkynes. Strain-promoted cycloadditions of cyclic alkenes and alkynes established themselves as powerful tools in bioconjugations. Cycloadditions of strained cycloalkynes were exclusively limited to azides, despite the large number of Huisgen reactions of alkynes with other dipoles such as nitrile oxides, diazo compounds, azomethines, and nitrones. Only recently were two independent papers reported on cycloadditions of dibenzocyclooctyne and dibenzoazacyclooctyne with nitrones, reactions that proceed up to 300 times more rapidly than those with azides. Other bioorthogonal reaction pairs not involving strained alkynes were recently developed, in particular thiol-ene reactions, alkene-azomethine cycloaddition, and the cycloaddition of tetrazine with *trans*-cyclooctene.^{268,269}

Table 8. Use of the Second-Generation DIFO and Azides for Bioorthogonal Labeling

			Purpose(s)	Detection	Ref.
1.	 X = CH ₂ or CH ₂ Ph		metabolic conversion of Ac4ManNAz into SiaNAz and detection in Jurkat and CHO cell-surface glycoproteins	avidin-FITC, flow cytometry (Jurkat) fluorescence microscopy (CHO)	273
2.	 X = CH ₂ Ph		bottom-up synthesis of microtissues composed of multiple cell types	flow cytometry, fluorescence and brightfield microscopy	293
3.	 X = CH ₂ Ph		probing protein interactions between COM domains of NRPS enzymes	SDS-PAGE	294
4.	 X = CH ₂		tailoring biophysical properties of cell microenvironments by cell encapsulation/patterning	rheology, confocal microscopy	295

Strain-promoted alkyne–azide cycloaddition (SPAAC) with cyclooctynes is ideal for bioconjugation with no additional reagents required. Cyclooctyne reactivity could be greatly enhanced by structural modification, for example, by fluorination, by sp^2 -hybridization of ring atoms, or by fusion to cyclopropane. It was going beyond the scope of this account to discuss in detail all cyclooctyne variants applied in bioconjugation. This topic was covered by several excellent recent reviews and papers with some highlights of cyclooctynes applied in bioconjugation used in the literature.²⁶⁸

For a reaction to be suitable for bioconjugation, two basic features are of high importance: reactivity and selectivity. First, high reactivity is clearly a requirement for application under highly dilute conditions, for example, in vivo. Second, it is obvious that any bioorthogonal ligation becomes severely upset in the case of lipophilic binding to proteins and/or when cross-reactivity with natural biomolecular functionality is operative. Several of the strained systems currently in use involve hydrocarbon scaffolds with limited solubility in water. Apart from solubility issues, the bioavailability of a highly hydrophobic probe may be decreased due to sequestration by membranes or nonspecific binding to serum protein, and $c \log P$ values are a measure of lipophilic efficiency and give complete information about solubility. In that respect, the DIMAC system (Table 4, entry 6) clearly stands out as indicated by the

provided calculated $c \log P$ values. Generation cyclooctynes (Table 4, entries 1 and 2) were relatively easy to prepare (4–5 steps, 12–52% overall yields) and provided the basis for current developments in copper-free ligation chemistries. In particular, the development of the DIFOs (Table 4, entry 3) heralded an era of novel opportunities for strain-promoted cycloadditions with azides, with reaction rates over 10 times greater than those of earlier cyclooctynes. Moreover, the troublesome synthesis of DIFOs (10 steps, 1.2% overall yield) was recently overcome by development of the so-called “second-generation” DIFOs (Table 4, entry 4), which can be prepared in acceptable overall yields (about 25%). The most reactive cyclooctyne reported to date is benzofused lactam BARAC (entry 8). Rate enhancement by benzofusion was earlier demonstrated by Boons et al. in the development of DIBO (entry 5),²⁷⁴ while introduction of an amide nitrogen in the ring as in DIBAC (entry 7) sprouted.²⁷⁶ The order of reactivity of DIBO < DIBAC < BARAC, that is, 0.17, 0.36, and 0.96 $M^{-1} s^{-1}$, respectively, is suggestive of a direct correlation between the number of sp^2 -hybridized atoms and reactivity. Lipophilic compounds were not only poorly water-soluble but, more importantly, may engage in hydrophobic interactions with proteins. A poor-yielding synthesis blocked full flourishing of the first cyclooctyne with suitable reactivity, that is, DIFO (entry 9). Second-generation DIFOs (entries 4 and 9) were more easily accessible

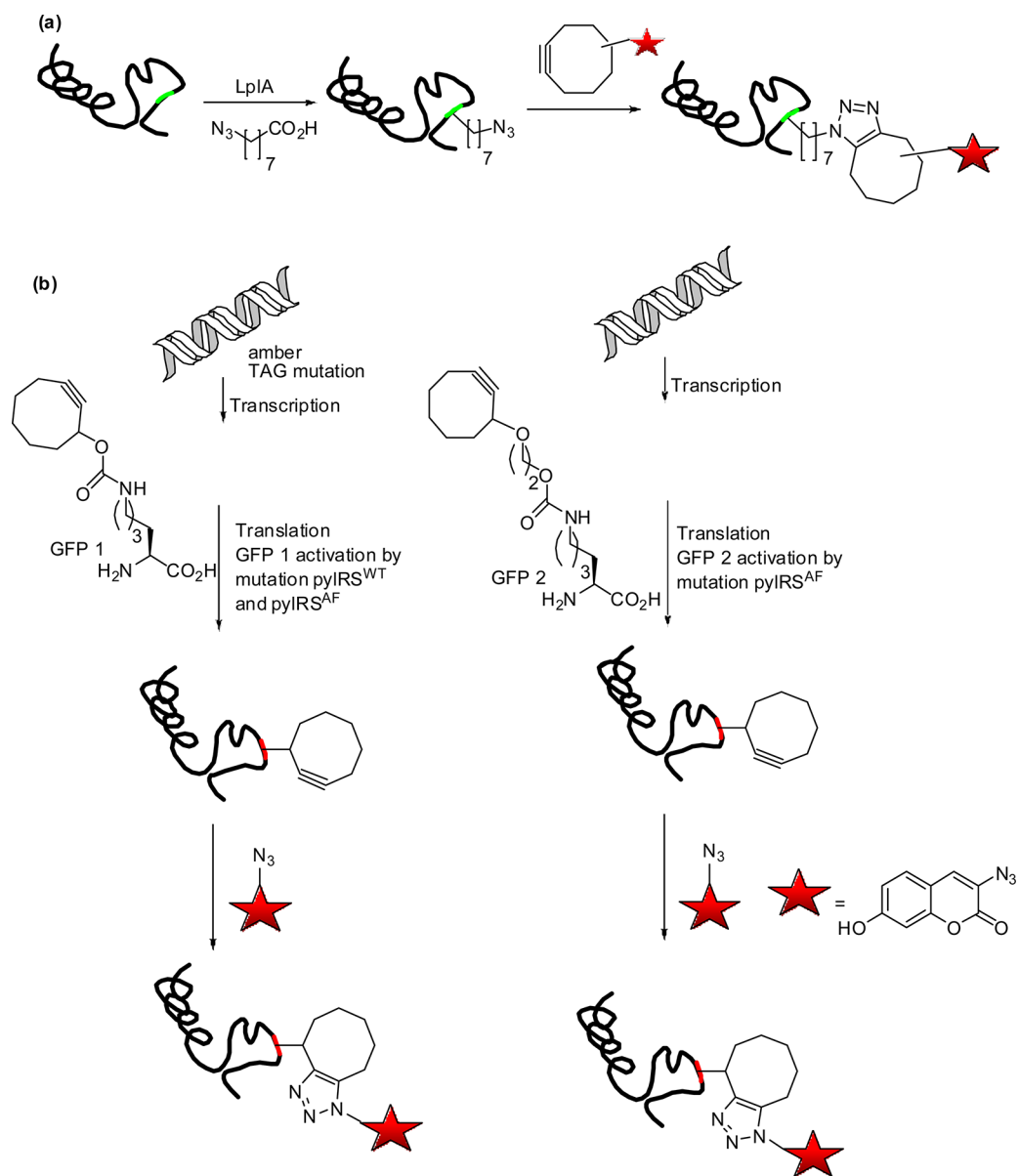


Figure 57. Genetically encoded chemical reporter. (a) Incorporation of lipoic acid ligase followed by copper click chemistry for cell surface protein labeling. (b) Incorporation of noncanonical amino acids during translation for in vivo labeling *E. coli*.

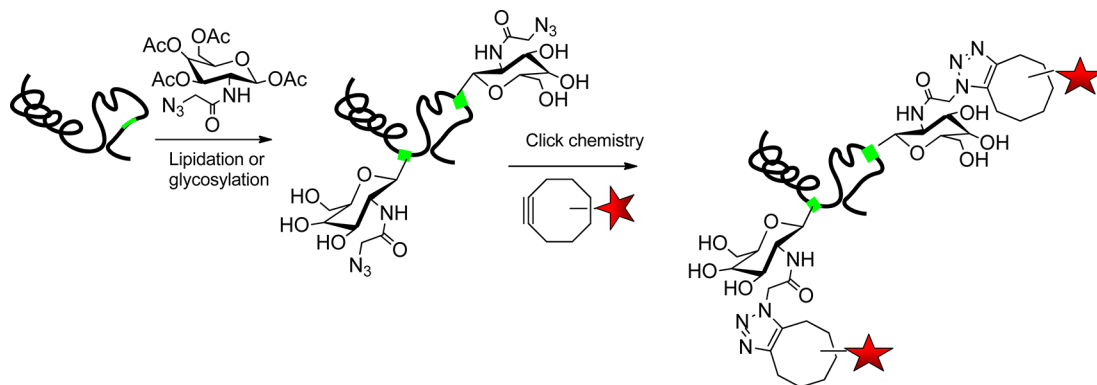


Figure 58. Post-translational incorporation of noncanonical lipids and glycans using click chemistry for monitoring glycans on cells, on tissues, and on zebrafish embryos surface.

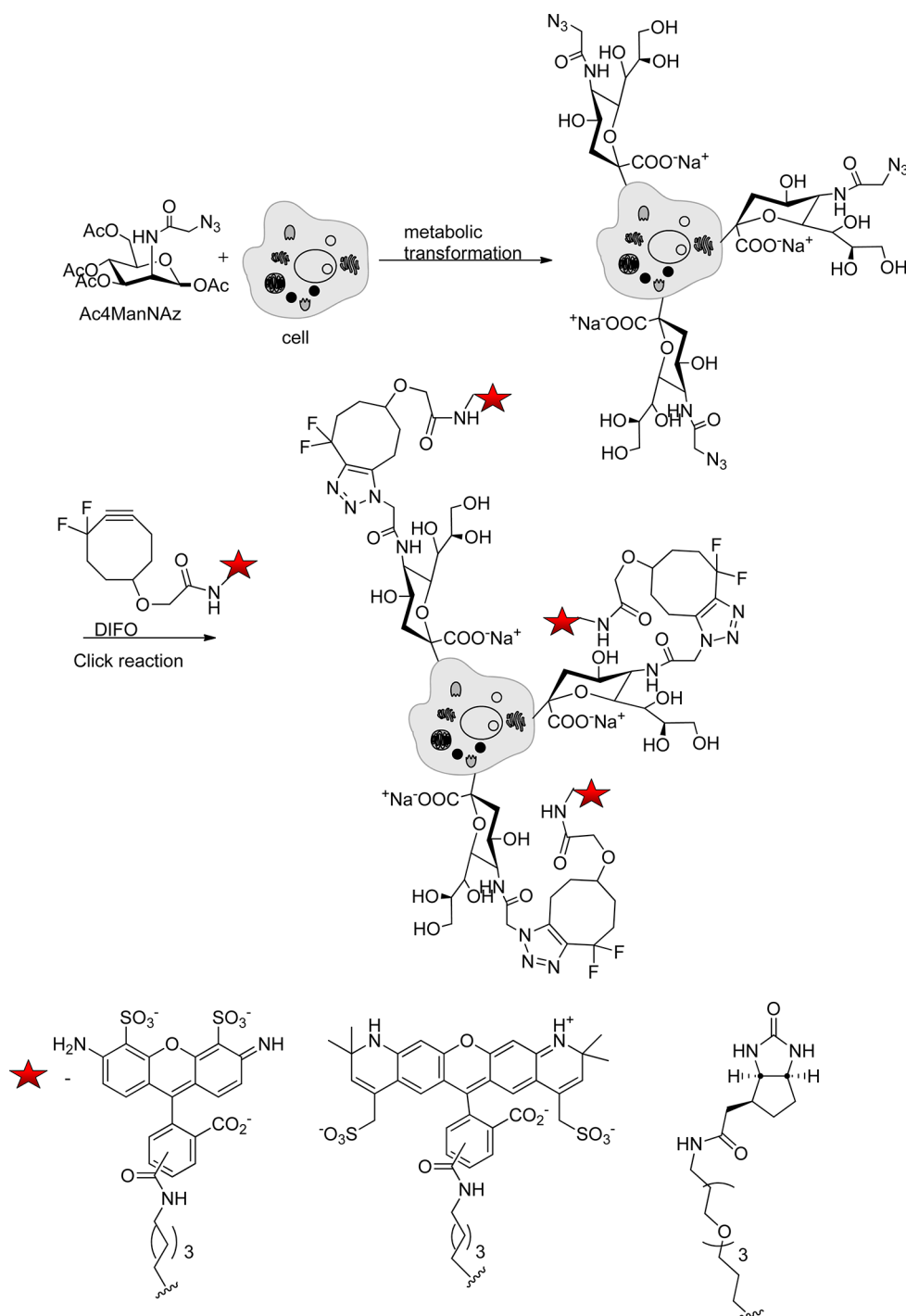


Figure 59. Bioorthogonal copper-free click chemistry for dynamic monitoring of cell-surface glycans by in vivo imaging using various fluorophores and DIFO.

(8–10 steps, overall yields ~25%), while the synthesis of DIBAC proved more straightforward and high yielding (nine steps, 40% overall yield).²⁶⁹

8.2. Cyclooctyne Derivatives Used in Copper-Free Click Bioorthogonal Chemistry

The use of bioorthogonal reactions to tag biomolecules with probes requires that one reagent was installed in the target molecule. Also, the reagent must be sufficiently stable so as to persist during the installation process. There were numerous applications of cyclooctynes in the context of biological systems. The cyclooctynes were able to selectively label cells

of metabolically incorporated azidosugars onto their surface as glycoproteins in the living cells.

The potential bioapplication of 3-alkoxycyclooctyne was established using labeling of glycoprotein in the cell-surface, development of polymeric carriers for drug delivery, and labeling of lipids. Jurkat cells were incubated with Ac₄ManNAz to introduce azide-containing sialic acid on cell-surface glycans through metabolic incorporation. After 3 days, the azide-modified cells were treated with 3-alkoxycyclooctyne at several concentrations and with different densities of cell-surface azides and varying reaction times. It was found that more efficient

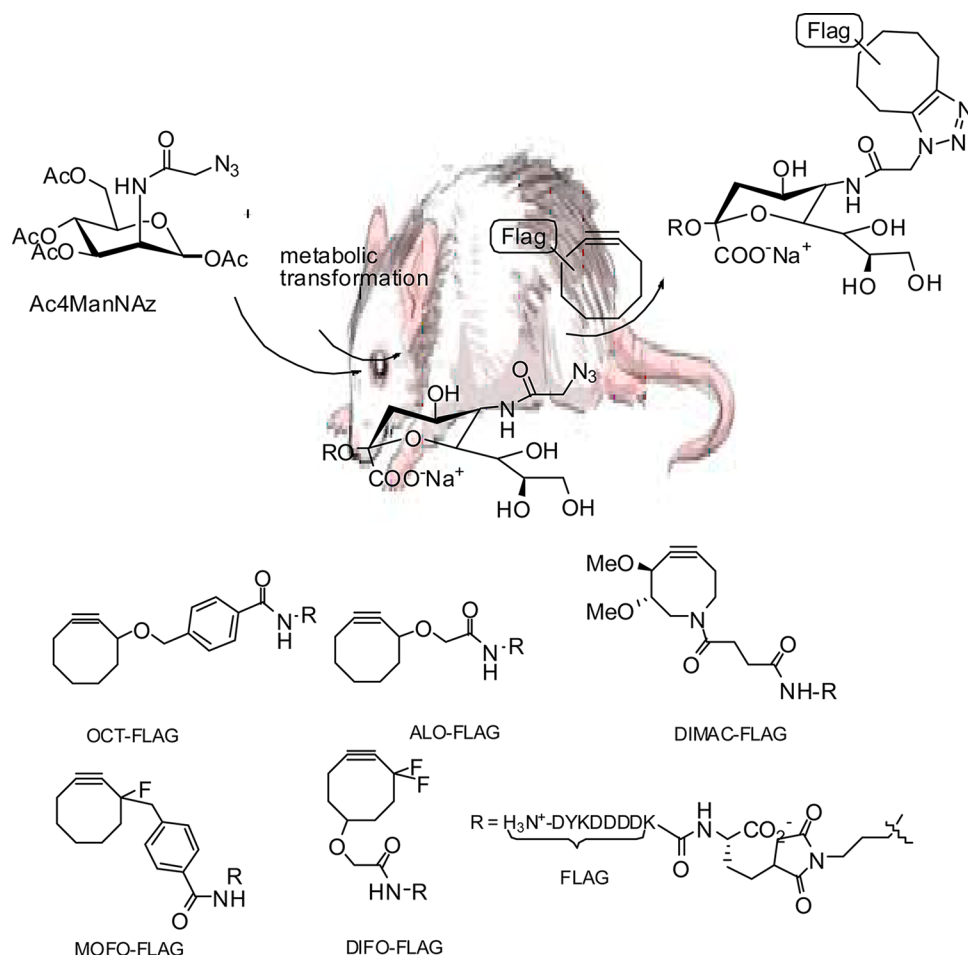


Figure 60. Copper-free click chemistry in mice. (A) Mice were injected with Ac4ManNAz once daily for 1 wk to allow for metabolic labeling of glycans with SiaNAz. The mice were then injected with a cyclooctyne-FLAG conjugate for in vivo covalent labeling of azido glycans. (B) Panel of FLAG conjugates used in this study.

labeling could be achieved with higher concentrations of 3-alkoxycyclooctyne, higher azide densities, and longer reaction times. Importantly, no negative effects on cell viability were observed. An overview of the use of 3-alkoxycycloalkyne conjugates is provided in Table 5.

Tirrell and co-workers' incorporation of noncanonical amino acids into cellular proteins often requires engineering new aminoacyl-tRNA synthetase activity into the cell.²⁸⁰ A screening strategy that relies on cell-surface display of reactive amino acid side-chains was used to identify a diverse set of methionyl-tRNA synthetase (MetRS) mutants that allows efficient incorporation of the methionine (Met) analogue azidonorleucine (Anl). We demonstrate that the extent of cell-surface labeling in vivo is a good indicator of the rate of Anl activation by the MetRS variant harbored by the cell. By screening at low Anl concentrations in Met-supplemented media, MetRS variants with improved activities toward Anl and better discrimination against Met were identified.²⁸⁰

Lallana et al. and co-workers observed a strong depolymerizing effect of CuI when CuAAC was applied on nanostructures based on azide-containing polymeric chitosan-PEG conjugates. Therefore, cyclooctynes were linked to fluorescein isothiocyanate (FITC) and an anti-BSA antibody.²⁸¹ The FITC-cyclooctyne conjugate was ligated to chitosan-PEG-N₃ and mixed with unfunctionalized chitosan-PEG to provide fluorescent nanoparticles. The nanoparticles were in turn

decorated with cyclooctynes conjugated to anti-BSA rabbit IgG, as judged by dynamic light scattering (DLS) and staining of BSA-agarose beads (Table 5, entry 7).²⁸²

The easy synthetic preparation of 3-alkylcyclooctyne was facilitated in several biological applications, as summarized in Table 6. A microbial lipoyl ligase (LplA), for example (entry 2), was redirected to attach azide-containing fatty acids, ideally 8-azido-octanoic acid, onto an engineered LplA acceptor peptide (LAP). Cyclooctynes conjugated to cyanine-3 (Cy3), Alexa Fluor 568, or biotin were subsequently used to visualize HEK cells containing fusion proteins either of LAP with cyan fluorescent protein (in turn fused to a transmembrane receptor) or of LAP with the low-density lipoprotein receptor.²⁸³

Wolfbeis et al. prepared synthetic peptides containing both propargylglycine and an N-terminal cyclooctyne moiety.²⁸⁴ Subsequent labeling with SPAAC followed by CuAAC with different fluorophores afforded peptide substrates for MMP2, a diagnostic tumor indicator. Cleavage of the peptide by MMP2 could be effectively monitored by Förster resonance energy transfer (FRET). Alternatively, the cyclooctyne-labeled peptide could be loaded onto azido-functionalized silica nanoparticles (predoped with triazolylcoumarin), followed by CuI-catalyzed introduction of a fluorescent label to obtain dually labeled nanoparticles for FRET detection. In another contribution, the same authors demonstrated that a 3-alkylcyclooctyne con-

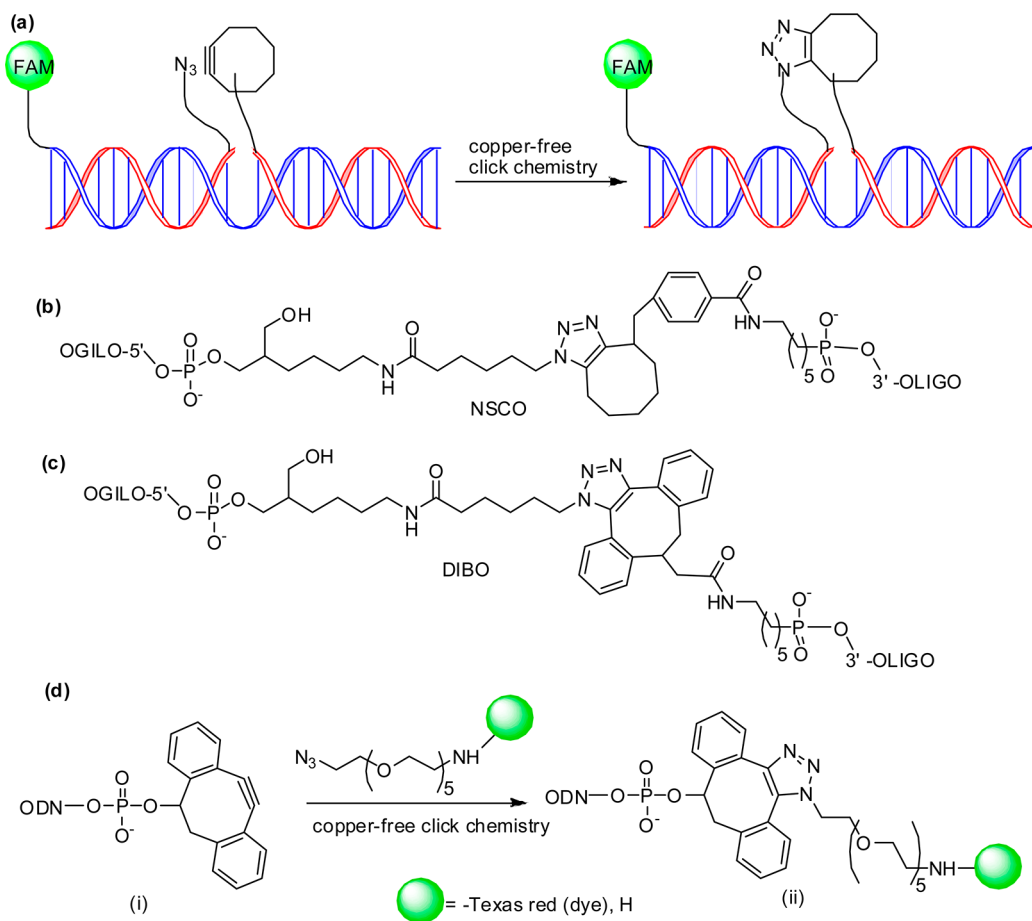


Figure 61. Strain-promoted click chemistry for terminal labeling of DNA. (a) Schematic of representation of SPAAC click DNA ligation between azide-labeled and cyclooctyne-labeled oligonucleotides (FAM = 6-carboxyfluorescein). (b,c) Chemical structures of NSCO and DIBO alkynes, respectively, at the ligation point. (d) 5'-DIBO-modified ODN (i) and Texas red derivatives of azide used as precursors to label terminal DNA.

jugated to a red fluorophore can be useful for cell-surface staining of Chinese hamster ovary (CHO) cells.²⁸⁴

Bertozzi et al. applied the fluorinated cyclooctyne in the same cell-surface glycoprofiling experiments as for the previously reported cyclooctynes (Table 6, entry 1). 3-Alkoxy-cyclooctyne conjugates found one application in the cross-linking of azido-terminated star polymers prepared by ATRP (entry 8).²⁷⁰ Treatment of star polymers with a dimeric derivative led to time-dependent formation of a gel that could subsequently be photodegraded by irradiation with 350 nm light for 2 days.

The high reactivity of the DIFO was also reflected in the staining of Jurkat cells bearing SiaNAz with the biotinylated DIFO (Table 7, entry 1), which proceeded with a 20-times higher efficiency than with other cyclooctynes.²⁷⁰ Again, no cellular toxicity was observed. A DIFO derivative fluorescently labeled with Alexa Fluor 488 was synthesized and applied for time-lapse imaging of labeled cell-surface glycans in CHO cells (entry 3). Moreover, in combination with another Alexa Fluor 568 conjugate, dynamic multicolor imaging of glycan internalization and trafficking by two consecutive rounds of incubation with Ac₄ManNAz, followed by labeling with different fluorophores, indicated that glycan labeling did not perturb normal glycan trafficking to lysosomes. Finally, in vivo labeling of splenocyte glycans in mice was demonstrated by daily injection (1 week) with DIFO-FLAG (entry 6). In follow-up papers, in vivo labeling was also successfully demonstrated in zebrafish and *Caenorhabditis elegans*. Zebrafish embryos (entry

4) were incubated in media containing Ac₄GalNAz at 3–72 h after fertilization and then treated with a DIFO-647 probe, to obtain a fluorescent signal. Alternatively, embryos were incubated with Ac₄GalNAz from 3 h after fertilization, and GalNAz incorporation was followed by labeling with DIFO-647 at time intervals of 12 h. Finally, the time dependency of sugar synthesis in certain regions was demonstrated by three-color detection with conjugates of the DIFO to Alexa Fluor 488, 555, and 647. Similar research has been reported for the incorporation of ManNAz, GalNAz, and GlcNAz into mucin O-glycans in the nematode *C. elegans* (Table 7, entry 5).²⁸⁷

Finally, Turro et al. elegantly demonstrated that the gelation times of azido-terminated star polymers can be simply tuned through the choice of cyclooctyne probe: the bis-DIFO functionalized ethylene-1,2-diamine (Table 7, entry 7) gave significantly faster cross-linking than a dimer of cyclooctyne **28** (Table 6, entry 8).²⁸⁹

The alternative DIFO derivative, lacking the phenyl ring in the linker, was also prepared to reduce nonspecific protein and cell binding as a result of the lipophilic character of DIFO. Live-cell imaging was also performed with CHO cells, with no notable difference with respect to earlier cyclooctyne probes.

For the preparation of microtissues (Table 8, entry 2), azide-containing Jurkat cells were conjugated to DIFO-containing single-stranded DNA. Multicellular structures were devised by selective hybridization of cells functionalized with complementary DNA sequences, eventually leading to microtissues

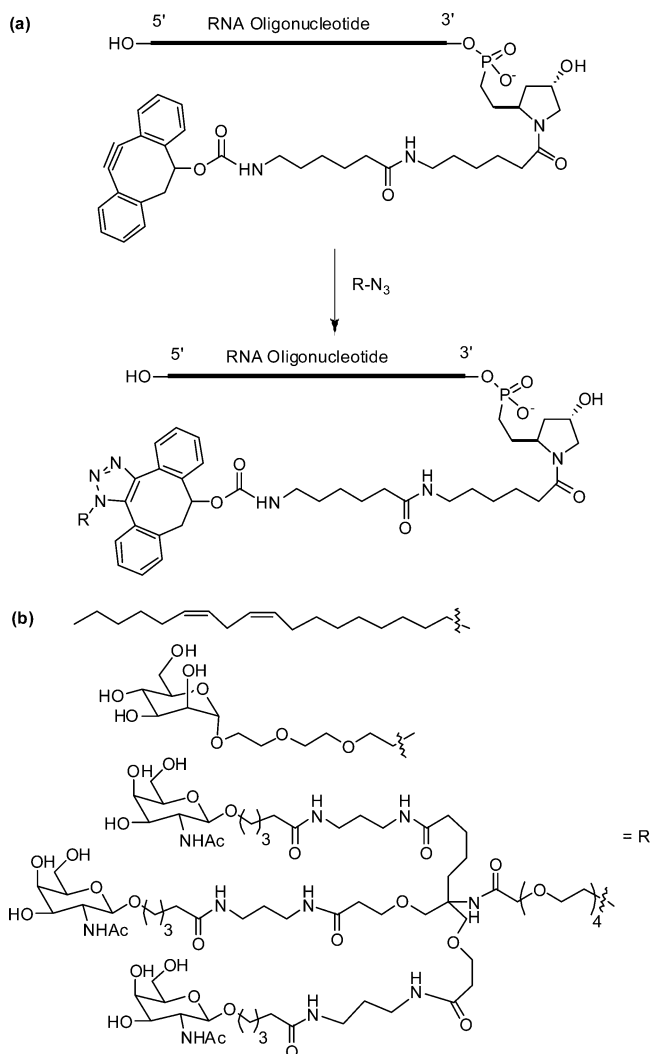


Figure 62. (a) RNA oligonucleotides functionalized at 5' or 3' terminal end or at an internal position generated via copper-assisted and copper-free click chemistry for the efficient synthesis of RNA conjugates. (b) Various substituted azides used for the functionalization of RNA.

with defined cell composition and stoichiometry.²⁹³ Burkart et al. used the second-generation DIFO 32 to probe the protein interactions between communication-mediating (COM) domains of nonribosomal peptide synthetase (NRPS). To ensure smooth processing of biosynthetic intermediates, individual catalytic protein domains must properly interact by intramodular communication. A panel of pantetheine cycloalkynes and azides (Table 8, entry 3) was loaded onto PCP domains of NRPS modules to trap the transient protein–protein interaction during NRP biosynthesis. Cyclooctyne–azide conjugation was faster and more selective than CuI-catalyzed [3 + 2] conjugation, which also showed conjugation between noninteracting proteins.²⁹⁴ Second-generation DIFOs have also found application in the patterning of microtissues. A doubly functionalized DIFO-labeled peptide was prepared (entry 4) and subsequently treated with poly(ethylene glycol) tetraazide to form hydrogels.²⁹⁵ Through the application of a peptide sequence with a metalloproteinase cleavage site, it was found that encapsulated cells could spread and migrate through the material.

8.3. Chemical Tagging Strategies Used Copper-Free Click Chemistry

Live cell imaging is a powerful method to study protein dynamics at the cell surface, but conventional imaging probes are bulky, or interfere with protein function, or dissociate from proteins after internalization. Fluorescent labeling of cell surface proteins enables imaging of the trafficking and function of receptors, channels, and transporters. Many protein labeling methods have been developed in recent years, but none currently allows the covalent attachment of small fluorophores onto cell surface proteins modified only by a small peptide tag, with short labeling times and with extremely high specificity over a wide range of expression levels and labeling conditions. Bertozzi and his co-workers applied lipoic acid ligase for cell surface protein labeling using copper-free click chemistry. Researchers developed a new technology for covalent, specific tagging of cellular proteins with chemical probes. Through rational design, researchers redirected a microbial lipoic acid ligase (LplA) to specifically attach an alkyl azide onto an engineered LplA acceptor peptide (LAP). The alkyl azide was then selectively derivatized with cyclooctyne conjugates to various probes. Researchers labeled LAP fusion proteins expressed in living mammalian cells with Cy3, Alexa Fluor 568, and biotin. Researchers combined LplA labeling with our previous biotin ligase labeling, to simultaneously image the dynamics of two different receptors, coexpressed in the same cell. This methodology was useful for the access to biochemical and imaging studies of cell surface proteins, using small fluorophores introduced via a short peptide tag (Figure 57a).^{200,283}

Recently, the monitoring of biomolecules in a physiological environment, such as time-lapse imaging of genetically encoded UAAs in live cells, was achieved by bioorthogonal “click chemistry” strategies. In contrast to proteins, which normally require a genetically GFP (green fluorescent protein) encoded tag, Lemke et al. reported genetically encoding one of the most potent functional groups for in vivo chemistry into *E. coli* and for in vivo labeling using high-resolution single-molecule measurements.²⁹⁶ SPAAC chemistry was used to site-specifically and noninvasively modify proteins in living cells. Two cyclooctynes derivatives of unnatural amino acids were incorporated during translation using amber stop codon TAG. The cyclooctyne derivatives of unnatural amino acids were incorporated by using a two mutation in the tRNA^{pyl}/pyIRS^{WT} and tRNA^{pyl}/pyIRS^{AF} by coexpressing a green fluorescent protein (GFP) reporter construct. GFP was efficiently expressed only in the presence of cyclooctynes derivatives of unnatural amino acids for this mutant tRNA^{pyl}/pyIRS^{AF} pair, and mass spectrometry confirmed the site-specific incorporation of the UAA into the protein (Figure 57b).²⁹⁶ As the tRNA^{pyl}/pyIRS^{AF} showed no obvious dependence on linker length, it was conceivable that slightly altered derivatives, such as mono- and difluorinated cyclooctynes, and possibly bicyclonones, were used in this system, as pyIRS from *M. mazei* is orthogonal in a variety of eukaryotic organisms.

Glycans are attractive targets for molecular imaging, but were inaccessible because of their incompatibility with genetically encoded reporters. Metabolic labeling of proteins using bioorthogonal chemical reporters is not restricted to monitoring global de novo protein synthesis as analogous techniques capitalize on the manifold potential of alkynes and azides to target other classes of biomolecules such as glycans and lipids. Bertozzi and his co-workers demonstrated the noninvasive

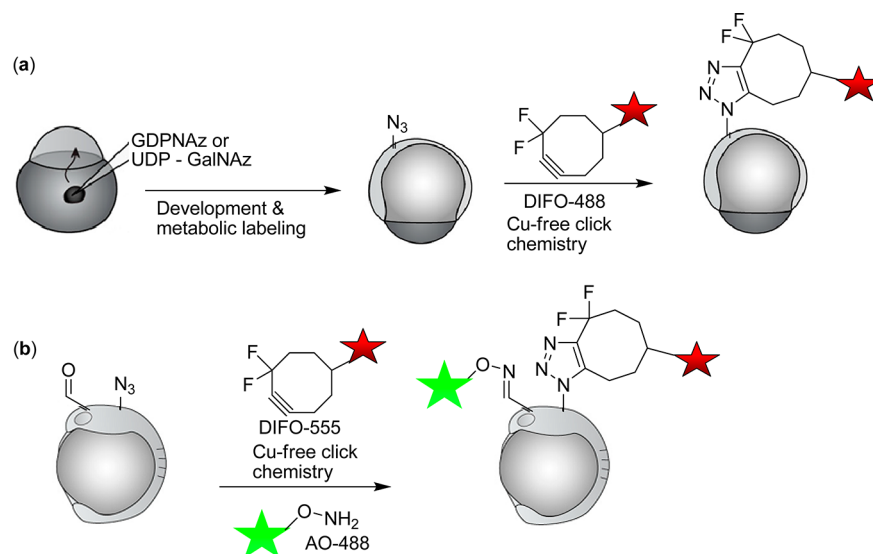


Figure 63. Metabolic labeling of fucosylated glycans in developing zebrafish using copper-free click chemistry. (a) Two-step strategy for imaging glycans in vivo. Zebrafish embryos were microinjected with UDP-GalNAz, GalNAz, UDPGalNAc, or no sugar (D, bottom), along with the tracer dye rhodamine-dextran, allowed to develop to 7 hpf, reacted with DIFO-488 (100 μM , 1 h), and imaged by confocal microscopy. (b) Schematic depicting dual labeling of O-glycans and sialylated glycans. Zebrafish embryos were microinjected with GalNAz, allowed to develop to 10 hpf, and then bathed in NaIO_4 (500 μM , 30 min) or no reagent. Embryos were reacted in a mixture of DIFO-555 (100 μM) and AO-488 (100 μM) in PBS (pH 6.7) for 1 h, rinsed, and imaged by confocal microscopy.

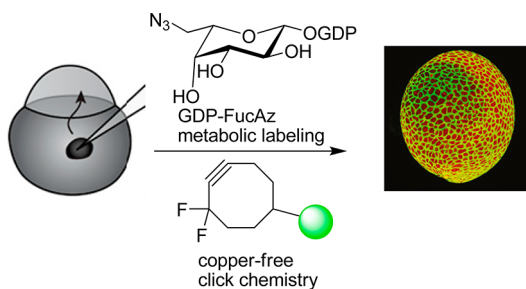


Figure 64. Microinjection of GDP-FucAz followed by copper-free click chemistry enables imaging of fucosylated glycans during the first 5 days of development. Zebrafish embryos were microinjected with vehicle alone (top) or 75 pmol of GDP-FucAz (bottom), allowed to develop, then treated with DIFO-488, and imaged at the time indicated.

imaging of glycans in live developing zebrafish, using a chemical reporter strategy. Zebrafish embryos were treated with an unnatural sugar to metabolically label their cell-surface glycans with azides.^{291,297} Subsequently, the embryos were reacted with fluorophore conjugates by means of copper-free click chemistry, enabling the visualization of glycans in vivo at subcellular resolution during development. At 60 h after fertilization, researchers observed an increase in de novo glycan biosynthesis in the jaw region, pectoral fins, and olfactory organs. Using a multicolor detection strategy, the researchers performed a spatiotemporal analysis of glycan expression and trafficking and identified patterns that would be undetectable with conventional molecular imaging approaches. The Bertozzi group impressively applied the metabolic labeling strategy to track glycoproteins with different unnatural monosaccharides azides, monitor glycans on cells, tissues, and in whole organisms, as well as perform profiling of glycosylation dynamics at the proteomic level (Figure 58).^{291,297}

The same research group again demonstrated the use of the metabolic pathway to include a bioorthogonal azide group in an

unnatural substrate, such as the azide-bearing ManNAc analogue (ManNAz), into a target glycoconjugate on the cell-surface, to detect the modified sialic acid metabolite, which further reacted covalently with an alkyne-modified functional probe by cycloaddition to form triazole conjugates with minimal physiological perturbation. The fast click reaction to visualize biological processes was accomplished using hydrophilic cyclooctynes, activated by a difluoromethylene moiety as an electron-withdrawing substituent in the ring, and a chemical tag, such as a small fluorophore, for the consolidated detection, compatible with the aqueous biological environment, neutral pH, and room temperature conditions. By combining the kinetic stability and the high thermodynamic energy of azide, as an interesting bioorthogonal species, which did not interact with the functionality presented in biological systems, and exploring the high reactivity of DIFO-based reagents for azide detection, it was possible to perform a nonhazardous copper-free click reaction, for covalent labeling of the cell-surface (Figure 59) and intracellular glycans.²⁹¹

Bertozzi and co-workers again explored copper-free click chemistry for labeling in the living animal.²⁹⁸ The researchers took the mice as the model for labeling of living animal. Mice were administered peracetylated *N*-azidoacetylmannosamine (Ac_4ManNAz) to metabolically label cell-surface sialic acids with azides (Figure 60a). After subsequent injection with cyclooctyne reagents, glycoconjugate labeling was observed on isolated splenocytes and in a variety of tissues including the intestines, heart, and liver, with no apparent toxicity. The researchers used various substituted cyclooctynes (Figure 60b) for labeling the mice. The relative amounts of ligation products observed with different cyclooctynes suggest that both intrinsic reaction kinetics and other properties such as solubility and tissue access govern the efficiency of Cu-free click chemistry in mice. More broadly, Cu-free click chemistry appears to possess the requisite bioorthogonality to achieve specific biomolecules labeling in this important model organism. The cyclooctynes tested displayed various labeling efficiencies that likely reflect

the combined influence of intrinsic reactivity and bioavailability. The researchers established Cu-free click chemistry as a bioorthogonal reaction that can be executed in the physiologically relevant context of a mouse.²⁹⁸

Oligonucleotide labeling using the copper-free SPAAC reaction would constitute a significant advance and could in principle be carried out *in vivo*. Brown and his co-workers employed ring-strain promoted alkyne–azide cycloaddition reaction for copper-free click DNA ligation. Two cyclooctynes (NSCO and DIBO) were successfully incorporated into oligonucleotides and used in SPAAC reactions (Figure 61a).²⁹⁹ Initially, both alkynes were attached postsynthetically to the 5′-end of an aminohexyl-labeled oligonucleotide. Templated DNA ligation was very fast, and a single base pair mismatch was sufficient to strongly inhibit the reaction. The NHS ester of 6-azidohexanoic acid was added to a 3′-amino alkyl labeled oligonucleotide to provide the azide oligonucleotide (ODN-3), which had a fluorescein dye at the 5′-end to allow visualization at low concentrations. HPLC purification was carried out on all oligonucleotides, and the products were characterized by mass spectrometry (ESI). Templated and nontemplated ligation reactions between azide ODN-3 and alkyne ODN-1 and ODN-2 were carried out in the absence of CuI. Of the two cyclooctynes tested, DIBO (Figure 61c) was much faster in templated ligation. Reactions with this alkyne proceeded cleanly and were essentially complete within 1 min at 2 μM DNA concentration. NSCO (Figure 61b) also reacted quickly but required more than 30 min for complete reaction. In both cases, the nontemplated reactions gave little or no product under otherwise identical conditions. Importantly, introduction of a single mismatch base pair between template ODN-11 and DIBO-labeled ODN-1 was sufficient to inhibit the ligation reaction, pointing to future applications in genetic analysis. It should be possible to use this approach for multiple simultaneous templated DNA ligation reactions if participating oligonucleotides were labeled with either two alkynes or two azides.

Taton and his co-workers explored strain-promoted click chemistry for terminal labeling of DNA.³⁰⁰ The researcher described the solid-phase synthesis and characterization of 5′-dibenzocyclooctyne (DIBO)-modified oligonucleotides, using a new DIBO phosphoramidite, which reacts with azides via copper-free, strain-promoted alkyne–azide cycloaddition (SPAAC) (Figure 61d). Researchers found that the DIBO group not only survived the standard acidic and oxidative reactions of solid-phase oligonucleotide synthesis (SPOS), but it also survived the thermal cycling and standard conditions of the polymerase chain reaction (PCR). As a result, PCR with DIBO-modified primers yielded “clickable” amplicons that could be tagged with azide-modified fluorophores or immobilized on azide-modified surfaces. From this methodology, it is clear that SPAAC on DNA could streamline the bioconjugate chemistry of nucleic acids in a number of modern biotechnologies.

Novel non-nucleoside alkyne monomers compatible with oligonucleotide were synthesized and efficiently incorporated into RNA and RNA analogues during solid-phase synthesis. These modifications allowed site-specific conjugation of ligands to the RNA oligonucleotides through copper-free strain-promoted azide–alkyne cycloaddition (SPAAC) reactions.³⁰¹ The SPAAC click reactions of cyclooctyne-oligonucleotides with various classes of azido-functionalized ligands in solution phase and on solid phase were efficient and quantitative and

occurred under mild reaction conditions (Figure 62a). All common steps of phosphoramidite chemistry, including the oxidation with iodine, were compatible with the activated, strained cyclooctyne derivative. Copper-free click reactions of RNA oligonucleotides functionalized at 5′ or 3′ termini or at an internal position were efficient in the solution phase as well as on solid support. The various azides were evaluated quantitatively and efficiently as determined by HPLC analysis (Figure 62b).³⁰¹

Bertozi and co-workers employed copper-free click chemistry for visualizing enveloping layer glycans during zebrafish early embryogenesis.³⁰² The same research group previously described a chemical method to image glycans during zebrafish larval development; however, they were unable to detect glycans during the first 24 h of embryogenesis, a very dynamic period in development. Researchers then demonstrated that microinjection of simple nucleotide azidosugars followed by labeling using copper-free click chemistry could enable visualization of glycan biosynthesis in the enveloping layer of zebrafish embryos as early as 4 h after the onset of zygotic gene expression. Researchers microinjected embryos with azidosugars at the one-cell stage, allowed the zebrafish to develop, and detected the metabolically labeled glycans with copper-free click chemistry. Mucin-type O-glycans were imaged as early as 7 h postfertilization, during the gastrula stage of development. Additionally, researchers used a nonmetabolic approach to label sialylated glycans with an independent chemistry, enabling the simultaneous imaging of these two distinct classes of glycans. Imaging analysis of glycan trafficking revealed the dramatic reorganization of glycans on the second time scale, including rapid migration to the cleavage furrow of mitotic cells. These studies yield insight into the biosynthesis and dynamics of glycans in the enveloping layer during embryogenesis and provide a platform for imaging other biomolecular targets by microinjection of appropriately functionalized biosynthetic precursors. Simultaneous visualization of O-glycans and sialylated glycans using these independent targeting strategies exposed subtle differences in the distributions of these two partially overlapping sectors of the glycome during embryogenesis (Figure 63).

Fucosylation is essential for proper cell signaling and embryonic development. Many developmental processes depend on proper fucosylation, but this post-translational modification is difficult to monitor *in vivo*. Bertozi and co-worker successfully applied the chemical reporter strategy to enable visualization of fucosylation during zebrafish development.³⁰³ Using azide-derivatized analogues of fucose, researchers metabolically labeled cell-surface glycans and then detected the incorporated azides via copper-free click chemistry with a difluorinated cyclooctyne probe. During these studies, researchers found that the fucose salvage pathway enzymes were expressed during zebrafish embryogenesis, but that they process the azide-modified substrates inefficiently and they were able to bypass the salvage pathway by using an azide-functionalized analogue of GDP-fucose. This nucleotide sugar was readily accepted by fucosyltransferases and provided robust cell-surface labeling of fucosylated glycans, as determined by flow cytometry and confocal microscopy analysis. Researchers used this technique to image fucosylated glycans in the enveloping layer of zebrafish embryos during the first 5 days of development (Figure 64).

9. CONCLUSION

Life on earth requires the construction of carbon–heteroatom–carbon bonds in an aqueous environment. Following nature's lead, researchers endeavor to generate substances by joining small units together with heteroatom links (C–X–C). To address this problem, several chemical and technological advancements in the very recent past have radically improved today's research fields in chemical biology and molecular biology. Recently, click chemistry is one of the powerful tools for the construction of heteroatom links (C–X–C) for chemistry and biological applications. We have demonstrated from this rReview that click chemistry is one of the powerful versatile synthetic tools applicable for chemistry and biology in drug development and investigation of biological systems. The copper(I)-catalyzed 1,2,3-triazole forming reaction between azides and terminal alkynes has become the gold standard reaction due to its reliability, specificity, and biocompatibility.

In the development of enzyme inhibitors, click chemistry plays an important active role. It has been identified as a convenient strategy toward fragment-based inhibitor assembly, where large libraries of potential bidentate inhibitors were generated with minimum synthetic efforts by several research groups. Many research groups developed a nanomolar potent ligand for specific enzyme inhibition using click chemistry. Ingenious strategies, such as in situ click chemistry, have so far shed some light onto new ways of generating extremely potent inhibitors against certain enzymes. Nevertheless, click chemistry is used for the development of agonists, antagonist, and selective ligand in receptor–ligand binding studies for drug development in the field of medicinal chemistry.

Bioorthogonal-click chemistry reactions are paving the way for new innovations in biology. These reactions possess extreme selectivity and biocompatibility, such that their participating reagents can form covalent bonds within richly functionalized biological systems. The bioorthogonal reactions described in this Review and related transformations have proven powerful tools for bioconjugation. Thus, the click chemistry reaction was successfully used for site-specific protein, glycans, lipids, and cell surfaces, inside living animals under physiological conditions. Click-ABPP platforms enable both the discovery of various disease relevant enzymes and the selective pharmacological probes to perturb and characterize these proteins in cells. Activity-based proteomics can provide insight into the metabolic and signaling pathways that support illuminate new strategies for disease diagnosis and treatment.

The portability of azide labeling and Cu-free click chemistry enables applications in many areas of chemical biology. Cu-free click chemistry has been used to monitor azidosugars, proteins bearing azido amino acids, lipids, and site-specifically labeled proteins, DNA, and RNA in live cells.

In the short period since click chemistry was conceived, it has had a dramatic and diverse impact in many areas of modern chemistry. In particular, strain-promoted cycloadditions of cyclic alkenes and alkynes have now established themselves as powerful tools in (reagent-free) bioconjugations. Research and development in this field are still increasing exponentially, and this Review is intended to provide an introductory overview of click chemistry to demonstrate the diversity of applications of this chemical strategy.

AUTHOR INFORMATION

Corresponding Author

*E-mail: krzysztof.jozwiak@umlub.pl

Notes

The authors declare no competing financial interest.

Biographies



Dr. Prakasam Thirumurugan was born in Tirupattur (TN), India. He received his Ph.D in Organic Chemistry in 2010 at University of Madras, under the guidance of Dr. P. T. Perumal in CLRI-CSIR. After completion of his doctorate, he joined as a postdoctoral researcher at University of Oklahoma, OK. Later, he joined the Medical University of Lublin, Poland, and carried out postdoctoral research under Prof. Krzysztof Jozwiak in 2010. His research focuses on the synthesis of N-modified dextromethan derivatives for ligand–receptor binding studies for the development of new agonist and antagonists using click chemistry.



Prof. Dariusz Matosiuk obtained his M.Sc. in Organic Chemistry at Maria Curie-Skłodowska University in 1982. That same year he obtained a position at the Department of Synthesis and Chemical Technology of Pharmaceutical Substances, Faculty of Pharmacy, Medical University of Lublin, where he works still. He commissioned his Ph.D. thesis in 1991 and got habilitation in 2003. He has been a Head of Department since 1996. Since the beginning of his scientific work, he has been interested in the synthesis as well as structure and activity elucidation of new derivatives, potentially acting in the central nervous system, as anticancer or antineurodegenerative drugs. His main interests between molecular targets are opioid receptors (analgesia, depression, allosteric modulation), glutamate ion channels (iGluR) and receptors (mGluR) (inhibition in neurodegeneration, activation in cancer), nicotinic acetylcholine ion channels (non-competitive inhibitors of the channel pore), histamine H3 and H4

(antagonists and reversed agonists), and serine and threonine kinases (GSK3 β inhibitors). He is a founder and Member of the Board of the Polish Society of Medicinal Chemistry.



Professor Krzysztof Jozwiak is Head of the Laboratory of Medicinal Chemistry and Neuroengineering of the Medical University of Lublin, Lublin, Poland. Following graduation in 2000 he was a postdoctoral fellow in the Gerontology Research Center at the National Institutes of Health USA, under the supervision of Irving W. Wainer; in 2005 started his second postdoc in the International Institute of Molecular and Cell Biology in Warsaw in Prof. Slawomir Filipek's group and in late 2007 assumed Associate Professor position at the Medical University of Lublin. Prof. Jozwiak's main research interests focus on elucidation of molecular mechanisms of interactions between medicinal molecules and their protein targets, development of novel approaches in both experimental and theoretical characterization of drug–receptor interactions, and their applications in medicinal chemistry projects. In 2012, Prof. Jozwiak was awarded the UCB-Ehrlich Award for Excellence in Medicinal Chemistry granted by the European Federation for Medicinal Chemistry.

REFERENCES

- (1) (a) Boyce, M.; Bertozzi, C. R. *Nat. Methods* **2011**, *8*, 638. (b) Nören-Müller, A.; Reis-Corrêa, I.; Prinz, H.; Rosenbaum, C.; Saxena, K.; Schwalbe, H. J.; Vestweber, D.; Cagna, G.; Schunk, S.; Schwarz, O.; Schiewe, H.; Waldmann, H. *Proc. Natl. Acad. Sci. U.S.A.* **2006**, *103*, 10606.
- (2) Baran, P. S.; Maimone, T. J.; Richter, J. M. *Nature* **2007**, *446*, 404.
- (3) Besanceney-Webler, C.; Jiang, H.; Zheng, T.; Feng, L.; Soriano del Amo, D.; Wang, W.; Klivansky, L. M.; Marlow, F. L.; Liu, Y.; Wu, P. *Angew. Chem., Int. Ed.* **2011**, *50*, 8051.
- (4) (a) Kolb, H. C.; Finn, M. G.; Sharpless, K. B. *Angew. Chem., Int. Ed.* **2001**, *40*, 2004. (b) Wu, P.; Feldman, A. K.; Nugent, A. K.; Hawker, C. J.; Scheel, A.; Voit, B.; Pyun, J.; Fréchet, J. M. J.; Sharpless, K. B.; Fokin, V. V. *Angew. Chem., Int. Ed.* **2004**, *43*, 3928.
- (5) (a) Kolb, H. C.; Sharpless, K. B. *Drug Discovery Today* **2003**, *8*, 1128. (b) Moses, J. E.; Moorhouse, A. D. *Chem. Rev.* **2007**, *36*, 1249.
- (6) Rostovtsev, V. V.; Green, L. G.; Fokin, V. V.; Sharpless, K. B. *Angew. Chem.* **2002**, *114*, 2708.
- (7) (a) Appukkuttan, P.; Dehaen, W.; Fokin, V. V.; Van der Eycken, E. *Org. Lett.* **2004**, *6*, 4223. (b) Binder, W. H.; Sachsenhofer, R. *Macromol. Rapid Commun.* **2007**, *28*, 15.
- (8) Bouillon, C.; Meyer, A.; Vidal, S.; Jochum, A.; Chevolut, Y.; Cloarec, J.-P.; Praly, J.-P.; Vasseur, J.-J.; Morvan, F. *J. Org. Chem.* **2006**, *71*, 4700.
- (9) Finn, M. G.; Fokin, V. V. *Chem. Rev.* **2010**, *39*, 1231.
- (10) Tron, G. C.; Piralì, T.; Billington, R. A.; Canonico, P. L.; Sorba, G.; Genazzani, A. A. *Med. Res. Rev.* **2008**, *28*, 278.
- (11) (a) Röper, S.; Kolb, H. C. *Fragment-based Approaches in Drug Discovery*; Wiley-VCH Verlag GmbH & Co. KGaA: Weinheim, Germany, 2006; p 311. (b) Colombo, M.; Peretto, I. *Drug Discovery Today* **2008**, *13*, 677.
- (12) (a) Borshell, N.; Papp, T.; Congreve, M. *Nat. Rev. Drug Discovery* **2011**, *10*, 166. (b) Welsch, M. E.; Snyder, S. A.; Stockwell, B. R. *Curr. Opin. Chem. Biol.* **2010**, *14*, 347.
- (13) Macarron, R.; Banks, M. N.; Bojanic, D.; Burns, D. J.; Cirovic, D. A.; Garyantes, T.; Green, D. V. S.; Hertzberg, R. P.; Janzen, W. P.; Paslay, J. W.; Schopfer, U.; Sittampalam, G. S. *Nat. Rev. Drug Discovery* **2011**, *10*, 188.
- (14) Simon, C. G.; Lin-Gibson, S. *Adv. Mater.* **2011**, *23*, 369.
- (15) An, W.; Tolliday, N. *Mol. Biotechnol.* **2010**, *45*, 180.
- (16) Uttamchandani, M. *Biointerphases* **2010**, *5*, FA24.
- (17) Inglese, J. *ChemMedChem* **2010**, *5*, 1398.
- (18) Andricopulo, A. D.; Salum, L.; Via, B.; Abraham, D. J. *Curr. Top. Med. Chem.* **2009**, *9*, 771.
- (19) Mayr, L. M.; Bojanic, D. *Curr. Opin. Pharmacol.* **2009**, *9*, 580.
- (20) Ricardo, M. *Drug Discovery Today* **2006**, *11*, 277.
- (21) Congreve, M.; Chessari, G.; Tisi, D.; Woodhead, A. J. *J. Med. Chem.* **2008**, *51*, 3661.
- (22) Hajduk, P. J.; Greer, J. *Nat. Rev. Drug Discovery* **2007**, *6*, 211.
- (23) Murray, C. W.; Rees, D. C. *Nat. Chem.* **2009**, *1*, 187.
- (24) de Kloe, G. E.; Bailey, D.; Leurs, R.; de Esch, I. J. P. *Drug Discovery Today* **2009**, *14*, 630.
- (25) Schulz, M. N.; Hubbard, R. E. *Curr. Opin. Pharmacol.* **2009**, *9*, 615.
- (26) Salum, L. B.; Andricopulo, A. D. *Expert Opin. Drug Discovery* **2010**, *5*, 405.
- (27) (a) Murray, C. W.; Blundell, T. L. *Curr. Opin. Struct. Biol.* **2010**, *20*, 497. (b) Brik, A.; Wu, C.-Y.; Wong, C.-H. *Org. Biomol. Chem.* **2006**, *4*, 1446.
- (28) Schmidt, M. F.; Rademann, J. *Trends Biotechnol.* **2009**, *27*, 512.
- (29) Corbett, P. T.; Leclaire, J.; Vial, L.; West, K. R.; Wietor, J.-L.; Sanders, J. K. M.; Otto, S. *Chem. Rev.* **2006**, *106*, 3652.
- (30) Beeren, S. R.; Sanders, J. K. M. *History and Principles of Dynamic Combinatorial Chemistry. Dynamic Combinatorial Chemistry*; Wiley-VCH Verlag GmbH & Co. KGaA: Weinheim, Germany, 2010.
- (31) Johnson, D. S.; Weerapana, E.; Cravatt, B. F. *Future Med. Chem.* **2010**, *2*, 949.
- (32) Kalesh, K. A.; Shi, H.; Ge, J.; Yao, S. Q. *Org. Biomol. Chem.* **2010**, *8*, 1749.
- (33) Lu, L.; Zhu, M. *Anticancer Agents Med. Chem.* **2011**, *11*, 164.
- (34) He, R.; Yu, Z.; He, Y.; Zeng, L.-F.; Xu, J.; Wu, L.; Gunawan, A. M.; Wang, L.; Jiang, Z.-X.; Zhang, Z.-Y. *ChemMedChem* **2010**, *5*, 2051.
- (35) He, X.-P.; Deng, Q.; Gao, L.-X.; Li, C.; Zhang, W.; Zhou, Y.-B.; Tang, Y.; Shi, X.-X.; Xie, J.; Li, J.; Chen, G.-R.; Chen, K. *Bioorg. Med. Chem.* **2011**, *19*, 3892.
- (36) Li, C.; He, X.-P.; Zhang, Y.-J.; Li, Z.; Gao, L.-X.; Shi, X.-X.; Xie, J.; Li, J.; Chen, G.-R.; Tang, Y. *Eur. J. Med. Chem.* **2011**, *46*, 4212.
- (37) Zhou, B.; He, Y.; Zhang, X.; Xu, J.; Luo, Y.; Wang, Y.; Franzblau, S. G.; Yang, Z.; Chan, R. J.; Liu, Y.; Zheng, J.; Zhang, Z.-Y. *Proc. Natl. Acad. Sci. U.S.A.* **2010**, *107*, 4573.
- (38) Srinivasan, R.; Tan, L. P.; Wu, H.; Yang, P.-Y.; Kalesh, K. A.; Yao, S. Q. *Org. Biomol. Chem.* **2009**, *7*, 1821.
- (39) Wang, J.; He, X.; Gao, L.; Sheng, L.; Shi, X.; Li, J.; Chen, G. *Chin. J. Chem.* **2011**, *29*, 1227.
- (40) Srinivasan, R.; Uttamchandani, M.; Yao, S. Q. *Org. Lett.* **2006**, *8*, 713.
- (41) Xie, J.; Seto, C. T. *Bioorg. Med. Chem.* **2007**, *15*, 458.
- (42) Tan, L. P.; Wu, H.; Yang, P.-Y.; Kalesh, K. A.; Zhang, X.; Hu, M.; Srinivasan, R.; Yao, S. Q. *Org. Lett.* **2009**, *11*, 5102.
- (43) Zhang, X.; He, Y.; Liu, S.; Yu, Z.; Jiang, Z.-X.; Yang, Z.; Dong, Y.; Nabinger, S. C.; Wu, L.; Gunawan, A. M.; Wang, L.; Chan, R. J.; Zhang, Z.-Y. *J. Med. Chem.* **2010**, *53*, 2482.
- (44) He, X.-P.; Li, C.; Jin, X.-P.; Song, Z.; Zhang, H.-L.; Zhu, C.-J.; Shen, Q.; Zhang, W.; Sheng, L.; Shi, X.-X.; Tang, Y.; Li, J.; Chen, G.-R.; Xie, J. *New J. Chem.* **2011**, *35*, 622.
- (45) Duval, R.; Kolb, S. P.; Braud, E.; Genest, D.; Garbay, C. J. *Comb. Chem.* **2009**, *11*, 947.

- (46) Song, Z.; He, X.-P.; Li, C.; Gao, L.-X.; Wang, Z.-X.; Tang, Y.; Xie, J.; Li, J.; Chen, G.-R. *Carbohydr. Res.* **2011**, *346*, 140.
- (47) Yang, J.-W.; He, X.-P.; Li, C.; Gao, L.-X.; Sheng, L.; Xie, J.; Shi, X.-X.; Tang, Y.; Li, J.; Chen, G.-R. *Bioorg. Med. Chem. Lett.* **2011**, *21*, 1092.
- (48) Lin, L.; Shen, Q.; Chen, G.-R.; Xie, J. *Bioorg. Med. Chem.* **2008**, *16*, 9757.
- (49) Zhang, Y.-J.; He, X.-P.; Li, C.; Li, Z.; Shi, D.-T.; Gao, L.-X.; Qiu, B.-Y.; Shi, X.-X.; Tang, Y.; Li, J.; Chen, G.-R. *Chem. Lett.* **2010**, *39*, 1261.
- (50) Bahta, M.; Burke, T. R. *ChemMedChem* **2011**, *6*, 1363.
- (51) (a) Titball, R. W.; Leary, S. E. *Br. Med. Bull.* **1998**, *54*, 625. (b) Zhang, Z. Y.; Clemens, J. C.; Schubert, H. L.; Stuckey, J. A.; Fischer, M. W.; Hume, D. M.; Saper, M. A.; Dixon, J. E. *J. Biol. Chem.* **1992**, *267*, 23759. (c) Bahta, M.; Lountos, G. T.; Dyas, B.; Kim, S.-E.; Ulrich, R. G.; Waugh, D. S.; Burke, T. R. *J. Med. Chem.* **2011**, *54*, 2933.
- (52) Matthews, D. J.; Gerritsen, M. E. *Targeting Protein Kinases for Cancer Therapy*; John Wiley & Sons, Inc.: Weinheim, Germany, 2010.
- (53) Poot, A. J.; van Ameijde, J.; Slijper, M.; van den Berg, A.; Hilhorst, R.; Ruijtenbeek, R.; Rijkers, D. T. S.; Liskamp, R. M. J. *ChemBioChem* **2009**, *10*, 2042.
- (54) van Ameijde, J.; Poot, A. J.; van Wandelen, L. T. M.; Wammes, A. E. M.; Ruijtenbeek, R.; Rijkers, D. T. S.; Liskamp, R. M. J. *Org. Biomol. Chem.* **2010**, *8*, 1629.
- (55) Kumar, D.; Reddy, V. B.; Kumar, A.; Mandal, D.; Tiwari, R.; Parang, K. *Bioorg. Med. Chem. Lett.* **2011**, *21*, 449.
- (56) Le Corre, L.; Girard, A.-L.; Aubertin, J.; Radvanyi, F.; Benoist-Lasselin, C.; Jonquoy, A.; Mugniery, E.; Legeai-Mallet, L.; Busca, P.; Le Merrer, Y. *Org. Biomol. Chem.* **2010**, *8*, 2164.
- (57) Kumar, A.; Ahmad, I.; Chhikara, B. S.; Tiwari, R.; Mandal, D.; Parang, K. *Bioorg. Med. Chem. Lett.* **2011**, *21*, 1342.
- (58) Klein, M.; Diner, P.; Dorin-Semblat, D.; Doerig, C.; Grotli, M. *Org. Biomol. Chem.* **2009**, *7*, 3421.
- (59) (a) Gu, G.; Wang, H.; Liu, P.; Fu, C.; Li, Z.; Cao, X.; Li, Y.; Fang, Q.; Xu, F.; Shen, J.; Wang, P. G. *Chem. Commun.* **2012**, *48*, 2788. (b) Kalesh, K. A.; Liu, K.; Yao, S. Q. *Org. Biomol. Chem.* **2009**, *7*, 5129.
- (60) Roychoudhury, R.; Pohl, N. L. B. *Curr. Opin. Chem. Biol.* **2010**, *14*, 168.
- (61) Hosoguchi, K.; Maeda, T.; Furukawa, J. I.; Shinohara, Y.; Hinou, H.; Sekiguchi, M.; Togame, H.; Takemoto, H.; Kondo, H.; Nishimura, S.-I. *J. Med. Chem.* **2010**, *53*, S607.
- (62) Lee, L. V.; Mitchell, M. L.; Huang, S.-J.; Fokin, V. V.; Sharpless, K. B.; Wong, C.-H. *J. Am. Chem. Soc.* **2003**, *125*, 9588.
- (63) Colombano, G.; Travelli, C.; Galli, U.; Caldarelli, A.; Chini, M. G.; Canonico, P. L.; Sorba, G.; Bifulco, G.; Tron, G. C.; Genazzani, A. A. *J. Med. Chem.* **2009**, *53*, 616.
- (64) Galli, U.; Ercolano, E.; Carraro, L.; Blasi Roman, C. R.; Sorba, G.; Canonico, P. L.; Genazzani, A. A.; Tron, G. C.; Billington, R. A. *ChemMedChem* **2008**, *3*, 771.
- (65) Li, T.; Guo, L.; Zhang, Y.; Wang, J.; Li, Z.; Lin, L.; Zhang, Z.; Li, L.; Lin, J.; Zhao, W.; Li, J.; Wang, P. G. *Carbohydr. Res.* **2011**, *346*, 1083.
- (66) Cheng, K.; Liu, J.; Sun, H.; Xie, J. *Chem. Biodiversity* **2010**, *7*, 690.
- (67) Cheng, K.; Liu, J.; Liu, X.; Li, H.; Sun, H.; Xie, J. *Carbohydr. Res.* **2009**, *344*, 841.
- (68) Cheng, K.; Liu, J.; Sun, H.; Bokor, E.; Czifrak, K.; Konya, B.; Toth, M.; Docsa, T.; Gergely, P.; Somsak, L. *New J. Chem.* **2010**, *34*, 1450.
- (69) Alexacou, K.-M.; Hayes, J. M.; Tiraidis, C.; Zographos, S. E.; Leonidas, D. D.; Chrysina, E. D.; Archontis, G.; Oikonomakos, N. G.; Paul, J. V.; Varghese, B.; Loganathan, D. *Proteins: Struct., Funct., Bioinf.* **2008**, *71*, 1307.
- (70) Cheng, K.; Liu, J.; Sun, H.; Xie, J. *Synthesis* **2010**, *2010*, 1046.
- (71) Chrysina, E. D.; Bokor, É.; Alexacou, K.-M.; Charavgi, M.-D.; Oikonomakos, G. N.; Zographos, S. E.; Leonidas, D. D.; Oikonomakos, N. G.; Somsák, L. *Tetrahedron: Asymmetry* **2009**, *20*, 733.
- (72) Adibekian, A.; Martin, B. R.; Wang, C.; Hsu, K.-L.; Bachovchin, D. A.; Niessen, S.; Hoover, H.; Cravatt, B. F. *Nat. Chem. Biol.* **2011**, *7*, 469.
- (73) Tornøe, C. W.; Sanderson, S. J.; Mottram, J. C.; Coombs, G. H.; Meldal, M. *J. Comb. Chem.* **2004**, *6*, 312.
- (74) (a) Smith, R. A.; Copp, L. J.; Coles, P. J.; Pauls, H. W.; Robinson, V. J.; Spencer, R. W.; Heard, S. B.; Krantz, A. *J. Am. Chem. Soc.* **1988**, *110*, 4429. (b) Powers, J. C.; Asgian, J. L.; Ekici, Ö. D.; James, K. E. *Chem. Rev.* **2002**, *102*, 4639. (c) Baskin-Bey, E. S.; Washburn, K.; Feng, S.; Oltersdorf, T.; Shapiro, D.; Huyghe, M.; Burgart, L.; Garrity-Park, M.; Van Vilsteren, F. G. I.; Oliver, L. K.; Rosen, C. B.; Gores, G. *Am. J. Transplant.* **2007**, *7*, 218.
- (75) Brak, K.; Kerr, I. D.; Barrett, K. T.; Fuchi, N.; Debnath, M.; Ang, K.; Engel, J. C.; McKerrow, J. H.; Doyle, P. S.; Brinen, L. S.; Ellman, J. A. *J. Med. Chem.* **2010**, *53*, 1763.
- (76) Loh, Y.; Shi, H.; Hu, M.; Yao, S. Q. *Chem. Commun.* **2010**, *46*, 8407.
- (77) Siles, R.; Kawasaki, Y.; Ross, P.; Freire, E. *Bioorg. Med. Chem. Lett.* **2011**, *21*, 5305.
- (78) Ng, S. L.; Yang, P.-Y.; Chen, K. Y. T.; Srinivasan, R.; Yao, S. Q. *Org. Biomol. Chem.* **2008**, *6*, 844.
- (79) Mohapatra, D. K.; Maity, P. K.; Shabab, M.; Khan, M. I. *Bioorg. Med. Chem. Lett.* **2009**, *19*, 5241.
- (80) Gillet, L. C. J.; Namoto, K.; Ruchti, A.; Hoving, S.; Boesch, D.; Inverardi, B.; Mueller, D.; Coulot, M.; Schindler, P.; Schweigler, P.; Bernardi, A.; Gil-Parrado, S. *Mol. Cell. Proteomics* **2008**, *7*, 1241.
- (81) Zapico, J. M.; Serra, P.; Garcia-Sanmartin, J.; Filipiak, K.; Carbajo, R. J.; Schott, A. K.; Pineda-Lucena, A.; Martinez, A.; Martin-Santamaria, S.; de Pascual-Teresa, B.; Ramos, A. *Org. Biomol. Chem.* **2011**, *9*, 4587.
- (82) Wang, J.; Uttamchandani, M.; Li, J.; Hu, M.; Yao, S. Q. *Org. Lett.* **2006**, *8*, 3821.
- (83) Forino, M.; Johnson, S.; Wong, T. Y.; Rozanov, D. V.; Savinov, A. Y.; Li, W.; Fattorusso, R.; Becattini, B.; Orry, A. J.; Jung, D.; Abagyan, R. A.; Smith, J. W.; Alibek, K.; Liddington, R. C.; Strongin, A. Y.; Pellecchia, M. *Proc. Natl. Acad. Sci. U.S.A.* **2005**, *102*, 9499.
- (84) Minond, D.; Saldanha, S. A.; Subramaniam, P.; Spaargaren, M.; Spicer, T.; Fotsing, J. R.; Weide, T.; Fokin, V. V.; Sharpless, K. B.; Galleni, M.; Bebrone, C.; Lassaux, P.; Hodder, P. *Bioorg. Med. Chem.* **2009**, *17*, 5027.
- (85) Kolb, H.; Joseph, C.; Dhanalakshmi, K.; Vani, P.; Bing, W.; Umesh, B. G.; Brian, A. D.; Kai, C.; Wei, Z.; Gang, C.; Clifton, H. P.; Farhad, K.; Peter, J. H. S.; Zhiyong, G.; Qianwa, Lee, C. T.; Tieming, Z.; Chunfang, X. U.S. Patent US20100317842 A1, 2010; WO2008124703.
- (86) Singer, M.; Lopez, M.; Bornaghi, L. F.; Innocenti, A.; Vullo, D.; Supuran, C. T.; Poulsen, S.-A. *Bioorg. Med. Chem. Lett.* **2009**, *19*, 2273.
- (87) Wilkinson, B. L.; Bornaghi, L. F.; Houston, T. A.; Innocenti, A.; Vullo, D.; Supuran, C. T.; Poulsen, S.-A. *J. Med. Chem.* **2007**, *50*, 1651.
- (88) Winum, J.-Y.; Poulsen, S.-A.; Supuran, C. T. *Med. Res. Rev.* **2009**, *29*, 419.
- (89) Salmon, A. J.; Williams, M. L.; Innocenti, A.; Vullo, D.; Supuran, C. T.; Poulsen, S.-A. *Bioorg. Med. Chem. Lett.* **2007**, *17*, 5032.
- (90) Lopez, M.; Salmon, A.; Supuran, C.; Poulsen, S.-A. *Curr. Pharm. Des.* **2010**, *16*, 3277.
- (91) Monceaux, C. J.; Hirata-Fukae, C.; Lam, P. C. H.; Totrov, M. M.; Matsuoka, Y.; Carlier, P. R. *Bioorg. Med. Chem. Lett.* **2011**, *21*, 3992.
- (92) Fischer, C.; Zultanski, S. L.; Zhou, H.; Methot, J. L.; Brown, W. C.; Mampreian, D. M.; Schell, A. J.; Shah, S.; Nuthall, H.; Hughes, B. L.; Smotrov, N.; Kenific, C. M.; Cruz, J. C.; Walker, D.; Bouthillette, M.; Nikov, G. N.; Savage, D. F.; Jeliakova-Mecheva, V. V.; Diaz, D.; Szewczak, A. A.; Bays, N.; Middleton, R. E.; Munoz, B.; Shearman, M. S. *Bioorg. Med. Chem. Lett.* **2011**, *21*, 4083.
- (93) Liu, K.; Shi, H.; Xiao, H.; Chong, A. G. L.; Bi, X.; Chang, Y.-T.; Tan, K. S. W.; Yada, R. Y.; Yao, S. Q. *Angew. Chem.* **2009**, *121*, 8443.
- (94) Brik, A.; Muldoon, J.; Lin, Y.-C.; Elder, J. H.; Goodsell, D. S.; Olson, A. J.; Fokin, V. V.; Sharpless, K. B.; Wong, C.-H. *ChemBioChem* **2003**, *4*, 1246.

- (95) Brik, A.; Alexandratos, J.; Lin, Y.-C.; Elder, J. H.; Olson, A. J.; Wlodawer, A.; Goodsell, D. S.; Wong, C.-H. *ChemBioChem* **2005**, *6*, 1167.
- (96) Jia, Z.; Zhu, Q. *Bioorg. Med. Chem. Lett.* **2010**, *20*, 6222.
- (97) Doiron, J.; Boudreau, L. H.; Picot, N.; Villebonnet, B.; Surette, M. E.; Touaibia, M. *Bioorg. Med. Chem. Lett.* **2009**, *19*, 1118.
- (98) Moorhouse, A. D.; Spiteri, C.; Sharma, P.; Zloh, M.; Moses, J. E. *Chem. Commun.* **2011**, 47, 230.
- (99) Maurya, S. K.; Gollapalli, D. R.; Kirubakaran, S.; Zhang, M.; Johnson, C. R.; Benjamin, N. N.; Hedstrom, L.; Cuny, G. D. *J. Med. Chem.* **2009**, *52*, 4623.
- (100) Chen, L.; Wilson, D. J.; Xu, Y.; Aldrich, C. C.; Felczak, K.; Sham, Y. Y.; Pankiewicz, K. W. *J. Med. Chem.* **2010**, *53*, 4768.
- (101) Tran, A. T.; Cergol, K. M.; Britton, W. J.; Imran Bokhari, S. A.; Ibrahim, M.; Laphorn, A. J.; Payne, R. J. *MedChemComm* **2010**, *1*, 271.
- (102) Chakrabarty, S. P.; Ramapanicker, R.; Mishra, R.; Chandrasekaran, S.; Balaran, H. *Bioorg. Med. Chem.* **2009**, *17*, 8060.
- (103) Shen, J.; Woodward, R.; Kedenburg, J. P.; Liu, X.; Chen, M.; Fang, L.; Sun, D.; Wang, P. G. *J. Med. Chem.* **2008**, *51*, 7417.
- (104) Hou, J.; Feng, C.; Li, Z.; Fang, Q.; Wang, H.; Gu, G.; Shi, Y.; Liu, P.; Xu, F.; Yin, Z.; Shen, J.; Wang, P. *Eur. J. Med. Chem.* **2011**, *46*, 3190.
- (105) Horne, W. S.; Olsen, C. A.; Beierle, J. M.; Montero, A.; Ghadiri, M. R. *Angew. Chem., Int. Ed.* **2009**, *48*, 4718.
- (106) Chen, Y.; Lopez-Sanchez, M.; Savoy, D. N.; Billadeau, D. D.; Dow, G. S.; Kozikowski, A. P. *J. Med. Chem.* **2008**, *51*, 3437.
- (107) Chen, P. C.; Patil, V.; Guarrant, W.; Green, P.; Oyelere, A. K. *Bioorg. Med. Chem.* **2008**, *16*, 4839.
- (108) Ferreira, S. B.; Sodero, A. C. R.; Cardoso, M. F. C.; Lima, E. S.; Kaiser, C. R.; Silva, F. P.; Ferreira, V. F. *J. Med. Chem.* **2010**, *53*, 2364.
- (109) Diaz, L. A.; Bujons, J.; Casas, J.; Llebaria, A.; Delgado, A. J. *Med. Chem.* **2010**, *53*, 5248.
- (110) Diaz, L. A.; Casas, J.; Bujons, J.; Llebaria, A.; Delgado, A. J. *Med. Chem.* **2011**, *54*, 2069.
- (111) Weïwer, M.; Chen, C.-C.; Kemp, M. M.; Linhardt, R. J. *Eur. J. Org. Chem.* **2009**, 2009, 2611.
- (112) Diot, J. D.; Moreno, I. G.; Twigg, G.; Mellet, C. O.; Haupt, K.; Butters, T. D.; Kovensky, J.; Gouin, S. b. G. *J. Org. Chem.* **2011**, *76*, 7757.
- (113) Diot, J.; Garcia-Moreno, M. I.; Gouin, S. G.; Ortiz Mellet, C.; Haupt, K.; Kovensky, J. *Org. Biomol. Chem.* **2009**, *7*, 357.
- (114) Aragão-Leoneti, V.; Campo, V. L.; Gomes, A. S.; Field, R. A.; Carvalho, I. *Tetrahedron* **2010**, *66*, 9475.
- (115) Antonow, D. *Drug Discovery Today* **2010**, *15*, 801.
- (116) Sharpless, K. B.; Manetsch, R. *Expert Opin. Drug Discovery* **2006**, *1*, 525.
- (117) Mamidyala, S. K.; Finn, M. G. *Chem. Rev.* **2010**, *39*, 1252.
- (118) Cox, H. S.; Ford, N.; Reeder, J. C. *Lancet Infect. Dis.* **2009**, *9*, 138.
- (119) DeBarber, A. E.; Mdluli, K.; Bosman, M.; Bekker, L.-G.; Barry, C. E. *Proc. Natl. Acad. Sci. U.S.A.* **2000**, *97*, 9677.
- (120) Engohang-Ndong, J.; Baillat, D.; Aumercier, M.; Bellefontaine, F.; Besra, G. S.; Loch, C.; Baulard, A. R. *Mol. Microbiol.* **2004**, *51*, 175.
- (121) Willand, N.; Dirie, B.; Carette, X.; Bifani, P.; Singhal, A.; Desroses, M.; Leroux, F.; Willery, E.; Mathys, V.; Deprez-Poulain, R.; Delcroix, G.; Frenois, F.; Aumercier, M.; Loch, C.; Villeret, V.; Deprez, B.; Baulard, A. R. *Nat. Med.* **2009**, *15*, 537.
- (122) Willand, N.; Desroses, M.; Toto, P.; Dirie, B.; Lens, Z.; Villeret, V.; Rucktooa, P.; Loch, C.; Baulard, A.; Deprez, B. *ACS Chem. Biol.* **2010**, *5*, 1007.
- (123) Hu, X.; Manetsch, R. *Chem. Rev.* **2010**, *39*, 1316.
- (124) Suzuki, T. *Chem. Pharm. Bull.* **2009**, *57*, 897.
- (125) Suzuki, T.; Ota, Y.; Kasuya, Y.; Mutsuga, M.; Kawamura, Y.; Tsumoto, H.; Nakagawa, H.; Finn, M. G.; Miyata, N. *Angew. Chem., Int. Ed.* **2010**, *49*, 6817.
- (126) Berg, T. *Angew. Chem., Int. Ed.* **2003**, *42*, 2462.
- (127) Arkin, M. R.; Wells, J. A. *Nat. Rev. Drug Discovery* **2004**, *3*, 301.
- (128) Wells, J. A.; McClendon, C. L. *Nature* **2007**, *450*, 1001.
- (129) Kulkarni, S. S.; Hu, X.; Doi, K.; Wang, H.-G.; Manetsch, R. *ACS Chem. Biol.* **2011**, *6*, 724.
- (130) Lee, S. S.; Lim, J.; Tan, S.; Cha, J.; Yeo, S. Y.; Agnew, H. D.; Heath, J. R. *Anal. Chem.* **2010**, *82*, 672.
- (131) (a) Agnew, H. D.; Rohde, R. D.; Millward, S. W.; Nag, A.; Yeo, W.-S.; Hein, J. E.; Pitram, S. M.; Tariq, A. A.; Burns, V. M.; Krom, R. J.; Fokin, V. V.; Sharpless, K. B.; Heath, J. R. *Angew. Chem., Int. Ed.* **2009**, *48*, 4944. (b) Millward, S. W.; Henning, R. K.; Kwong, G. A.; Pitram, S.; Agnew, H. D.; Deyle, K. M.; Nag, A.; Hein, J.; Lee, S. S.; Lim, J.; Pfeilsticker, J. A.; Sharpless, K. B.; Heath, J. R. *J. Am. Chem. Soc.* **2011**, *133*, 18280.
- (132) Manetsch, R.; Krasinski, A.; Radić, Z.; Raushel, J.; Taylor, P.; Sharpless, K. B.; Kolb, H. C. *J. Am. Chem. Soc.* **2004**, *126*, 12809.
- (133) Krasinski, A.; Radić, Z.; Manetsch, R.; Raushel, J.; Taylor, P.; Sharpless, K. B.; Kolb, H. C. *J. Am. Chem. Soc.* **2005**, *127*, 6686.
- (134) (a) Bourne, Y.; Radić, Z.; Taylor, P.; Marchot, P. *J. Am. Chem. Soc.* **2010**, *132*, 18292. (b) Grimster, N. P.; Stump, B.; Fotsing, J. R.; Weide, T.; Talley, T. T.; Yamauchi, J. G.; Nemezc, A.; Kim, C.; Ho, K.-Y.; Sharpless, K. B.; Taylor, P.; Fokin, V. V. *J. Am. Chem. Soc.* **2012**, *134*, 6732.
- (135) Louis, J. M.; Aniana, A.; Weber, I. T.; Sayer, J. M. *Proc. Natl. Acad. Sci. U.S.A.* **2011**, *108*, 9072.
- (136) Whiting, M.; Muldoon, J.; Lin, Y.-C.; Silverman, S. M.; Lindstrom, W.; Olson, A. J.; Kolb, H. C.; Finn, M. G.; Sharpless, K. B.; Elder, J. H.; Fokin, V. V. *Angew. Chem., Int. Ed.* **2006**, *45*, 1435.
- (137) Hirose, T.; Sunazuka, T.; Mura, S. *Proc. Jpn. Acad., Ser. B* **2010**, *86*, 85.
- (138) Hirose, T.; Sunazuka, T.; Sugawara, A.; Noguchi, Y.; Tanaka, T.; Iguchi, K.; Yamamoto, T.; Gouda, H.; Shiomi, K.; Omura, S. *J. Antibiot.* **2009**, *62*, 495.
- (139) Lopez, M.; Salmon, A.; Supuran, C.; Poulsen, S.-A. *Curr. Pharm. Des.* **2010**, *16*, 3277.
- (140) Mocharla, V. P.; Colasson, B.; Lee, L. V.; Röper, S.; Sharpless, K. B.; Wong, C.-H.; Kolb, H. C. *Angew. Chem., Int. Ed.* **2005**, *44*, 116.
- (141) Wollack, J. W.; Zeliadt, N. A.; Mullen, D. G.; Amundson, G.; Geier, S.; Falkum, S.; Wattenberg, E. V.; Barany, G.; Distefano, M. D. *J. Am. Chem. Soc.* **2009**, *131*, 7293.
- (142) Ochocki, J. D.; Mullen, D. G.; Wattenberg, E. V.; Distefano, M. D. *Bioorg. Med. Chem. Lett.* **2011**, *21*, 4998.
- (143) Ye, S.; Huber, T.; Vogel, R.; Sakmar, T. P. *Nat. Chem. Biol.* **2009**, *5*, 397.
- (144) Haar, E.; Koth, C. M.; Abdul-Manan, N.; Swenson, L.; Coll, J. T.; Lippke, J. A.; Lepre, C. A.; Garcia-Guzman, M.; Moore, J. M. *Structure* **2010**, *18*, 1083.
- (145) Huber, T.; Sakmar, T. P. *Trends Pharmacol. Sci.* **2011**, *32*, 410.
- (146) Grunbeck, A.; Huber, T.; Sachdev, P.; Sakmar, T. P. *Biochemistry* **2011**, *50*, 3411.
- (147) Devigny, C.; Perez-Balderas, F.; Hoogeland, B.; Cuboni, S.; Wachtel, R.; Mauch, C. P.; Webb, K. J.; Deussing, J. M.; Hausch, F. J. *Am. Chem. Soc.* **2011**, *133*, 8927.
- (148) Cosyn, L.; Palaniappan, K. K.; Kim, S.-K.; Duong, H. T.; Gao, Z.-G.; Jacobson, K. A.; Van Calenbergh, S. *J. Med. Chem.* **2006**, *49*, 7373.
- (149) Tosh, D. K.; Chinn, M.; Yoo, L. S.; Kang, D. W.; Luecke, H.; Gao, Z.-G.; Jacobson, K. A. *Bioorg. Med. Chem.* **2010**, *18*, 508.
- (150) Tosh, D. K.; Yoo, L. S.; Chinn, M.; Hong, K.; Kilbey, S. M.; Barrett, M. O.; Fricks, I. P.; Harden, T. K.; Gao, Z.-G.; Jacobson, K. A. *Bioconjugate Chem.* **2010**, *21*, 372.
- (151) Ciocoiu, C. C.; Nikolic, N.; Nguyen, H. H.; Thoresen, G. H.; Aasen, A. J.; Hansen, T. V. *Eur. J. Med. Chem.* **2010**, *45*, 3047.
- (152) Zhang, J.; Zhang, H.; Cai, W.; Yu, L.; Zhen, X.; Zhang, A. *Bioorg. Med. Chem.* **2009**, *17*, 4873.
- (153) Jorgensen, W. L.; Gandavadi, S.; Du, X.; Hare, A. A.; Trofimov, A.; Leng, L.; Bucala, R. *Bioorg. Med. Chem. Lett.* **2010**, *20*, 7033.
- (154) Sakmar, T. P. *Nat. Chem. Biol.* **2011**, *7*, 500.
- (155) Kecskés, A.; Tosh, D. K.; Wei, Q.; Gao, Z.-G.; Jacobson, K. A. *Bioconjugate Chem.* **2011**, *22*, 1115.
- (156) Gopi, H. N.; Tirupula, K. C.; Baxter, S.; Ajith, S.; Chaiken, I. M. *ChemMedChem* **2006**, *1*, 54.

- (157) Gopi, H.; Umashankara, M.; Pirrone, V.; LaLonde, J.; Madani, N.; Tuzer, F.; Baxter, S.; Zentner, I.; Cocklin, S.; Jawanda, N.; Miller, S. R.; Schön, A.; Klein, J. C.; Freire, E.; Krebs, F. C.; Smith, A. B.; Sodroski, J.; Chaiken, I. *J. Med. Chem.* **2008**, *51*, 2638.
- (158) Huber, D.; Hübner, H.; Gmeiner, P. *J. Med. Chem.* **2009**, *52*, 6860.
- (159) Kühhorn, J.; Hübner, H.; Gmeiner, P. *J. Med. Chem.* **2011**, *54*, 4896.
- (160) Alam, M. S.; Huang, J.; Ozoe, F.; Matsumura, F.; Ozoe, Y. *Bioorg. Med. Chem.* **2007**, *15*, 5090.
- (161) Bonnet, D.; Ilien, B.; Galzi, J.-L.; Riché, S.; Antheaune, C.; Hibert, M. *Bioconjugate Chem.* **2006**, *17*, 1618.
- (162) Michel, K.; Büther, K.; Law, M. P.; Wagner, S.; Schober, O.; Hermann, S.; Schäfers, M.; Riemann, B.; Höltke, C.; Kopka, K. *J. Med. Chem.* **2011**, *54*, 939.
- (163) Sun, H.; Liu, L.; Lu, J.; Qiu, S.; Yang, C.-Y.; Yi, H.; Wang, S. *Bioorg. Med. Chem. Lett.* **2010**, *20*, 3043.
- (164) Wijtmans, M.; de Graaf, C.; de Kloe, G.; Istyastono, E. P.; Smit, J.; Lim, H.; Boonnak, R.; Nijmeijer, S.; Smits, R. A.; Jongejan, A.; Zuiderveld, O.; de Esch, I. J. P.; Leurs, R. *J. Med. Chem.* **2011**, *54*, 1693.
- (165) Sander, K.; Kottke, T.; Hoffend, C.; Walter, M.; Weizel, L.; Camelin, J.-C.; Ligneau, X.; Schneider, E. H.; Seifert, R.; Schwartz, J.-C.; Stark, H. *Org. Lett.* **2010**, *12*, 2578.
- (166) Ye, N.; Wu, Q.; Zhu, L.; Zheng, L.; Gao, B.; Zhen, X.; Zhang, A. *Bioorg. Med. Chem.* **2011**, *19*, 1999.
- (167) Loaiza, P. R.; Löber, S.; Hübner, H.; Gmeiner, P. *Bioorg. Med. Chem.* **2009**, *17*, 5482.
- (168) Loaiza, P. R.; Löber, S.; Hübner, H.; Gmeiner, P. *J. Comb. Chem.* **2006**, *8*, 252.
- (169) Trabocchi, A.; Menchi, G.; Cini, N.; Bianchini, F.; Raspanti, S.; Bottoncetti, A.; Pupi, A.; Calorini, L.; Guarna, A. *J. Med. Chem.* **2010**, *53*, 7119.
- (170) Shu, H.; Izenwasser, S.; Wade, D.; Stevens, E. D.; Trudell, M. L. *Bioorg. Med. Chem. Lett.* **2009**, *19*, 891.
- (171) Stanley, N. J.; Pedersen, D. S.; Nielsen, B.; Kvist, T.; Mathiesen, J. M.; Bräuner-Osborne, H.; Taylor, D. K.; Abell, A. D. *Bioorg. Med. Chem. Lett.* **2010**, *20*, 7512.
- (172) (a) Mazella, J.; Vincent, J.-P. *Peptides* **2006**, *27*, 2488. (b) Richter, S.; Ramenda, T.; Bergmann, R.; Kniess, T.; Steinbach, J.; Pietzsch, J.; Wuest, F. *Bioorg. Med. Chem. Lett.* **2010**, *20*, 3306.
- (173) Choi, W. J.; Shi, Z.-D.; Worthy, K. M.; Bindu, L.; Karki, R. G.; Nicklaus, M. C.; Fisher, R. J.; Burke, T. R., Jr. *Bioorg. Med. Chem. Lett.* **2006**, *16*, 5265.
- (174) Beierle, J. M.; Horne, W. S.; van Maarseveen, J. H.; Waser, B.; Reubi, J. C.; Ghadiri, M. R. *Angew. Chem., Int. Ed.* **2009**, *48*, 4725.
- (175) Nicholas, K. T. *Drug Discovery Today Technol.* **2010**, *7*, e97.
- (176) Walsh, J. C.; Kolb, H. C. *Pure Appl. Chem.* **2010**, *64*, 29.
- (177) Jorgensen, W. L. *Acc. Chem. Res.* **2009**, *42*, 724.
- (178) Edwards, A. M.; Bountra, C.; Kerr, D. J.; Willson, T. M. *Nat. Chem. Biol.* **2009**, *5*, 436.
- (179) Peterson, L. B.; Blagg, B. S. J. *Bioorg. Med. Chem. Lett.* **2010**, *20*, 3957.
- (180) Day, J. E. H.; Sharp, S. Y.; Rowlands, M. G.; Aherne, W.; Workman, P.; Moody, C. J. *Chem.-Eur. J.* **2010**, *16*, 2758.
- (181) Kamal, A.; Shankaraiah, N.; Devaiah, V.; Laxma Reddy, K.; Juvekar, A.; Sen, S.; Kurian, N.; Zingde, S. *Bioorg. Med. Chem. Lett.* **2008**, *18*, 1468.
- (182) Zhang, J.; Garrossian, M.; Gardner, D.; Garrossian, A.; Chang, Y.-T.; Kim, Y. K.; Chang, C.-W. T. *Bioorg. Med. Chem. Lett.* **2008**, *18*, 1359.
- (183) Yoon, J.; Ryu, J.-S. *Bioorg. Med. Chem. Lett.* **2010**, *20*, 3930.
- (184) Reddy, D. M.; Srinivas, J.; Chashoo, G.; Saxena, A. K.; Sampath Kumar, H. M. *Eur. J. Med. Chem.* **2011**, *46*, 1983.
- (185) Reddy, P. B.; Agrawal, S. K.; Singh, S.; Bhat, B. A.; Saxena, A. K.; Kumar, H. M. S.; Qazi, G. N. *Chem. Biodiversity* **2008**, *5*, 1792.
- (186) Lee, Y.-S.; Park, S. M.; Kim, H. M.; Park, S.-K.; Lee, K.; Lee, C. W.; Kim, B. H. *Bioorg. Med. Chem. Lett.* **2009**, *19*, 4688.
- (187) Lei, X.; Danishefsky, S. J. *Adv. Synth. Catal.* **2008**, *350*, 1677.
- (188) Chen, J.; Nikolovska-Coleska, Z.; Yang, C.-Y.; Gomez, C.; Gao, W.; Krajewski, K.; Jiang, S.; Roller, P.; Wang, S. *Bioorg. Med. Chem. Lett.* **2007**, *17*, 3939.
- (189) Chen, J.; Nikolovska-Coleska, Z.; Yang, C.-Y.; Gomez, C.; Gao, W.; Krajewski, K.; Jiang, S.; Roller, P.; Wang, S. *Bioorg. Med. Chem. Lett.* **2007**, *17*, 3939.
- (190) Pintér, G.; Bereczki, I.; Batta, G.; Ötvös, R.; Sztaricskai, F.; Roth, E.; Ostorházi, E.; Rozgonyi, F.; Naesens, L.; Szarvas, M.; Boda, Z.; Herczegh, P. *Bioorg. Med. Chem. Lett.* **2010**, *20*, 2713.
- (191) Howell, L. A.; Howman, A.; O'Connell, M. A.; Mueller, A.; Searcey, M. *Bioorg. Med. Chem. Lett.* **2009**, *19*, 5880.
- (192) Perez-Castro, I.; Caamano, O.; Fernandez, F.; Garcia, M. D.; Lopez, C.; Clercq, E. D. *Org. Biomol. Chem.* **2007**, *5*, 3805.
- (193) Boechat, N.; Ferreira, V. F.; Ferreira, S. B.; Ferreira, M. D. L. G.; da Silva, F. d. C.; Bastos, M. M.; Costa, M. d. S.; Lourenço, M. C. S.; Pinto, A. C.; Krettli, A. U.; Aguiar, A. C.; Teixeira, B. M.; da Silva, N. V.; Martins, P. R. C.; Bezerra, F. A. F. M.; Camilo, A. L. S.; da Silva, G. P.; Costa, C. C. P. *J. Med. Chem.* **2011**, *54*, 5988.
- (194) Tron, G. C.; Pirali, T.; Billington, R. A.; Canonico, P. L.; Sorba, G.; Genazzani, A. A. *Med. Res. Rev.* **2008**, *28*, 278.
- (195) (a) Kharb, R.; Sharma, P. C.; Yar, M. S. *J. Enzyme Inhib. Med. Chem.* **2011**, *26*, 1. (b) Pagliai, F.; Pirali, T.; Del Grosso, E.; Di Brisco, R.; Tron, G. C.; Sorba, G.; Genazzani, A. A. *J. Med. Chem.* **2005**, *49*, 467.
- (196) Best, M. D. *Biochemistry* **2009**, *48*, 6571.
- (197) Sletten, E. M.; Bertozzi, C. R. *Acc. Chem. Res.* **2011**, *44*, 666.
- (198) Baskin, J. M.; Bertozzi, C. R. *QSAR Comb. Sci.* **2007**, *26*, 1211.
- (199) Chen, Y.-X.; Triola, G.; Waldmann, H. *Acc. Chem. Res.* **2011**, *44*, 762.
- (200) (a) Dieterich, D. C. *Curr. Opin. Neurobiol.* **2010**, *20*, 623. (b) Hao, Z.; Hong, S.; Chen, X.; Chen, P. R. *Acc. Chem. Res.* **2011**, *44*, 742.
- (201) Lim, R. K. V.; Lin, Q. *Chem. Commun.* **2010**, *46*, 1589.
- (202) Berry, A. F. H.; Heal, W. P.; Tarafder, A. K.; Tolmachova, T.; Baron, R. A.; Seabra, M. C.; Tate, E. W. *ChemBioChem* **2010**, *11*, 771.
- (203) Devaraj, N. K.; Hilderbrand, S.; Upadhyay, R.; Mazitschek, R.; Weissleder, R. *Angew. Chem.* **2010**, *122*, 2931.
- (204) Deiters, A.; Cropp, T. A.; Mukherji, M.; Chin, J. W.; Anderson, J. C.; Schultz, P. G. *J. Am. Chem. Soc.* **2003**, *125*, 11782.
- (205) Torrice, M. M.; Bower, K. S.; Lester, H. A.; Dougherty, D. A. *Proc. Natl. Acad. Sci. U.S.A.* **2009**, *106*, 11919.
- (206) Kiick, K. L.; Saxon, E.; Tirrell, D. A.; Bertozzi, C. R. *Proc. Natl. Acad. Sci. U.S.A.* **2002**, *99*, 19.
- (207) Dieterich, D. C.; Link, A. J.; Graumann, J.; Tirrell, D. A.; Schuman, E. M. *Proc. Natl. Acad. Sci. U.S.A.* **2006**, *103*, 9482.
- (208) Dieterich, D. C.; Hodas, J. J. L.; Gouzer, G.; Shadrin, I. Y.; Ngo, J. T.; Triller, A.; Tirrell, D. A.; Schuman, E. M. *Nat. Neurosci.* **2010**, *13*, 897.
- (209) Ngo, J. T.; Champion, J. A.; Mahdavi, A.; Tanrikulu, I. C.; Beatty, K. E.; Connor, R. E.; Yoo, T. H.; Dieterich, D. C.; Schuman, E. M.; Tirrell, D. A. *Nat. Chem. Biol.* **2009**, *5*, 715.
- (210) Koudelka, K. J.; Manchester, M. *Curr. Opin. Chem. Biol.* **2010**, *14*, 810.
- (211) Hong, V.; Presolski, S. I.; Ma, C.; Finn, M. G. *Angew. Chem., Int. Ed.* **2009**, *48*, 9879.
- (212) (a) Gupta, S. S.; Kuzelka, J.; Singh, P.; Lewis, W. G.; Manchester, M.; Finn, M. G. *Bioconjugate Chem.* **2005**, *16*, 1572. (b) Bruckman, M. A.; Kaur, G.; Lee, L. A.; Xie, F.; Sepulveda, J.; Breitenkamp, R.; Zhang, X.; Joralemon, M.; Russell, T. P.; Emrick, T.; Wang, Q. *ChemBioChem* **2008**, *9*, 519.
- (213) Yi, L.; Shi, J.; Gao, S.; Li, S.; Niu, C.; Xi, Z. *Tetrahedron Lett.* **2009**, *50*, 759.
- (214) Besanceney-Webler, C.; Jiang, H.; Wang, W.; Baughn, A. D.; Wu, P. *Bioorg. Med. Chem. Lett.* **2011**, *21*, 4989.
- (215) Hong, V.; Steinmetz, N. F.; Manchester, M.; Finn, M. G. *Bioconjugate Chem.* **2010**, *21*, 1912.
- (216) Soriano del Amo, D.; Wang, W.; Jiang, H.; Besanceney, C.; Yan, A. C.; Levy, M.; Liu, Y.; Marlow, F. L.; Wu, P. *J. Am. Chem. Soc.* **2010**, *132*, 16893.

- (217) Nomura, W.; Tanabe, Y.; Tsutsumi, H.; Tanaka, T.; Ohba, K.; Yamamoto, N.; Tamamura, H. *Bioconjugate Chem.* **2008**, *19*, 1917.
- (218) Oishi, S.; Masuda, R.; Evans, B.; Ueda, S.; Goto, Y.; Ohno, H.; Hirasawa, A.; Tsujimoto, G.; Wang, Z.; Peiper, S. C.; Naito, T.; Kodama, E.; Matsuoka, M.; Fujii, N. *ChemBioChem* **2008**, *9*, 1154.
- (219) Ye, S.; Köhrer, C.; Huber, T.; Kazmi, M.; Sachdev, P.; Yan, E. C. Y.; Bhagat, A.; RajBhandary, U. L.; Sakmar, T. P. *J. Biol. Chem.* **2008**, *283*, 1525.
- (220) Daggett, K. A.; Sakmar, T. P. *Curr. Opin. Chem. Biol.* **2011**, *15*, 392.
- (221) Kolodziejek, I.; van der Hoorn, R. A. L. *Curr. Opin. Biotechnol.* **2010**, *21*, 225.
- (222) Nomura, D. K.; Dix, M. M.; Cravatt, B. F. *Nat. Rev. Cancer* **2010**, *10*, 630.
- (223) Raghavan, A. S.; Hang, H. C. *Drug Discovery Today* **2009**, *14*, 178.
- (224) Sleno, L.; Emili, A. *Curr. Opin. Chem. Biol.* **2008**, *12*, 46.
- (225) Pernemalm, M.; Lewensohn, R.; Lehtiö, J. *Proteomics* **2009**, *9*, 1420.
- (226) Krishnamurthy, D.; Barrios, A. M. *Curr. Opin. Chem. Biol.* **2009**, *13*, 375.
- (227) Viertler, M.; Schittmayer, M.; Birner-Gruenberger, R. *Bioorg. Med. Chem.* **2011**, *20*, 628.
- (228) Böttcher, T.; Sieber, S. A. *J. Am. Chem. Soc.* **2010**, *132*, 6964.
- (229) Shi, H.; Liu, K.; Xu, A.; Yao, S. Q. *Chem. Commun.* **2009**, *33*, 5030.
- (230) Fuwa, H.; Takahashi, Y.; Konno, Y.; Watanabe, N.; Miyashita, H.; Sasaki, M.; Natsugari, H.; Kan, T.; Fukuyama, T.; Tomita, T.; Iwatsubo, T. *ACS Chem. Biol.* **2007**, *2*, 408.
- (231) Dijkstra, H. P.; Sprong, H.; Aerts, B. N. H.; Kruithof, C. A.; Egmond, M. R.; Klein Gebbink, R. J. M. *Org. Biomol. Chem.* **2008**, *6*, 523.
- (232) Gillet, L. C. J.; Namoto, K.; Ruchti, A.; Hoving, S.; Boesch, D.; Inverardi, B.; Mueller, D.; Coulot, M.; Schindler, P.; Schweigler, P.; Bernardi, A.; Gil-Parrado, S. *Mol. Cell. Proteomics* **2008**, *7*, 1241.
- (233) Haedke, U.; Götz, M.; Baer, P.; Verhelst, S. H. L. *Bioorg. Med. Chem.* **2012**, *20*, 633.
- (234) Hang, H. C.; Loureiro, J.; Spooner, E.; van der Velden, A. W. M.; Kim, Y.-M.; Pollington, A. M.; Maehr, R.; Starnbach, M. N.; Ploegh, H. L. *ACS Chem. Biol.* **2006**, *1*, 713.
- (235) Böttcher, T.; Sieber, S. A. *Angew. Chem., Int. Ed.* **2008**, *47*, 4600.
- (236) Cohen, M. S.; Hadjivassiliou, H.; Taunton, J. *Nat. Chem. Biol.* **2007**, *3*, 156.
- (237) Stubbs, K. A.; Scaffidi, A.; Debowski, A. W.; Mark, B. L.; Stick, R. V.; Vocadlo, D. J. *J. Am. Chem. Soc.* **2007**, *130*, 327.
- (238) Vila, A.; Tallman, K. A.; Jacobs, A. T.; Liebler, D. C.; Porter, N. A.; Marnett, L. J. *Chem. Res. Toxicol.* **2008**, *21*, 432.
- (239) Saario, S. M.; McKinney, M. K.; Speers, A. E.; Wang, C.; Cravatt, B. F. *Chem. Sci.* **2012**, *3*, 77.
- (240) Raghavan, A.; Charron, G.; Flexner, J.; Hang, H. C. *Bioorg. Med. Chem. Lett.* **2008**, *18*, 5982.
- (241) Salisbury, C. M.; Cravatt, B. F. *J. Am. Chem. Soc.* **2008**, *130*, 2184.
- (242) Salisbury, C. M.; Cravatt, B. F. *Proc. Natl. Acad. Sci. U.S.A.* **2007**, *104*, 1171.
- (243) Xu, C.; Soragni, E.; Chou, C. J.; Herman, D.; Plasterer, H. L.; Rusche, J. R.; Gottesfeld, J. M. *Chem. Biol.* **2009**, *16*, 980.
- (244) Evans, M. J.; Saghatelyan, A.; Sorensen, E. J.; Cravatt, B. F. *Nat. Biotechnol.* **2005**, *23*, 1303.
- (245) Wright, A. T.; Cravatt, B. F. *Chem. Biol.* **2007**, *14*, 1043.
- (246) Sieber, S. A.; Niessen, S.; Hoover, H. S.; Cravatt, B. F. *Nat. Chem. Biol.* **2006**, *2*, 274.
- (247) MacKinnon, A. L.; Garrison, J. L.; Hegde, R. S.; Taunton, J. J. *Am. Chem. Soc.* **2007**, *129*, 14560.
- (248) Qiu, W.-W.; Xu, J.; Li, J.-Y.; Li, J.; Nan, F.-J. *ChemBioChem* **2007**, *8*, 1351.
- (249) Weerapana, E.; Speers, A. E.; Cravatt, B. F. *Nat. Protoc.* **2007**, *2*, 1414.
- (250) Speers, A. E.; Adam, G. C.; Cravatt, B. F. *J. Am. Chem. Soc.* **2003**, *125*, 4686.
- (251) Speers, A. E.; Cravatt, B. F. *Chem. Biol.* **2004**, *11*, 535.
- (252) Macpherson, L. J.; Dubin, A. E.; Evans, M. J.; Marr, F.; Schultz, P. G.; Cravatt, B. F.; Patapoutian, A. *Nature* **2007**, *445*, 541.
- (253) El-Sagheer, A. H.; Brown, T. *Chem. Rev.* **2010**, *39*, 1388.
- (254) Gutschiedl, K.; Fazio, D.; Carell, T. *Chem.-Eur. J.* **2010**, *16*, 6877.
- (255) Jao, C. Y.; Salic, A. *Proc. Natl. Acad. Sci. U.S.A.* **2008**, *105*, 15779.
- (256) Salic, A.; Mitchison, T. J. *Proc. Natl. Acad. Sci. U.S.A.* **2008**, *105*, 2415.
- (257) Song, C.-X.; He, C. *Acc. Chem. Res.* **2011**, *44*, 709.
- (258) Xu, Y. *Chem. Rev.* **2011**, *40*, 2719.
- (259) Collie, G. W.; Sparapani, S.; Parkinson, G. N.; Neidle, S. *J. Am. Chem. Soc.* **2011**, *133*, 2721.
- (260) Xu, Y.; Suzuki, Y.; Komiyama, M. *Angew. Chem., Int. Ed.* **2009**, *48*, 3281.
- (261) Dash, J.; Waller, Z. A. E.; Pantoş, G. D.; Balasubramanian, S. *Chem.-Eur. J.* **2011**, *17*, 4571.
- (262) Moorhouse, A. D.; Santos, A. M.; Gunaratnam, M.; Moore, M.; Neidle, S.; Moses, J. E. *J. Am. Chem. Soc.* **2006**, *128*, 15972.
- (263) (a) Huisgen, R. *Angew. Chem., Int. Ed. Engl.* **1963**, 565. (b) Meldal, M.; Tornøe, C. W. *Chem. Rev.* **2008**, *108*, 2952. (c) Jewett, J. C.; Bertozzi, C. R. *Chem. Rev.* **2010**, *39*, 1272.
- (264) Manova, R.; van Beek, T. A.; Zuilhof, H. *Angew. Chem., Int. Ed.* **2011**, *50*, 5428.
- (265) Sletten, E. M.; Bertozzi, C. R. *Acc. Chem. Res.* **2011**, *44*, 666.
- (266) Henriksson, A.; Friedbacher, G.; Hoffmann, H. *Langmuir* **2011**, *27*, 7345.
- (267) Becer, C. R.; Hoogenboom, R.; Schubert, U. S. *Angew. Chem., Int. Ed.* **2009**, *48*, 4900.
- (268) Debets, M. F.; van der Doelen, C. W. J.; Rutjes, F. P. J. T.; van Delft, F. L. *ChemBioChem* **2010**, *11*, 1168.
- (269) Debets, M. F.; van Berkel, S. S.; Dommerholt, J.; Dirks, A. J.; Rutjes, F. P. J. T.; van Delft, F. L. *Acc. Chem. Res.* **2011**, *44*, 805.
- (270) Agard, N. J.; Prescher, J. A.; Bertozzi, C. R. *J. Am. Chem. Soc.* **2004**, *126*, 15046.
- (271) Agard, N. J.; Baskin, J. M.; Prescher, J. A.; Lo, A.; Bertozzi, C. R. *ACS Chem. Biol.* **2006**, *1*, 644.
- (272) Baskin, J. M.; Prescher, J. A.; Laughlin, S. T.; Agard, N. J.; Chang, P. V.; Miller, I. A.; Lo, A.; Codelli, J. A.; Bertozzi, C. R. *Proc. Natl. Acad. Sci. U.S.A.* **2007**, *104*, 16793.
- (273) Codelli, J. A.; Baskin, J. M.; Agard, N. J.; Bertozzi, C. R. *J. Am. Chem. Soc.* **2008**, *130*, 11486.
- (274) Ning, X.; Guo, J.; Wolfert, M. A.; Boons, G.-J. *Angew. Chem., Int. Ed.* **2008**, *47*, 2253.
- (275) Sletten, E. M.; Bertozzi, C. R. *Org. Lett.* **2008**, *10*, 3097.
- (276) Debets, M. F.; van Berkel, S. S.; Schoffelen, S.; Rutjes, F. P. J. T.; van Hest, J. C. M.; van Delft, F. L. *Chem. Commun.* **2010**, *46*, 97.
- (277) Jewett, J. C.; Sletten, E. M.; Bertozzi, C. R. *J. Am. Chem. Soc.* **2010**, *132*, 3688.
- (278) Baskin, J. M.; Prescher, J. A.; Laughlin, S. T.; Agard, N. J.; Chang, P. V.; Miller, I. A.; Lo, A.; Codelli, J. A.; Bertozzi, C. R. *Proc. Natl. Acad. Sci. U.S.A.* **2007**, *104*, 16793.
- (279) Dommerholt, J.; Schmidt, S.; Temming, R.; Hendriks, L. J. A.; Rutjes, F. P. J. T.; van Hest, J. C. M.; Lefebvre, D. J.; Friedl, P.; van Delft, F. L. *Angew. Chem., Int. Ed.* **2010**, *49*, 9422.
- (280) Tanrikulu, I. C.; Schmitt, E.; Mechulam, Y.; Goddard, W. A.; Tirrell, D. A. *Proc. Natl. Acad. Sci. U.S.A.* **2009**, *106*, 15285.
- (281) Lallana, E.; Fernandez-Megia, E.; Riguera, R. *J. Am. Chem. Soc.* **2009**, *131*, 5748.
- (282) Neef, A. B.; Schultz, C. *Angew. Chem., Int. Ed.* **2009**, *48*, 1498.
- (283) Fernandez-Suarez, M.; Baruah, H.; Martinez-Hernandez, L.; Xie, K. T.; Baskin, J. M.; Bertozzi, C. R.; Ting, A. Y. *Nat. Biotechnol.* **2007**, *25*, 1483.
- (284) Kele, P.; Mezö, G.; Achatz, D.; Wolfbeis, O. S. *Angew. Chem., Int. Ed.* **2009**, *48*, 344.

- (285) Kele, P.; Li, X.; Link, M.; Nagy, K.; Herner, A.; Lorincz, K.; Beni, S.; Wolfbeis, O. S. *Org. Biomol. Chem.* **2009**, *7*, 3486.
- (286) Nessen, M. A.; Kramer, G.; Back, J.; Baskin, J. M.; Smeenk, L. E. J.; de Koning, L. J.; van Maarseveen, J. H.; de Jong, L.; Bertozzi, C. R.; Hiemstra, H.; de Koster, C. G. *J. Proteome Res.* **2009**, *8*, 3702.
- (287) Back, J. W.; David, O.; Kramer, G.; Masson, G.; Kasper, P. T.; de Koning, L. J.; de Jong, L.; van Maarseveen, J. H.; de Koster, C. G. *Angew. Chem., Int. Ed.* **2005**, *44*, 7946.
- (288) Kasper, P. T.; Back, J. W.; Vitale, M.; Hartog, A. F.; Roseboom, W.; de Koning, L. J.; van Maarseveen, J. H.; Muijsers, A. O.; de Koster, C. G.; de Jong, L. *ChemBioChem* **2007**, *8*, 1281.
- (289) Johnson, J. A.; Baskin, J. M.; Bertozzi, C. R.; Koberstein, J. T.; Turro, N. J. *Chem. Commun.* **2008**, *26*, 3064.
- (290) Zou, Y.; Yin, J. *Bioorg. Med. Chem. Lett.* **2008**, *18*, 5664.
- (291) Laughlin, S. T.; Baskin, J. M.; Amacher, S. L.; Bertozzi, C. R. *Science* **2008**, *320*, 664.
- (292) Laughlin, S. T.; Bertozzi, C. R. *ACS Chem. Biol.* **2009**, *4*, 1068.
- (293) Gartner, Z. J.; Bertozzi, C. R. *Proc. Natl. Acad. Sci. U.S.A.* **2009**, *106*, 4606.
- (294) Hur, G. H.; Meier, J. L.; Baskin, J.; Codelli, J. A.; Bertozzi, C. R.; Marahiel, M. A.; Burkart, M. D. *Chem. Biol.* **2009**, *16*, 372.
- (295) DeForest, C. A.; Polizzotti, B. D.; Anseth, K. S. *Nat. Mater.* **2009**, *8*, 659.
- (296) Plass, T.; Milles, S.; Koehler, C.; Schultz, C.; Lemke, E. A. *Angew. Chem., Int. Ed.* **2011**, *50*, 3878.
- (297) Laughlin, S. T.; Agard, N. J.; Baskin, J. M.; Carrico, I. S.; Chang, P. V.; Ganguli, A. S.; Hangauer, M. J.; Lo, A.; Prescher, J. A.; Bertozzi, C. R.; Minoru, F. *Methods Enzymol.* **2006**, *415*, 230.
- (298) Chang, P. V.; Prescher, J. A.; Sletten, E. M.; Baskin, J. M.; Miller, I. A.; Agard, N. J.; Lo, A.; Bertozzi, C. R. *Proc. Natl. Acad. Sci. U.S.A.* **2010**, *107*, 1821.
- (299) Shelbourne, M.; Chen, X.; Brown, T.; El-Sagheer, A. H. *Chem. Commun.* **2011**, *47*, 6257.
- (300) Marks, I. S.; Kang, J. S.; Jones, B. T.; Landmark, K. J.; Cleland, A. J.; Taton, T. A. *Bioconjugate Chem.* **2011**, *22*, 1259.
- (301) Jayaprakash, K. N.; Peng, C. G.; Butler, D.; Varghese, J. P.; Maier, M. A.; Rajeev, K. G.; Manoharan, M. *Org. Lett.* **2010**, *12*, 5410.
- (302) Baskin, J. M.; Dehnert, K. W.; Laughlin, S. T.; Amacher, S. L.; Bertozzi, C. R. *Proc. Natl. Acad. Sci. U.S.A.* **2010**, *107*, 10360.
- (303) Dehnert, K. W.; Beahm, B. J.; Huynh, T. T.; Baskin, J. M.; Laughlin, S. T.; Wang, W.; Wu, P.; Amacher, S. L.; Bertozzi, C. R. *ACS Chem. Biol.* **2011**, *6*, 547.